

Biotransformation of Perfluorooctane Sulfonamide (FOSA), 8:2 Fluorotelomer Alcohol (8:2 FTOH), and 6:2 Fluorotelomer Sulfonate (6:2 FTS) in Aqueous Film-Forming Foam (AFFF)-Impacted Soils under Oxic and Anoxic Conditions

by

Pengfei Yan

A Dissertation submitted to the Graduate Faculty of
Auburn University
in partial fulfillment of the
requirements for the Degree of
Doctor of Philosophy

Auburn, Alabama
Dec 10, 2022

Keywords: Aqueous film-forming foam, Per- and polyfluoroalkyl substances, Biotransformation, Redox condition, Microbial community, Natural environment

Copyright 2022 by Pengfei Yan

Approved by

Natalie L. Cápiro, Ph.D., Chair, Assistant Professor, Department of Civil and Environmental
Engineering

Lauren E. Beckingham, Ph.D., Associate Professor, Department of Civil and Environmental
Engineering

Joel S. Hayworth, Ph.D., P.E., Associate Professor, Department of Civil and Environmental
Engineering

Ann S. Ojeda, Ph.D., Assistant Professor, Department of Geosciences

Abstract

The use of aqueous film-forming foams (AFFFs) for fire suppression over decades has resulted in contamination of numerous sites by per- and polyfluoroalkyl substances (PFAS). However, the environmental fate and transformation of the polyfluoroalkyl substances (referred to as “precursors”) in AFFF-impacted sites remain largely unknown. This study focused on investigating the biotransformation of three AFFF-derived precursors by native microbial communities under conditions representative of AFFF-impacted sites.

Aerobic soil biotransformation of perfluorooctane sulfonamide (FOSA) was first examined. Half-lives of 203.0-335.1 days for FOSA, and the production of perfluorooctanoic sulfonate (PFOS) with molar yields of 21.6-29.5 mol% were observed in two studied soils. Then, biotransformation of 8:2 fluorotelomer alcohol (8:2 FTOH) was investigated under various redox conditions. The biotransformation was much slower under sulfate- and iron-reducing conditions with >60 mol% of initial 8:2 FTOH remained after ~400 days, compared to a half-life of 12.5-36.5 days under nitrate-reducing conditions. Perfluorooctanoic acid (PFOA) was only formed under nitrate-reducing conditions. Further, biotransformation of 6:2 fluorotelomer sulfonate (6:2 FTS) was studied in two AFFF-impacted soils. A half-life of 43.3 days was obtained for one soil, while >60 mol% of initial 6:2 FTS remained in the other soil after a 224-day incubation. A novel “fluorotelomer ketone to PFCA” pathway during 6:2 FTS biotransformation is proposed. These microcosm studies demonstrate that biotransformation of FOSA, 8:2 FTOH, and 6:2 FTS could be strongly influenced by some environmental factors (e.g., redox condition, microbial community), and highlight the need to characterize biogeochemical site properties to accurately assess the potential for precursors’ biotransformation at AFFF-impacted sites.

To assess the potential effects of dynamic flow conditions in natural environments, biotransformation of 6:2 FTS was further examined in one-dimensional flow-through columns. By increasing hydraulic residence time from 4.1 to 6.3 days, 22-26% lower concentrations of 6:2 FTS were measured in column effluents. Flow interruptions (2-7 days) posed substantial promoting effects on 6:2 FTS biotransformation after flow resumption. Results revealed that flow conditions play important roles in the 6:2 FTS biotransformation in natural environment. The need to

incorporate system conditions (e.g., hydraulic parameters) into experimental systems for PFAS biotransformation investigation is highlighted.

Acknowledgements

I would like to express my heartfelt gratitude to my advisor Dr. Natalie Cápiro for giving me a chance to start my PhD study in the field of Environmental Engineering. Thank you for your continuous guidance and support throughout the course of my study. I also acknowledge the financial support from the Strategic Environmental Research and Development Program (SERDP), the China Scholarship Council, Auburn University Graduate School and Office of International Programs (OIP). Additional thanks to Dr. Andrew Gillespie and other staff from OIP for your kind help.

Thank you to my committee members, Dr. Lauren Beckingham, Dr. Joel Hayworth, and Dr. Ann Ojeda, and my dissertation outside reader, Dr. Anna Linhoss, for your time and valuable advice on my research and dissertation.

Thank you, Sheng. You have always been a great help at every aspect of research, thinking, writing, experimenting, plotting, etc. It was a good journey working with you throughout the PhD career. I also want to thank other collaborators, Dr. Katherine Manz, Matthew Woodcock, Dr. Chen Liu, Dr. Melissa Mezzari, Dr. Kurt Pennell, and Dr. Linda Abriola for your invaluable help and input to my research. Also, thanks to prior and current lab members, Spencer Cothran, Harry Vaslo, Savannah Cummins, Temitope Popoola. It was good to be at the same lab with you.

Special gratitude to my Mom and Dad for your unconditional love and support in my life. No matter where I am and what I am doing, I know you are always with me. Sorry, for not being at your side for such long time. Also, special thank you to all my family, friends, Huan, Yang, for your continuous emotional support and encouragement over these years.

Table of Contents

Abstract	ii
Acknowledgements	iv
List of Tables	viii
List of Figures	x
List of Abbreviations and Acronyms	xiv
Chapter 1 Introduction	1
1.1 Background	1
1.2 Motivation for this research	2
1.3 Objectives	3
1.4 Dissertation organization.....	3
Chapter 2 Literature review on per- and polyfluoroalkyl substances in aqueous film-forming foams (AFFFs) and AFFF-impacted environment	6
2.1 Introduction	6
2.2 PFAS concentrations in AFFF formulations	8
2.2.1 PFAS concentrations in ECF-based AFFF formulations	9
2.2.2 PFAS concentrations in FT-based AFFF formulations	10
2.3 The occurrence of PFAS in the environment impacted by AFFFs	12
2.3.1 PFAS concentrations in AFFF-impacted groundwater	13
2.3.2 PFAS concentrations in AFFF-impacted surface water	15
2.3.3 PFAS concentrations in AFFF-impacted surface and subsurface soil	16
2.3.4 PFAS concentrations in AFFF-impacted sediment	19
2.4 Comparison of PFAS compositions in AFFF formulations and AFFF-impacted environment.....	19
2.5 Microbial transformation of AFFF-derived PFAS	21
2.5.1 Aerobic biotransformation of ECF-based precursors.....	21
2.5.2 Aerobic biotransformation of FT-based precursors	25
2.5.3 Anaerobic biotransformation of AFFF-derived precursors	30
2.6 Environmental implications and future research recommendations	31
Chapter 3 Production of perfluorooctane sulfonate (PFOS) from biotransformation of perfluorooctane sulfonamide (FOSA) in aerobic soils	33
3.1 Introduction	33
3.2 Materials and methods.....	35
3.2.1 Chemicals and Materials	35
3.2.2 Microcosm Set-up and Sampling	35
3.2.3 PFAS analysis.....	37
3.2.4 Microbial community analysis	37
3.3 Results and discussion.....	38
3.3.1 Experimental system	38
3.3.2 Biotransformation of FOSA in Loring and Hudson soil microcosms	39
3.3.3 Comparison of the biotransformation of FOSA and FOSA precursors	42

3.3.4 Microbial communities in Loring and Hudson soil microcosms	43
3.4 Environmental implications	47
Chapter 4 Biotransformation of 8:2 Fluorotelomer Alcohol in Soil from Aqueous Film-Forming Foams (AFFFs)-impacted Sites under Nitrate-, Sulfate-, and Iron-reducing Conditions.....	48
4.1 Introduction	48
4.2 Materials and methods.....	50
4.2.1 Microcosm Set-up	50
4.2.2 Sample Collection and Preparation	51
4.2.3 Targeted and Non-targeted PFAS Analysis	52
4.2.4 Microbial community analysis	53
4.3 Results and discussion.....	53
4.3.1 Biotransformation of 8:2 FTOH under nitrate-reducing conditions.....	54
4.3.2 Biotransformation of 8:2 FTOH under sulfate-reducing and iron-reducing conditions.....	59
4.3.3 Distinct 8:2 FTOH biotransformation pathways under different redox conditions	62
4.3.4 Comprehensive biotransformation pathways of 8:2 FTOH	65
4.4. Environmental implications	69
Chapter 5 Aerobic Biotransformation of 6:2 Fluorotelomer Sulfonate in Soils from Two Aqueous Film-Forming Foam (AFFF)-Impacted Sites	70
5.1 Introduction	70
5.2 Materials and methods.....	71
5.2.1 Chemicals and Materials	71
5.2.2 Microcosm Set-up and Sampling	72
5.2.3 Targeted and Non-Targeted PFAS Analysis	73
5.2.4 Microbial community analysis	74
5.3 Results and discussion.....	74
5.3.1 Experimental system	74
5.3.2 Biotransformation of 6:2 FTS in Loring and Robins soil microcosms	75
5.3.3 Identification of novel biotransformation products by LC-HRMS analysis	83
5.3.4 Biotransformation pathways of 6:2 FTS in AFFF-impacted soil.....	84
5.4 Environmental implications	87
Chapter 6 Biotransformation of 6:2 Fluorotelomer Sulfonate in Aqueous Film-Forming Foam (AFFF)-impacted Soil under Continuous Flow Conditions	88
6.1 Introduction	88
6.2 Materials and methods.....	89
6.2.1 Chemicals and Materials	89
6.2.2 Column design and preparation	90
6.2.3 Synthetic groundwater preparation.....	91
6.2.4 Column operation and sampling.....	91
6.3 Results and discussion.....	93
6.3.1 Biotransformation of 6:2 FTS under dynamic flow conditions.....	94

6.3.2 Biotransformation of 6:2 FTS along the flowing path	100
6.3.3 Comparison of 6:2 FTS biotransformation between microcosm and column experiments.....	103
6.4 Environmental implications	105
Chapter 7 Key findings, publications, and recommendations for future work	107
7.1 Key Findings	107
7.1.1 Production of PFOS from biotransformation of FOSA in aerobic soils	107
7.1.2 Biotransformation of 8:2 FTOH in soil from AFFF-impacted sites under nitrate-, sulfate-, and iron-reducing conditions	107
7.1.3 Aerobic biotransformation of 6:2 FTS in soils from two AFFF-impacted sites	108
7.1.4 Biotransformation of 6:2 FTS in AFFF-impacted soil under continuous flow conditions	108
7.2 Publications and Presentations	109
7.2.1 Publications	109
7.2.2 Selected presentations	110
7.3 Recommendations for Future Research	110
Reference	112

Appendix A. Supporting Information for Chapter 2: Literature review on per- and polyfluoroalkyl substances in aqueous film-forming foams (AFFFs) and AFFF-impacted environment.....	131
--	------------

Appendix B. Supporting Information for Chapter 3: Production of perfluorooctane sulfonate (PFOS) from biotransformation of perfluorooctane sulfonamide (FOSA) in aerobic soils.....	139
--	------------

Appendix C. Supporting Information for Chapter 4: Biotransformation of 8:2 Fluorotelomer Alcohol in Soil from Aqueous Film-Forming Foams (AFFFs)-impacted Sites under Nitrate-, Sulfate-, and Iron-reducing Conditions	148
---	------------

C-S1. Materials and Methods	148
C-S2. Establishment of nitrate-, sulfate-, and iron-reducing microcosms	151
C-S3. Background levels of legacy PFAS in Loring AFB soil	152

Appendix D. Supporting Information for Chapter 5: Aerobic Biotransformation of 6:2 Fluorotelomer Sulfonate in Soils from Two Aqueous Film-Forming Foam (AFFF)-Impacted Sites	179
---	------------

D-S1. Materials and Methods.....	179
D-S2. Background levels of 6:2 FTS and its potential transformation products in Loring and Robins soils.	181
D-S3. Diversity and richness of microbial community	182
D-S4. The impacts of 6:2 FTS and its biotransformation products on the microbial community compositions.....	183

Appendix E. Supporting Information for Chapter 6: Biotransformation of 6:2 Fluorotelomer Sulfonate in Aqueous Film-Forming Foam (AFFF)-impacted Soil under Continuous Flow Conditions.....	211
---	------------

List of Tables

Table 2-1. Summary statistics of the concentration of selected PFAS previously reported in the groundwater samples (n=383) collected from AFFF-impacted sites.....	14
Table 3-1. Microcosm set-up of FOSA aerobic biotransformation in Loring and Hudson soils.	36
Table 3-2. An overview of the prior and current studies investigating biotransformation of FOSA and FOSA precursors.....	43
Table A-1. PFAS class acronym, class name, structure of the class, and the example of acronym of one analogue.....	131
Table A-2. Summary statistics of the concentration of selected PFAS previously reported in the surface water samples (n=204) collected from AFFF-impacted sites	134
Table A-3. Summary statistics of the concentration of selected PFAS previously reported in the surface soil samples (n=274) collected from AFFF-impacted sites.....	135
Table A-4. Summary statistics of the concentration of selected PFAS previously reported in the subsurface soil samples (n=169) collected from AFFF-impacted sites	137
Table A-5. Summary statistics of the concentration of selected PFAS previously reported in the sediment samples (n=78) collected from AFFF-impacted sites	138
Table B-1. Physical and chemical properties of Loring and Hudson soils	139
Table B-2. Targeted mass inclusion list used in LC-MS analysis	140
Table B-3. Limits of detection (LODs) and limits of quantification (LOQs) of targeted PFAS	141
Table B-4. Changes in the mass (nmole) of FOSA and PFOS in Loring soil microcosms	142
Table B-5. Partitioning of FOSA and PFOS in aqueous and solid phases of Loring and Hudson live treatments (percentage (%) of mass in each phase relative to the total mass).....	143
Table B-6. Microbial richness and diversity in Loring and Hudson soils.....	144
Table C-1. Experimental set-up of 8:2 FTOH biotransformation microcosms under nitrate-, sulfate-, and iron-reducing conditions	153
Table C-2. Chemical names, acronyms, molecular structures, and suppliers of target poly- and perfluoroalkyl substances (PFAS) for LC-MS/MS quantitative analysis.....	154
Table C-3. Instrument conditions and LC gradient used for the detection and quantification of 8:2 FTOH and its polyfluorinated transformation products by UPLC-MS/MS	155
Table C-4. Multiple reaction monitoring (MRM) parameters used for the detection and quantification of 8:2 FTOH and its polyfluorinated transformation products by UPLC-MS/MS	156
Table C-5. Instrument conditions and LC gradient used for the detection and quantification of PFAAs by UPLC-MS/MS.....	157
Table C-6. Multiple reaction monitoring (MRM) parameters used for the detection and quantification of PFAAs by UPLC-MS/MS	158
Table C-7. Limits of detection (LODs) and limits of quantification (LOQs) of target PFAS...	159

Table C-8. Concentrations (nanomole per gram soil/dry weight) of individual PFAS in Loring AFB soil	160
Table C-9. Potential biotransformation products of 8:2 FTOH identified by LC-HRMS analysis	161
Table D-1. Chemical names, acronyms, molecular structures, and suppliers of target poly- and perfluoroalkyl substances (PFAS) for LC-MS/MS targeted analysis	184
Table D-2. Physical and chemical properties of Loring and Robins soils	185
Table D-3. Microcosm set-up of 6:2 FTS aerobic biotransformation in Loring and Robins soils	186
Table D-4. Instrument conditions and LC gradient used for the detection and quantification of 6:2 FTS and its polyfluorinated transformation products by UPLC-MS/MS	187
Table D-5. Multiple reaction monitoring (MRM) parameters used for the detection and quantification of 6:2 FTS and its polyfluorinated transformation products by UPLC-MS/MS .	188
Table D-6. Instrument conditions and LC gradient used for the detection and quantification of PFAAs by UPLC-MS/MS	189
Table D-7. Multiple reaction monitoring (MRM) parameters used for the detection and quantification of PFAAs by UPLC-MS/MS	190
Table D-8. Limits of detection (LODs) and limits of quantification (LOQs) of target PFAS ...	191
Table D-9. Background levels (nmole/g dw) of 6:2 FTS and its potential per- and polyfluorinated transformation products in Loring and Robins soils	192
Table D-10. Changes in the mass (nmole) of 6:2 FTS and its potential transformation products in Loring soil microcosms	193
Table D-11. Changes in the mass (nmole) of 6:2 FTS and its potential transformation products in Robins soil microcosms	194
Table D-12. Comparison of 6:2 FTS biotransformation in environmental matrices and pure cultures under aerobic conditions	195
Table D-13. Microbial richness and diversity in Loring and Robins soils	196
Table D-14. Potential biotransformation products of 6:2 FTS identified by HRMS analysis ...	197
Table E-1. Chemical names, acronyms, molecular structures, and suppliers of target poly- and perfluoroalkyl substances (PFAS) for LC-MS/MS targeted analysis	211
Table E-2. Packed dry porous media mass, total porosity, and pore volume (PV) for experimental columns	212
Table E-3. Oxidation-reduction potential (ORP) of biotic column samples collected at different time points	213
Table E-4. The average molar percent of 6:2 FTS and its biotransformation products (unit: mol%) at different time points in prior microcosm study	214
Table E-5. The average molar percent of 6:2 FTS and its biotransformation products (unit: mol%) at different phases	215

List of Figures

Figure 2-1. Concentration of PFAS detected in ECF-based AFFF formulations (top figure), and corresponding detection frequency (bottle figure).....	10
Figure 2-2. Concentration of PFAS detected in FT-based AFFF formulations (top figure), and corresponding detection frequency (bottle figure).....	12
Figure 2-3. Microbial transformation of primary and secondary ECF-based precursors derived from AFFF formulations.....	23
Figure 2-4. Microbial transformation of primary and secondary FT-based precursors derived from AFFF formulations.....	27
Figure 3-1. Changes in molar ratios of residual FOSA during aerobic biotransformation in Loring (Panel A) and Hudson (Panel B) soil microcosms.....	40
Figure 3-2. The formation of PFOS during FOSA aerobic biotransformation in Loring (Panel A) and Hudson (Panel B) soil microcosms.....	41
Figure 3-3. The relative abundance of microbial community composition at the phylum level in Loring (left) and Hudson (right) soil microcosms.....	46
Figure 4-1. Changes in molar ratios of residual 8:2 FTOH during biotransformation under nitrate-reducing conditions in the electron-donor (ED) treatment, natural attenuation (NA) treatment, abiotic controls, and positive controls microcosms (Panel A). Molar yields of 8:2 FTOH biotransformation products (squares: 8:2 FTCA, circles: 8:2 FTUA, up triangles: 7:2 sFTOH, down triangles: PFOA) in the ED (solid black lines and solid symbols) and NA treatments (dash red lines and open symbols) (Panel B). Panel C is a zoom view of B, showing the time course trends of PFOA molar yields.....	55
Figure 4-2. Changes in concentrations of targeted PFAS during 8:2 FTOH biotransformation under sulfate-reducing (Panels A and B), and iron-reducing conditions (Panels C and D). Panels A and C show 8:2 FTOH in the electron-donor (ED) treatment, natural attenuation (NA) treatment, abiotic control, and positive control. Panels B and D show the biotransformation products of 8:2 FTOH in ED and NA treatments.....	61
Figure 4-3. The relative abundance of microbial community composition at the phylum level (Panel A) and genus level (Panel B) in the initial Loring soil (Day 0), and in the nitrate-, sulfate-, and iron-reducing microcosms at the end of ca. 400 days incubation.....	64
Figure 4-4. Proposed comprehensive biotransformation pathways of 8:2 FTOH under various redox conditions. O ₂ , NO ₃ ⁻ , SO ₄ ²⁻ , Fe ³⁺ , and CO ₂ represent oxidic, nitrate-reducing, sulfate-reducing, iron-reducing, and methanogenic conditions, respectively.....	67
Figure 5-1. Changes in molar ratios of residual 6:2 FTS during aerobic biotransformation in Loring (Panel A) and Robins (Panel B) soil microcosms.....	76
Figure 5-2. Changes in concentrations of per- (Panels A and C) and polyfluorinated (Panels B and D) biotransformation products during 6:2 FTS aerobic biotransformation in Loring (Panels A and B) and Robins (Panels C and D) soil microcosms.....	78
Figure 5-3. Proposed aerobic biotransformation pathways of 6:2 FTS in AFFF-impacted soils. The compounds in the rectangular boxes were detected by LC-MS/MS analysis, and the	

compounds in the oval boxes were identified using non-targeted LC-HRMS analysis. The compounds in the brackets are proposed transformation products and were not detected in this study 85

Figure 6-1. Schematic of column experimental set-up 93

Figure 6-2. Time-course of 6:2 FTS concentration in the effluents from abiotic and biotic columns 95

Figure 6-3. Time-courses of the concentrations of biotransformation products during 6:2 FTS biotransformation in biotic columns 97

Figure 6-4. The average molar percent of 6:2 FTS and biotransformation products along the flowing path (i.e., Port 1, Port 2, Port 3, and Effluent, See Figure 6-1) in different phases..... 101

Figure B-1. Concentrations of dissolved organic carbon in Loring (Panel A) and Hudson (Panel B) soil microcosms.....145

Figure B-2. Principal coordinate analysis (PCoA) plot of phylogenetic microbial community changes among the treatments from Loring and Hudson soil microcosms, as described by weighted UniFrac distance matrices 146

Figure B-3. The relative abundance of microbial community composition at the genus level in Loring (left) and Hudson (right) soil microcosms. 147

Figure C-1. Concentrations of nitrate and organic acids in ED treatment/positive control (Panel A); concentrations of nitrate and total organic carbon (TOC) in NA treatment (Panel B); concentrations of nitrate and lactate in abiotic control (Panel C) 162

Figure C-2. Concentrations of sulfate and organic acids in ED treatment/positive control (Panel A); concentrations of sulfate and total organic carbon (TOC) in NA treatment (Panel B); concentrations of sulfate and lactate in abiotic control (Panel C) 163

Figure C-3. Concentrations of Fe(II) and organic acids in ED treatment/positive control (Panel A); concentrations of Fe(II) and total organic carbon (TOC) in NA treatment (Panel B); concentrations of Fe(II) and lactate in abiotic control (Panel C) 164

Figure C-4. Changes in molar ratio of residual 8:2 FTOH, and the fitting curves of single first-order kinetic models in ED and NA treatment under nitrate-reducing condition..... 165

Figure C-5. Changes in the concentrations (nanomole per gram soil/dry weight) of 7:3 acid, and C4-C9 PFCAs in ED, NA treatment, abiotic controls, and positive controls under nitrate-reducing condition throughout the experiments 166

Figure C-6. The total molar recoveries (8:2 FTOH and quantifiable biotransformation products) during 8:2 FTOH biotransformation in ED, NA treatment, and abiotic controls under nitrate-reducing conditions (Panel A), sulfate-reducing conditions (Panel B), iron-reducing conditions (Panel C) 167

Figure C-7. The MS2 spectra of potential biotransformation products identified in the ED and/or NA treatments under nitrate-, sulfate-, or iron-reducing conditions. Panel A, 7:3 U acid ($F(CF_2)_7CH=CHCOOH$, m/z 438.9822); Panel B, 3-OH-7:3 acid ($F(CF_2)_7CHOHCH_2COOH$, m/z 456.9930); Panel C, 3-F-7:3 acid ($F(CF_2)_7CFHCH_2COOH$, m/z 458.9885)..... 168

Figure C-8. The time trend of 7:3 U acid during 8:2 FTOH biotransformation in each treatment under (A) nitrate-reducing; (B) sulfate-reducing; and (C) iron-reducing conditions based on peak areas of extracted ion chromatograms	169
Figure C-9. The time trend of 3-OH-7:3 acid during 8:2 FTOH biotransformation in each treatment under (A) nitrate-reducing; (B) sulfate-reducing; and (C) iron-reducing conditions based on peak areas of extracted ion chromatograms.....	170
Figure C-10. The time trend of 7:3 U amide during 8:2 FTOH biotransformation in each treatment under (A) nitrate-reducing; (B) sulfate-reducing; and (C) iron-reducing conditions based on peak areas of extracted ion chromatograms.....	171
Figure C-11. The MS2 spectra of a novel biotransformation product identified as 1H-perfluoroheptane (m/z 368.9764). Panel A is the spectrum of samples collected from 8:2 FTOH nitrate-reducing microcosms. Panel B is the spectrum of 1 ppb 1H-perfluoroheptane standard	172
Figure C-12. The molar yields of 1H-perfluoroheptane during 8:2 FTOH biotransformation in each treatment under nitrate-reducing conditions, based on the GC-HRMS quantification results	173
Figure C-13. Changes in the concentrations (nanomole per gram soil/dry weight) of 7:3 acid, and C4-C9 PFCAs in ED, NA treatment, abiotic controls, and positive controls under sulfate-reducing condition throughout the experiments.	174
Figure C-14. Changes in the concentrations (nanomole per gram soil/dry weight) of 7:3 acid, and C4-C9 PFCAs in ED, NA treatment, abiotic controls, and positive controls under iron-reducing condition throughout the experiments.	175
Figure C-15. The time trend of 3-F-7:3 acid during 8:2 FTOH biotransformation in each treatment under (A) nitrate-reducing; (B) sulfate-reducing; and (C) iron-reducing conditions based on peak areas of extracted ion chromatograms.....	176
Figure C-16. Principal coordinate analysis (PCoA) plot of phylogenetic microbial community changes among the microcosms under different redox conditions, as described by weighted UniFrac distance matrices.....	177
Figure C-17. Compound Discoverer Workflow.	178
Figure D-1. Concentrations of dissolved organic carbon (DOC) in Loring (Panel A) and Robins (Panel B) soil microcosms	198
Figure D-2. Changes in sulfate concentrations during 6:2 FTS aerobic biotransformation in Loring (Panel A) and Robins (Panel B) soil microcosms.....	199
Figure D-3. Principal coordinate analysis (PCoA) plot of phylogenetic microbial community changes among the treatments from Loring or Robins soil microcosms, as described by weighted UniFrac distance matrices.....	200
Figure D-4. The relative abundance of microbial community composition at the phylum level in Loring (left) and Robins (right) soil microcosms	201
Figure D-5. The relative abundance of microbial community composition at the genus level in Loring (left) and Robins (right) soil microcosms	202

Figure D-6. The total molar recoveries (6:2 FTS and quantifiable biotransformation products) in live treatments and abiotic controls from Loring and Robins soil microcosms	203
Figure D-7. The time trends of 1H-perfluoropentane (C_5HF_{11} , m/z 268.98271) and 1H-perfluorobutane (C_4HF_9 , m/z 218.98587) during 6:2 FTS biotransformation in each treatment of Loring and Robins soil microcosms based on peak areas of extracted ion chromatograms.....	204
Figure D-8. The time trends of 1,2,2,3,3,4,4,4-Octafluorobutan-1-ol ($C_4H_2F_8O$, m/z 216.98912) and Perfluoropentanal (C_5HF_9O , m/z 246.9808) during 6:2 FTS biotransformation in each treatment of Loring and Robins soil microcosms based on peak areas of extracted ion chromatograms.....	205
Figure D-9. The time trends of $C_7H_2F_8$ (m/z 236.99543), $C_7H_3F_9$ (m/z 257.00159), and m/z 292.98316 during 6:2 FTS biotransformation in each treatment of Loring and Robins soil microcosms based on peak areas of extracted ion chromatograms	206
Figure D-10. MS ² spectra of 1H-perfluoropentane (C_5HF_{11} , m/z 268.98271) obtained from the analysis of microcosm sample (Panel A), and the analysis of 1 ppb reference standard (Panel B)	207
Figure D-11. MS ² spectra of 1H-perfluorobutane (C_4HF_9 , m/z 218.98587) obtained from the analysis of microcosm sample (Panel A), and the analysis of 1 ppb reference standard (Panel B)	208
Figure D-12. MS ² spectra of potential 6:2 FTS biotransformation products. Panel A, 1,2,2,3,3,4,4,4-octafluorobutan-1-ol ($C_4H_2F_8O$, m/z 216.98912); Panel B, $C_7H_2F_8$ (m/z 236.99543)	209
Figure D-13. Compound Discoverer Workflow	210
Figure E-1. Concentrations of dissolved organic carbon (DOC) in the effluent samples collected from abiotic and biotic columns	216

List of Abbreviations and Acronyms

16S rRNA	16S ribosomal ribonucleic acid
AFB	Air Force Base
AFFF	Aqueous film-forming foam
CEC	Cation exchange capacity
C _m	Median concentration
DF	Detection frequency
DGBE	Diethylene glycol butyl ether
DOC	Dissolved organic carbon
DT50	Half-life or time for 50% of a substance to disappear
ECF	Electrochemical fluorination
EtFASA	N-ethyl perfluoroalkane sulfonamide
FASA	Perfluoroalkane sulfonamide
FASAA	Perfluoroalkane sulfonamido acetic acid
FOSA	Perfluorooctane Sulfonamide
FT	Fluorotelomer
FTAB	Fluorotelomer sulfonamidoalkyl betaine
FTAL	Fluorotelomer aldehyde
FTB	Fluorotelomer betain
FTCA	Fluorotelomer saturated carboxylic acid
FTI	Fluorotelomer iodide
FTOH	Fluorotelomer alcohol
FTS	Fluorotelomer sulfonate
FtTAoS	Fluorotelomer thioether amido sulfonate
FTUA	Fluorotelomer unsaturated carboxylic acid
GC	Gas chromatography
HPLC	High-performance liquid chromatography
HRMS	High-resolution mass spectrometry
IC	Ion chromatography
LC-MS/MS	Liquid chromatography-tandem mass spectrometry
LOD	Limit of detection
LOQ	Limit of quantitation

MSDS	Material Safety Data Sheets
ORP	Oxidation-reduction potential
OTU	Operational Taxonomic Unit
PAP	Polyfluoroalkyl phosphate
PCR	Polymerase chain reaction
PFAA	Perfluoroalkyl acid
PFAI	Perfluoroalkyl iodide
PFAS	Per- and polyfluoroalkyl substances
PFBA	Perfluorobutanoic acid
PFBS	Perfluorobutanoic sulfonate
PFCA	perfluoroalkyl carboxylic acid
PFHpA	Perfluoroheptanoic acid
PFHpS	Perfluoroheptanoic sulfonate
PFHxA	Perfluorohexanoic acid
PFHxS	Perfluorohexanoic sulfonate
PFOA	Perfluorooctanoic acid
PFOS	Perfluorooctanoic sulfonate
PFOSI	Perfluorooctane sulfinate
PFPeA	Perfluoropentanoic acid
PFPeS	Perfluoropentanoic sulfonate
PFSA	Perfluoroalkane sulfonic acid
POSF	Perfluorooctane sulfonyl fluoride
PV	Pore volume
SHE	Standard hydrogen electrode
TOC	Total organic carbon

Chapter 1 : Introduction

1.1 Background

Per- and polyfluoroalkyl substances (PFAS, $C_nF_{2n+1}R$) refer to a family of thousands of man-made chemicals that include a perfluoroalkyl moiety ($C_nF_{2n+1}^-$) of varying carbon chain length.¹ PFAS have been mass-produced starting from 1950s for a wide variety of industrial and consumer products (e.g., textiles, apparel, carpet, paints, adhesives, food packaging, firefighting foams) owing to their unique properties such as chemical and thermal stability, water- and oil-repellency, and surface tension reduction.¹ As a result, PFAS have been widely detected in the global environment.²⁻⁵ Further, the concerns over the impacts of these compounds on the environmental and human health are growing due to their persistence, bioaccumulation potential, and toxicity.^{1,6,7}

Aqueous film-forming foams (AFFFs) are water-based chemical mixtures containing solvents, hydrocarbon- and fluorocarbon-based surfactants.^{8,9} Since the 1960s, AFFFs have been used to extinguish hydrocarbon-fuel fires at civil airports, oil refineries, and military bases during the emergency response and regular training exercise.^{10,11} AFFFs contain various PFAS classes which are the primary fire-extinguishing components, as well as the vapor sealants that prevent the re-ignition of fuel and solvents.⁹ Those PFAS include perfluoroalkyl acids (PFAAs) such as perfluoroalkyl carboxylates (PFCAs) and perfluoroalkyl sulfonates (PFSAs), as well as a wide variety of polyfluoroalkyl substances (referred hereafter to as “precursors”).¹²⁻¹⁵ The repeated application of AFFFs at fire training areas have resulted in particularly heavy PFAS contamination at AFFF-impacted sites, and in the adjacent surface water, groundwater, soil, sediment, and biota.^{4,16-18} Recent studies identified the large variations between the PFAS compositions in AFFF formulations and those detected in the AFFF-impacted environmental matrices.^{13,14} In particular, precursors that were dominant in AFFF formulations were either not detected or sporadically detected at a low abundance in AFFF-impacted environment.^{13,14} Also, the increase in the relative mass of PFAAs was observed.^{13,14} These findings indicate that the biotic or abiotic transformation, or other environmental processes (e.g., sorption, photodegradation) occur to the precursors after release into the environment. Understanding the environmental fate and behavior of these precursors, including their susceptibility to microbial transformation under conditions representative of natural environments, can provide crucial knowledge for the management and remediation of hundreds of AFFF-impacted sites.

1.2 Motivation for this research

Precursors can be categorized into electrochemical fluorination (ECF)-based and fluorotelomer (FT)-based precursors based on the manufacturing process.⁹ Biotransformation of these precursors has been increasingly investigated in the last decades.^{19–22} Compared to ECF-based ones, the biotransformation of FT-based precursors was more widely studied.^{19–22} Those biotransformation studies were mostly conducted in the laboratory microcosms under oxic conditions, utilizing microorganisms from activated sludge,^{23,24} river sediments,²⁵ aerobic bacterial enrichments,^{26,27} constructed wetlands,²⁸ landfill leachate,^{29,30} and surface soils.^{31–34} It was demonstrated that the aerobic biotransformation rate and/or pathways of one precursor often differ between experimental systems established with different environmental matrices. For example, the half-life of one FT-based precursor, 6:2 fluorotelomer sulfonate (6:2 FTS) was less than 5 days in the river sediment, but was ca. 86 days in landfill leachate sediment and 2 years in activated sludge.^{24,25,29} Another example is perfluorooctane sulfonamide (FOSA, an ECF-based precursor), which was reported with a half-life of 9.2 days in activated sludge,³⁵ whereas its half-life was predicted as 712 days in an aerobic soil.³⁶ These results indicate that microbial communities in various environmental matrices could influence the biotransformation of precursors, further complicating assessments of their behaviors in the environment.

Limited information is available on the biotransformation of precursors under anoxic conditions including nitrate-reducing,²⁸ sulfate-reducing,^{25,37} and methanogenic conditions.^{38–40} Those studies demonstrated that the biotransformation of precursors under anoxic conditions was always different from that under oxic conditions. For example, half-lives of *n*:2 fluorotelomer alcohol (FTOH, *n*=6, 8) were reported to be 30-145 days under methanogenic conditions,⁴¹ whereas the half-lives of less than 7 days were observed in various environmental matrices under oxic conditions.^{23,26,27,29,42–50} The formation of PFAAs was also at least 20-fold less under methanogenic conditions than oxic conditions.⁴¹ In addition, biotransformation of 6:2 FTS occurred under oxic^{24,51} and nitrate-reducing conditions,⁵² with the most rapid biotransformation rate in aerobic sediment;²⁵ however, biotransformation did not occur under sulfate-reducing²⁵ and methanogenic⁴⁰ conditions. These findings suggest that redox condition plays an important role in the biotransformation of precursors.

To date, only a few studies investigated the biotransformation of precursors using the native microorganisms present at AFFF-impacted sites.^{31,37,53} Compared to the pristine environment, microbial communities at AFFF-impacted sites may have evolved to be more tolerant to PFAS and more capable of PFAS biotransformation due to the historical exposure. Moreover, other environmental factors such as redox condition, pH, ionic strength, reactive mineral species, as well as co-contaminants (e.g., chlorinated solvents) typically present at AFFF-impacted sites might influence the biotransformation behavior of precursors. Therefore, the overall goal of this research is to study the biotransformation of precursors by native microbial communities under conditions representative of AFFF-impacted sites. An ECF-based precursor (i.e., FOSA), and two FT-based precursors (i.e., 8:2 FTOH and 6:2 FTS) were selected as the primary parent compounds of interest, given their widespread occurrences in AFFF-impacted environments.^{13,14,54-58} The aerobic and/or anaerobic biotransformation of FOSA, 8:2 FTOH and 6:2 FTS were investigated in the soil microcosms constructed with AFFF-impacted soils. In addition, to fill a key knowledge gap on biotransformation of PFAS in natural porous media under dynamic flow conditions, the fate and transformation of 6:2 FTS was also investigated in one-dimensional column experiments.

1.3 Objectives

The specific objectives will be addressed to accomplish the overall goal of this research:

1. Identify the key knowledge gaps on microbial transformation of precursors by conducting a thorough literature review (Chapter 2).
2. Assess the biotransformation of FOSA in two soil microcosms constructed with a pristine soil and an AFFF-impacted soil, respectively (Chapter 3).
3. Investigate the biotransformation of 8:2 FTOH in AFFF-impacted soil under nitrate-, sulfate-, and iron-reducing conditions (Chapter 4).
4. Evaluate the biotransformation of 6:2 FTS in soils collected from two AFFF-impacted sites (Chapter 5).
5. Investigate the biotransformation of 6:2 FTS in AFFF-impacted soil under continuous flow conditions (Chapter 6).

1.4 Dissertation organization

The dissertation is organized into seven chapters, as described below.

In Chapter 1 (current chapter), the research background and motivation are provided. Accordingly, the overall goal and specific objectives of this research are outlined.

In Chapter 2, a literature review is presented regarding PFAS detections in AFFF formulations and AFFF-contaminated environment, as well as impact of microbial transformation on the environment fate of AFFF-derived PFAS. Specifically, the concentrations of PFAS reported to date in various AFFF formulations and AFFF-impacted environmental matrices were summarized. The shift of PFAS composition in AFFF formulations to that in AFFF-impacted environmental matrices was then noted. Further, the microbial transformation processes affecting the occurrence and fate of PFAS in AFFF-impacted sites was delineated. Last, key research gaps and future research needs were identified.

In Chapter 3, aerobic biotransformation kinetics and product formation of FOSA were examined in the two soil microcosms over a 308-day incubation period. Two distinct soils, in terms of soil properties and contamination history (i.e., one pristine and one AFFF-contaminated soil), were used for the assessment of FOSA biotransformation. The interactive influence of FOSA and transformation products on the soil microbial community structure was also investigated. Further, the microbial species that are more tolerant to FOSA and transformation products, and might be the potential FOSA degraders were identified.

In Chapter 4, the biotransformation of 8:2 FTOH was, for the first time, investigated under nitrate-, sulfate-, and iron-reducing conditions in laboratory microcosm reactors. The molar yields of known 8:2 FTOH biotransformation products were determined in the soil microcosms (constructed using an AFFF-impacted soil) under each redox condition. High-resolution mass spectrometry (HRMS) was employed to identify potential unknown transformation products. Based on the findings in the study and results from previous investigations, comprehensive biotransformation pathways for 8:2 FTOH under various redox conditions representative of natural environments were presented.

In Chapter 5, the biotransformation of 6:2 FTS in the soils collected two AFFF-impacted sites were investigated under oxic conditions. Biotransformation rates and product formation in two sets of microcosms were examined over a 224-day incubation period. HRMS was also employed to identify previously undocumented transformation products. By comparing the results observed

in the two AFFF-impacted soils, environmental factors (e.g., sulfur source, microbial community composition) that impact 6:2 FTS biotransformation were identified.

In Chapter 6, the fate and transformation of 6:2 FTS in AFFF-impacted soil was, for the first time, investigated in one-dimensional column experiments. Incorporation of water flowing into experimental systems represents more closely the realistic scenario. Two different seepage velocities were used in column experiments to evaluate the effects of hydraulic residence time in porous media on 6:2 FTS biotransformation. In addition, flow interruptions were performed to assess if the biotransformation is rate-limited under the experimental column conditions. Last, 6:2 FTS biotransformation behaviors in the column experiments were compared to those in microcosm experiments (Chapter 5), to better understand the effects of dynamic flowing conditions on the environmental fate of 6:2 FTS.

In Chapter 7, the major findings of the present study, and the environmental implications for the fate and transformation of ECF- and FT-based precursors in AFFF-impacted sites are summarized. In addition, the recommendations of future research are provided.

Chapter 2 : Literature review on per- and polyfluoroalkyl substances in aqueous film-forming foams (AFFFs) and AFFF-impacted environment

2.1 Introduction

Aqueous film-forming foams (AFFFs) are complex proprietary mixtures containing solvents, hydrocarbon- and fluorocarbon-based surfactants, which, when combined, render AFFFs the characteristics required for their applications.^{8,9} Since the 1960s, AFFFs have been used to extinguish hydrocarbon-fuel fires during the emergency response and regular training exercise at civil airports and military bases.^{10,11} Fluorinated surfactants in AFFFs are made up of per- and polyfluoroalkyl substances (PFAS), which exhibit both hydrophobic and oleophobic characteristics, and serve as the primary fire-extinguishing components and as the vapor sealants that prevent the fuel and solvents from re-igniting.⁹

PFAS ($C_nF_{2n+1}-R$) refer to a family of thousands of anthropogenic chemicals that contain a perfluoroalkyl moiety ($C_nF_{2n+1}-$) of varying carbon chain length.¹ Due to the high electronegativity of fluorine, and the overlap between the 2s, 2p orbitals of fluorine and the corresponding orbitals of carbon, the carbon-fluorine bond is highly polarized as one of the strongest single bonds in chemistry.⁸ The fluorination also typically strengthens the adjacent carbon-carbon bonds.⁸ As a result, PFAS molecules are imparted with unique properties (e.g., chemical and thermal stability, hydrophobicity, and lipophobicity), and thus have been mass-produced starting from 1940s for a wide variety of industrial and consumer applications (e.g., textiles, packaging, AFFFs).¹ However, PFAS have recently attracted global attentions among the public and scientific communities due to their widespread occurrence in the environment, and their persistence, bioaccumulation potential, and toxicity to humans.¹ Accordingly, PFAS compounds are increasingly regulated by the US Environmental Protection Agency (EPA) and other U.S. state agencies. In 2009, US EPA published provisional health advisory levels for two primary PFAS compounds, perfluorooctanoic acid (PFOA) and perfluorooctanoic sulfonate (PFOS) in drinking water.⁵⁹ Those lifetime health advisories for PFOA and PFOS concentrations (individually or combined) in drinking water were subsequently revised to 70 ng/L by EPA in 2016.^{60,61} Since then, several U.S. states have published even more stringent limits for PFOA, PFOS, as well as other PFAS (e.g., perfluorobutane sulfonate-PFBS, perfluorohexane sulfonate-PFHxS) for drinking

water.⁶² On June, 2022, EPA again issued interim updated life health advisories for PFOA and PFOS, which were steeply lowered to 0.004 ng/L and 0.02 ng/L, respectively.^{63,64}

Two principal processes have been used in the manufacturing of PFAS: electrochemical fluorination (ECF) and telomerization (TM).⁹ With ECF, an organic raw material (e.g., octane sulfonyl fluoride ($C_8H_{17}SO_2F$), octane fluoride ($C_7H_{15}COF$)) undergoes electrolysis in anhydrous hydrofluoric acid, resulting in the replacement of all hydrogen atoms by fluorine atoms.^{9,65} A mixture of even- and odd-numbered, cyclic, branched as well as linear perfluoroalkyl chains is then generated due to the carbon chain rearrangement and breakage resulting from the free-radical nature of ECF process.^{9,65} The ECF of $C_8H_{17}SO_2F$ and $C_7H_{15}COF$ yields the perfluorooctane sulfonyl fluoride ($C_8F_{17}SO_2F$, POSF) and perfluorooctanoyl fluoride ($C_7F_{15}COF$), respectively, which are further reacted to manufacture PFOS and PFOA, as well as the perfluoroalkane sulfonamide ($F(CF_2)_n-S(O)_2NH-$) and amide derivatives ($F(CF_2)_n-C(O)NH-$), respectively. TM process reacts a perfluoroalkyl iodide (PFAI, referred to as the “telogen”; perfluoroethyl iodide (C_2F_5I) is the most common telogen) with tetrafluoroethylene ($CF_2=CF_2$) (referred to as the “taxogen”) to yield a mixture of PFAIs with longer perfluoroalkyl chains. As opposed to ECF process, TM process typically yields even-numbered, linear perfluorinated carbon chains.⁹ The mixture of PFAIs often reacts further with ethylene ($CH_2=CH_2$) to form $n:2$ fluorotelomer iodides ($n:2$ FTIs, n of perfluorinated carbons followed by 2 of aliphatic hydrocarbons), which, along with PFAIs, are the raw material intermediates for the manufacture of additional building blocks (e.g., fluorotelomer alcohols, FTOHs) that are further used to produce numerous fluorotelomer-based surfactants and polymer products.¹

Broadly speaking, AFFFs can be categorized as ECF- or fluorotelomer (FT)-based AFFFs according to the manufacture process for the PFAS contained. Prior to 2002, the AFFF formulations manufactured by 3M predominantly contained ECF-based PFAS, including perfluoroalkyl sulfonates (PFSAs) and other polyfluoroalkyl substances (the so-called “precursors”).¹² Due to the rising concerns about PFSAs (e.g., PFOS) and the associated precursors,⁹ the manufacture of such ECF-based AFFFs was voluntarily discontinued by 3M in 2002, which accordingly resulted in the proliferation of FT-based AFFFs containing $n:2$ fluorotelomers ($n=4, 6, 8$).¹² In the last decades, an increasing number of studies are published regarding the environmental occurrence and fate of PFAS in AFFF-impacted sites.^{4,13,14,58,66,67} The composition of PFAS in historical and contemporary AFFF formulations has also been

increasingly investigated.^{12,13,15,68,69} Moreover, growing efforts are being made to investigate the microbial transformation of AFFF-derived PFAS upon the release into environment.^{19,31–34} Recent reviews have addressed the occurrence, fate, and transport of PFAS in landfills,⁷⁰ soil,¹⁶ groundwater,³ vadose zone,⁷¹ and subsurface environment.² In addition, the laboratory studies on biotransformation of PFAS in various environmental matrices have been reviewed lately.^{19,22,72} However, few reviews have exclusively focused on the PFAS detections in AFFF formulations and in associated AFFF-contaminated environment, as well as the impact of microbial transformation on the environment fate of AFFF-derived PFAS.²⁰

Thus, the aims of the present study are, (1) to overview the concentrations of PFAS reported to-date in ECF- and FT-based AFFF formulations, (2) to summarize the occurrence of PFAS in various environmental matrices (i.e., groundwater, surface water, surface soil, subsurface soil, and sediment) with known contamination by use of AFFFs, (3) to identify the shift of PFAS composition in AFFF formulations to that in AFFF-impacted environmental matrices, (4) to delineate the microbial transformation affecting the occurrence and fate of PFAS in AFFF-impacted sites, (5) to identify the research gaps and future research needs.

2.2 PFAS concentrations in AFFF formulations

Although the Material Safety Data Sheets (MSDS) and patent pertaining to the AFFFs typically list that fluorinated surfactants are contained in the formulations, the exact elemental composition of these chemicals is proprietary.⁸ The only exception is the presence of PFSA salts, as indicated in the MSDS for 3M's AFFFs (e.g., Light Water).⁷³ Over the last decades, continuous efforts have been made by researchers to identify and quantify the PFAS compounds included in the AFFFs used around the world, while the lack of commercially available standards for most identified PFAS restrained quantitative detection using targeted analysis (e.g., liquid- chromatography tandem mass spectroscopy (LC-MS/MS)).

In this section, the quantitative detections of PFAS in a total of 42 ECF-based^{13,14,69,74–77} and 88 FT-based AFFFs^{13,14,56,69,74,75,77,78} that reported in previous studies are analyzed (Figures 2-1 and 2-2). It should be noted that some of ECF-based AFFFs were repeatedly analyzed in a few studies, namely, less than 42 of AFFF formulations is expected.^{13,14,76} In addition, the concentrations of analytes (AmPr-FASA and AmPr-FASA-PrA in ECF-based AFFFs; *n*:2 FtTAoS, *n*:2 FTAB, *n*:2 FtSaAm, *n*:2 FtTHN, *n*:2 H-FTB, and *n*:3 FTB in FT-based AFFFs; See Appendix A Table A-1

for the PFAS class acronym, name, and structure) reported in two studies were not generated based on the calibration curves of analytical standards that were not available.^{13,14} Instead, the concentration was estimated by either using a reference material, or assuming equal molar response to a related analyte of which the standard was available. The reader is referred to the original publications for a detailed explanation.^{13,14} Last, although hundreds of novel and infrequently reported PFAS were identified recently in various AFFF formulations by employing non-targeted high-resolution mass spectrometry (HRMS),^{15,68,69} no associated quantitative data was available, and most of them are very likely the impurities that are in the forms of synthetic intermediates, side products, and/or degradation products. Therefore, those PFAS compounds are not focused in the present study.

2.2.1 PFAS concentrations in ECF-based AFFF formulations

As shown in Figure 2-1, PFOS was reported at highest levels than any other PFAS in ECF-based AFFFs, with the median concentration (C_m) of 4,900 mg/L and detection frequency (DF) of 100%. Among PFAAs, much greater quantities of PFSAs were present relative to PFCAs; PFHxS had a C_m of 600 mg/L (DF=94.6%) and other PFSAs ($n = 3, 4, 5, 7$) had a C_m of 120-200 mg/L, while the highest C_m for PFCAs was 100 mg/L (PFHxA). The results are to be expected, as PFOS and related PFSAs such as PFHxS represent significant components in the historic 3M ECF-based AFFF formulations.^{12,13} In addition to the commonly investigated PFAAs ($n = 4-8$ PFSAs and $n = 3-7$ PFCAs), the ultra-short-chain PFSAs ($n = 2-3$), and the ultra-long-chain PFSAs ($n = 9-10$) and PFCAs ($n = 8-12$) were also detected in some of the ECF-based AFFFs (Figure 2-1). In particular, two ultra-short-chain PFSAs ($n = 2-3$) were both detected by one study, in all tested five AFFFs (DF=100%) with the concentrations of 7-13 mg/L ($n = 2$) and 120-270 mg/L ($n = 3$), respectively.⁷⁶ More quantification of the two PFSAs is needed for a better understanding of their presence in ECF-based AFFFs. For the ultra-long-chain PFAAs, PFSAs ($n = 9-10$) had a relatively higher abundance ($C_m = 20.1-28.5$ mg/L) than PFCAs ($n = 8-12$) ($C_m = 0.1-4.1$ mg/L), and all of those are likely not the intended component of AFFF formulations.

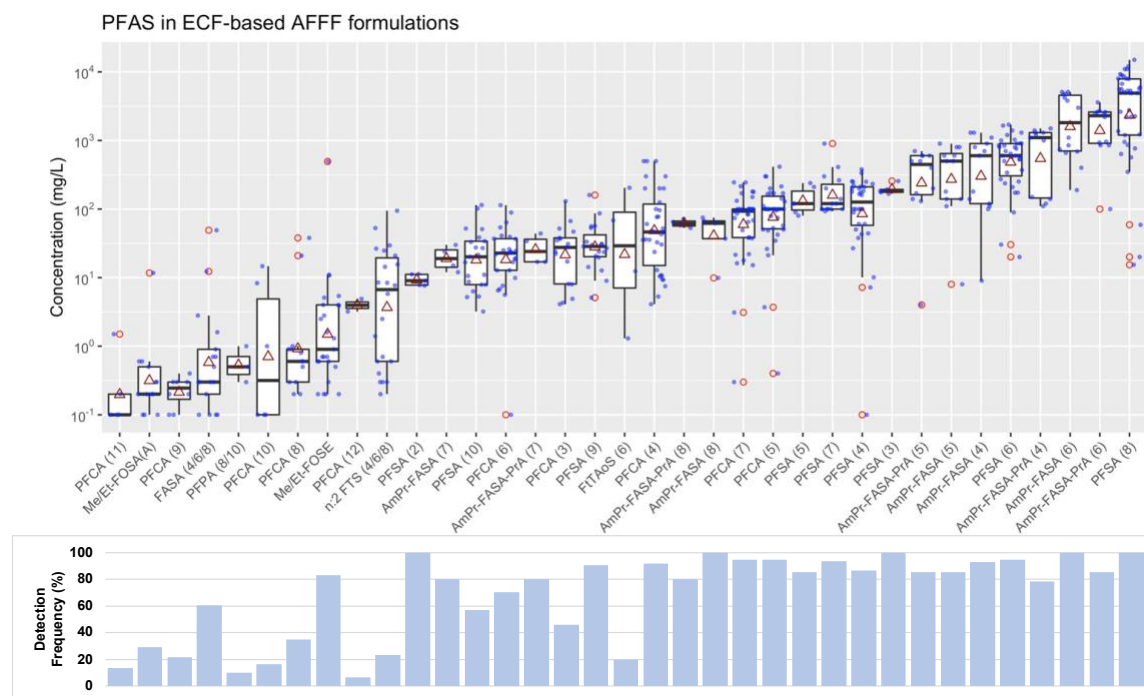


Figure 2-1. Concentration of PFAS detected in ECF-based AFFF formulations (top figure), and corresponding detection frequency (bottom figure). The box plots represent the minimum, 1st quartile, median, 3rd quartile and maximum values. Dark red triangle and red circle represent mean value and outlier, respectively. The number in the parenthesis of PFAS acronym represents the number of perfluorinated carbon in the compound. Boxplots are sorted out in ascending order of median concentration.

Compared to PFAAs, limited data are available on the concentrations of ECF-based precursors in AFFF formulations, mainly because of the unavailability of the analytical standards. In two prior studies, the concentrations of two classes of precursors: AmPr-FASA ($n = 4-8$) and AmPr-FASA-PrA ($n = 4-8$) were estimated.^{13,14} It was shown that these classes of PFAS were in a great abundance in the ECF-based AFFF formulations. Except PFOS and PFHxS, they were the most predominant PFAS species, with C_m ranging from 450 mg/L to 2,300 mg/L (Figure 2-1). Within the two classes, C6 is the most abundant homologue in AFFFs (Figure 2-1). AmPr-FASA ($n = 6$) and AmPr-FASA-PrA ($n = 6$) had the C_m of 2,050-2,300 mg/L, more than 3-fold greater than that of PFHxS ($C_m = 600$ mg/L).

2.2.2 PFAS concentrations in FT-based AFFF formulations

Unlike the ECF-based AFFF formulations that were almost exclusively manufactured by 3M, FT-based AFFF formulations were created by several manufacturers since 1970s such as Ansul,

National Foam, Angus, Chemguard, Buckeye.¹² As reported previously, the primary PFAS species (i.e., FT-based precursor) varied by the manufacturer.¹²⁻¹⁴ For example, *n*:2 FtTAoS were demonstrated to represent the significant PFAS mass in the AFFF formulations manufactured by Ansul, Angus and Chemguard.¹²⁻¹⁴ In contrast, *n*:2 FTAB and *n*:2 FtSaAm were the main PFAS detected in the AFFF formulations manufactured by National Foam and Fire Service Plus.¹²⁻¹⁴ Two other classes of FT-based precursors, *n*:2 H-FTB and *n*:3 FTB, were only detected in Buckeye AFFF formulations.¹²⁻¹⁴ Since different classes of FT-based precursors predominated in various FT-based AFFF formulations, the DFs of those precursors were generally lower (<70%), compared to the PFSAs and associated precursors in ECF-based AFFF formulations (Figures 2-1 and 2-2). C6 homologue was typically the dominant species in each class of FT-based precursors present in the AFFFs (Figure 2-2). Among the aforementioned FT-based precursors in different manufacturers' AFFFs, 6:2 FtTAoS and 6:2 FTAB were reported with the greatest number of detections (>10 concentrations), as well as the highest C_m of 3,188-7,100 mg/L (Figure 2-2).

Although it was not reported as a major component,¹²⁻¹⁴ 6:2 FTS has been widely detected in FT-based AFFF formulations, with the highest number of detections (63), DF (71.6%), and C_m (53.7 mg/L) (Figure 2-2). Potential transformation of the main ingredient of AFFF (e.g., 6:2 FtTAoS, 6:2 FTAB) during the AFFF storage might result in the formation of 6:2 FTS (discussed in Section 5).^{31,79,80} Similarly, the detection of some other PFAS such as *n*:2 FTCA, *n*:2 FTOH, PFCAs at low levels in FT-based AFFF formulations might be due to the potential further transformation of 6:2 FTS (discussed in Section 5).^{25,31,75} Also, *n*:2 FTOH, PFCAs, and PFSAs could be present in FT-based AFFF formulations as impurities (e.g., synthetic intermediates, side products) during the manufacturing process. Overall, the abundance of *n*:2 FTCA, *n*:2 FTOH, PFCAs, and PFSAs was very low; for example, the highest C_m for all PFAAs reported was 1.6 mg/L (PFPeA) (Figure 2-2).

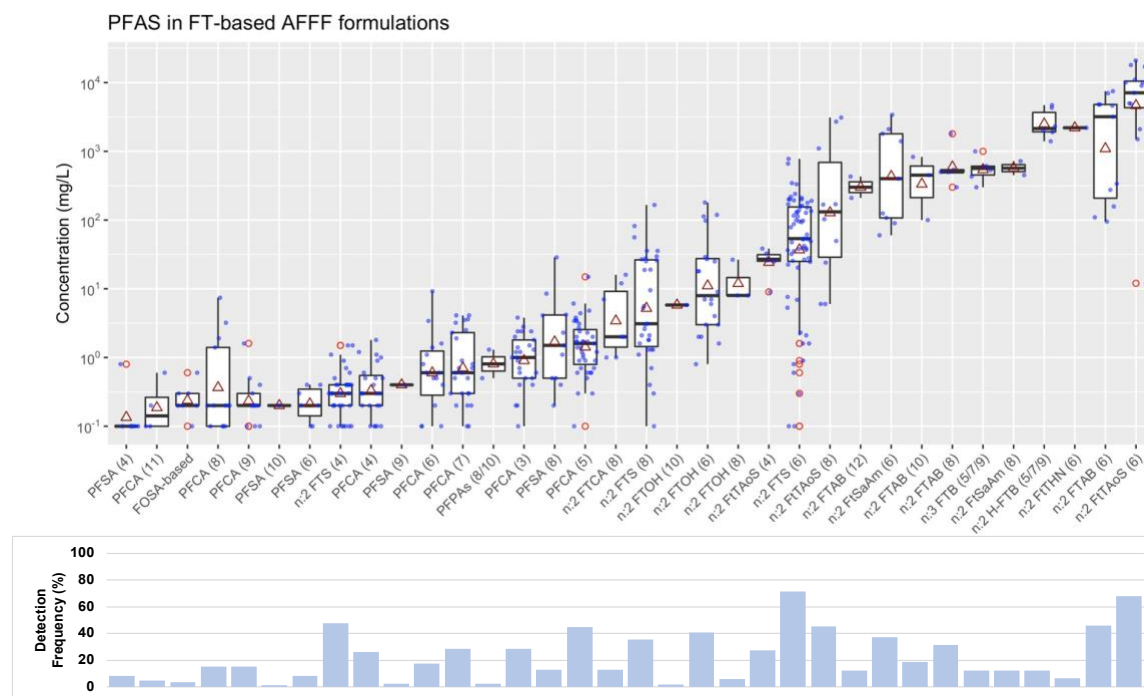


Figure 2-2. Concentration of PFAS detected in FT-based AFFF formulations (top figure), and corresponding detection frequency (bottom figure). The box plots represent the minimum, 1st quartile, median, 3rd quartile and maximum values. Dark red triangle and red circle represent mean value and outlier, respectively. The number in the parenthesis of PFAS acronym represents the number of perfluorinated carbon in the compound. Boxplots are sorted out in ascending order of median concentration.

2.3 The occurrence of PFAS in the environment impacted by AFFFs

The use of ECF- and FT-based AFFFs has resulted in the widespread occurrence of PFAS in the adjacent surface water, groundwater, soil, sediment, and biota.^{4,16–18} In this section, PFAS concentrations reported previously in the AFFF-impacted sites are aggregated as a function of environmental matrices (i.e., surface water, groundwater, surface soil, subsurface soil and sediment). The compiled data is critical towards understanding the fate and transport of PFAS upon the release by AFFF application. In general, most of the reported concentrations were for the anionic PFAS, including PFCAs, PFSAs, and commonly investigated polyfluorinated compounds such as *n*:2 FTS, FHxSA, FOSA. Although cationic and zwitterionic PFAS (e.g., AmPr-FASA, TAmPr-FASA, AmPr-FASA-PrA, *n*:2 FtTAoS) have been increasingly detected in the environmental matrices impacted by AFFFs, the associated concentration data is scarce possibly because the unavailability of the authentic standards limited the quantification.^{13,57,58,81} Therefore,

those polyfluorinated compounds that were reported previously with less than 10 concentrations available are not included in the present analysis.

2.3.1 PFAS concentrations in AFFF-impacted groundwater

The first definitive identification of PFAS (i.e., C6-C8 PFCAs) in groundwater impacted by AFFF application was reported by Moody and Field in 1999.¹⁰ The research group later demonstrated the presence of PFSAs (i.e., PFHxS and PFOS) in AFFF-impacted groundwater.⁸² Since then, especially after 2010s, PFAS compounds have been widely detected in AFFF-impacted groundwater around the globe. In the present section, the PFAS concentrations of 383 AFFF-impacted groundwater samples that were reported in 16 peer-reviewed articles were analyzed.^{10,13,14,55,56,58,76,78,82-89} The summary statistics of the reported PFAS concentrations are shown in Table 2-1.

Based on the number of detections (~290) and DFs (>80%), PFHxS and PFOS were the predominant PFAS reported in the AFFF-impacted groundwater (Table 2-1). This is to be expected given that the two PFAS are the main ingredients of ECF-based AFFFs which were widely used. The maximum reported concentrations for PFHxS and PFOS reached to over 1,000,000 ng/L (Table 2-1). Out of all reported detections, the mean and median values for both PFAS were more than 55,000 ng/L and 1,000 ng/L, respectively (Table 2-1). Although less attentions have been paid (i.e., less detection attempts), PFPrS and PFPeS surprisingly had the highest DFs (86.5-93.3%), with the mean and median values of over 25,000 ng/L and 7,000 ng/L, respectively (Table 2-1). Such high DFs and detected concentrations, along with the potentially high solubility and mobility, suggest that these short-chain PFSAs need to be more often monitored in groundwater impacted by AFFFs.

Table 2-1. Summary statistics of the concentration of selected PFAS previously reported in the groundwater samples (n=383) collected from AFFF-impacted sites. C3-C13 PFCAs, C2-C10 PFASs, and polyfluorinated compounds that were prevalently detected are included in the table. Other polyfluorinated compounds such as newly identified precursors in AFFF formulations (e.g., AmPr-FASAs) with <10 concentrations reported are not included.

PFAS	Detection Frequency	Concentration range (ng/L)	Mean (ng/L)	Median (ng/L)
PFPrA	3/9 (33.3%)	400-18,000	10,467	13,000
PFBA	160/309 (51.8%)	0.82-87,000	8,009	656
PFPeA	194/312 (62.2%)	0.11-300,000	15,802	517
PFHxA	245/346 (70.8%)	0.13-480,000	27,772	440
PFHpA	213/320 (66.6%)	0.12-149,000	5,679	205
PFOA	243/346 (70.2%)	0.11-6,570,000	76,867	568
PFNA	121/312 (38.8%)	0.14-66,700	1,505	110
PFDA	60/312 (19.2%)	0.16-143,040	2,817	18
PFUnA	49/266 (18.4%)	3-534	40	17
PFDoA	17/245 (6.9%)	0.52-36	13	14
PFTTrA	5/97 (5.2%)	2.21-14.4	6	4
PFEtS	8/11 (72.7%)	11-7500	1,716	375
PFPrS	32/37 (86.5%)	19-176,000	25,919	10,800
PFBS	199/331 (60.1%)	0.39-210,000	16,634	430
PFPeS	42/45 (93.3%)	49-220,000	31,893	7,200
PFHxS	290/357 (81.2%)	0.14-1,300,000	55,777	1,062
PFHpS	88/134 (65.7%)	0.26-32,000	4,312	1,550
PFOS	289/357 (81.0%)	0.11-4,600,000	70,265	2,048
PFNS	24/49 (49.0%)	7-20,000	2,966	445
PFDS	40/301 (13.3%)	1.22-1,700	53	9
4:2 FTS	28/115 (24.3%)	5.2-12,000	3,196	835
6:2 FTS	187/328 (57.0%)	0.15-14,600,000	183,787	2,700
8:2 FTS	105/325 (32.3%)	0.11-98,000	3,649	628
FHxSA	62/88 (70.5%)	28-1,520,000	98,439	11,000
FOSA	37/251 (14.7%)	1-22,000	2,442	119
6:2 FTAB	10/79 (12.7%)	45-91,000	10,216	291

C4-C8 PFCAs were also prevalently detected in AFFF-impacted groundwater samples, with a DF of more than 50%. The detected concentrations were relatively lower than PFSAs, with C_m for C4-C8 PFCAs ranging from 200-700 ng/L (Table 2-1). However, it is worthy to mention that PFOA was measured at surprisingly high concentrations in 3 groundwater samples (i.e., 2,400,000 ng/L, 4,800,000 ng/L, and 6,570,000 ng/L) considering PFOA is not a main component of either ECF- or FT-based AFFFs. In addition to PFAAs, *n*:2 FTS, FHxSA, FOSA, and 6:2 FTAB were often detected in groundwater among the polyfluorinated compounds. FHxSA and 6:2 FTS had the highest DFs (57.0-70.5%) and highest reported concentrations with C_m of 2,700-11,000 ng/L (Table 2-1). Even with relatively lower DFs (12.7-32.3%), other potential PFAA precursors (i.e., 4:2 FTS, 8:2 FTS, FOSA, and 6:2 FTAB) could also exist at a high abundance in the groundwater, with mean and median values of greater than 2,000 ng/L and 100 ng/L, respectively (Table 2-1).

In a recent review on the concentration of PFAS in global groundwater systems, PFBS, PFHxS, PFOS, PFBA, PFOA, and PFNA were frequently detected, with the mean concentrations of 0.4-11,016 ng/L, 0-355 ng/L, 0-413 ng/L, 0.2-1544 ng/L, 0.5-1,422 ng/L, and 0.1-4.7 ng/L, respectively.³ These mean values are substantially lower than that summarized from AFFF-impacted groundwater samples in this study. For example, the mean concentrations of PFHxS, PFOS, and PFOA are 55,777 ng/L, 70,265 ng/L, and 76,867 ng/L, respectively (Table 2-1). The results indicate that compared to other sources of PFAS (e.g., industrial facility, wastewater), AFFF application could be a predominant source contributing to the PFAS occurrence in groundwater.

2.3.2 PFAS concentrations in AFFF-impacted surface water

The contamination of PFAS in AFFF-impacted surface water was first demonstrated for PFHxS, PFOS and PFOA by Moody et al.⁹⁰ In the study, a total of 54 surface water samples were collected following a discharge of 22,000-liter of AFFF formulations into the water body over a 153-day sampling period. A combined concentration ranging from <17-2,260,000 ng/L for PFHxS and PFOS, and <9-11,300 ng/L PFOA were detected in those surface water samples.⁹⁰ The highest concentrations reported for PFHxS (134,000 ng/L), PFOS (2,210,000 ng/L) and PFOA (11,300 ng/L) in that study remained as the highest values for the three PFAS compounds, although another 150 of AFFF-impacted surface water samples were analyzed since 2011 (Table A-2).

In general, PFAS concentrations in surface water impacted by AFFFs were much lower than that in groundwater. For instance, the C_m for C4-C8 PFCAs in surface water were 10-32 ng/L, more than one order of magnitude lower than those in groundwater (205-656 ng/L) (Table 2-1 and A-2). Similarly, C4-C8 PFSAAs had C_m of 430-7,200 ng/L in groundwater, which were much higher than 13-140 ng/L in surface water (PFPeS is not included due to limited detections). Among the PFAAs, PFHxS and PFOS are still predominant in the surface water, with a DF of 73.5-84.3% and C_m of 46-140 ng/L (Table A-2). However, PFCAs were more frequently detected in surface water relative to the groundwater; for example, the DFs for C4-C9 PFCAs were 60.6-88.2% and 38.8-70.8% in surface water and groundwater, respectively (Table 2-1 and A-2).

Similar to PFAAs, concentration of the precursors detected in surface water was also substantially lower than that in groundwater (Table A-2). The C_m for 4:2 FTS, 6:2 FTS, 8:2 FTS, and FOSA (5, 28, 22, 1.8 ng/L, respectively) in surface water were nearly two orders of magnitude lower than those in groundwater (835, 2,700, 628, 119 ng/L, respectively). However, there is an exception, 6:2 FTAB, which had a DF of 68.8% and C_m of 426 ng/L (Table A-2). Both DF and C_m were higher than that in groundwater (12.7% and 291 ng/L). In a previous study, high abundance of 6:2 FTAB (59-17,874 ng/L) was detected in 11 out of 16 surface water samples contaminated by AFFFs.⁵⁶ By far, although only a small number of detections/measurements for 6:2 FTAB have been reported, it is clearly shown that AFFF use could lead to a high concentration of 6:2 FTAB in the adjacent surface water and groundwater. Thus, more investigations on the occurrence of 6:2 FTAB in the areas potentially impacted by AFFFs are needed. Another precursor, 6:2 FTS, also frequently existed (DF=60.6%) in the AFFF-impacted surface water with a high abundance (C_m =28 ng/L) (Table A-2).

2.3.3 PFAS concentrations in AFFF-impacted surface and subsurface soil

The PFAS occurrence and transport in the soil has been increasingly focused by researchers since 2010s, and soil was demonstrated as a significant reservoir for PFAS, especially at the contaminated sites, serving as a potential long-term PFAS source to the atmosphere, surface water, and groundwater. Strynar et al. found that PFAS was widely detected in the surface soil samples collected from 60 locations in 6 countries, and estimated total global surface soil loadings of 1,860 and >7,000 metric tons for PFOA and PFOS, respectively.⁹¹ Based on the concentrations of 32 PFAS measured in surface soil samples collected from 62 locations across all continents,⁹²

Washington et al. estimated a summed loading of 1,500 to 9,000 metric tons for 8 PFAS around the globe, with mean estimates of ca. 1,000 metric tons for PFOS and PFOA.⁹³

In this study, PFAS concentrations that have been reported in the soil impacted by AFFF applications are reviewed. A total of 13 peer-reviewed articles were identified that included measured concentrations of PFAS in soil.^{14,55,57,58,67,81,83–86,89,94,95} In most studies, “surface soil”, “subsurface soil”, or “aquifer solid” were clearly specified to the samples in which PFAS concentrations were reported. As for the soil cores analyzed in two studies, samples from 0-1 m were taken as surface soil samples, and the rest were taken as subsurface soil samples.^{84,86} In sum, PFAS concentrations reported in 274 surface soil samples and 169 subsurface samples were analyzed.

Among the PFAAs, PFOS was the most predominant PFAS detected in the AFFF-impacted soils, followed by PFHxS (Tables A-3 and A-4). In surface soil samples, the maximum reported concentrations for PFHxS and PFOS were 23,875 µg/kg and 55,197 µg/kg, respectively (Table A-3). PFOS had a C_m of 78 µg/kg, which was nearly one order of magnitude higher than that of PFHxS (8 µg/kg), and both PFAS had the most detections with high DFs (81.7-90.9%) (Table A-3). In subsurface soils, PFOS and PFHxS were detected with an even higher C_m (80 µg/kg and 25 µg/kg), although the mean values of reported concentrations were lower than that in surface soil (84-231 µg/kg vs. 288-1,485 µg/kg) (Tables A-3 and A-4). The summed C_m of all detected PFCAs and PFSAs in surface soils were calculated as 26.9 µg/kg and 94.4 µg/kg, respectively (Table A-3), while the corresponding values in subsurface soils were 36.2 µg/kg and 120.3 µg/kg, respectively (Table A-4). The results indicate that after the AFFF release to the ground, PFAS could transport and infiltrate into deeper soil and groundwater, resulting in even heavier contamination in the subsurface soil. In particular, the PFAS which have higher solubility and mobility (e.g., short-chain PFAAs), could transport more rapidly and reach to deeper soil. For example, the summed C_m of short-chain PFCAs (C4-C7) and PFSAs (C3-C6) were 16.6 µg/kg and 10.6 µg/kg in surface soils, but 26 µg/kg and 34.3 µg/kg in subsurface soils (Tables A-3 and A-4). In contrast, the long-chain PFAS tend to be retained in relatively shallower surface soil. The summed C_m of long-chain PFCAs (C8-C14) and PFSAs (C7-C10) were 10.3 µg/kg and 83.8 µg/kg in surface soils, which were comparable to that in subsurface soils (10.2 µg/kg and 86 µg/kg) (Tables A-3 and A-4).

A great abundance of precursors was also detected in the AFFF-impacted soil (Tables A-3 and A-4). The occurrence of precursors in the environment has attracted growing attentions in the last decade, though relatively less efforts were made for their detections, if compared to PFAAs. However, some of the precursors could be often present at a high concentration in AFFF-impacted surface and subsurface soils. With more than 100 detections reported, 6:2 FTS had a high DF of 77.4-81.3%, and a C_m of 27-40 $\mu\text{g}/\text{kg}$ (Tables A-3 and A-4). The concentration of 6:2 FTS was reported as high as 6,200 $\mu\text{g}/\text{kg}$ (Tables A-3 and A-4). The longer-chain analogue to 6:2 FTS, 8:2 FTS was also shown as one of primary PFAS contaminants, with a C_m of 10-14 $\mu\text{g}/\text{kg}$ (Tables A-3 and A-4). Other two FT-based precursors, 6:2 FTAB and 6:2 FtSaAm, which are direct ingredients of some FT-based AFFF formulations, were also reported in the surface soil. In particular, 6:2 FTAB was shown as the most predominant species in both surface and subsurface soils. In surface soil, the maximum, mean, and median concentrations of 6:2 FTAB were reported as 631,338 $\mu\text{g}/\text{kg}$, 12,975 $\mu\text{g}/\text{kg}$ and 494 $\mu\text{g}/\text{kg}$, respectively (Table A-3). Moreover, the DF was 69.2% (81 detections out of 117 soil samples). With lower DF (48.6%) and lower concentration reported, 6:2 FTAB had a C_m of 280 $\mu\text{g}/\text{kg}$ in subsurface soil (Table A-4). Surprisingly, the C_m of 6:2 FTAB (280-494 $\mu\text{g}/\text{kg}$) in AFFF-impacted soils were even 3-6 times higher than those of PFOS (78-80 $\mu\text{g}/\text{kg}$). Based on the high C_m (116 $\mu\text{g}/\text{kg}$) and a small number of detections/measurements (i.e., 19/83), 6:2 FtSaAm should be more often monitored in the AFFF-impacted sites moving forward (Table A-3). Last, FHxSA and FOSA were found in AFFF-impacted soils at a high abundance, although both were not the components of AFFF formulations. With more than 65% DF, FOSA and FHxSA had maximum concentrations of 1,800-3,400 $\mu\text{g}/\text{kg}$ reported in surface soils. The C_m of combined concentrations for FOSA and FHxSA reported in surface and subsurface soils were 15 $\mu\text{g}/\text{kg}$ and 22.8 $\mu\text{g}/\text{kg}$, respectively (Tables A-3 and A-4). Such C_m were comparable to that for combined PFCAs (C4-C14) in surface (26.9 $\mu\text{g}/\text{kg}$) and subsurface soils (36.2 $\mu\text{g}/\text{kg}$).

There is a database generated by U.S. Air Force during an ongoing investigation on PFAS contamination in AFFF-impacted sites since 2016.⁹⁶ As of 2019, the database comprises almost 25,000 soil and vadose-zone samples from 2,452 borehole sampling locations across 1000 AFFF-impacted sites.⁴ Although these data could not be incorporated into the present study, Brusseau et al.⁴ conducted an analysis on the soil concentrations for the selected PFAS (i.e., PFCAs (C4, C6, C8, C10), PFSAAs (C4, C6, C8, C10), FOSA, and 6:2 FTS) retrieved from the database. In the surface soils, PFOS, PFHxS, PFOA, and PFHxA were shown as the four species with the greatest

number of detections. Followed by 6:2 FTS, PFOS had the highest maximum, mean, and median concentrations of 373,000, 22, 18 $\mu\text{g}/\text{kg}$, respectively. In addition, the C_m for all 10 PFAS are close to or higher than 1 $\mu\text{g}/\text{kg}$. Moreover, Brusseau et al.⁴ investigated the depth distribution of PFAS in the soil as a function of chain length. It was found that long-chain PFAS comprise the majority of PFAS mass at the shallower depths, while short-chain PFAS represent the majority at deeper depths. All those findings from Brusseau et al.⁴ based on the AFFF-impacted soil metadata are in a good agreement with the results presented in this study (Tables A-3 and A-4), indicating that although the number of sites and samples analyzed were relatively limited, the present study could provide some insights into the overall occurrence of PFAS in the AFFF-impacted sites, especially for those precursors that were often ignored (e.g., FHxSA, 6:2 FTAB).

2.3.4 PFAS concentrations in AFFF-impacted sediment

Compared to other environmental matrices, less sediment samples impacted by AFFFs have previously been analyzed on the occurrence of associated PFAS. A total of 78 contaminated sediment samples were analyzed in 7 peer-reviewed publications,^{56,83,87,89,97-99} and the statistics of related PFAS concentrations are summarized in Table A-5. In general, much lower concentration of PFAS was reported in the sediment, along with the low DF (i.e., DFs of all PFAAs except PFOS are less than 50%). The summed C_m of all detected PFCAs and PFSAs in sediment were 3.0 $\mu\text{g}/\text{kg}$ and 2.5 $\mu\text{g}/\text{kg}$, respectively, which were 12-fold and 48-fold lower than those in subsurface soils (36.2 $\mu\text{g}/\text{kg}$ and 120.3 $\mu\text{g}/\text{kg}$). PFOS, PFOA, and 6:2 FTS are the three PFAS with the greatest number of detections (Table A-5). PFOS had the highest mean (15 $\mu\text{g}/\text{kg}$) and median (1.1 $\mu\text{g}/\text{kg}$) concentrations (Table A-5). One point of interest is, instead of 6:2 FTAB which was often detected in surface water, groundwater, and soil samples (Table 2-1 and Tables A-2 to A-4), 8:2 FTAB and 10:2 FTAB were more frequently detected in the sediment samples (Table A-5).^{98,99}

2.4 Comparison of PFAS compositions in AFFF formulations and AFFF-impacted environment

Although some similarities (e.g., the prevalence of PFOS or PFSAs) exist, a larger discrepancy between the PFAS compositions in AFFF formulations and those in the AFFF-impacted matrices could be appreciated (Figures 2-1 and 2-2; Table 2-1 and Tables A-2 to A-5). The similarity might be due to the globally historical use of ECF-based AFFF formulations, and the superior persistence of PFSAs in the environment.^{12,77} For the discrepancy, the most apparent one is that the

polyfluoroalkyl substances that were dominant in ECF- or FT-based AFFF formulations were either not detected or detected at a low level in AFFF-impacted environment. For example, the predominant ECF-based precursors, AmPr-FASA and AmPr-FASA-PrA (C_m ranging from 450 mg/L to 2,300 mg/L in AFFF formulations, Figure 2-1), were rarely detected in the AFFF-impacted soil and groundwater despite the attempts of detections.^{13,14} Likewise, several predominant FT-based precursors such as 6:2 FtTAoS ($C_m = 7,100$ mg/L), 6:2 FTAB ($C_m = 3,188$ mg/L), 8:2 FtSaAm ($C_m = 585$ mg/L) in FT-based AFFFs (Figure 2-2), were sporadically detected in the AFFF-impacted soil and groundwater.^{13,14} In contrast, the concentrations of 6:2 FTS, which were generally low in the AFFF formulations ($C_m = 53.7$ mg/L), were reported with higher concentrations ($C_m = 2,700$ ng/L) than 6:2 FtTAoS (limited detections), 8:2 FtSaAm (limited detections), or 6:2 FTAB ($C_m = 291$ ng/L) in AFFF-impacted groundwater (Table 2-1). The second discrepancy is that some PFAS species were not included in the AFFF formulations, but were frequently detected in the AFFF-impacted sites, even with high abundances. For example, FHxSA which was not present in ECF- or FT-based AFFF formulations, were detected in the AFFF-impacted groundwater with a DF of 70.5% and a C_m of 11,000 ng/L (Table 2-1), and were detected in the AFFF-impacted soils with a DF of 69.2-86.0% and a C_m of 12-17 μ g/kg (Tables A-3 and A-4). Lastly, the fraction of PFAAs was greater in AFFF-impacted groundwater and solid samples compared to that in AFFF formulations. For example, PFHxS and PFOS were mainly contained in ECF-based AFFF formulations with C_m of 600 mg/L and 4,900 mg/L, respectively (C_m of 0.2-1.5 mg/L in FT-based AFFFs) (Figures 2-1 and 2-2). The mass ratio of PFHxS to PFOS could be estimated as ca. 0.1 based on the median values. However, the ratios between the median concentrations of PFHxS and PFOS in the AFFF-impacted groundwater (Table 2-1), surface water (Table A-2), surface soil (Table A-3), subsurface soil (Table A-4), and sediment (Table A-5) were 0.5, 0.3, 0.1, 0.3, 0.6, respectively. In addition, PFCAs accounted for a very small percentage of total mass in both ECF- and FT-based AFFF formulations (Figures 2-1 and 2-2); the ratios between the summed C_m of Σ PFCAs (C4-C12) and Σ PFAS are 0.02 and <0.01 in ECF- and FT-based AFFF formulations, respectively. However, such ratios are 0.06, 0.14, 0.03, 0.07, and 0.47, respectively in the AFFF-impacted groundwater (Table 2-1), surface water (Table A-2), surface soil (Table A-3), subsurface soil (Table A-4), and sediment (Table A-5).

All the variations described above between PFAS compositions in AFFF formulations and those detected in the AFFF-impacted environmental matrices prevalingly indicate the occurrence

of the biotic or abiotic transformation to the AFFF-derived PFAS after release into the environment. The on-site transformation resulted in the decrease in the relative mass of some polyfluoroalkyl substances (e.g., AmPr-FASA, 6:2 FtTAoS), and the increase in the relative mass of corresponding transformation products (e.g., 6:2 FTS, PFCAs), as well as the formation of non-AFFF components (e.g., FHxSA). In the next section, the microbial transformation of AFFF-derived PFAS that could affect the occurrence and fate of PFAS in AFFF-impacted sites, are specifically reviewed.

2.5 Microbial transformation of AFFF-derived PFAS

Although the microbial transformation of perfluoroalkyl substances (e.g., PFOA, PFOS) have been demonstrated very recently,^{100–102} those reaction would be less likely to occur to the AFFF-derived PFAS in the environment, given the incubation condition (i.e., incubations with pure cultures of *Acidimicrobium* sp. strain A6¹⁰⁰), or the special structure of the starting PFAS compounds (e.g., unsaturated structure^{101,102}) used in the studies. Therefore, the biotransformation of PFOA, PFOS or the unsaturated PFAS reported in the above studies is beyond the scope of this review, and will not be discussed here.

Studies on biotransformation of PFAS in the last decades has been mostly focusing on the polyfluoroalkyl substances (“precursors”), in which the non-fluorinated head groups were typically reported to be transformed, on some occasions (e.g., for FT-based precursors), followed by the partial defluorination of perfluoroalkyl chains. The precursors discussed in this section are categorized into primary and secondary precursors derived from AFFF formulations (Table A-1). Primary precursors represent the precursors that were present in AFFF formulations as an intended PFAS component (e.g., at a high abundance), such as 6:2 FtTAoS in FT-based AFFFs (Figure 2-2). Secondary precursors represent the precursors that were not major PFAS components of AFFF formulations, whereas they were frequently detected in AFFF formulations or AFFF-impacted environment (e.g., 6:2 FTS) (Figure 2-2). Typically, the biotransformation of primary precursors may result in the formation of secondary precursors.

2.5.1 Aerobic biotransformation of ECF-based precursors

In recent years, AFFF-derived ECF-based precursors have been receiving growing attentions, with an increasing number of these compounds being identified by using advanced mass spectrometry techniques.^{12,13,15,68} However, the studies on biotransformation of AFFF-derived

ECF-based precursors are still limited, possibly due to the absence of chemical standards for most precursors and associated potential biotransformation products.

For the primary ECF-precursors, the microbial transformation potential of polyfluoroalkyl tertiary amines (AmPr-FASA and AmPr-FAAd),³⁴ polyfluoroalkyl amine oxides (OAmPr-FASA and OAmPr-FAAd),³³ quaternary ammonium polyfluoroalkyl surfactants (TAmPr-FASA and TAmPr-FAAd),³² and polyfluoroalkyl amine betaines (CMeAmPr-FASA and CMeAmPr-FAAd),³⁴ were investigated in aerobic soil microcosms (See Table A-1 for the PFAS class acronym, name, and structure). Class of AmPr-FASA was identified as a major component of AFFF formulations (Figure 2-1, Section 2.1)^{13,14}, and the other classes investigated in above studies were also detected in AFFFs or AFFF-impacted sites.^{15,57,68} Containing a sulfonamide (R-S(=O)₂N-R'R'') or carboxamide (R-C(=O)N-R'R'') group, these classes shared similarities in their structures: -S(=O)₂N(H)-C₃H₆-N(CH₃)₂- or -C(=O)N(H)-C₃H₆-N(CH₃)₂- (Figure 2-3 and Table A-1). The structure similarities resulted in the associated biotransformation pathways being mostly shared (Figure 2-3). Also, in general, same reactions occurred to the sulfonamide- (e.g., AmPr-FASA) and amide-containing precursors (e.g., AmPr-FAAd).³²⁻³⁴ Since the sulfonamide-containing precursors were primarily used in ECF-based AFFF formulations,^{12,13,34} and were detected in AFFF-impacted sites,¹⁴ the biotransformation of these precursors are focused in the present review (Figure 2-3).

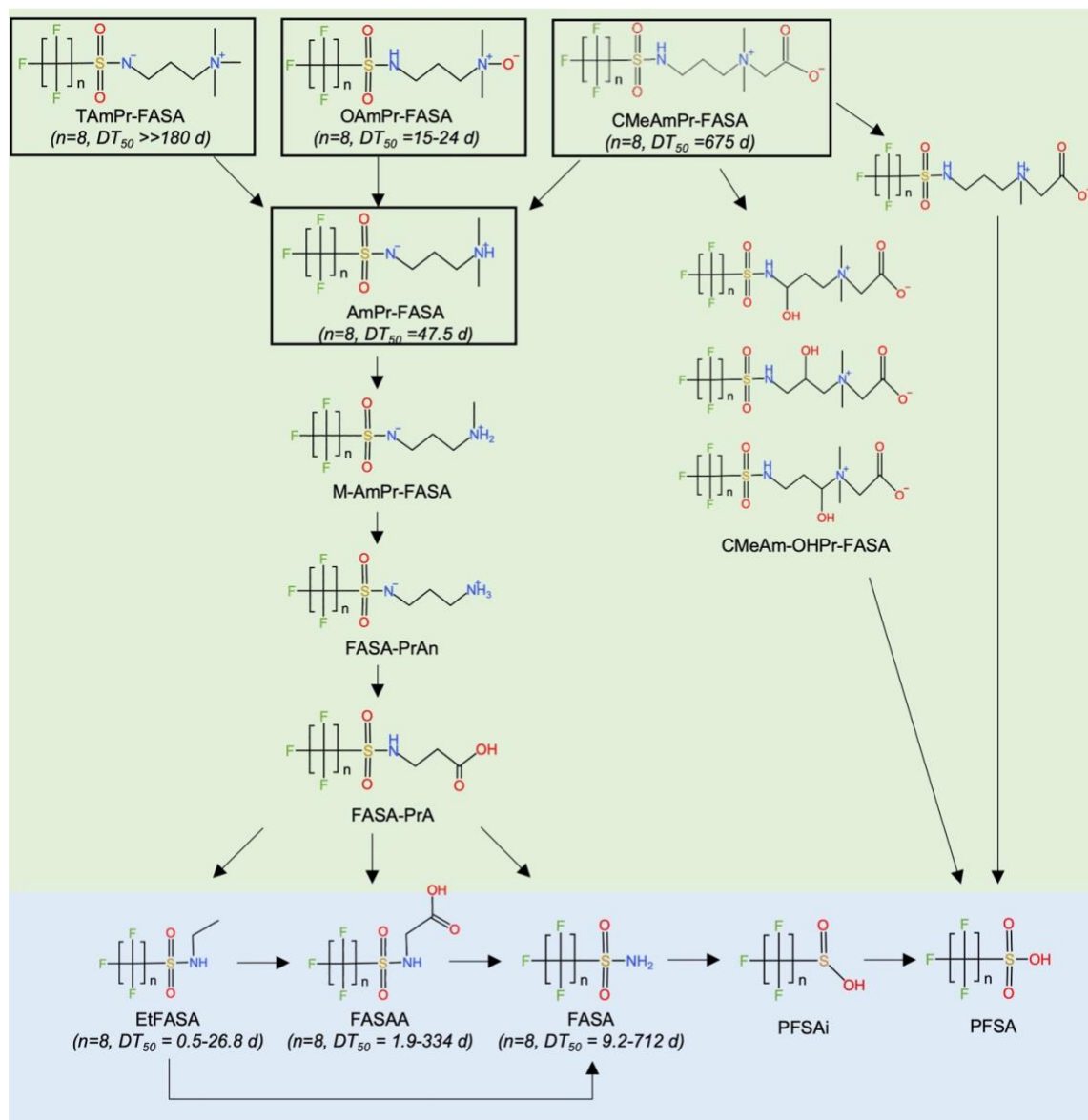


Figure 2-3. Microbial transformation of primary and secondary ECF-based precursors derived from AFFF formulations. The biotransformation pathways and rates (DT_{50} : half-life or time for 50% of a substance to disappear) of primary precursors (shaded in green) were reported in aerobic soils.³²⁻³⁴ The biotransformation pathways and rates of secondary precursors (shaded in blue) are summarized based on prior studies using aerobic soil,^{36,103,104} activated sludge,³⁵ and wetland slurry.¹⁰⁵ Note some biotransformation products (e.g., M-AmPr-FASA) included in the pathways were not verified due to the absence of chemical standard. A few minor pathways proposed in the above studies were not included here.

The biotransformation of TAmPr-FASA, OAmPr-FASA, CMeAmPr-FASA initiated by the alteration of the amine groups (i.e., *N*-dealkylation, *N*-reduction, and *N*-deacetylation,

respectively) on the molecules' head group (Figure 2-3). Accordingly, AmPr-FASA is formed with a tertiary amine group. Through multiple *N*-dealkylations, the tertiary amine is transformed to secondary (M-AmPr-FASA), then to primary amine (i.e., FASA-PrAn). Subsequently, the primary amine compound is oxidized to polyfluoroalkyl carboxylic acids (FASA-PrA), which could be further transformed to the compounds that were often detected in AFFF-impacted sites (referred to as the secondary ECF-precursors) such as FASA (Figure 2-3). In prior studies, with eight perfluorinated carbons ($n=8$), TAmPr-FASA ($DT_{50} \gg 180$ d) and CMeAmPr-FASA ($DT_{50} = 675$ d) showed much higher microbial stability than OAmPr-FASA ($DT_{50} = 15-24$ d) and AmPr-FASA ($DT_{50} = 47.5$ d) in aerobic soils.³²⁻³⁴ The susceptibility to biotransformation for AmPr-FASA could explain the absence or extremely low detection of this PFAS class in the AFFF-impacted groundwater and soil, despite the high abundance in the AFFF formulations (Figure 2-1).^{13,14} Likewise, the other major class of AFFF-derived ECF-based precursors, AmPr-FASA-PrA (Figure 2-1),^{13,14} might also have low microbial stability, resulting in its absence in the AFFF-impacted sites. For TAmPr-FASA and CMeAmPr-FASA, it is unclear that if the two classes have ever been used as major PFAS compounds in some AFFF formulations. These two PFAS classes would be more persistent in the environment, and conversion to AmPr-FASA can be a rate-limiting step for the natural attenuation. Recently, a few detections of TAmPr-FASA were reported in AFFF-impacted groundwater and soil samples (not included in Table 2-1 and Tables A-2 to A-5 due to <10 detections reported).^{57,67,81,88} The concentration of TAmPr-FASA ($n=8$) in one groundwater sample was 280 ng/L,⁸⁸ whereas the concentrations of TAmPr-FASA ($n=6$) in surface and subsurface soil were reported up to 140,000 $\mu\text{g}/\text{kg}$ and 2,192 $\mu\text{g}/\text{kg}$, respectively.⁵⁷

For the secondary ECF-based precursors, EtFASA, FASAA, and FASA could be formed by the biotransformation of primary ECF-based precursors in aerobic soils (Figure 2-3). Comparatively, the biotransformation of these secondary ECF-based precursors has been more investigated.^{35,36,103-105} Through direct *N*-dealkylation or the ethyl group oxidation, EtFASA could be biotransformed to FASA or FASAA in aerobic soils,^{36,103,104} activated sludge,³⁵ and wetland plant microcosms (Figure 2-3).¹⁰⁵ The *N*-dealkylation reaction leading to FASA production was demonstrated to be more favored; for example, the rate constant of reaction EtFOSA to FOSA was 0.92 d^{-1} , more than 2-fold faster than that of reaction EtFOSA to FOSAA (0.45 d^{-1}) in wetland plant microcosms.¹⁰⁵ The low microbial stability of EtFOSA was reported in various environmental matrices, with the half-lives ranging 0.5 to 26.8 days.^{35,36,103-105} The low stability is

in agreement with the absence or low detections of EtFASA class in AFFF-impacted environmental samples (Table 2-1 and Tables A-2 to A-5). FOSAA was shown to convert to FOSA by removal of the acetate group in aerobic soils,^{103,104} activated sludge,³⁵ and wetland plant microcosms (Figure 2-3).¹⁰⁵ However, the biotransformation rate varied substantially among the studies, with a half-life of 1.9 days in activated sludge,³⁵ 3.9 days in wetland plant microcosms,¹⁰⁵ and 96.2-334 days in aerobic soils.¹⁰⁴ The biotransformation of FOSAA to FOSA was even not feasible in another aerobic soil.³⁶ The variations observed for FOSAA biotransformation rate are likely due to the different microbial communities used in prior studies.^{35,36,104,105} Therefore, the persistence of class of FASAA in the environment might be site-dependent, namely, dependent on if the associated microbial degraders are present or not. As shown in Table A-3, a few detections of FOSAA (DF=9.5%) were reported in AFFF-impacted surface soils. FOSA could be further biotransformed to PFOS through the proposed transient intermediate perfluorooctane sulfinate (PFOSI) in aerobic soils,^{36,103,104} activated sludge,³⁵ and wetland plant microcosms (Figure 2-3).¹⁰⁵ However, FOSA showed a much higher microbial stability than EtFOSA and FOSAA, with a half-lives of 9.2-712 days.^{35,36,104,105} These findings might explain the prevalent detections of FOSA and its C6 analogue, FHxSA in AFFF-impacted environments (Table 2-1 and Tables A-2 to A-5).

Overall, sulfonamide-containing ECF-based precursors have been demonstrated to be precursors to PFSA in laboratory microcosms, despite the variations in biotransformation rate and PFSA yield associated with the distinct types of hydrophilic head groups in the precursors. Therefore, those ECF-based precursors are the short- or long-term sources to PFSA in the environment impacted by historical AFFF usages. For some classes such as TAMPr-FASA, they could be quite persistent in the fields, and serve as PFSA source even years, decades after AFFF releases. It is noteworthy that the biotransformation of ECF-based precursors that have been reported to-date is limited to the non-fluorinated moieties without the occurrence of defluorination and shortening of perfluoroalkyl chains. In other words, a C6 homologue of ECF-based precursor such as AmPr-FHxSA is a precursor to PFHxS, while a C8 precursor is likely biotransformed to PFOS eventually.

2.5.2 Aerobic biotransformation of FT-based precursors

Compared to ECF-based precursors, the aerobic biotransformation of FT-based precursors was more studied.^{19,31,75,80,106,107} Three classes of primary FT-based precursors in AFFF formulations

are $n:2$ FtTAoS, $n:2$ FTAB and $n:2$ FtSaAm (Figure 2-2, Section 2.2).^{12-14,68} The aerobic biotransformation of a C6 homologue (i.e., $n=6$) in these three classes was investigated in microcosms constructed with activated sludge,^{75,80} or aerobic soil,^{31,107,108} or by a pure bacterial culture.¹⁰⁶ In addition, C4 and C8 homologues in class of $n:2$ FtTAoS were investigated along with C6 homologue in a soil microcosm, in which similar biotransformation pathways were shared among three homologues.³¹ To facilitate the illustration and discussion, in this section, the biotransformation of FT-based precursors will focus on the C6 homologue in each class (Figure 2-4).

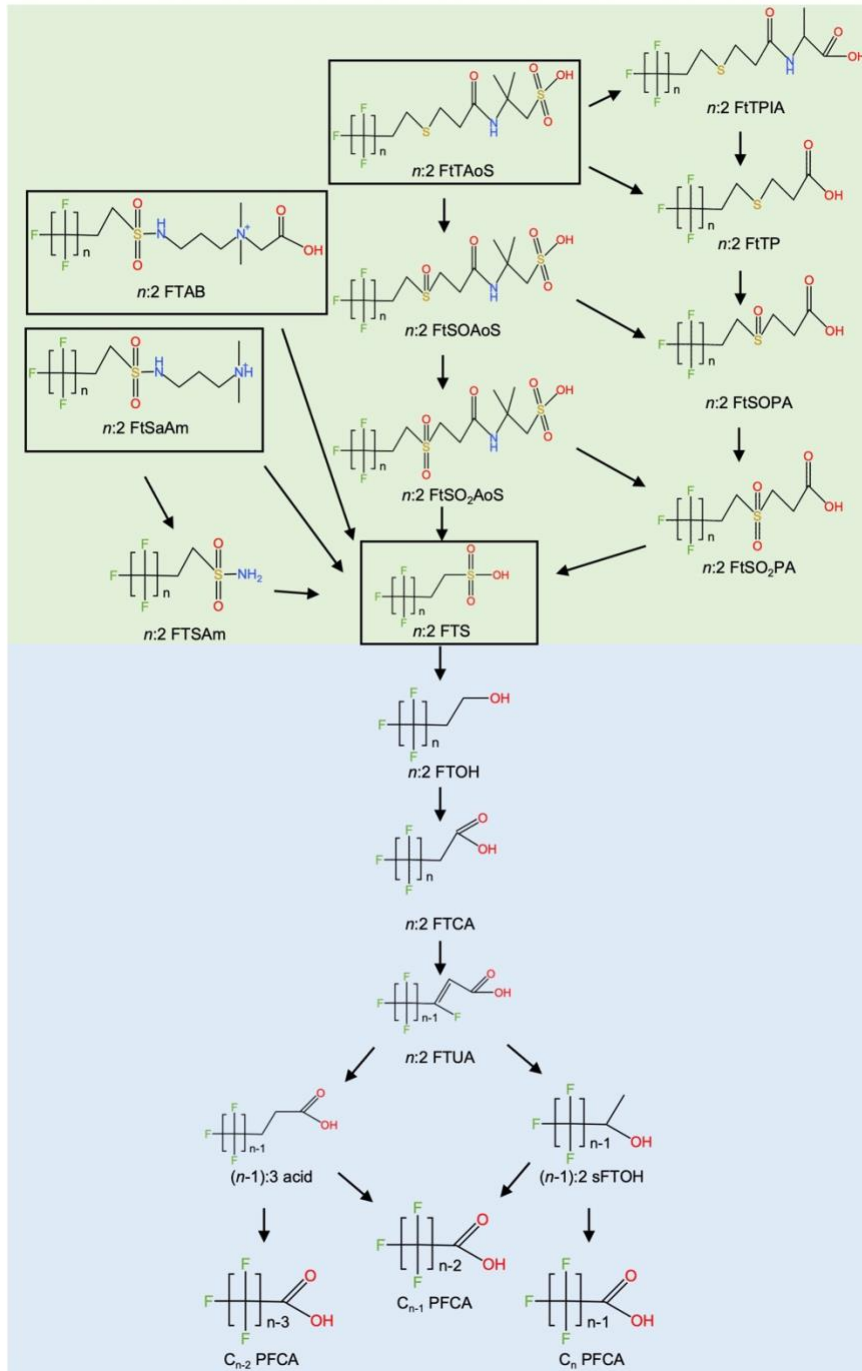


Figure 2-4. Microbial transformation of primary and secondary FT-based precursors derived from AFFF formulations. The biotransformation pathways of primary precursors (shaded in green) were reported in aerobic soils,^{31,107,108} and activated sludge.^{75,80} The biotransformation pathways of secondary precursors (shaded in blue) are summarized based on prior studies using activated sludge,²⁴ river sediment,²⁵ wetland slurry,²⁸ and landfill leachate.^{29,30} Note some biotransformation products (e.g., $n:2$ FtSOAoS) included in the pathways were not verified due to the absence of chemical standard. A few minor pathways proposed in the above studies were not included here.

The biotransformation of 6:2 FtTAoS has been investigated in aerobic soil^{31,107} and activated sludge.^{75,109} As shown in Figure 2-4, one of the biotransformation pathways for 6:2 FtTAoS involves direct oxidation of thioether into sulfoxide and sulfone, leading to the formations of 6:2 FtSOAoS and 6:2 FtSO₂AoS.^{31,75,107,109} Then, 6:2 FtSO₂AoS could be further oxidized to 6:2 FTS involving the cleavage of a carbon-carbon bond.^{31,75,107,109} The other parallel biotransformation pathways for 6:2 FtTAoS include alkylsulfonate oxidation to form 6:2 FtTPIA, and amide hydrolysis to form 6:2 FtTP (Figure 2-4).^{107,109} Similar as 6:2 FtTAoS, through sequential oxygen addition on the thioether group, 6:2 FtTP can be oxidized to 6:2 FtSOPA, 6:2 FtSO₂PA, and eventually to 6:2 FTS (Figure 2-4).^{107,109} The formations of 6:2 FtSOPA and 6:2 FtSO₂PA are also possible from the amide hydrolysis of 6:2 FtSOAoS and 6:2 FtSO₂AoS, respectively (Figure 2-4). Limited data are available on the biotransformation pathways of 6:2 FTAB and 6:2 FtSaAm.^{80,106,108} Although only a few of intermediates were identified (e.g., 6:2 FTSAm), 6:2 FTAB and 6:2 FtSaAm were demonstrated as the precursors of 6:2 FTS in aerobic soil and activated sludge (Figure 2-4).^{80,108} Among the three classes of primary FT-based precursors in AFFF formulations, 6:2 FtTAoS was consistently shown to be readily biotransformed in aerobic soil^{31,107} and activated sludge,^{75,109} with the complete disappearance in <42 days. The low microbial stability of 6:2 FtTAoS agrees with the rare detection of this class in AFFF-impacted environment (Table 2-1 and Tables A-2 to A-5), despite the high concentration in the AFFF formulations (Figure 2-2). In contrast, the class of *n*:2 FTAB was frequently detected in the AFFF-impacted environmental matrices; in particular, 81 detections (DF=69.2%, C_m=494 μg/kg) and 54 detections (DF=48.6%, C_m=280 μg/kg) of 6:2 FTAB were reported in AFFF-impacted surface and subsurface soils, respectively (Tables A-3 and A-4). In addition, 6:2 FtSaAm was detected in the surface soil (DF=22.9%) with a C_m of 116 μg/kg (Table A-3). The occurrence of *n*:2 FTAB and *n*:2 FtSaAm in the AFFF-impacted sites is possibly due to their higher microbial stability and thus persistence. D'Agostino and Mabury reported that the 6:2 FTAB biotransformation was quite slow, while 6:2 FtSaAm biotransformation was relatively faster in the activated sludge, although the mass losses complicated the quantitative assessment of the associated rates.⁸⁰ Li et al. reported an estimated half-life of 31 days for 6:2 FTAB in the aerobic soil, however, the high nutrient condition used in their study likely promoted the biotransformation.¹⁰⁸

The biotransformation of primary FT-based precursors described above always leads to the formation of *n*:2 FTS, which is the predominant secondary FT-based precursor (Figure 2-4).

Because of those biotransformation processes occurring in the fields, a great number of detections of $n:2$ FTS, especially $6:2$ FTS, was reported throughout the AFFF-impacted environment (Table 2-1 and Tables A-2 to A-5). Biotransformation of $6:2$ FTS has been investigated by pure bacterial strains (e.g., *Gordonia* sp. strain NB4-1Y) under well-controlled cultivation conditions,^{110–114} and by various mixed microbial cultures from activated sludge,²⁴ river sediment,²⁵ wetland slurry,²⁸ and landfill leachate.^{29,30} In general, the initial step of $6:2$ FTS biotransformation is the microbial desulfonation catalyzed by monooxygenases,^{111,112} resulting in the formation of $6:2$ FTOH (Figure 2-4). However, the presence of more easily assimilated sulfur sources (e.g., sulfate) in the environment was reported to suppress the desulfonation, making it often a rate-limiting step for $6:2$ FTS biotransformation.^{24,28,29} Accordingly, large discrepancies in the $6:2$ FTS biotransformation rate were associated with the above studies. For example, the half-life of $6:2$ FTS was <5 days in the river sediment, but approximately 86 days in landfill leachate sediment and 2 years in activated sludge.^{24,25,29} These results suggest that $6:2$ FTS biotransformation is influenced by the environmental factors, and the compound can be persistent in some environment where biotransformation is not favored. The widespread detection of $n:2$ FTS in AFFF-impacted sites further supports the environmental persistence of this class (Table 2-1 and Tables A-2 to A-5). Following the conversion to $n:2$ FTOH by desulfonation, the biotransformation of $n:2$ FTOH ($n=6, 8$) have been widely studied in various environmental matrices.^{23,26,27,29,42–50} Among those studies, generally rapid biotransformation (e.g., half-life <7 days) was observed, and the majority of biotransformation pathways was shared in activated sludge, aerobic soils and river sediment.^{23,26,27,29,42–50} Specifically, $n:2$ FTOH is oxidized to $n:2$ fluorotelomer aldehyde (not shown) by an alcohol dehydrogenase, which is then oxidized to $n:2$ FTCA catalyzed by an aldehyde dehydrogenase (Figure 2-4). Through a dehydrohalogenation reaction, $n:2$ FTCA is transformed to $n:2$ FTUA involving elimination of a hydrogen fluoride (HF). The biotransformation of $n:2$ FTOH to $n:2$ FTAL, to $n:2$ FTCA, and then to $n:2$ FTUA is a rapid process,^{23,26,27,42–47,50} which explains the absence of classes of $n:2$ FTOH, $n:2$ FTAL, and $n:2$ FTCA in AFFF-impacted sites (Table 2-1 and Tables A-2 to A-5). Yet some detections in AFFF-impacted surface soils (Table A-3) likely indicates a higher microbial stability of $n:2$ FTUA. Further biotransformation of $n:2$ FTUA usually processes into two ways.^{42,43,115} Through multiple enzymatic steps (e.g., defluorination and decarboxylation), $n:2$ FTUA can be metabolized to $(n-1):2$ sFTOH, which is the precursor to C_n and C_{n-1} PFCAs via currently unknown reactions

involving the removal of fluorine and carbon atoms (Figure 2-4). The other transformation pathway for $n:2$ FTUA leads to the formation of $(n-1):3$ acid possibly via reductive defluorination and hydrogenation (Figure 2-4). It has been demonstrated that $(n-1):3$ acid is a precursor to C_{n-1} and C_{n-2} PFCAs, however, the biotransformation rate can be quite slow in activated sludge and soil due to the binding of $(n-1):3$ acid and organic components of environmental matrices (i.e., low bioavailability).^{43,116} In addition, with a longer perfluoroalkyl chain, $(n-1):3$ acid has a lower bioavailability.^{43,116} These findings are in a good agreement with the detections of 5:3 acid and 7:3 acid in AFFF-impacted surface soil (Table A-3), as well as a higher DF for 7:3 acid (100%) than 5:3 acid (30.5%).

Overall, AFFF-derived FT-based precursors are likely to be biotransformed to PFCAs in aerobic environment. $n:2$ FTS is a key intermediate class during the biotransformation. Given the potential persistence, $n:2$ FTS and associated transformation products (e.g., $(n-1):3$ acid and PFCAs) could be accumulated in AFFF-impacted environments. One distinct difference between the biotransformation of FT- and ECF-based precursors is the potential defluorination and shortening of perfluoroalkyl chains, which has only been observed for FT-based precursors to-date.

2.5.3 Anaerobic biotransformation of AFFF-derived precursors

Very limited studies were reported on the anaerobic biotransformation of AFFF-derived precursors.^{25,28,37,39,41,53,117} Most of them were associated with the biotransformation of FT-based precursors. More importantly, the biotransformation of those precursors under anoxic conditions were found distinctly different from that under oxic conditions. Zhang et al.⁴¹ reported the half-lives of $n:2$ FTOH ($n=6, 8$) biotransformation under methanogenic conditions as 30-145 days, which were much longer than those reported in various environmental matrices under oxic conditions (i.e., <7 days).^{23,26,27,29,42-50} The PFAA yields were also at least 20-time lower under methanogenic condition than oxic conditions.⁴¹ The biotransformation of 6:2 FTS occurred under oxic^{24,51} and nitrate-reducing conditions,⁵² with the most rapid transformation rate occurring in aerobic sediment;²⁵ whereas, transformations did not occur under sulfate-reducing²⁵ and methanogenic conditions.⁴⁰ An AFFF-derived primary FT-based precursor, 6:2 FtTAoS, was reported to be biotransformed much more slowly under sulfate-reducing conditions (ca. 75 mol% of initially spiked 6:2 FtTAoS biotransformed after a 270-day incubation)³⁷ than under oxic

conditions (100 mol% of initially spiked 6:2 FtTAoS biotransformed in <20 days) in soil microcosms.³¹ Under nitrate-reducing condition with the same biomass, however, the biotransformation rate of 6:2 FtTAoS was approximately 10-fold slower than under oxic condition, but approximately 2.7-fold faster than under sulfate-reducing conditions.⁵³ Moreover, the distinct biotransformation pathways were observed among the three redox conditions; for example, 6:2 FTS was the most abundant biotransformation product (8 mol%) and production of PFCAs (1.5 mol%) were observed under oxic condition,³¹ whereas none or minimal of 6:2 FTS and PFCAs were detected under sulfate- and nitrate-reducing conditions.^{37,53} All these findings to-date indicate the complexity of PFAS biotransformation, and the important role of redox condition and the associated microbial communities in the biotransformation processes.

2.6 Environmental implications and future research recommendations

The present study demonstrates a widespread occurrence of AFFF-derived PFAS in various environmental matrices that were potentially impacted by the historical use of AFFFs. Concentrations of PFOA and PFOS in hundreds of AFFF-impacted groundwater (C_m of 568 and 2,048 ng/L) and surface water (C_m of 32 and 140 ng/L) were several orders of magnitude greater than the latest EPA life health advisories (0.004 ng/L and 0.02 ng/L for PFOA and PFOS, respectively).^{63,64} The AFFF-contaminated soils were shown as a significant PFAS reservoir, serving as potential long-term PFAS sources to the atmosphere, surface water, and groundwater. These observations have the implications for human exposure to PFAS through multiple routes, which poses the adverse health impacts. In addition to the commonly investigated anionic PFAS (i.e., C4 to C8 PFCAs and PFSAs), the presence of other PFAS such as ultra-short PFSAs (e.g., PFEtS and PFPrS), cationic and zwitterionic PFAS (e.g., 6:2 FTAB, FHxSA) in AFFF-impacted environment was reported with high detection frequency and concentration. Given the potentially high solubility, mobility, and persistence, these PFAS should be more investigated for the associated occurrence in the environment impacted by AFFFs and other PFAS sources. Further, the potential exposure and adverse human health effects from those PFAS need to be explored in the future studies.

Microbial transformation of AFFF-derived PFAS including primary and secondary precursors, was demonstrated as an important factor affecting the occurrence and fate of PFAS upon the release to the ground. The biotransformation rates and pathways for secondary precursors (e.g.,

EtFOSA, 6:2 FTS) in aerobic environment were relatively more investigated, and the findings reported to-date could provide explanations to the field observations (e.g., high detections of 6:2 FTS and FOSA due to the potential persistence). However, limited data are available on the biotransformation pathways of primary ECF- and FT-based precursors, despite an increasing number of identifications of those precursors in AFFF formulations^{13,15,68} and AFFF-impacted sites.^{13,57,58,81} The biotransformation pathways of those precursors (e.g., 6:2 FTAB) were often incomplete due to the missing of transformation intermediates.⁸⁰ More laboratory studies as well as the field data collection (i.e., detection of precursors and intermediate compounds in the field) in the future are needed to elucidate the biotransformation pathways for AFFF-derived precursors.

The impact of redox condition and related microbial community on the biotransformation of AFFF-derived precursors has been demonstrated.^{31,37,52,53} Such impact complicates the assessment of the fate and transformation of PFAS in natural environment. By far, the biotransformation of AFFF-derived precursors under anoxic conditions have only been investigated in few studies,^{25,37,53} leaving a critical knowledge gap on the fate of a large number of precursors including newly identified cationic and zwitterionic PFAS in the subsurface soil and the aquifer. Research efforts with respect to anaerobic biotransformation of PFAS need to be continuously made in the future, which will help better predict the PFAS fate in the subsurface environment and design of effective remediation strategies.

Chapter 3 : Production of perfluorooctane sulfonate (PFOS) from biotransformation of perfluorooctane sulfonamide (FOSA) in aerobic soils

The work presented in this chapter is being prepared as a manuscript for publication.

3.1 Introduction

Perfluorooctane sulfonate (PFOS) is one of the predominant per- and polyfluoroalkyl substances (PFAS) detected in the environment, wildlife, and humans.^{4,82,90,118–120} Due to the great concerns for its extreme persistence, bioaccumulation potential, and toxicological effects, the production of PFOS and related substances has been phased out in North America in early 2000s, and in Europe since 2010.^{121,122} In 2009, those compounds were also added to the list of the United Nations Stockholm Convention on Persistent Organic Pollutants (UNSCPOP). However, the increased production and application of PFOS and related substances in other parts of the world poses continuous threats to the health of global environment and humans.¹²³ The widespread presence of PFOS in the environment can be attributed to the historical uses of PFOS in commercial products (e.g., aqueous film forming foam-AFFF).⁹⁰ In addition, a large number of sulfonamide-containing derivatives (referred to as “PFOS precursor candidates”) present in the environment may transform to PFOS through abiotic¹²⁴ or biotic processes.^{35,103,125} Those PFOS precursor candidates have been historically used in a wide range of commercial products (e.g., carpets, textiles, packaging and insecticide), and the total production and emission may have exceeded those of PFOS.¹²⁰ Therefore, the relative contribution of PFOS precursor candidates to the overall environmental burden of PFOS is likely significant. Understanding the environmental fate of those precursor candidates is of importance, not only to identify sources of emission and exposures to PFOS, but also to predict the future burden of PFOS in wildlife and humans.¹²⁶

Perfluorooctane sulfonamide (FOSA) is a neutral PFOS precursor candidate, which has been used in food packaging and other consumer applications to repel grease and water.¹²⁷ FOSA was also reported as a biotransformation product of other PFOS precursor candidates such as N-ethyl perfluorooctane sulfonamide ethanol (EtFOSE) and N-ethyl perfluorooctane sulfonamide (EtFOSA).^{35,36,103–105,128} Consequently, FOSA has been widely detected in the environment, with concentrations up to 22,000 ng/L and 3,400 µg/kg reported in an AFFF-impacted groundwater⁵⁸ and soil,¹⁴ respectively. The toxicological effects of FOSA on biota^{129,130} and humans¹³¹ were

reported previously. Moreover, FOSA was known as a developmental neurotoxicant, posing an even higher toxicity than PFOS.¹³²

To date, only a few studies have investigated the biotransformation potential of FOSA.^{133,134} Indigenous microorganisms in groundwater were demonstrated to be able to biotransform FOSA to PFOS, and the amendment of nutrients and soil promoted the PFOS formation (i.e., molar yield increased from 0.5% to 4.9%).¹³³ Zhao et al. reported that FOSA could be biotransformed to PFOS by the microorganisms in soil, though the molar yield of PFOS was not provided.¹³⁴ However, the biotransformation kinetics of FOSA were not investigated in these two studies.^{133,134} In other biotransformation studies in which EtFOSE or EtFOSA was the starting compound, FOSA was formed as an intermediate and the associated biotransformation rate was reported.^{35,36,104,105} These studies reported a wide range in the FOSA biotransformation kinetics and the potentially associated PFOS yields.^{35,36,104,105} For example, a half-life of 9.2 days was reported for FOSA in activated sludge,³⁵ whereas the half-life was predicted as 712 days in an aerobic soil.³⁶ Resulting from EtFOSA biotransformation, PFOS molar yield was reported to be 4.0% after a 182-day incubation in an aerobic soil,¹⁰³ but was 85.1% in wetland plant microcosms after 91 days.¹⁰⁵ Those results suggest that the factors such as the microbial community composition in various environmental matrices might play an important role in the biotransformation of FOSA. Understanding the interaction between microbial community and FOSA biotransformation, and further providing the information on potential FOSA degraders and microbial toxicity of FOSA, would be critical towards the assessments of its behavior in the environment.

The present study is intended to provide more insights into the biotransformation kinetics of FOSA and PFOS yields in soil. Soil is a significant reservoir for organic pollutants including PFAS, serving as a potential long-term contaminants source to the atmosphere, surface water, and groundwater. Soil is also highly rich in microorganisms that are capable of biotransforming PFAS.^{31,43,107} In this study, two distinctly different soils, in terms of both soil properties and contamination history (i.e., one pristine and one AFFF-contaminated soil), were used for separate FOSA microcosm investigation. FOSA and other PFAS have been frequently detected in AFFF-impacted sites.^{14,58} The microbial communities in historically AFFF-contaminated soil may evolve to be more tolerant to PFAS and more capable of transforming PFAS. Yet, the biotransformation of PFAS have been rarely investigated in these contaminated matrices.^{31,37} In this study, the biotransformation kinetics and product formation of FOSA in the two soil microcosms were

examined over a 308-day incubation period. Also, the interactive influence of FOSA and transformation products on the soil microbial community structure was investigated. Further, the microbial species that are more tolerant to FOSA and transformation products, and might be the potential FOSA degraders were identified.

3.2 Materials and methods

3.2.1 Chemicals and Materials

FOSA was obtained from Sigma-Aldrich (St. Louis, MO, USA) with 98% purity. The chemical standard of FOSA (>98%, in isopropanol, $50 \pm 2.5 \mu\text{g/mL}$), FHxSA (>98%, in isopropanol, $50 \pm 2.5 \mu\text{g/mL}$) and PFAC-MXC stock solution including 21 native PFCAs and PFSA were purchased from Wellington Laboratories (Ontario, Canada). Other chemicals used in this study were reagent grade or higher. Ultrapure deionized water ($18.2 \text{ M}\Omega \text{ cm}$) from an Evoqua water purification system (Evoqua Water Technologies, USA) was used for all purposes. Two aerobic soils were used in this study for microcosm construction. Following the procedure described previously,¹³⁵ an AFFF-contaminated soil was collected from former Loring Air Force Base (Aroostook County, ME), and another soil was collected from a location close to Hudson River in Rensselaer County, New York (Coordinates: $42^{\circ}29'02''\text{N } 73^{\circ}44'29''\text{W}$) (referred to hereafter as Loring soil and Hudson soil). The physical and chemical properties (pH, moisture content, organic matter content, cation exchange capacity (CEC), soil particle size distribution) of Loring and Hudson soils are provided in Appendix B, Table B-1.

3.2.2 Microcosm Set-up and Sampling

Two sets of microcosms were constructed in 160-mL Wheaton serum bottles with either Loring or Hudson soil. Each set consisted of triplicate live treatments, duplicate abiotic controls, and duplicate positive controls (composition described in Table 3-1). In each bottle, 10 g (dry weight) of Loring or Hudson soil and 100 mL of bicarbonate-buffered growth medium were added. The medium was prepared based on the recipe previously reported,¹³⁶ with modifications to omit resazurin, L-cysteine, and sodium sulfide due to their potential to serve as carbon sources under oxic conditions. For live treatments, each bottle was spiked with 85 μL of FOSA stock solution (100 mg/L) prepared in diethylene glycol butyl ether (DGBE) to yield an initial FOSA concentration of ca. 85 $\mu\text{g/L}$. DGBE was used to prepare the stock, because it was a primary organic solvent in AFFF formulations and was demonstrated as an electron donor and carbon

source in previous aerobic soil microcosms.^{13,29} Abiotic controls were constructed similarly to live treatments, but additional 1 g/L NaN₃ was dosed to inhibit microbial growth (effective concentration determined by preliminary experiments, data not shown). Abiotic controls were used to evaluate potential abiotic transformation of FOSA and/or other legacy PFAS present in Loring and Hudson soils. In the positive controls, only 85 µL DGBE (no FOSA) was dosed, and all other procedures were same as the live treatments. The positive controls aimed to monitor background levels of legacy PFAS in Loring and Hudson soils, and the associated potential biotransformation products. All bottles were crimp-sealed with rubber septa and aluminum caps (Chemglass; Vineland, NJ). To ensure the aeration in the soil microcosms throughout experiment, a 0.22-µm sterile syringe filter (polyethersulfone (PES), VWR) connected to an 18G×1" needle was pierced through the septum into the headspace of each bottle. The microcosms were continuously shaken at 150 rpm on an orbital shaker (Innova 2350, New Brunswick Scientific) at room temperature for 308 days.

Table 3-1. Microcosm set-up of FOSA aerobic biotransformation in Loring and Hudson soils.

Treatment	Soil	Spiked FOSA ^a	Carbon source & electron donor	Electron acceptor	Other ^c
<i>Loring AFB soil microcosms</i>					
Live treatment	Loring AFB soil	Yes	DGBE ^b	Oxygen	/
Abiotic control	Loring AFB soil	Yes	DGBE	Oxygen	NaN ₃
Positive control	Loring AFB soil	No	DGBE	Oxygen	/
<i>Hudson AFB soil microcosms</i>					
Live treatment	Hudson soil	Yes	DGBE	Oxygen	/
Abiotic control	Hudson soil	Yes	DGBE	Oxygen	NaN ₃
Positive control	Hudson soil	No	DGBE	Oxygen	/

^aThe initial concentration of FOSA spiked into the microcosms was ca. 85 µg/L.

^bDGBE was added into the microcosms with an initial concentration of ca. 5 mM.

^cOne gram per liter sodium azide was added to inhibit the microbial activity.

On days 0, 28, 56, 98, 154, 224, and 308, all microcosm bottles were taken into a biological safety cabinet (Labconco, Purifier Class II model, Kansas City, MO). The 0.22-µm syringe filter was removed from each bottle, and a 3-mL sterile syringe (BD Luer-Lok disposable syringe) was connected to the 18G×1" needle. After shaking the bottle vigorously, 2 mL of well-mixed slurry was collected into a 2-mL microcentrifuge tube and centrifuged at 15,000 rpm for 10 minutes.

After centrifugation, the supernatant (0.5-mL) was added into methanol (9.5-mL), which was filtered through a 0.2- μ m nylon filter (Corning Inc., Corning, NY) and stored at -20 °C prior to PFAS analysis. The remaining supernatant was transferred into a new 2-mL microcentrifuge tube for dissolved organic carbon (DOC) analysis (TOC-L CPH, Shimadzu). Subsequently, the soil pellet was resuspended with 1.5 mL methanol and vortexed for 20 min, followed by 20 min sonication (operating frequency of 35 kHz) at 60 °C. The methanol extract of soil was then collected after centrifugation (15,000 rpm, 10 minutes), and further filtered through a 0.22- μ m nylon filter. The soil extract was also stored at -20 °C for PFAS analysis.

3.2.3 PFAS analysis

The analysis of FOSA, PFOS, and other targeted PFAS in the aqueous and solid phases samples, was performed on an Vanquish Flex Binary Ultra Performance Liquid Chromatography (UPLC) system (Thermo Scientific) fitted with a PFC-free kit (P/N 80100-62142) coupled to a quadrupole orbitrap mass spectrometer (Orbitrap Exploris 120, Thermo Scientific) with heated electrospray ionization (H-ESI) in negative mode using Xcalibur software (V4.4.16.14). A delay column was placed between the pump and autosampler (HypersilGOLD, 1.9 μ m, 175 Å, 3 x 50 mm) to separate any PFAS in the LC system and solvents from the analytes. The standard or sample (10 μ L) was injected onto a C18 column (Accucore RP-MS, 2.6 μ m, 2.1 x 100 mm) maintained at 40°C, with a 200 μ L/min flow rate of mobile phase of solution A (2 mM ammonium acetate in water) and solution B (100% acetonitrile) beginning at 20% B for the first 1.8 min to 95% B at 13.4 min, held at 95% B for 0.5 min, back to 20% B at 14.5 min, and with re-equilibration of 3.5 min. The MS scan range was 100-1000 m/z with resolution of 60,000, standard AGC target, 70% RF lens, maximum injection time auto, with EASY-IC run-start on. The spray voltage was 2200 V, ion transfer tube temperature was 250 °C, and the vaporizer temperature was 175 °C and mild trapping was on. The sheath gas was 30 and aux gas 5 (arbitrary units). A targeted inclusion mass list with retention time windows was used for comparing the standard and sample fragmentation pattern with a 5-ppm mass tolerance as shown in Table B-2. The instrument limits of detection (LODs) and limits of quantification (LOQs) for targeted PFAS are provided in Table B-3.

3.2.4 Microbial community analysis

To provide insights on the role of native microbial communities in FOSA biotransformation in the investigated contaminated and pristine soils, duplicate microcosm samples at three sampling

points (day 0, 154, and 308) were collected from Loring and Hudson live treatments and positive controls for microbial community analysis. Sample DNA extraction was performed using DNeasy PowerSoil Pro Kit (Qiagen, Hilden, Germany) according to the manufacturer's instructions. Amplification and sequencing of DNA samples were performed at the Alkek Center for Metagenomics and Microbiome Research at Baylor College of Medicine, following the method described previously.¹³⁵

3.3 Results and discussion

3.3.1 Experimental system

Throughout the 308-day incubations, the continuous consumption of DGBE was observed in Loring and Hudson soil bioactive microcosms (i.e., live treatments and positive controls), in which multiple amendments of 5-10 mM DGBE were made (Figure B-1). In contrast, no obvious change in DOC concentration was observed in abiotic controls (Figure B-1). These results suggested that aeration was sufficient to support the growth of aerobic microorganisms (i.e., DGBE biodegradation) in both soils. Moreover, no differences in biodegradation rates of DGBE were observed between live treatments and positive controls (Figure B-1), indicating that the addition of FOSA and/or the formation of FOSA biotransformation products (e.g., PFOS) did not negatively impact the substrate consumption by the native microbial communities in Loring and Hudson soils.

The background levels of legacy PFAS in the contaminated Loring soil has been reported previously.¹³⁵ PFOS was found as the predominant PFAS in the Loring soil, with around 3.4 nmol/g dw. Although FOSA concentration was not reported in that study, it could be approximately determined as 0.06 nmol/g dw from the day 0 positive control samples of Loring microcosms in the present study (Table B-4). The total mass of FOSA initially spiked into live treatments and abiotic controls was 30-40 folds greater than the legacy FOSA in Loring soil (Table B-4). The high spiked amounts allowed for the identification and quantification of FOSA transformation products. In contrast to Loring soil, all the targeted PFAS was below the LODs in Hudson soil. Therefore, Loring and Hudson soils were hereafter sometimes referred to as contaminated and pristine soils, respectively. The investigation of FOSA biotransformation in these two soil microcosms were to reveal if previous exposure to PFAS contamination for native microbial community affected the biotransformation behavior.

As shown in Figure 3-1, 95.2 ± 7.8 mol% and 93.0 ± 4.3 mol% of the initially spiked FOSA remained in Loring and Hudson abiotic controls, respectively, with no significant changes ($p > 0.05$) over the 308-day incubation period, indicating the integrity of the experimental system and the efficacy of extraction methods used in the present study, and that FOSA was stable under abiotic experimental conditions.

3.3.2 Biotransformation of FOSA in Loring and Hudson soil microcosms

3.3.2.1 Biotransformation rates. In the live treatments of Loring soil microcosms, a gradual decrease in the initially spiked FOSA was observed during the 308-day incubation, with 54.7 ± 3.0 mol% of spiked FOSA remaining at the end (Figure 3-1A). The half-life ($t_{1/2}$) was determined to be 335.1 days by fitting 7 data points using a first-order kinetic model (coefficient of determination $R^2 = 0.92$). Biotransformation of legacy FOSA was not appreciated in positive controls, where the total mass of FOSA remained constant (0.6-0.8 nmol) during the incubation (Table B-4). The low bioavailability of the small amount of legacy FOSA (>90 mol% of mass partitioned in the solid phase) likely restrained the biotransformation. Surprisingly, a faster biotransformation of FOSA was observed in the pristine soil (i.e., Hudson soil), with 32.7 ± 5.2 mol% of initially spiked FOSA remaining in live treatments after the 308-day incubation (Figure 3-1B). The half-life was calculated to be 203.0 days ($R^2 = 0.99$), indicating the FOSA biotransformation rate in Hudson soil was about 1.7-fold faster than that in Loring soil. One of the reasons contributing to a faster biotransformation in Hudson soil could be the higher bioavailability of FOSA to Hudson soil microbial community than Loring's. Classified as a Loam/Sandy Loam, Loring soil has a higher organic carbon (OC) content of $3.5 \pm 0.1\%$ than Hudson soil ($1.1 \pm 0.0\%$) (Table B-1). The higher OC content likely resulted in a greater partitioning of spiked FOSA into the solid phase of Loring soil microcosms (Table B-5), which reduced the bioavailability of FOSA to the microorganisms. During the 308-day incubation, 88.6-91.8 mol% of FOSA in the Loring soil live treatments was in the solid phase, whereas only 69.6-82.7 mol% of FOSA partitioned into the solid phase of Hudson live treatments (Table B-5). In addition, the differences in microbial community compositions could also lead to the different biotransformation rates, which will be discussed in the later sections.

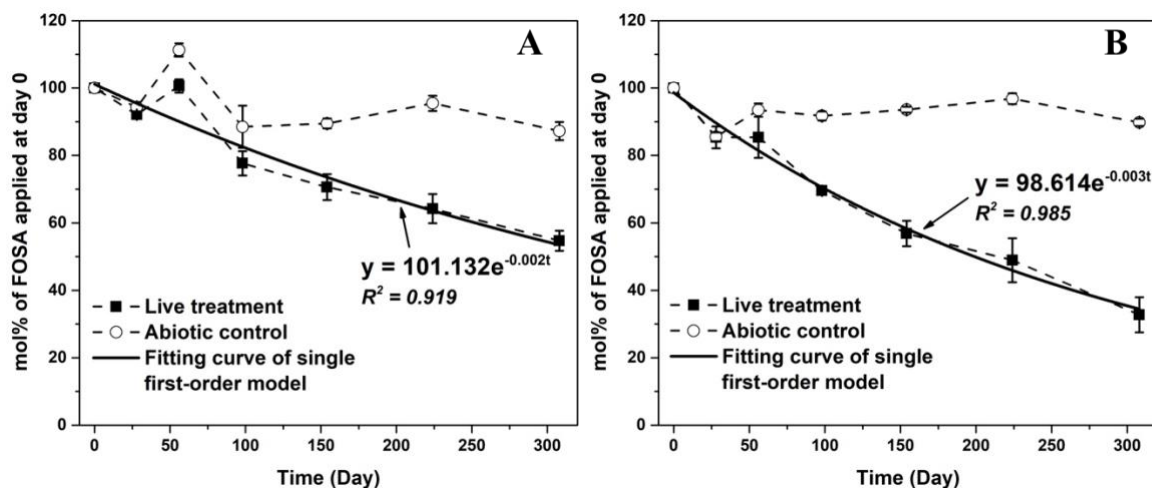


Figure 3-1. Changes in molar ratios of residual FOSA during aerobic biotransformation in Loring (Panel A) and Hudson (Panel B) soil microcosms. Error bars represent the standard deviation of triplicate live treatment microcosms, and of duplicate control microcosms.

3.3.2.2 Quantification of biotransformation products and mass balance. Analysis of samples collected from Loring and Hudson soil microcosms indicated the production of PFOS which was previously observed as a biotransformation product of FOSA.^{35,36,103–105,133} In the live treatments of Hudson soil microcosms, the formation of PFOS was observed at day 28 with a molar yield of 1.7 ± 0.1 mol% (Figure 3-2B). Then, PFOS was continuously produced, reaching a molar yield of 29.2 ± 7.9 mol% at day 224 (Figure 3-2B). During day 224 to day 308, PFOS yield stayed relatively constant, and the final yield was 29.5 ± 3.8 mol% (Figure 3-2B). PFOS was below LODs in the abiotic controls and positive controls throughout the experiment, suggesting that PFOS production only resulted from the biotransformation of FOSA in Hudson soil. Since PFOS was the predominant legacy PFAS in the contaminated Loring soil, high abundance of PFOS was detected in all Loring soil microcosms, with a total mass ranging from 47.0 nmol to 57.9 nmol (Table B-4). Therefore, the production of PFOS by FOSA biotransformation in Loring soil was determined by subtracting the PFOS mass in the positive controls from that in the live treatments (Table B-4). As shown in Figure 3-2A, the production of PFOS was observed at day 56, then gradually increased to 25.6 ± 3.4 mol% at day 154. The level of PFOS decreased slightly afterwards, and was determined to be 21.6 ± 5.2 mol% by day 308 (Figure 3-2A). Cautions should be taken regarding these calculated molar yields of PFOS, since the high background level of PFOS in Loring soil and slight variations in PFAS analysis on different batches of samples complicated the assessment of the PFOS yield resulting from the FOSA biotransformation. For example, a 1-nmol variation in

PFOS mass would lead to a difference of 4.2 mol% in molar yield, given the total mass of initially spiked FOSA (i.e., 24 nmol). Overall, the PFOS yield in Loring soil was slightly lower than that in Hudson soil (Figure 3-2), which is consistent with the observation that less of spiked FOSA was biotransformed in Loring soil than Hudson soil (Figure 3-1).

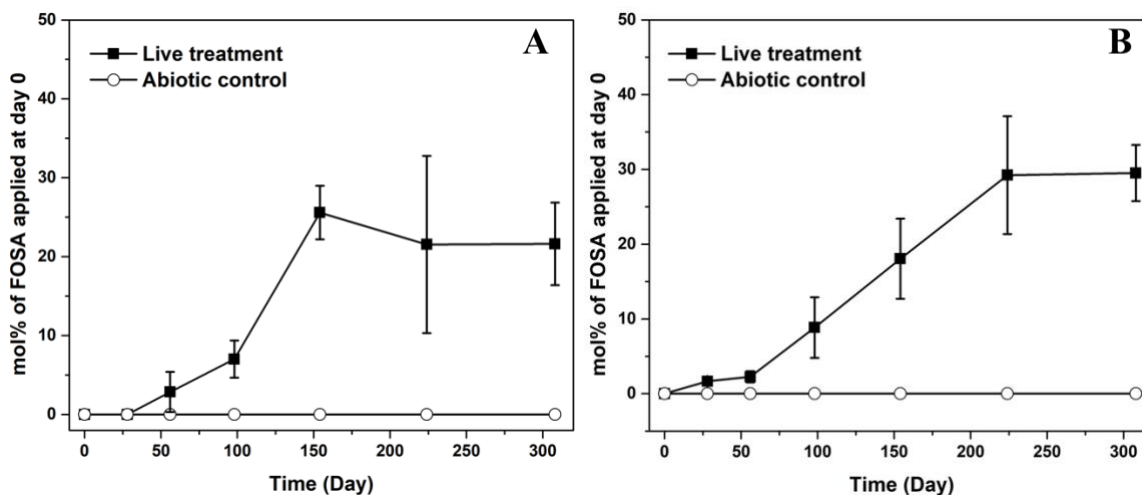


Figure 3-2. The formation of PFOS during FOSA aerobic biotransformation in Loring (Panel A) and Hudson (Panel B) soil microcosms. Error bars represent the standard deviation of triplicate live treatment microcosms, and of duplicate control microcosms.

At the end of the biotransformation experiments, 45.3 ± 3.0 mol% and 67.3 ± 5.2 mol% of spiked FOSA was biotransformed in Loring and Hudson soil microcosms (Figure 3-1), whereas PFOS formation only accounted for 21.6 ± 5.2 mol% and 29.5 ± 3.8 mol% of the initially spiked mass (Figure 3-2). As good mass recoveries were obtained from Loring and Hudson soil abiotic controls (95.2 ± 7.8 mol% and 93.0 ± 4.3 mol%, respectively) throughout the experiments, the incomplete mass balance in the live treatments was likely caused by the formation of other biotransformation products that were not quantified, or the irreversible bindings of FOSA and/or PFOS to the biomass. Previously studies reported that perfluorooctane sulfinate (PFOSI) was a key intermediate during the biotransformation of FOSA to PFOS.^{35,103} PFOSI was not quantified in the present study due to the unavailability of the authentic chemical standard. Regardless, PFOSI was likely formed in Loring and Hudson soil microcosms, based on the observed greater mass loss in Hudson soil (37.8 mol% loss) than Loring soil (23.7 mol% loss), which could be explained by the increased extent of FOSA biotransformation (Figure 3-1) and the associated greater PFOSI formation in Hudson soil.

3.3.3 Comparison of the biotransformation of FOSA and FOSA precursors

To provide more understandings of the biotransformation kinetics of FOSA and the associated PFOS yields in the environment, prior and current studies investigating the biotransformation of FOSA are summarized (Table 3-2).^{133,134} Given a limited number of studies on direct FOSA biotransformation,^{133,134} those previous studies that investigated the biotransformation of other sulfonamide derivatives which were reported as FOSA precursors were also included (Table 3-2).^{34-36,103-105,128} Those precursors included EtFOSE, EtFOSA, and perfluorooctane sulfonamido betaine (PFOSB). The half-lives of those precursors and FOSA during the biotransformation, if reported, were listed (Table 3-2). Compared to its precursors, FOSA showed a higher microbial stability in activated sludge,³⁵ wetland plants,¹⁰⁵ and aerobic soils.^{34,36} The results might explain the frequent detection of FOSA rather than those precursors (i.e., EtFOSE, EtFOSA, PFOSB) in the contaminated soils,^{14,137} surface water,^{97,137} and groundwater.¹⁴ Regardless of the potential persistence in the environment, large variations in the biotransformation rate of FOSA are also observed (Table 3-2). While shorter half-lives of FOSA ranging from 9.2 to 39 days were reported in three different environmental matrices (i.e., activated sludge,³⁵ aerobic soil,¹⁰⁴ and wetland plant microcosm¹⁰⁵), half-lives up to 712 days³⁶ and >1000 days³⁴ were measured or predicted in other aerobic soils. In the present study, a half-life of 203.0-335.1 days which lied in between the low and high values reported in prior studies, was observed in two distinct aerobic soils (i.e., contaminated and pristine soils), further supporting the potential persistence of FOSA in the soil compartment.

PFOS has been always reported as the final biotransformation product of sulfonamide derivatives (e.g., FOSA and FOSA precursors).^{34-36,103-105,128} However, the yields of PFOS from those biotransformation varied (Table 3-2). In previous studies, low PFOS yields (0.4-12 mol%) were observed under various incubation conditions (Table 3-2), with one exception that 85.1 mol% PFOS was formed during the biotransformation of EtFOSA in wetland plant microcosms.¹⁰⁵ In the present study, relatively high molar yields of PFOS (21.6-29.5 mol%) from FOSA biotransformation were observed in Loring and Hudson soils (Table 3-2). The high PFOS yields might be partially attributed to a long-term incubation (i.e., 308 days) performed in this study, confirming that FOSA could serve as a long-term source to PFOS in the environment.

Table 3-2. An overview of the prior and current studies investigating biotransformation of FOSA and FOSA precursors.

Parent compound	Microcosm	Incubation duration	Estimated t _{1/2} of parent compound	Estimated t _{1/2} of FOSA	PFOS yield (mol%)	Reference
EtFOSE	Activated sludge	10 d	0.7 d	9.2 d	N/A	35
EtFOSE	Marine sediment	120 d	44 d (25 °C); 160 d (4 °C)	N/A	12% (25 °C); 0.4% (4 °C)	128
EtFOSE	Aerobic soil	180-210 d	25.2-30.8 d	35.6-39 d	1.1-5.5%	104
EtFOSE	Aerobic soil	105 d	9.6 d	712 d	7.9%	36
EtFOSA	Aerobic soil	182 d	13.9 ± 2.1 d	N/A	4.0 %	103
EtFOSA	Wetland plants	91 d	0.5 d	39 d	85.1%	105
PFOSB	Aerobic soil	90 d	675 d	>1000 d	1.5%	34
FOSA	Groundwater and soil	49 d	/	N/A	0.5-4.9%	133
FOSA	Aerobic soil	30 d	/	N/A	N/A	134
FOSA	AFFF-impacted soil	308 d	/	335.1 d	21.6 %	This study
FOSA	Aerobic soil	308 d	/	203.0 d	29.5%	This study

N/A: Not available.

3.3.4 Microbial communities in Loring and Hudson soil microcosms

3.3.4.1 Diversity and Richness. The mapped reads of 16S rRNA gene amplicons from Loring and Hudson soil microcosms varied in the range of 4606 to 8298 (Table B-6). To facilitate the comparison of diversity and richness of microbial community, the number of reads in all samples was rarefied to the lowest value within the plateau range of the rarefaction curves. The quality-filtered reads were then clustered into operational taxonomic units (OTUs) at a 97% similarity level. The number of OTUs in all samples ranged from 150 to 687 (Table B-6).

The alpha diversity (i.e., mean diversity of species in a community¹³⁸) and species richness, (i.e., the number of species or OTUs present in a community) of Loring and Hudson soil microbial community was investigated using the Shannon and Simpson, and Chao1 indices, respectively

(Table B-6). The overall diversity of the microbial community native to Loring soil is substantially higher than that in Hudson soil, as the Shannon (5.85 ± 0.07 vs. 4.87 ± 0.05), Simpson (0.99 ± 0.00 vs. 0.98 ± 0.00), and Chao1 (1019.8 ± 30.8 vs. 586.6 ± 35.6) indices are much higher in the day 0 samples from Loring soil microcosms than Hudson soil microcosms (Table B-6). The higher diversity in Loring soil might be partially attributed to a more sufficient carbon sources for the microbial growth at the site; the total organic carbon content in Loring soil is about 3.5% which is more than 3-fold greater than that in Hudson soil (Table B-1). After the biostimulation with amendment of DGBE over 308 days, the microbial diversity and richness of both Loring and Hudson soil microbial communities decreased dramatically, as indicated by lower Chao1, Shannon, and Simpson indices at day 154 and day 308 samples relative to day 0 samples (Table B-6). Such decreases might be due to the biased stimulated growth of certain microbial species over others by the amendment of DGBE.

In Loring or Hudson soil microcosms, significant differences ($p < 0.05$) in Chao1, Shannon, or Simpson indices were not found in day 154 or day 308 samples between the live treatment (85 $\mu\text{g/L}$ FOSA spiked) and the positive control (0 $\mu\text{g/L}$ FOSA spiked) (Table B-6). Results indicate that the presence of spiked FOSA and biotransformation products did not significantly alter the microbial diversity in the present study. Previous studies reported that microbial diversity in river sediment and soil was reduced by the exposure to PFAS compounds (e.g., PFCAs).^{139–141} However, the PFAS concentrations in those studies were much higher (e.g., 15 mg/L) than that in the present study (i.e., 85 $\mu\text{g/L}$).^{139–141} Principle coordinate analysis (PCoA) was also analyzed on the Weighted Unifrac distance matrices as a measurement of beta diversity to visualize microbial community alteration among the different treatments in Loring and Hudson microcosms. The negligible impact of spiked FOSA on overall diversity is further supported by the obvious grouping of samples from the live treatment and positive controls (Figure B-2). Moreover, a separation of Loring and Hudson soil samples revealed the differences between the microbial community compositions at the two sites (Figure B-2).

3.3.4.2 Shifts in microbial community compositions. The microbial community composition in Loring and Hudson soils was further analyzed on various taxonomic levels. A total of 35 classified phyla in the domain Bacteria and 4 phyla in the domain Archaea were shared. Figure 3-3 shows the relative abundance of microbial community composition at the phylum level in Loring

and Hudson soil microcosms. In general, Proteobacteria was the most dominant phylum in Loring and Hudson soils, especially after the bioaugmentation (relative abundance >40% in day 154 and day 308 samples) (Figure 3-3). Prior studies identified Proteobacteria as the predominant phylum in aerobic soils and river sediments that were contaminated by PFAS.^{141–143} In addition, an obvious increase (12.5–65.7%) in Proteobacteria was observed previously in wetland slurry and fresh water following exposure to PFAS.^{28,144} Those results indicate that Proteobacteria might be more tolerant to PFAS than other phyla. In the present study, two classes of Proteobacteria, Alpha- and Gamma-proteobacteria, were found in Loring and Hudson soils; microorganisms belonging to the two classes were reported to degrade various hydrocarbon compounds,^{145,146} as well as PFAS (e.g., fluorotelomer compounds).^{113,115,147,148} In addition, Actinobacteriota, Chloroflexi, Acidobacteriota, and Planctomycetota were observed as primary phyla in Loring and Hudson soil samples (Figure 3-3). Some genera from Actinobacteriota were reported as PFAS degraders; for example, *Mycobacterium*, *Gordonia*, *Rhodococcus*, and *Dietzia* have been shown to biodegrade 6:2 fluorotelomer alcohol or 6:2 fluorotelomer sulfonate.^{110–112,114,147} Chloroflexi, Acidobacteriota, and Planctomycetota were previously found to be enriched in the environment where chlorinated solvents or PFAS were present.^{28,105,149} Taken together with prior work, microorganisms belonging to the aforementioned phyla might play a role in the biotransformation of FOSA observed in this study.

Distinct differences in the relative abundances of phyla discussed above (i.e., Proteobacteria, Actinobacteriota, Chloroflexi, Acidobacteriota, and Planctomycetota) were not observed in day 154/day 308 samples between the live treatment (85 µg/L FOSA spiked) and the positive control (0 µg/L FOSA spiked) (Figure 3-3), suggesting that these phyla were not sensitive to the spiked FOSA and associated transformation products. In contrast, a substantially greater relative abundance of Cyanobacteria was found in the live treatments than positive controls in both Loring and Hudson soil microcosms (Figure 3-3). In the absence of FOSA, relative abundances of Cyanobacteria were $3.1 \pm 0.6\%$ and $2.2 \pm 0.3\%$ at day 154 and day 308, respectively; whereas relative abundances increased to $7.3 \pm 2.3\%$ and $4.6 \pm 2.4\%$, respectively, in the FOSA-spiked Loring soil microcosms. Similar increase was also observed in Hudson soil microcosms with $0.6 \pm 0.1\%$ of Cyanobacteria in day 308 samples from live treatment, compared to $0.1 \pm 0.1\%$ from positive control. Another phylum, Bacteroidota was also found with a substantially greater relative abundance in the live treatment than positive control in Hudson soil microcosms (Figure 3-3). For

example, relative abundances of Bacteroidota were $1.4 \pm 0.6\%$ and $0.8 \pm 0.2\%$ at day 154 and day 308, respectively in the positive controls while were $3.3 \pm 0.8\%$ and $8.0 \pm 3.2\%$, respectively in the live treatments. These results indicate that Cyanobacteria and Bacteroidota were relatively more tolerant to FOSA and/or the associated transformation products. Bacteroidota were reported to be associated with diesel- and PFAS-contaminated soils,^{139,146,150} and Cyanobacteria species were shown to degrade aromatic hydrocarbons and xenobiotics using various enzymes.¹⁵¹

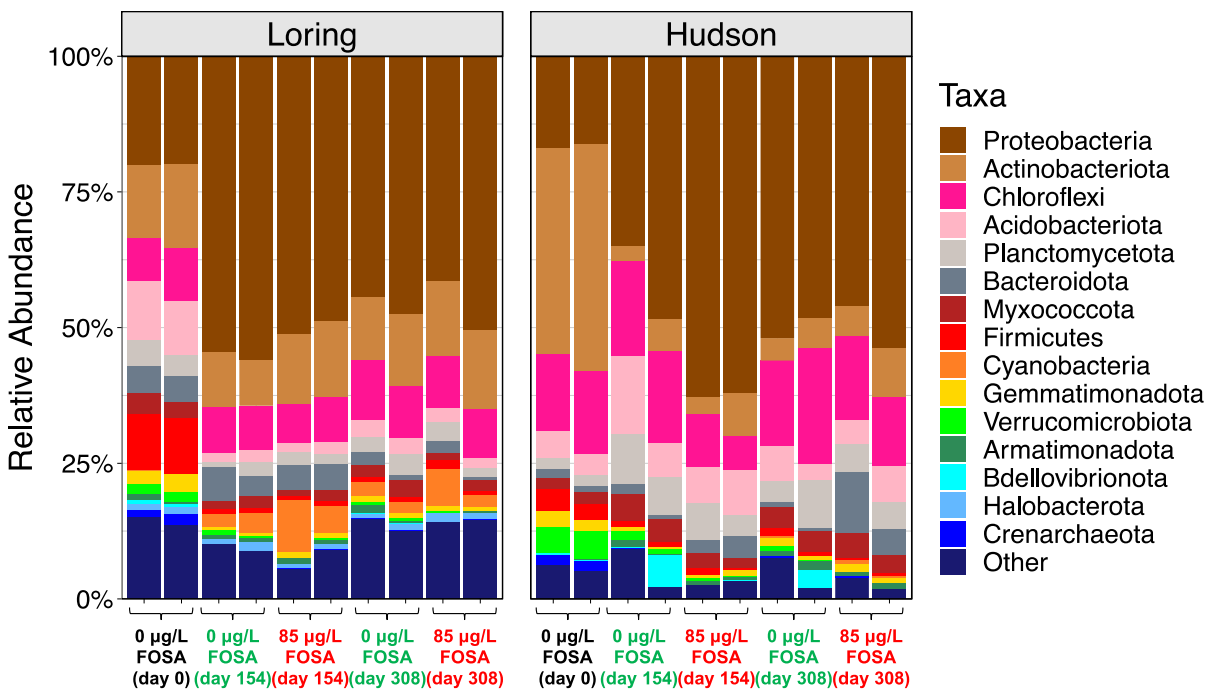


Figure 3-3. The relative abundance of microbial community composition at the phylum level in Loring (left) and Hudson (right) soil microcosms.

On the genus level, a total of 568 genera were identified in the samples from Loring and Hudson microcosms. The relative abundances of predominant 19 genera are shown in Figure B-3. During the incubation, *Afipia* was the most dominant genus in Loring and Hudson soil microcosms, with a relative abundance of $20.7 \pm 5.9\%$ in day 154 and day 308 samples (Figure B-3). Previous studies showed that *Afipia* strains were capable of degradation of various environmental contaminants (e.g., 1,4-dioxane, methanesulfonate, and haloacetic acids).¹⁵²⁻¹⁵⁴ Therefore, microorganisms in *Afipia* might be involved in the FOSA biotransformation in Loring and Hudson soils. The Welch t-test with Benjamini-Hochberg false discovery rate (FDR) for multiple test corrections was employed to compare the relative abundance of each genus in the live treatments and positive

controls. No genus was found to significantly (adjusted $p < 0.05$) increase in live treatments compared to positive controls in both Loring and Hudson soil microcosm samples (day 154 and day 308). Instead, *Pajaroellobacter* was found to significantly decrease in live treatments compared to positive controls in Loring soil microcosms. At day 154, the relative abundance of *Pajaroellobacter* was $0.0 \pm 0.0\%$ in live treatments compared to positive controls ($0.2 \pm 0.1\%$); at day 308, the relative abundance was $0.0 \pm 0.0\%$ in live treatments compared to positive controls ($0.6 \pm 0.0\%$). These results suggest that the relatively low concentration of spiked FOSA and associated biotransformation products may not exert much pressure on the microbial communities in Loring and Hudson soils. Regardless, *Pajaroellobacter* might be more sensitive to FOSA and transformation products such as PFOS.

3.4 Environmental implications

This study demonstrates that the biotransformation of FOSA in natural environment might be soil/site dependent. With a tendency to partition to the solid phase, the bioavailability of FOSA to the native microbial community appears to a critical parameter for the evaluation of FOSA biotransformation in the soil compartment. Thus, soil properties such as organic carbon content that could impact the sorption behaviors and bioavailability of FOSA need to be assessed. Moreover, the differences in microbial community compositions could also lead to the different biotransformation of FOSA. Microorganisms belonging to Proteobacteria, Actinobacteriota, Chloroflexi, Acidobacteriota, and Planctomycetota might play a role in the biotransformation of FOSA, while Cyanobacteria and Bacteroidota might be relatively more tolerant to FOSA and/or the associated transformation products. Overall, the findings in the present study suggest that evaluations of site geochemical and biological attributes are important towards achieving a better understanding of FOSA biotransformation in the field, as well as gaining insights into the management and remediation of contaminated sites.

Chapter 4 : Biotransformation of 8:2 Fluorotelomer Alcohol in Soil from Aqueous Film-Forming Foams (AFFFs)-impacted Sites under Nitrate-, Sulfate-, and Iron-reducing Conditions

This chapter was reproduced with permissions from Yan, P.-F.; Dong, S.; Manz, K. E.; Liu, C.; Woodcock, M. J.; Mezzari, M. P.; Abriola, L. M.; Pennell, K. D.; Cápiro, N. L. Biotransformation of 8:2 Fluorotelomer Alcohol in Soil from Aqueous Film-Forming Foams (AFFFs)-Impacted Sites under Nitrate-, Sulfate-, and Iron-Reducing Conditions. *Environ. Sci. Technol.* **2022**, 56, 19, 13728–13739.

© 2022 American Chemical Society.

4.1 Introduction

Aqueous film-forming foams (AFFFs) are water-based chemical mixtures that have been used since the 1960's to effectively extinguish hydrocarbon-fuel fires at airports and military bases.^{10,11} AFFFs contain various classes of per- and polyfluoroalkyl substances (PFAS),⁵⁵ and the repeated application of AFFF at fire training areas has resulted in high PFAS concentrations in soil and groundwater.^{14,155} Recently, a few studies have identified a wide variety of perfluoroalkyl acid (PFAA) precursors (referred to hereafter as “precursors”) as well as PFAAs in various AFFF formulations.^{12–15} PFAAs are persistent compounds that can cause adverse effects on human health,^{14,156,157} and they may come from direct release of AFFFs or from the transformation of AFFF-derived precursors.^{31–33,37} However, information on the environmental fate of precursors identified in AFFFs,^{12–15} including their susceptibility to biotransformation under conditions representative of natural groundwater environments, is limited, which complicates the management and remediation of AFFF-impacted sites.

The biotransformation of some AFFF-derived precursors have been investigated previously, and most of these studies were conducted under oxic conditions, utilizing microorganisms from activated sludge,^{23,24} river sediments,²⁵ and surface soils.^{31–34} In contrast, limited studies were conducted under anoxic conditions.^{25,37,38} The biotransformation of precursors under anoxic conditions was found to be distinctly different from that under oxic conditions. For instance, the half-life of 6:2 fluorotelomer alcohol resulting from the biotransformation under methanogenic conditions was reported as ca. 30 days,³⁸ which was much longer than that reported in aerobic activated sludge, sediment, and soil (i.e., 1-2 days).^{26,42,45} The PFAA yields under methanogenic

conditions were also at least 20-times lower than under oxic conditions.³⁸ The biotransformation of 6:2 fluorotelomer sulfonate occurred under oxic^{24,51} and nitrate-reducing conditions,⁵² with the most rapid transformation rate occurring in aerobic sediment;²⁵ whereas, transformations did not occur under sulfate-reducing²⁵ and methanogenic⁴⁰ conditions. Another precursor, 6:2 fluorotelomer thioether amido sulfonates, was reported to be biotransformed much more slowly under sulfate-reducing conditions³⁷ than under oxic conditions,³¹ with distinct biotransformation pathways observed between both conditions. These findings indicate that redox condition plays an important role in precursor biotransformation.

Fluorotelomer alcohols [FTOHs, $F(CF_2)_nCH_2CH_2OH$] are primary raw materials used to manufacture surfactants and polymeric materials with water- and oil-repelling properties.¹⁵⁸ The unique properties have led to the use of FTOH-based products in a wide variety of applications including AFFFs.¹⁵⁸ Measurements of source fingerprints of new generation AFFF formulations acquired in Norway,⁷⁴ and commercially available AFFFs generated between 2012 and 2013 in Switzerland have detected 8:2 FTOH,¹⁵⁹ with the concentrations ranging from 8 to 26.5 mg/L. Furthermore, FTOHs are likely present as byproducts during the synthesis of the fluorotelomer-based precursors.¹⁶⁰ Therefore, the detection and prevalence of 8:2 FTOH at AFFF-impacted sites is anticipated to increase. Previous studies have demonstrated that 8:2 FTOH “readily undergoes” or “susceptible to” biotransformation under oxic conditions in various environmental matrices, including activated sludge,^{23,150} brackish water,¹⁶¹ and pristine soils.^{43,47} PFAAs, including perfluorohexanoic acid (PFHxA) and perfluorooctanoic acid (PFOA), were reported as the stable biotransformation products. In contrast, little information is available on the anaerobic biotransformation of 8:2 FTOH. Sáez et al.¹⁶² did not observe the anaerobic biotransformation of 8:2 FTOH in municipal sewage sludge after a 9-week incubation. However, Zhang et al.³⁸ reported 8:2 FTOH biotransformation in digester sludge with a half-life of ca. 145 days. Moreover, Li et al.³⁹ found that 8:2 FTOH biotransformation in anaerobic activated sludge was rapid with a half-life of only ca. 5 days. All three studies investigated 8:2 FTOH biotransformation under methanogenic conditions, and the discrepancy observed among these studies was likely due to the differences between the microbial communities. To date, there is still a paucity of information on the biotransformation of 8:2 FTOH and potential pathways under other redox conditions representative of natural aquifer environment (e.g., nitrate-, iron-, and sulfate-reducing

conditions). Addressing this knowledge gap is essential to elucidate the fate and transformation of 8:2 FTOH in natural groundwater systems.

In the present study, the biotransformation of 8:2 FTOH was, for the first time, investigated under nitrate-, sulfate-, and iron-reducing conditions in laboratory microcosm reactors. The objective of this study was to evaluate the environmental fate of 8:2 FTOH under the conditions typical of AFFF-impacted sites. To this end, AFFF-impacted soil was collected from a former U.S. military base and used for the construction of the microcosms. The subsurface microbial communities in AFFF-impacted soil are expected to differ from those in activated sludge, river sediment, and aerated surface soil, and they may evolve to be more resistant to PFAS and more capable of transforming PFAS due to the historical exposure. Therefore, potentially distinct 8:2 FTOH biotransformation (e.g., rate, pathway, etc.) from those reported previously was hypothesized under these experimental conditions. The molar yields of known biotransformation products were determined in the microcosms under each redox condition. High-resolution mass spectrometry (HRMS) was also employed to identify potential unknown transformation products. Based on the findings of the current investigation and results from previous studies, the comprehensive biotransformation pathways for 8:2 FTOH under various redox conditions representative of natural environments were proposed.

4.2 Materials and methods

4.2.1 Microcosm Set-up

The soil used in this study was collected from an AFFF-contaminated location at the former Loring Air Force Base (Limestone, ME). Detailed information on soil collection, taxonomic classification, and physical and chemical property characterization (pH, moisture content, organic matter content, cation exchange capacity (CEC), soil particle size distribution) are provided in the Appendix C-section S1. To minimize the loss of volatile 8:2 FTOH and transformation products, a closed-system using Wheaton glass serum bottles (60-mL), aluminum crimp-sealed with rubber septa was adopted for microcosm set-up. In each reactor, 30 mL of growth medium¹³⁶ and 3 g (dry weight) of Loring soil were added. Sodium nitrate (20 mM), sodium sulfate (20 mM), and goethite (100mM, mineral of Fe(III) oxide-hydroxide) was added in each batch of microcosms as the electron acceptor under nitrate-, sulfate-, and iron-reducing conditions, respectively. Each batch of microcosms included two sets of live-spiked treatments, one set of abiotic control and one set

of positive control (See Table C-1, Appendix C). For live-spiked treatments, each bottle was spiked with ~170 $\mu\text{g/L}$ of 8:2 FTOH prepared in diethylene glycol butyl ether (DGBE), which is a primary organic solvent in AFFF that has been shown to serve as a microbial electron donor and carbon source.¹⁶³ One set of live-spiked treatment mimicked natural attenuation (NA treatment) where 5 mM DGBE was introduced as the solvent for 8:2 FTOH and as the sole external potential electron donor, while the other set mimicked biostimulation where 20 mM sodium lactate was added as an additional electron donor and carbon source in conjunction with DGBE to enhance the microbial growth (ED treatment). Abiotic controls were prepared similarly to live-spiked treatments, but 1 g/L NaN_3 was added to inhibit the microbial activity (effective concentration was determined by preliminary experiments, data not shown here). Abiotic controls were used to evaluate the potential abiotic transformation of 8:2 FTOH and/or legacy PFAS originally in the Loring AFB soil. For the positive controls, only DGBE (without 8:2 FTOH) was dosed into the bottles, and all other procedures were identical to the live-spiked treatments. The positive controls were used to monitor the background levels of legacy PFAS in the Loring soil, and their potential transformation products. All the microcosms were incubated at room temperature with 150 rpm shaking over ~400 days.

4.2.2 Sample Collection and Preparation

At each sampling point, triplicate bottles from live-spiked treatments and duplicate bottles from abiotic and positive controls were sacrificed for sampling. The headspace of each bottle was purged through a C_{18} cartridge (Maxi-Clean™, Alltech, Deerfield, IL) by flushing N_2 to capture 8:2 FTOH and potential volatile transformation products. Each C_{18} cartridge was eluted with methanol (5mL) for further PFAS analysis. The supernatant (0.5 mL) from each bottle was then collected and immediately mixed with 9.5 mL of methanol to avoid potential loss of volatile PFAS. The diluted sample was filtered with a 0.2- μm Corning® nylon syringe filter (Corning Inc., Corning, NY) into a 15-mL centrifuge tube for PFAS quantification of the microcosm aqueous phase. Subsequently, each bottle was shaken vigorously, and 1 mL of well-mixed slurry was collected for the measurements of geochemical parameters (e.g., SO_4^{2-} , NO_3^- , F^- , lactate, etc., details in Appendix C-S1). All remaining slurry along with the rubber septum were transferred into a 50-mL centrifuge tube. The bottle was rinsed with 5 mL of ultrapure water (18.2 $\text{M}\Omega\text{ cm}$) and the rinse water was combined with the slurry. After centrifugation at 4,000 rpm for 20 min, the supernatant was discarded, and the soil pellet was resuspended in 30 mL methanol and vortexed

for 30 min, followed by sonication at 60 °C in a water bath for 30 min. The methanol extract was collected after centrifugation and further filtered with a 0.22- μm Corning® nylon filter for quantification of sorbed PFAS from the septum and microcosm solid phases. The C₁₈ cartridge eluent, methanol-diluted aqueous samples, and methanol extracts of soil and septum were stored at -20 °C before PFAS analysis.

4.2.3 Targeted and Non-targeted PFAS Analysis

Targeted LC-MS/MS analysis was performed using a Waters ACQUITY ultra high-performance liquid chromatograph coupled with a Waters Xevo triple quadrupole mass spectrometer (UPLC-MS/MS) (Waters Corporation, Milford, MA). Each of the three phases described above were analyzed by LC-MS/MS separately. The target PFAS in the LC-MS/MS analysis are listed in Table C-2. PFAAs analysis was performed following established methods.¹⁶⁴ Analysis of 8:2 FTOH and its polyfluorinated biotransformation products was performed following the method reported by Szostek et al.¹⁶⁵ with no ammonium acetate addition in mobile phase, as FTOHs form adducts under negative electrospray ionization. In both methods, analyte separation was achieved using a Waters ACQUITY UPLC BEH C18 Column (130Å, 1.7 μm , 2.1 mm X 50 mm). The solvent gradient and detailed instrumental parameters are specified in Tables C-3 to C-6. The detection limits of target analytes are provided in Table C-7. To quantify 1H-perfluoroheptane in each of the three sample phases, targeted gas chromatography (GC)-HRMS was performed using a high-resolution Thermo Q Exactive Orbitrap MS equipped with a Thermo Trace 1300 GC and a TriPlus RSH Autosampler. Operational details for GC-HRMS are described in the Appendix C-S1.

Aqueous samples and soil methanol extracts collected from each treatment at select sampling time points were pooled for non-targeted LC-HRMS analysis. Sampling time points were selected based on targeted LC-MS/MS analysis results to include the samples collected before and after the occurrence of 8:2 FTOH biotransformation. Non-targeted LC-HRMS analysis was performed using a Thermo QExactive HF-X Orbitrap MS equipped with a Vanquish UHPLC to provide high resolution, high mass accuracy, and high sensitivity over a large mass to charge (m/z) range. Detailed procedures for LC-HRMS are described in the Appendix C-S1.

4.2.4 Microbial community analysis

To better understand the effects of redox condition on the biotransformation of 8:2 FTOH, microbial community analysis was performed on samples from live-spiked treatments and positive controls under each redox condition. Duplicate soil samples were collected at the beginning and the end of incubation, and DNA was extracted using DNeasy PowerSoil Kit (Qiagen, Hilden, Germany) according to the manufacturer's protocols. Amplification and sequencing of soil DNA samples were performed at the Alkek Center for Metagenomics and Microbiome Research at Baylor College of Medicine. The V4 region of the 16S rRNA gene was amplified by polymerase chain reaction (PCR) using barcoded primer sets (515F/806R) and sequenced on the MiSeq platform (Illumina, San Diego, CA) using a 2×250 bp paired-end protocol.¹⁶⁶ The read pairs were demultiplexed based on the unique molecular barcodes, and reads were merged using the USEARCH v7.0.1090.¹⁶⁷ The 16S rRNA gene sequences were clustered into Operational Taxonomic Units (OTUs) at a similarity cutoff value of 97% using the UPARSE algorithm.¹⁶⁸ The generated sequences were mapped against the latest SILVA Database.¹⁶⁹ The ATIMA (Agile Toolkit for Incisive Microbial Analyses) was used to analyze and visualize trends in taxa abundance, alpha diversity, and beta diversity as they relate to sample metadata.

4.3 Results and discussion

Throughout the experiments, nitrate-, sulfate-, and iron-reducing activities were confirmed in the respective microcosms by monitoring the consumption of electron donor (i.e., lactate and/or DGBE) and electron acceptor (i.e., NO_3^- , SO_4^{2-} , or Fe(III)/Fe(II)) (Figures C-1, C-2, and C-3, Appendix C). Additional information related to the establishment of nitrate-, sulfate-, and iron-reducing microcosms is provided in Appendix C-S2. A total of 19 PFAS compounds were quantified in all microcosms (Table C-2). Some PFAS were detected in the day 0 samples, thus the background levels of legacy PFAS in Loring soil were determined (Table C-8). Additional discussion on the measurement of legacy PFAS in Loring soil is provided in Appendix C-S3. As shown in Figures 4-1 and 4-2, 94.9 ± 7.8 mol%, 88.1 ± 7.4 mol% and 90.7 ± 8.0 mol% of the initially spiked 8:2 FTOH remained in the abiotic controls of nitrate-, sulfate-, and iron-reducing microcosms, respectively, without significant changes ($p > 0.05$) throughout the experiments. These stable 8:2 FTOH concentrations under various abiotic experimental conditions verify the

integrity of the experimental system and the efficiency of the extraction method applied in the present study.

4.3.1 Biotransformation of 8:2 FTOH under nitrate-reducing conditions

4.3.1.1 Biotransformation rates. In the live-spiked treatments (i.e., ED and NA treatments), dramatic decreases in the spiked 8:2 FTOH were observed under nitrate-reducing conditions in the first 56-day incubations (Figure 4-1A). The half-life of 8:2 FTOH biotransformation in the NA treatment was calculated as ~36.5 days as determined by fitting 9 data points into a single first-order kinetic model (coefficient of determination $R^2 = 0.847$, Figure C-4). Amendment of 20 mM lactate (i.e., ED treatment) greatly enhanced the biotransformation rate by reducing the half-life of 8:2 FTOH to ~12.5 days ($R^2 = 0.931$, Figure C-4). Thus, the biostimulation of nitrate-reducing microorganisms with lactate as a supplemental and/or favorable electron donor and carbon source could promote more efficient biotransformation of 8:2 FTOH. Specifically, in the ED treatment, the residual 8:2 FTOH fraction decreased sharply from 99.9 ± 5.6 mol% at day 7 to 5.6 ± 3.3 mol% at day 28 and was further reduced to 0.4 ± 0.2 mol% by day 154 (Figure 4-1A). The residual 8:2 FTOH in the NA treatment, by comparison, did not decrease in the first 28 days. However, a rapid decrease was observed in the following 28 days with only 10.7 ± 3.0 mol% remaining by day 56, which was then gradually decreased to 0.2 ± 0.2 mol% by the end of incubation (Figure 4-1A). The relatively fast biotransformation of 8:2 FTOH under nitrate-reducing conditions in Loring soil, especially with lactate amendment, was comparable with those observed in aerobic soils (half-lives ranging from one to four weeks),^{43,170} and was much faster than previously documented in digester sludge under methanogenic conditions (half-life of ca. 145 days).³⁸

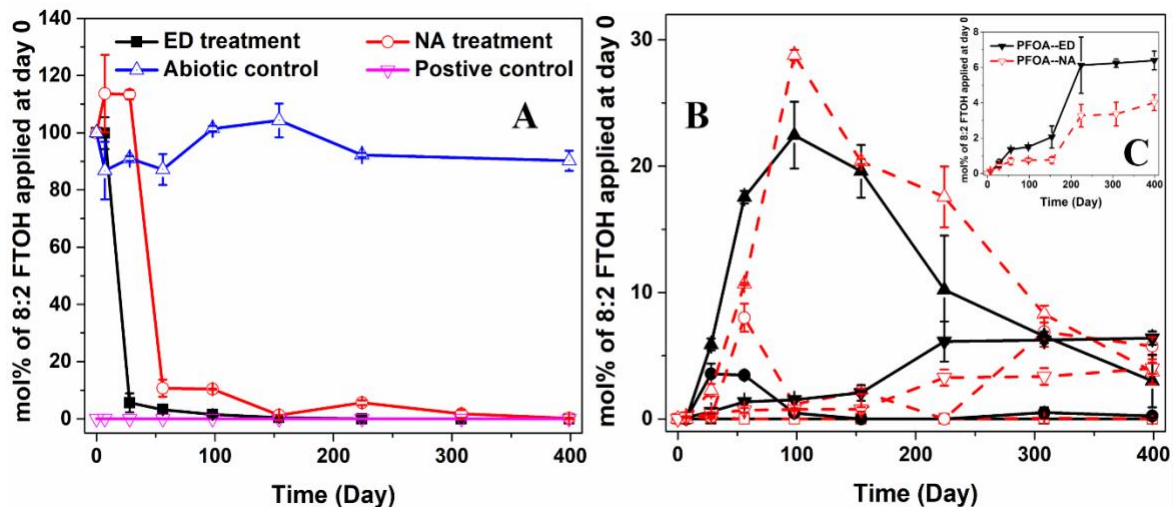


Figure 4-1. Changes in molar ratios of residual 8:2 FTOH during biotransformation under nitrate-reducing conditions in the electron-donor (ED) treatment, natural attenuation (NA) treatment, abiotic controls, and positive controls microcosms (Panel A). Molar yields of 8:2 FTOH biotransformation products (squares: 8:2 FTCA, circles: 8:2 FTUA, up triangles: 7:2 sFTOH, down triangles: PFOA) in the ED (solid black lines and solid symbols) and NA treatments (dash red lines and open symbols) (Panel B). Panel C is a zoom view of B, showing the time course trends of PFOA molar yields.

4.3.1.2 Biotransformation products quantified by LC-MS/MS targeted analysis. As shown in Figure 4-1B, 8:2 fluorotelomer saturated carboxylic acid (8:2 FTCA), 8:2 fluorotelomer unsaturated carboxylic acid (8:2 FTUA), and 7:2 secondary fluorotelomer alcohol (7:2 sFTOH), which were previously reported as polyfluorinated intermediates of 8:2 FTOH,^{39,43,46} were quantified in both ED and NA treatments during 8:2 FTOH biotransformation under nitrate-reducing conditions. None of these compounds were above the limits of detection (LOD) in abiotic and positive controls. The most abundant transformation product was 7:2 sFTOH, which reached peak molar yields of 22.5 ± 2.6 mol% and 28.8 ± 0.4 mol% of the initially applied 8:2 FTOH by day 98 in ED and NA treatments, respectively. Concentrations of 7:2 sFTOH then decreased to 10.2 ± 4.3 mol% and 17.6 ± 2.4 mol% at day 224, further to 3.0 ± 2.1 mol% and 3.7 ± 1.0 mol% at the end of incubation, respectively (Figure 4-1B). In contrast, 8:2 FTCA was only detected sporadically in the NA treatment (< 0.2 mol% of initially applied 8:2 FTOH) and was below the LOD in the ED treatment (Figure 4-1B), likely due to its rapid conversion to other products (e.g., 8:2 FTUA). In the ED treatment, 8:2 FTUA was produced with a peak molar yield of 3.6 ± 0.8 mol% by day 28, then later decreased to low levels (< 0.5 mol%). While in the NA treatment, 8:2

FTUA reached a peak molar yield of 8.0 ± 1.1 mol% by day 56 followed by some fluctuations and settled at 5.8 ± 0.7 mol% by the termination of the experiment (Figure 4-1B). The molar yields and time trends of these three polyfluorinated intermediates in the present study were consistent with 8:2 FTOH biotransformation reported in aerobic soils.⁴³ Another previously reported major polyfluorinated product of 8:2 FTOH was 7:3 acid;^{38,39,43} however, it was not measured as a product in this study. Although 7:3 acid was detected in ED and NA treatments, it was also detected in abiotic and positive controls without significant differences ($p > 0.05$) throughout the incubations (Figure C-5). This finding is in contrast to most previous studies on aerobic and anaerobic 8:2 FTOH biotransformation where 7:3 acid was a major stable transformation product.^{29,38,43} Only one study found that 7:3 acid and its known direct precursor, 7:3 U acid (7:3 unsaturated acid, $F(CF_2)_7CH=CHCOOH$), were absent in the biotransformation of 8:2 FTOH by an alkane-degrading strain, *Pseudomonas oleovorans*.¹⁵⁸ The researchers assumed that *P. oleovorans* might lack microbial enzymes capable of defluorinating 8:2 FTUA to 7:3 U acid and then reducing the latter to 7:3 acid. Therefore, the formation of 7:3 acid was absent or extremely minimal during 8:2 FTOH biotransformation under nitrate-reducing conditions could be interpreted by the lack of those enzymes responsible for 7:3 acid formation in the nitrate-reducers in Loring soil.

As potential perfluorinated transformation products of 8:2 FTOH,^{39,43} C4 to C9 perfluoroalkyl carboxylates (PFCAs) were detected in all treatments, indicating that these legacy PFAS were present in Loring soil (Figure C-5). However, a significant increase ($p < 0.05$) was only observed for PFOA after comparing the concentrations of these PFCAs in ED and NA treatments to positive controls (Figure C-5), demonstrating that PFOA was formed during 8:2 FTOH biotransformation under nitrate-reducing conditions. Although the concentrations of other PFCAs including perfluorobutanoic acid (PFBA), perfluoropentanoic acid (PFPeA), perfluorohexanoic acid (PFHxA), and perfluoroheptanoic acid (PFHpA) in live-spiked treatments were not significantly different from those in positive controls, some PFCAs might be biotransformation products as reported previously under both oxic^{29,47} and anoxic conditions,^{39,44} but with yields that were too low to be distinguished from the background levels in Loring soil. After subtracting the PFOA mass in positive controls at each sampling point, the molar yields of PFOA in both ED and NA treatments continued to increase during the incubations, reaching to 6.4 ± 0.5 mol% and 4.0 ± 0.4 mol% of the initially applied 8:2 FTOH at the end of incubation, respectively (Figures 4-1B and

4-1C). The PFOA yields measured here are much less than those previously reported in aerobic soils over ca.7 months incubation,⁴³ but substantially higher than yields measured in digester sludge under methanogenic conditions over the 181-day study.³⁸ In addition, higher molar yield of PFOA observed in the ED treatment compared to the NA treatment implies that the presence or amendment of additional and/or favorable electron donor and carbon source (e.g., lactate) at AFFF-impacted sites will likely result in more extensive and/or more rapid release of PFCAs to the environmental matrices under nitrate-reducing conditions.

4.3.1.3 Biotransformation products identified by LC-HRMS. In ED and NA treatments under nitrate-reducing conditions, total mass recovery of 8:2 FTOH and the transformation products quantified by LC-MS/MS decreased sharply during the periods when 8:2 FTOH was rapidly transformed (Figures 4-1A and C-6). Total mass recovery then further gradually decreased to only ca.10.0 mol% of the initially applied 8:2 FTOH by the end of incubation. Such a decrease was not observed in the abiotic controls (Figure C-6). The irreversible binding of 8:2 FTOH and/or biotransformation products in the soil, which has been reported in previous 8:2 FTOH studies in soils, resulted in those compounds not being recovered.^{43,47,171} This binding process, moreover, was likely catalyzed by microbial enzymatic activities,⁵⁰ which explains the overall satisfactory molar recovery (86.8-104.3 mol%) in abiotic controls. In addition, the formation of unknown 8:2 FTOH biotransformation products could contribute to the low mass recovery. Therefore, non-targeted LC-HRMS analysis was performed on the samples from each treatment under nitrate-reducing conditions, and a total of four potential biotransformation products of 8:2 FTOH were identified (Table C-9).

Tentatively identified as a biotransformation product of 8:2 FTOH at confidence level 3 (assigned based on the Schymanski Scale,¹⁷² detailed in Appendix C-S1), based on MS² spectrum (Figure C-7A), 7:3 U acid (m/z 438.9822) accumulated to a similar amount in ED and NA treatments after a 32-week incubation, but remained at a very low level in abiotic and positive controls under nitrate-reducing conditions (Figure C-8). In previous studies, 7:3 U acid has been recognized as a precursor to 7:3 acid under oxic and methanogenic conditions,^{38,43,46,158} and the absence of 7:3 U acid was attributed to the fast biotransformation to 7:3 acid.^{38,43} In this study, however, the formation of 7:3 acid was not observed in either ED or NA treatments under nitrate-reducing conditions, in spite of the gradual accumulation of 7:3 U acid. This finding was likely

due to a lack of microbial enzymes (e.g., reductase) capable of converting 7:3 U acid to 7:3 acid by the microorganisms in Loring soil under nitrate-reducing conditions.

In nitrate-reducing microcosms, 3-OH-7:3 acid ($\text{F}(\text{CF}_2)_7\text{CHOHCH}_2\text{COOH}$, m/z 456.9930) was identified as another biotransformation product of 8:2 FTOH (confidence level 2, based on MS^2 (Figure C-7B)). The authentic standard of 3-OH-7:3 acid was not available for further structure verification. This product gradually accumulated in only ED and NA treatments under nitrate-reducing conditions, as indicated by the increase in peak area over time (Figure C-9A). Only one previous study identified 3-OH-7:3 acid as a product during 8:2 FTOH biotransformation, and it was reported to form by the conversion of 7:3 U acid in aerobic soils.⁴³ This study represents the first reported identification of 3-OH-7:3 acid as a product during 8:2 FTOH biotransformation under nitrate-reducing conditions. During biotransformation, 3-OH-7:3 acid may be formed by the oxidation of 7:3 U acid by a hydratase type enzyme.

Non-targeted analysis also suggested the presence of a biotransformation product with potential structure as 7:3 U amide ($\text{F}(\text{CF}_2)_7\text{CH}=\text{CHCONH}_2$, m/z 437.9975). However, the MS^2 fragmentation data of this product was not available, resulting in the identification at confidence level 4. It was reported that 7:3 U amide was a potential product during 8:2 FTOH aerobic biotransformation,⁴⁶ but this compound was not observed in subsequent aerobic or anaerobic 8:2 FTOH biotransformation studies.^{38,39,43,47} In the present study, increases in the peak area of 7:3 U amide were observed only in ED and NA treatments under nitrate-reducing conditions (Figure C-10), indicating its formation during 8:2 FTOH biotransformation under nitrate-reducing conditions. The maximum peak area of 7:3 U amide was much larger in the NA treatment than the ED treatment, peaking at week 22 (Figures C-10A, A'). The formation of 7:3 U amide may result from the conversion of 7:3 U acid by a transaminase under nitrate-reducing conditions, and this reaction may be reversible.⁴⁶ In addition, decreases of 7:3 U amide in ED and NA treatments after week 22 indicated that it was likely an intermediate and was converted to downstream biotransformation products, such as PFHxA or PFOA as proposed previously.⁴⁶

A novel biotransformation product, 1H-perfluoroheptane ($\text{F}(\text{CF}_2)_6\text{CF}_2\text{H}$, m/z 368.9764), was identified during 8:2 FTOH biotransformation (confidence level 1 with a verified reference standard). Fragmentation analysis using MS^2 spectrum indicated the presence of characteristic moieties, including the deprotonated molecule ion (m/z 368.9764) and several fragment ions (m/z

218.9860, m/z 168.9893, and m/z 118.9929) with one or multiple losses of $-CF_2$ groups (50 Da) (Figure C-11A). The identification of this product as 1H-perfluoroheptane was further confirmed by the comparison with the compound standard (Figure C-11B). The quantification of 1H-perfluoroheptane was then conducted using a GC-HRMS. As shown in Figure C-12, 1H-perfluoroheptane was formed rapidly in ED and NA treatments, with a molar yield of 56.1-81.1 mol% at day 28. Then, 1H-perfluoroheptane gradually decreased to below the LOD (1,954 ng/L) by day 399 in the ED treatment; while in the NA treatment, its molar yield increased to 76.4 mol% at day 154 then decreased to below the LOD at day 399 (Figure C-12). In the abiotic and positive controls, 1H-perfluoroheptane was below the LOD during the incubation. As the concentration of 1H-perfluoroheptane measured in some solid and headspace samples were close to the LOD, caution should be taken regarding the quantification results, for example, the total mass of 1H-perfluoroheptane formed may be overestimated. Regardless, the substantial formation in the early incubation followed by the gradual decrease indicated that 1H-perfluoroheptane is a major intermediate during 8:2 FTOH biotransformation under nitrate-reducing conditions.

4.3.2 Biotransformation of 8:2 FTOH under sulfate-reducing and iron-reducing conditions

4.3.2.1 Biotransformation rates and products quantified by LC-MS/MS targeted analysis.

The biotransformation of 8:2 FTOH under sulfate-reducing and iron-reducing conditions was also observed in live-spiked microcosms based on the detections of known biotransformation products (Figures 4-2B and 4-2D). The biotransformation under both redox conditions, however, was less complete and much slower than that under nitrate-reducing conditions. At the end of the incubation (> 400 days), 64.4 ± 13.3 mol% and 75.2 ± 8.4 mol% of the initially applied 8:2 FTOH remained in ED and NA treatments, respectively, under sulfate-reducing conditions (Figure 4-2A). Similarly, under iron-reducing conditions, 71.8 ± 20.6 mol% and 90.0 ± 1.1 mol% remained in ED and NA treatments, respectively (Figure 4-2C). Among the known 8:2 FTOH biotransformation products reported previously^{29,43} and those under nitrate-reducing conditions, only 8:2 FTCA and 8:2 FTUA were measured as transformation products in the sulfate-reducing and iron-reducing live-spiked microcosms (Figures 4-2B and 4-2D). No significant differences ($p > 0.05$) in 7:2 sFTOH, 7:3 acid or C4-C9 PFCAs were observed among all treatments at each sampling event (Figures C-13 and C-14). Specifically, low concentrations of 8:2 FTCA and/or 8:2 FTUA were measured starting at day 56 in ED and NA treatment under sulfate-reducing conditions (Figure 4-2B). Both transformation products peaked at day 154 in the ED treatment with 3.5 ± 1.7 mol% of

8:2 FTCA and 0.2 ± 0.1 mol% of 8:2 FTUA, and then subsequently decreased (Figure 4-2B). In the NA treatment, however, 8:2 FTCA and 8:2 FTUA increased continuously to the molar yields of 6.5 ± 1.8 mol% and 1.1 ± 0.8 mol% at the end of incubation (Figure 4-2B). The slower biotransformation rate of 8:2 FTOH under iron-reducing conditions resulted in later detection of transformation products, which was not detected until day 154 (Figure 4-2D). Only trace amounts of 8:2 FTCA and 8:2 FTUA (< 0.1 mol%) were quantified throughout the incubation in the NA treatment (Figure 4-2D). Relatively more of 8:2 FTCA and 8:2 FTUA were formed in the ED treatment, continuously increasing to 4.2 ± 1.5 mol% and 0.2 ± 0.1 mol% by day 450 (Figure 4-2D). Based on the residual fractions of 8:2 FTOH and the amounts of quantified transformation products (i.e., 8:2 FTCA and 8:2 FTUA) in ED and NA treatments during biotransformation under sulfate- and iron-reducing conditions (Figure 4-2), it is likely that the lactate amendment resulted in the faster biotransformation of 8:2 FTOH, similar to observations under nitrate-reducing conditions.

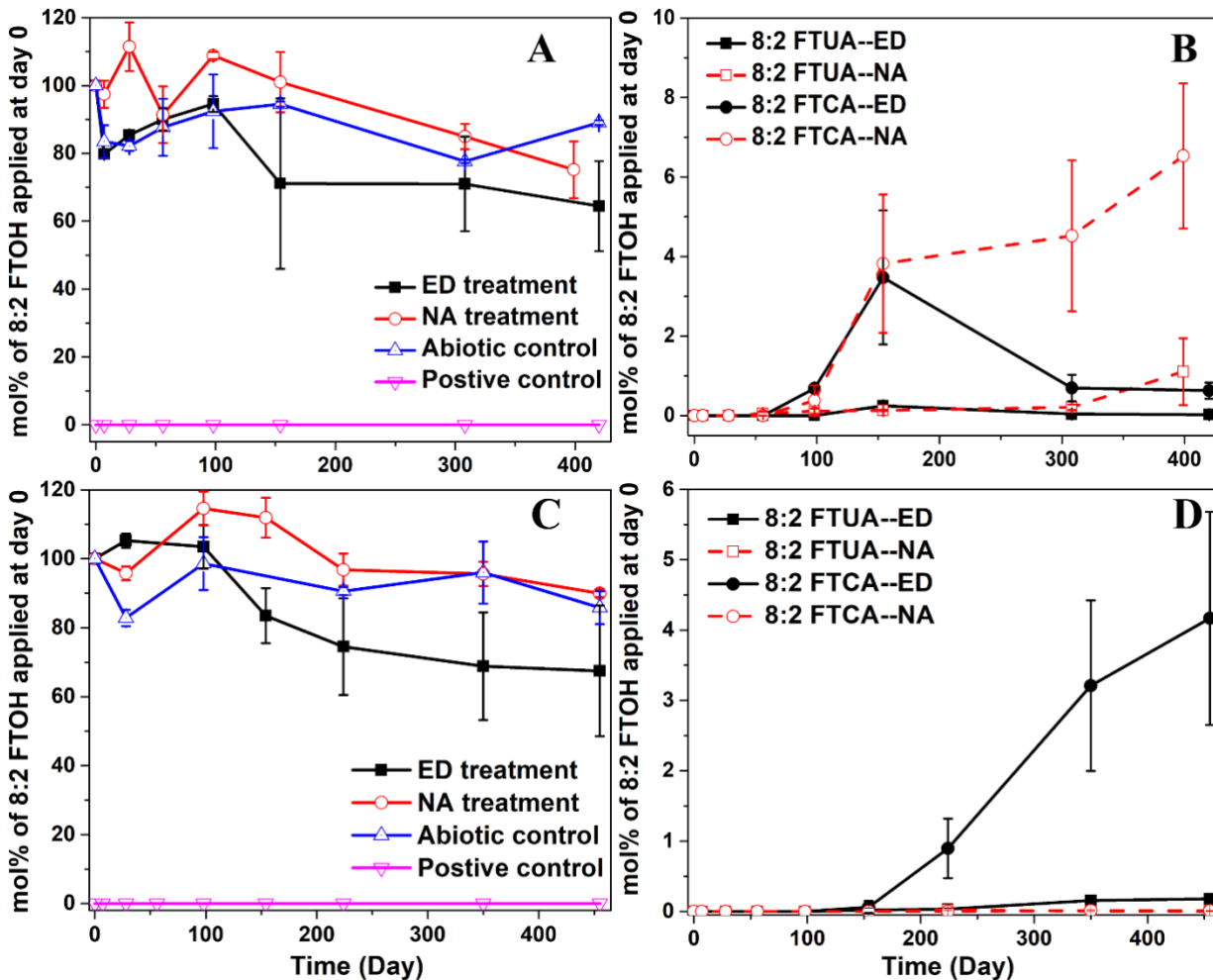


Figure 4-2. Changes in concentrations of targeted PFAS during 8:2 FTOH biotransformation under sulfate-reducing (Panels A and B), and iron-reducing conditions (Panels C and D). Panels A and C show 8:2 FTOH in the electron-donor (ED) treatment, natural attenuation (NA) treatment, abiotic control, and positive control. Panels B and D show the biotransformation products of 8:2 FTOH in ED and NA treatments. Note that the y-axis scale in Panel B is larger than the scale in Panel D.

4.3.2.2 Biotransformation product identified by LC-HRMS analysis. The molar recoveries were relatively higher in live-spiked treatments under sulfate- and iron-reducing conditions with 65.1 to 82.8 mol% and 71.8 to 90.0 mol% at the termination of the experiment, respectively. These higher molar recoveries were likely due to the decreased extent of 8:2 FTOH biotransformation (Figures 4-2 and C-6) relative to the nitrate-reducing conditions. Non-targeted LC-HRMS analysis was also performed on the samples from each treatment under sulfate- and iron-reducing conditions, and a novel biotransformation product of 8:2 FTOH, 3-F-7:3 acid

($\text{F}(\text{CF}_2)_7\text{CFHCH}_2\text{COOH}$, m/z 458.9885), was tentatively identified (confidence level 3, based on MS^2 (Figure C-7)) under both conditions (Table C-9). The obvious increases in the peak area were observed in ED and/or NA treatments under sulfate- and iron-reducing conditions, but not in abiotic and positive controls (Figure C-15). One analogue of 3-F-7:3 acid, 3-F-5:3 acid ($\text{F}(\text{CF}_2)_5\text{CFHCH}_2\text{COOH}$) was previously identified as a product during 6:2 FTOH biotransformation in digester sludge, and 3-F-7:3 acid was proposed as a product of 8:2 FTOH in the same system.³⁸ In this study, 3-F-7:3 acid was likely formed by the reduction of 8:2 FTUA with a reductase under sulfate- and iron-reducing conditions. In the ED treatment under sulfate-reducing condition, 3-F-7:3 acid increased at week 22 and then decreased at week 44 (Figure C-15B), indicating further biotransformation to other byproducts, or the possible conversion back to 8:2 FTUA as proposed previously.³⁸ The reverse reaction from 3-F-7:3 acid to 8:2 FTUA was less likely as the increase of 8:2 FTUA was not observed at week 44 in the ED treatment under sulfate-reducing condition (Figure 4-2B).

4.3.3 Distinct 8:2 FTOH biotransformation pathways under different redox conditions

4.3.3.1 Comparison of biotransformation under sulfate- and iron-reducing conditions with that under nitrate-reducing conditions. The biotransformation of 8:2 FTOH observed in the sulfate- and iron-reducing microcosms was distinctly different from that in nitrate-reducing microcosms, and also from those previously reported under oxic^{43,47} and methanogenic conditions.^{38,39} It has been proposed in prior studies that 8:2 FTOH was oxidized to 8:2 FTCA, which was further dehydrohalogenated to 8:2 FTUA.^{38,47} Transformation from 8:2 FTOH to 8:2 FTUA was shown to occur readily under nitrate-reducing conditions, as well as under oxic and methanogenic conditions.^{38,47} However, in the present study, 8:2 FTUA formation remained low (< 1.1 mol%) during incubation under sulfate- and iron-reducing conditions. These results suggest that the conversion of 8:2 FTCA to 8:2 FTUA may be the rate-limiting step for 8:2 FTOH biotransformation under sulfate-reducing and iron-reducing conditions, likely associated with the lack of (unknown) microbial enzymes involved in the dehydrohalogenation reaction.

Moreover, the conversion of 8:2 FTUA to either 7:2 sFTOH or 7:3 U acid, which has been previously reported^{43,158} and was also observed under nitrate-reducing conditions, did not occur under sulfate- and iron-reducing conditions. Instead, 3-F-7:3 acid was identified to be the likely transformation product of 8:2 FTUA under both conditions. Thus, under sulfate- and iron-reducing

conditions, the hydrogenation pathway for 8:2 FTUA leading to 3-F-7:3 acid formation was preferred over the reductive defluorination pathway, which is required for the formation of 7:2 sFTOH or 7:3 U acid. This observation resonates with a recent study¹⁰² that reported reductive defluorination of fluorinated carboxylic acids with one fluorine substitution on the unsaturated carbon (e.g., 6:2 FTUA) was much less favorable than hydrogenation by an anaerobic microbial enrichment culture (82.9% and 17.1% of 6:2 FTUA underwent hydrogenation and reductive defluorination pathways, respectively). The preference of the hydrogenation pathway under sulfate- and iron-reducing conditions observed herein could also be associated with a lack/inefficiency of relevant enzymes responsible for defluorinating 8:2 FTUA to 7:3 U acid and decarboxylating 8:2 FTUA to 7:2 sFTOH. The similar enzymatic inefficiency has been reported in aerobic and methanogenic microorganisms.^{38,115}

4.3.3.2 Comparison of microbial communities under different redox conditions. Microbial community analysis of the samples collected from nitrate-, sulfate-, and iron-reducing microcosms provided further insight into the effect of redox condition on the biotransformation of 8:2 FTOH. Principal coordinate analysis (PCoA), an ordination technique used to visualize microbial community alternation,¹⁷³ revealed distinct clustering of microbial communities in Loring soil on day 0 compared to those at the end of ca. 400 days incubation under each redox condition (Figure C-16). At the end of incubation, microbial communities in the nitrate-reducing microcosms substantially separated from those in sulfate- and iron-reducing microcosms, while separation between communities from the sulfate- and iron-reducing microcosms was not apparent (Figure C-16). These results indicate that the distinct biotransformation of 8:2 FTOH observed under sulfate- and iron-reducing conditions from that under nitrate-reducing condition was very likely due to the different microbial community compositions. As many sulfate-reducing bacteria are capable of using sulfate and iron (III) interchangeably as electron acceptors,^{174,175} the relatively close microbial community structures may explain the similar 8:2 FTOH biotransformation observed under sulfate- and iron-reducing conditions.

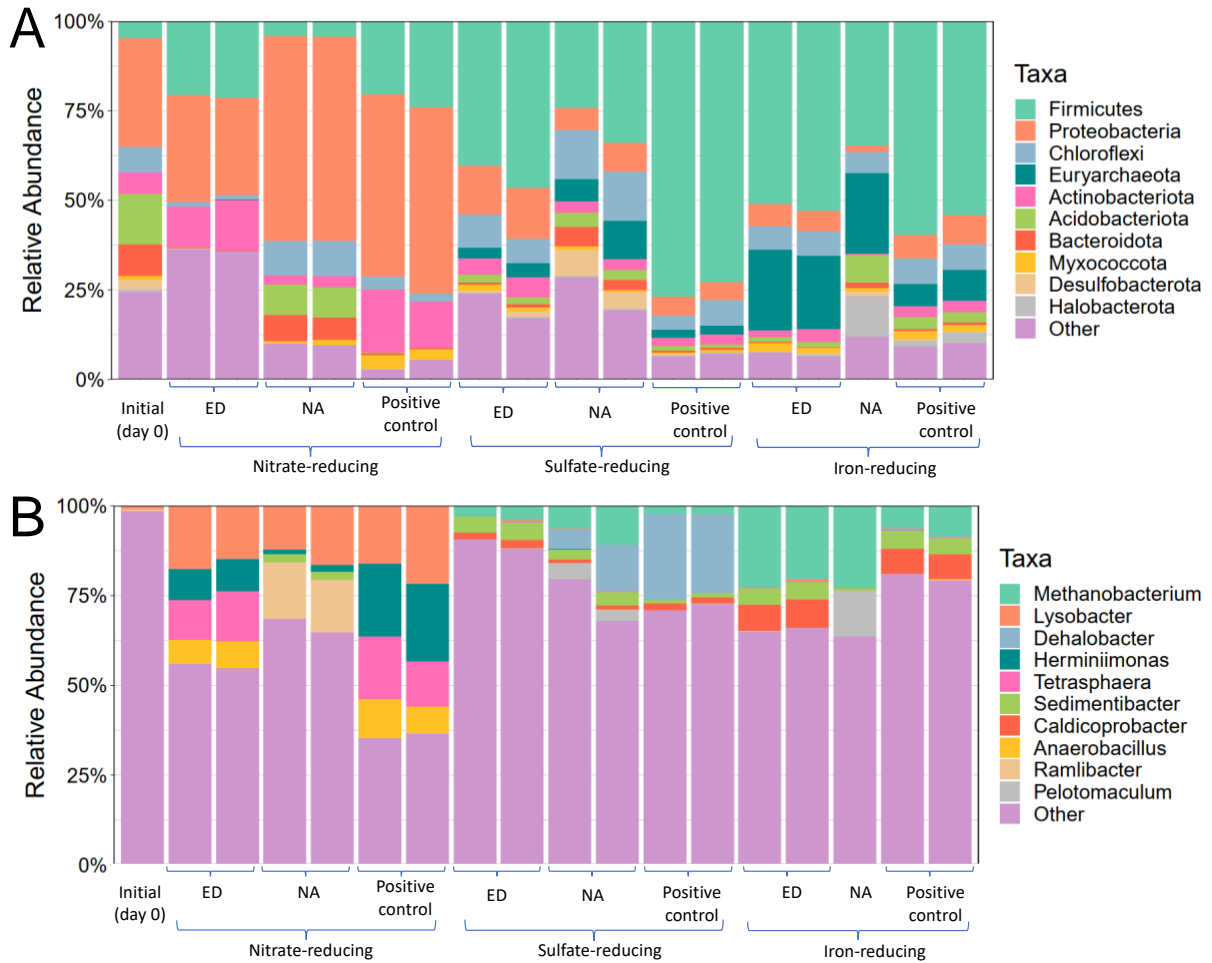


Figure 4-3. The relative abundance of microbial community composition at the phylum level (Panel A) and genus level (Panel B) in the initial Loring soil (Day 0), and in the nitrate-, sulfate-, and iron-reducing microcosms at the end of ca. 400 days incubation. Microcosms are classified as electron-donor (ED) treatment, natural attenuation (NA) treatment and positive control.

The microbial community composition in nitrate-, sulfate- and iron-reducing microcosms was further analyzed at the taxonomic level by evaluating the OTUs and making comparisons to the SILVA database.^{168,169} This additional analysis provided further support that distinctly different microbial communities were present under nitrate-reducing conditions compared to those under sulfate- and iron-reducing conditions (Figure 4-3). Proteobacteria was the most dominant phylum (relative abundance of 46.2 ± 12.2 %) in nitrate-reducing microcosms, whereas it only accounted for 8.8 ± 3.7 % and 5.4 ± 2.2 % in sulfate- and iron-reducing microcosms, respectively (Figure 4-3A). Microorganisms belonging to Proteobacteria have been reported to degrade various

hydrocarbon compounds,^{145,146} as well as PFAS (e.g., FTOHs).^{113,115,147,148} In this study, three genera in the Proteobacteria phylum, *Lysobacter*, *Herminiimonas*, and *Ramlibacter*, were exclusively found to be abundant in the ED and/or NA treatments under nitrate-reducing conditions (Figure 4-3B). Species in these genera may be responsible for the relatively rapid 8:2 FTOH biotransformation and transformation pathways observed under nitrate-reducing conditions. In sulfate- and iron-reducing microcosms, Firmicutes was the predominant phylum with relative abundances of $48.4 \pm 19.1\%$ and $51.0 \pm 8.7\%$, respectively (Figure 4-3A). Firmicutes was previously found as a dominant phylum in PFAS-contaminated soils,^{140,143} and are also capable of biotransformation of chlorinated solvents.^{176,177} In the present study, two genera in the Firmicutes phylum, *Caldicoprobacter* and *Sedimentibacter*, were found to be exclusively abundant at $1.6 \pm 0.5\%$ and $6.1 \pm 3.0\%$ in sulfate-reducing microcosms, respectively, and $3.0 \pm 1.6\%$ and $3.9 \pm 1.7\%$ in iron-reducing microcosms, respectively (Figure 4-3B). This prevalence suggests that the two genera may have contributed to the 8:2 FTOH biotransformation. However, the relevant enzymes for the transformation of 8:2 FTCA to 8:2 FTUA and further conversion of 8:2 FTUA to 7:2 sFTOH or 7:3 U acid may be absent in these genera.

Substantial differences between microbial communities under nitrate-reducing conditions and those under sulfate- and iron-reducing conditions described above likely resulted in the distinct 8:2 FTOH biotransformation (e.g., rate and pathways) observed in this study (Figure 4-4).

4.3.4 Comprehensive biotransformation pathways of 8:2 FTOH

Based on the biotransformation products detected by LC-MS/MS targeted analysis and by non-targeted HRMS under nitrate-, sulfate-, and iron-reducing conditions in this study, as well as the pathways proposed in previous studies on 8:2 FTOH biotransformation under oxic^{43,49,158} and methanogenic conditions,^{38,39} comprehensive biotransformation pathways for 8:2 FTOH were proposed under various redox conditions representative of most of natural environments (Figure 4-4). Although the pathways under oxic^{43,49,158} and methanogenic conditions^{38,39} were observed in various environmental matrices (e.g., aerobic soil, activated sludge, digester sludge), which likely possessed different microbial communities from those in Loring soil (i.e., a historically AFFF-contaminated soil), they were compiled here to compare with the pathways observed in Loring soil under nitrate-, sulfate-, and iron-reducing conditions to: (1) provide the insights into the role of

redox condition and/or microbial community in 8:2 FTOH biotransformation; (2) give a holistic understanding of the 8:2 FTOH biotransformation pathways that have been observed to-date.

Under all redox conditions, 8:2 FTOH biotransformation pathways shared the first three biotransformation steps before diverging into different paths. The first step was the oxidization of 8:2 FTOH aerobically or anaerobically to 8:2 fluorotelomer aldehyde (8:2 FTAL) by an alcohol dehydrogenase as described previously (pathway “a”; refers to Figure 4-4).^{38,43} Next, 8:2 FTAL was oxidized aerobically or anaerobically to 8:2 FTCA catalyzed by an aldehyde dehydrogenase (pathway “b”). Further, 8:2 FTCA was dehydrohalogenated to 8:2 FTUA with hydrogen fluoride (HF) elimination involved (pathway “c”). In the present study, 8:2 FTAL was not quantified by LC-MS/MS analysis due to the unavailability of an authentic standard and was not identified by HRMS analysis, indicating that this product was either unstable or rapidly oxidized under the tested conditions, as previously reported in 8:2 FTOH biotransformation under oxic^{23,46} and methanogenic³⁹ conditions.

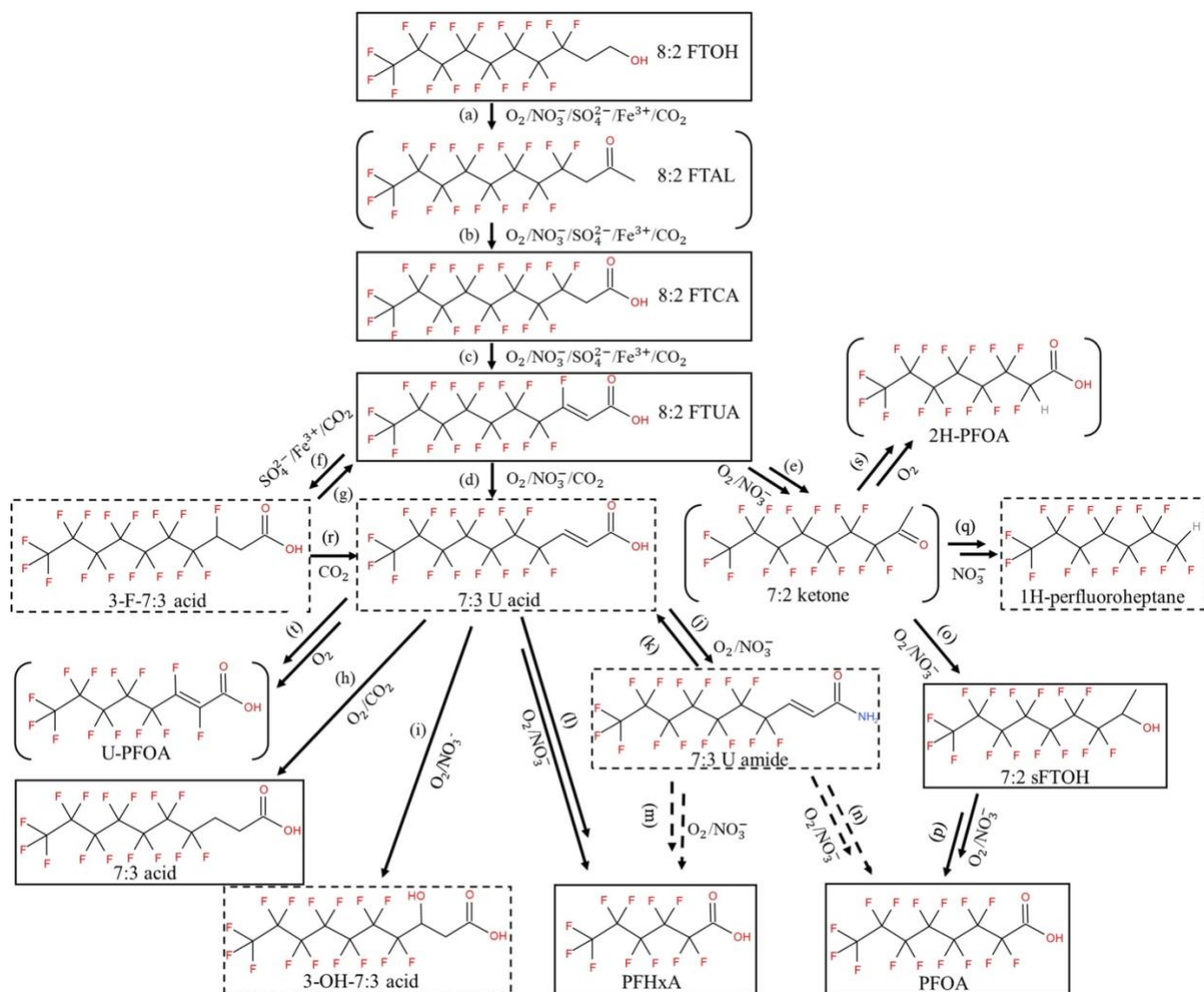


Figure 4-4. Proposed comprehensive biotransformation pathways of 8:2 FTOH under various redox conditions. O_2 , NO_3^- , SO_4^{2-} , Fe^{3+} , and CO_2 represent oxic, nitrate-reducing, sulfate-reducing, iron-reducing, and methanogenic conditions, respectively. The pathways under oxic and methanogenic conditions were proposed in previous studies,^{38,39,43,49,158} and they were observed in various environmental matrices (e.g., aerobic soil, activated sludge, digester sludge), which likely possessed different microbial communities from those in Loring soil (i.e., a historically AFFF-contaminated soil). The compounds in the solid rectangular boxes were quantitatively analyzed by LC-MS/MS, and the compounds in the dashed rectangular boxes were identified using non-targeted HRMS in the present study. The compounds in the brackets are the aerobic biotransformation products proposed and/or detected in previous studies whereas not detected in this study. The solid arrows indicate the biotransformation steps that would be expected to occur based on the current and/or previous studies. The dashed arrows indicate the potential reactions that may or may not occur. The double arrows indicate multiple enzymatic steps.

A key branch point for further biotransformation under the various redox conditions was 8:2 FTUA, after which the pathways diverged (i.e., pathways “d”, “e”, and “f”). On pathway “d”, 8:2 FTUA was converted to 7:3 U acid possibly via reductive defluorination, which was demonstrated for unsaturated PFAS by a commercially available microbial culture.¹⁰¹ This step has been commonly reported in the studies on 8:2 FTOH biotransformation under oxic and methanogenic conditions;^{29,38,39,43,46,158} however, it was only observed in the nitrate-reducing microcosms in the present study. Although previous studies showed that 7:3 U acid could be further transformed to 7:3 acid by reductases under oxic or methanogenic conditions (pathway “h”),^{38,39,43,46,158} transformation to 7:3 acid was not observed in the nitrate-reducing microcosms. Instead, 7:3 U acid was likely transformed to 3-OH-7:3 acid (pathway “i”) and 7:3 U amide (pathway “j”) by a hydratase and a transaminase, respectively, under nitrate-reducing conditions, and the latter reaction might be reversible (pathway “k”). The conversion of 7:3 U acid to PFHxA (pathways “l”), and 7:3 U amide to PFHxA/PFOA (pathways “m” and “n”) were proposed and/or demonstrated previously under oxic conditions.^{43,46,158} The reactions may also happen under nitrate-reducing conditions, and the rate of PFHxA production might be too slow to be appreciated.

Biotransformation of 8:2 FTUA to 7:2 ketone proceeded via multiple enzymatic steps involving defluorination and decarboxylation (pathway “e”).^{43,158} Then, 7:2 ketone was converted to 7:2 sFTOH (pathway “o”), which was further transformed to PFOA through some unknown enzymatic steps (pathway “p”). The sequence of pathways “e” to “o” and “p” have been reported as a major aerobic biotransformation pathway for 8:2 FTOH in the soil,⁴³ landfill leachate,⁵¹ and mixed bacterial cultures.¹⁵⁸ In this study, 7:2 ketone was not targeted in LC-MS/MS analysis due to the lack of an authentic standard, and was not detected in non-targeted analysis possibly due to its rapid conversion to downstream products. However, the substantial formations of 7:2 sFTOH and PFOA indicate that the pathways “e”, “o”, and “p” were likely prevailing during the 8:2 FTOH biotransformation under nitrate-reducing conditions. Moreover, 7:2 ketone might also be metabolized via multiple enzymatic reactions to form 1H-perfluoroheptane (pathway “q”), a major intermediate product during 8:2 FTOH biotransformation under nitrate-reducing conditions, though the transformation products of 1H-perfluoroheptane are unknown at this point.

Under sulfate- and iron-reducing conditions, 8:2 FTUA was potentially converted to 3-F-7:3 acid by a reductase (pathway “f”), which could be converted back to 8:2 FTUA (pathway “g”).

These reactions were proposed previously in digester sludge (i.e., under methanogenic conditions),³⁸ where 3-F-7:3 acid was also proposed to be transformed to 7:3 U acid via dehydrohalogenation (pathway “r”). Two other biotransformation products identified in previous aerobic biotransformation studies of 8:2 FTOH,^{43,49} 2H-PFOA (F(CF₂)₆CFHCOOH) and unsaturated PFOA (U-PFOA, F(CF₂)₅CF=CFCOOH) through pathways “s” and “t”, respectively, were not detected in non-targeted HRMS analysis under tested conditions in the present study.

4.4. Environmental implications

This study demonstrates that the biotransformation rates and pathways of 8:2 FTOH are highly dependent upon redox conditions. The biotransformation was much slower under sulfate- and iron-reducing conditions than under nitrate-reducing conditions, while the fastest biotransformation were reported under oxic conditions.^{43,47} The PFCAs, which were found as the terminal products of 8:2 FTOH biotransformation under oxic conditions, were produced with less yield under nitrate-reducing conditions, and were not formed under sulfate- and iron-reducing conditions. The production of two polyfluorinated acids (i.e., 8:2 FTCA and 8:2 FTUA), however, was observed under all redox conditions investigated in the current and previous studies.^{38,39,43,47,51,158} Biostimulation (e.g., lactate amendment) was shown to increase 8:2 FTOH biotransformation rates and products yields (e.g., PFOA) in the anaerobic microcosms tested in this study, implying that caution and considerations might be needed when the bioremediation is applied to treat other contaminants (e.g., chlorinated solvents) at sites where PFAS are also present.

The environmental fate of some newly identified products such as 1H-perfluoroheptane and 3-F-7:3 acid is not yet understood; therefore, future research is needed to elucidate the potential biotransformation and pathways of these compounds. In addition, genera potentially responsible for 8:2 FTOH biotransformation under each redox condition were identified including *Lysobacter*, *Herminiimonas*, and *Ramlibacter* under nitrate-reducing conditions, and *Caldicoprobacter* and *Sedimentibacter* under sulfate- and iron-reducing conditions. Future studies with isolated pure cultures would help to better assess the biotransformation of 8:2 FTOH with species from these genera. Overall, the presented research findings provide an improved understanding of the role of microbial communities in 8:2 FTOH biotransformation rates and pathways under various redox conditions, which impact its fate in different environmental matrices.

Chapter 5 : Aerobic Biotransformation of 6:2 Fluorotelomer Sulfonate in Soils from Two Aqueous Film-Forming Foam (AFFF)-Impacted Sites

The work presented in this chapter has been submitted to *Environ. Sci. Technol.*, and currently is under review.

5.1 Introduction

Per- and polyfluoroalkyl substances (PFAS) have been used in a wide variety of industrial and consumer products owing to their unique properties (e.g., water- and oil-repellency, surface tension reduction).¹ However, concerns over the impacts these compounds may pose to the environmental and human health are growing.^{6,7} Aqueous film-forming foams (AFFFs), which were commonly used to extinguish hydrocarbon-based fuel fires at airports and military bases,^{8,178} were identified as a major source of PFAS in the environment.^{14,179} 6:2 fluorotelomer sulfonate (6:2 FTS) has been identified as a component of AFFF formulations.^{12,13,74,75,78} Moreover, 6:2 FTS has been reported as a major transformation product of other PFAS compounds in AFFFs, such as 6:2 fluorotelomer thioether amido sulfonates (6:2 FtTAoS) and 6:2 fluorotelomer sulfonamidoalkyl betaine (6:2 FTAB).^{31,79,110} Consequently, 6:2 FTS has been widely detected at AFFF-impacted sites and in the nearby terrestrial and aquatic ecosystems,^{13,14,54–56} with concentrations up to 14,600 µg/L and 2,101 µg/kg reported in water and soil, respectively.^{78,83} Furthermore, the concentration of 6:2 FTS is anticipated to increase at AFFF-impacted sites as global manufacturers shifted to the production of shorter-chain length fluorotelomer-based AFFFs containing 6:2 FTS or its precursors.^{31,74,79}

Biotransformation of 6:2 FTS has been reported by pure bacterial strains (e.g., *Gordonia* sp. strain NB4-1Y, *Rhodococcus jostii* RHA1, and *Dietzia aurantiaca* J3) under well-controlled cultivation conditions,^{110–114} and by various mixed microbial cultures from activated sludge,²⁴ river sediment,²⁵ wetland slurry,²⁸ and landfill leachate.^{29,30} However, large discrepancies in the 6:2 FTS biotransformation rate and product formation were associated with those studies. For example, the half-life of 6:2 FTS was less than 5 days in the river sediment, but approximately 86 days in landfill leachate sediment and 2 years in activated sludge.^{24,25,29} Under sulfur-limiting conditions, rapid biotransformation of 6:2 FTS (>99 mol% disappearance of 6:2 FTS after 7 days) was achieved by pure bacterial cultures, while no biotransformation was observed in the presence of other sulfur sources (e.g., sulfate).^{110,112,114} Although the polyfluorinated compounds such as 5:3 fluorotelomer

carboxylic acid (5:3 acid) and short chain perfluoroalkyl carboxylates, including perfluoropentanoic acid (PFPeA) and perfluorohexanoic acid (PFHxA), were commonly reported as biotransformation products of 6:2 FTS, the detection frequencies and molar yields of those products varied among prior studies.^{24,25,28,29,110,112} These results suggest that environmental factors such as the microbial community composition and sulfur source concentrations could influence the biotransformation of 6:2 FTS, further complicating assessments of its behavior in the environment.

The environmental fate of 6:2 FTS at AFFF-impacted sites remains poorly understood. In the only laboratory study conducted to-date, Harding-Marjanovic et al. demonstrated that a native AFFF-impacted soil microbial community biotransformed 6:2 FtTAoS to 6:2 FTS, which was further transformed to products including 5:3 acid, PFPeA and PFHxA.³¹ However, the rate and pathway of 6:2 FTS biotransformation, as well as the environmental conditions that impact 6:2 FTS biotransformation, were not investigated. Therefore, the present study aims to assess the biotransformation of 6:2 FTS under conditions representative of AFFF-impacted sites using native microbial communities. To this end, surface soils collected from two U.S. military bases were used for separate 6:2 FTS microcosm studies. Biotransformation rates and product formation in two sets of microcosms were examined over a 224-day incubation period. High-resolution mass spectrometry (HRMS) was employed to identify previously undocumented transformation products. By comparing the results observed in the two AFFF-impacted soils, some environmental factors that impact 6:2 FTS biotransformation were identified.

5.2 Materials and methods

5.2.1 Chemicals and Materials

The chemical names, acronyms, molecular structures, and suppliers of PFAS targeted in liquid chromatography-tandem mass spectrometry (LC-MS/MS) analysis are listed in the Appendix D, Table D-1. 1H-perfluoropentane (purity 98%) and 1H-perfluorobutane (purity 99%) were purchased from Synquest Laboratories (Alachua, FL). The LC-MS grade water and methanol (>99.9%) were obtained from Honeywell Burdick & Jackson (Honeywell, Charlotte, NC). All other chemicals were reagent grade or higher. AFFF-impacted soils collected from two military sites, the former Loring Air Force Base (Aroostook County, ME) and Robins Air Force Base (Houston County, GA) were used in this study (referred to hereafter as Loring soil and Robins

soil). Detailed information on soil collection, and physical and chemical properties (pH, moisture content, organic matter content, cation exchange capacity (CEC), soil particle size distribution) are provided in Appendix D-section S1 and Table D-2.

5.2.2 Microcosm Set-up and Sampling

Two sets of microcosms were constructed in 60-mL Wheaton serum bottles with either Loring or Robins soil. Each set consisted of live treatments, abiotic controls, and positive controls (composition described in Table D-3). In each bottle, 3 g (dry weight) of Loring or Robins soil and 30 mL of synthetic groundwater (Appendix D-section S1) were added. For live treatments, each bottle was dosed with approximately 1,700 $\mu\text{g/L}$ of 6:2 FTS prepared in diethylene glycol butyl ether (DGBE), which is a primary organic solvent in AFFF formulations and has also been demonstrated as an electron donor and carbon source in prior microcosm studies.^{31,37} Abiotic controls were prepared similarly to live treatments, except with the addition of 1 g/L NaN_3 to inhibit microbial growth (1 g/L was determined to be effective in preliminary experiments; data not shown). Abiotic controls were used to evaluate potential abiotic transformation of 6:2 FTS and/or legacy PFAS originally present in Loring and Robins soils. In positive control bottles, only DGBE (no 6:2 FTS) was added to monitor legacy PFAS and potential PFAS biotransformation in Loring and Robins soils. Throughout the experiments, DGBE was amended into the live treatment and positive control microcosms as needed to support the microbial growth. All bottles were crimp-sealed with rubber septa and aluminum caps (Chemglass; Vineland, NJ). One C_{18} cartridge (Maxi-Clean™, Alltech, Deerfield, IL) pre-conditioned with methanol, was connected to an 18G \times 1" needle that was pushed through the septum into the headspace of each bottle. The cartridge ensured sufficient aeration, and captured potential volatile transformation products.⁴² All bottles were continuously agitated at 150 rpm on an orbital shaker (Innova 2350, New Brunswick Scientific) at room temperature until sampling.

On days 0, 7, 28, 56, 98, 154, and 224, triplicate bottles from live treatments, and duplicate bottles from abiotic and positive controls were destructively sampled. The headspace of each bottle was initially purged through the C_{18} cartridge using an aquarium air pump (Imagitarium, Petco Brand). The cartridges were then eluted with 5 mL methanol for further PFAS analysis. To ensure the efficiency of C_{18} cartridges during the long-term incubation (i.e., 224 days), new C_{18} cartridges were installed to replace the old ones on the remaining bottles on days 28, 56, 98, 126, 154, and

189. The cartridge eluents from each bottle were combined to account for the total volatile PFAS captured over the course of the experiment. After headspace sampling, supernatant (0.5-mL) was collected from each bottle and immediately added into methanol (9.5-mL) to minimize potential loss of volatile PFAS. The diluted sample was then filtered through a 0.2- μ m nylon filter (Corning Inc., Corning, NY). Each bottle was then shaken vigorously, and well-mixed slurry (1-mL) was withdrawn for dissolved organic carbon (DOC) analysis (TOC-L CPH, Shimadzu). All remaining slurry was transferred into a 50-mL centrifuge tube, along with the rubber septum. The bottle was rinsed with 5 mL ultrapure water and the rinse water was decanted to the 50-mL tube. The tube was then centrifuged at 4,000 rpm for 20 min, and the supernatant was discarded. The soil pellet was resuspended with 30 mL methanol and vortexed for 30 min, followed by 30 min sonication (operating frequency of 35 kHz) at 60 °C. The methanol extract of soil and septum was collected after centrifugation, and further filtered through a 0.22- μ m nylon filter. The C₁₈ cartridge eluents, and the filtrates of methanol-diluted aqueous samples and methanol extracts of soil and septum were stored at -20 °C prior to PFAS analysis.

5.2.3 Targeted and Non-Targeted PFAS Analysis

Targeted LC-MS/MS analysis was performed using a Waters ACQUITY ultra high-performance liquid chromatograph coupled with a Waters Xevo triple quadrupole mass spectrometer (UPLC-MS/MS) (Waters Corporation, Milford, MA). Each of the three phase samples (i.e., headspace, aqueous, and solid phases) was analyzed by LC-MS/MS separately. Target PFAS analytes are listed in Table D-1. Perfluoroalkyl acids (PFAAs) were analyzed following established methods,¹⁶⁴ while polyfluorinated compounds were analyzed using a method¹⁶⁵ with no ammonium acetate addition in mobile phase. A different method for polyfluorinated compounds was used because fluorotelomer alcohols (e.g., 6:2 FTOH) that are potential transformation products of 6:2 FTS could form adducts with ammonium acetate under negative electrospray ionization. In both methods, analyte separation was achieved using a Waters ACQUITY UPLC BEH C18 Column (130Å, 1.7 μ m, 2.1 mm X 50 mm). Details on the solvent gradient and instrumental parameters used in each targeted method are provided in Tables D-4 to D-7. The detection limits of target PFAS are provided in Table D-8.

For the non-targeted PFAS analysis, methanol-diluted aqueous samples and methanol extracts of soil and septum from each treatment at select sampling points were pooled. Sampling points

were selected to include the samples collected before and after the occurrence of 6:2 FTS biotransformation based on LC-MS/MS analysis. Non-targeted LC-HRMS analysis was performed using a Thermo QExactive HF-X Orbitrap MS equipped with a Vanquish UPLC to provide high resolution, high mass accuracy, and high sensitivity over a large mass to charge (m/z) range. Detailed procedures are described in the Appendix D-section S1.

5.2.4 Microbial community analysis

To provide insights on the role of native microbial communities in 6:2 FTS biotransformation in AFFF-impacted soils, duplicate microcosm samples at two sampling points (day 0 and 224) were collected from Loring and Robins live treatments and positive controls for microbial community analysis. Because the quantity of DNA extracted from Robins soil microcosms on day 0 was too low to be amplified, day 7 samples from the positive control (i.e., biostimulation with DGBE) were used as the initial samples. Amplification and sequencing of Loring and Robins soil DNA samples were performed at the Alkek Center for Metagenomics and Microbiome Research at Baylor College of Medicine. The V4 region of the 16S rRNA gene was amplified by polymerase chain reaction (PCR) using barcoded primer sets (515F/806R) and sequenced on the MiSeq platform (Illumina, San Diego, CA) using a 2×250 bp paired-end protocol.¹⁶⁶ The produced read pairs were demultiplexed, filtered and merged using parameters optimized for the 16Sv4 amplicon type.¹⁸⁰ Resulting reads were denoised using the Deblur algorithm following the default workflow and the length limit of 252 bp.¹⁸¹ The generated sequences were mapped against the latest SILVA Database.¹⁶⁹ The ATIMA (Agile Toolkit for Incisive Microbial Analyses) was used to analyze and visualize trends in taxa abundance, alpha diversity, and beta diversity as they relate to sample metadata.

5.3 Results and discussion

5.3.1 Experimental system

Throughout the experiments, the consumption of DGBE was monitored in Loring and Robins soil bioactive microcosms (i.e., live treatments and positive controls), which were amended 4-5 times of 10 mM DGBE (Figure D-1, Appendix D). No change in DOC concentration was detected in abiotic controls (Figure D-1). These results indicated aeration was sufficient to support DGBE biodegradation by the aerobic microorganisms in both soils. In addition, no differences in the consumption rates of DGBE were observed between live treatments and positive controls (Figure

D-1), suggesting that the addition of 6:2 FTS did not negatively impact substrate consumption by the native microbial community.

The background levels of 6:2 FTS and potential transformation products^{24,25} in Loring and Robins soils were determined from the day 0 positive control samples (Table D-9). Additional discussion on the occurrence of legacy PFAS in the two AFFF-impacted soils is provided in Appendix D-section S2. The total mass of 6:2 FTS initially spiked into live treatments and abiotic controls was approximately 180-fold and 22-fold greater than the legacy 6:2 FTS in Loring and Robins soils, respectively (Tables D-10 and D-11). Such spiked amounts allowed for the identification and quantification of 6:2 FTS transformation products. As shown in Figure 5-1, 102.9 ± 5.5 mol% and 95.9 ± 6.6 mol% of the initially spiked 6:2 FTS remained in Loring and Robins abiotic controls, respectively, with no significant changes ($p > 0.05$) over the 224-day incubation period, indicating the integrity of the experimental system and the efficiency of extraction methods used in this study, and that 6:2 FTS was stable under abiotic experimental conditions.

5.3.2 Biotransformation of 6:2 FTS in Loring and Robins soil microcosms

5.3.2.1 Biotransformation rates. In the live treatments of Loring soil microcosms, rapid 6:2 FTS biotransformation was observed with only 0.2 mol% of the initially spiked 6:2 FTS remaining after 154 days (Figure 5-1A). The half-life was determined to be 43.3 days by fitting 7 data points using a first-order kinetic model ($R^2 = 0.98$). Biotransformation of legacy 6:2 FTS was also observed in positive controls, where the total mass of 6:2 FTS decreased from 0.8 ± 0.2 nmol at day 0 to 0.0 ± 0.0 nmol at day 28 (Table D-10). In contrast, much slower 6:2 FTS biotransformation was observed in Robins soil, with 63.7 ± 6.0 mol% of initially spiked 6:2 FTS remaining in live treatments after the 224-day incubation (Figure 5-1B). Similarly, legacy 6:2 FTS in positive controls was biotransformed slowly, with 7.0 ± 2.0 nmol remaining at day 98 (8.3 ± 0.3 nmol at day 0, Table D-11). The presence of legacy 6:2 FTS biotransformation in Loring and Robins soils suggests that the lack of electron donor, carbon source or nutrients limited natural attenuation of 6:2 FTS at the field sites.

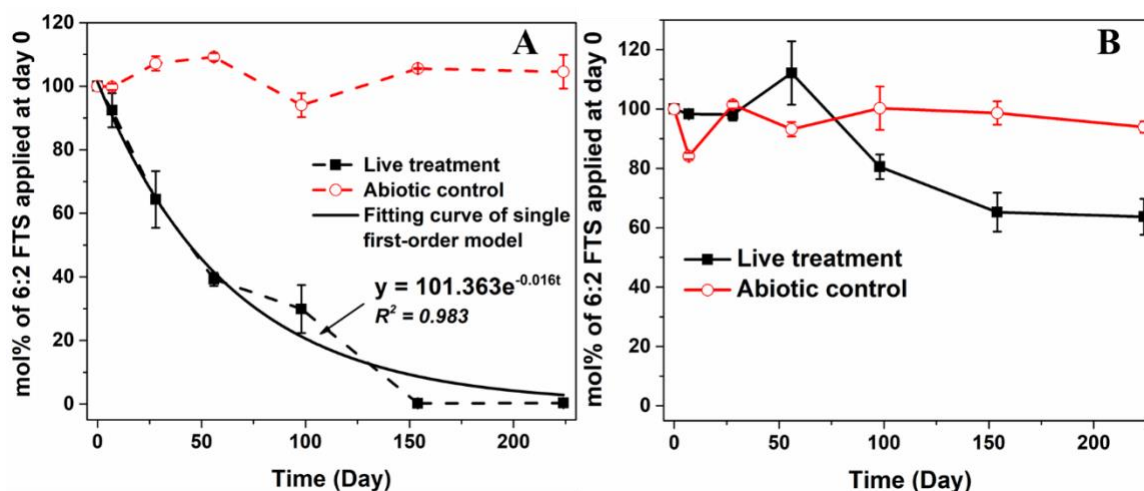


Figure 5-1. Changes in molar ratios of residual 6:2 FTS during aerobic biotransformation in Loring (Panel A) and Robins (Panel B) soil microcosms. Error bars represent the standard deviation of triplicate live treatments and duplicate abiotic controls.

5.3.2.2 Biotransformation products quantified by LC-MS/MS targeted analysis. Four polyfluorinated compounds including 6:2 fluorotelomer saturated carboxylic acid (6:2 FTCA), 6:2 fluorotelomer unsaturated carboxylic acid (6:2 FTUA), 5:2 secondary fluorotelomer alcohol (5:2 sFTOH) and 5:3 acid, and four perfluorinated compounds (perfluorobutanoic acid-PFBA, PFPeA, PFHxA, and perfluoroheptanoic acid-PFHpA) were identified as biotransformation products of 6:2 FTS in Loring soil using LC-MS/MS analysis. Significant increases ($p < 0.05$) in the mass of these compounds were detected in live treatments compared to abiotic and positive controls (Table D-10). Formation of 6:2 FTUA and 5:2 sFTOH in positive controls confirmed the occurrence of legacy 6:2 FTS biotransformation in Loring soil (Table D-10). An initial intermediate of 6:2 FTS biotransformation reported previously,²⁵ 6:2 FTOH, was below the limit of detection (LOD), suggesting that it was rapidly converted to downstream products. This finding is consistent with observations in activated sludge²⁴ and river sediment²⁵ where 6:2 FTOH was absent or detected at low levels (<2.5 mol%). Similarly, low levels of 6:2 FTCA (<0.5 mol%) were detected over the 224-day incubation likely due to its rapid biotransformation to 6:2 FTUA, which peaked at day 28 (3.7 ± 0.5 mol%) and decreased to less than 0.5 mol% by day 224 (Figure 5-2A). As a major intermediate product,²⁵ 5:2 sFTOH concentrations increased throughout the incubation period, reaching a peak molar yield of 13.3 ± 5.1 mol% by day 224 (Figure 5-2A). Higher production rates from upstream products (e.g., 6:2 FTUA) relative to conversion to downstream products likely resulted in this accumulation of 5:2 sFTOH. The slower accumulation rate observed in the

later stage of the incubation (i.e., day 56 to day 224) (Figure 5-2A) may be attributed to increasing conversion to downstream products (e.g., PFPeA, PFHxA, etc.). Another major transformation product of 6:2 FTS,^{24,25} 5:3 acid reached its peak molar yield at 8.9 ± 1.2 mol% by day 154 then decreased to 0.2 ± 0.1 mol% at day 224 (Figure 5-2A). The biotransformation of 5:3 acid was reported previously in activated sludge via “one-carbon removal pathways”, leading to the formation of two major products (4:3 acid and PFPeA) and two minor products (3:3 acid and PFBA).¹¹⁶ In the present study, the occurrence of a substantial decrease in 5:3 acid and increases in PFPeA and PFBA between day 154 and day 224 indicated that reactions in “one-carbon removal pathways” likely occurred in the later stage of incubation (Figure 5-2A). However, 4:3 acid could not be quantified due to the absence of an authentic standard, while the formation of 3:3 acid was not found to be significant ($p > 0.05$) in live treatments (Table D-10). Neither 4:3 acid nor 3:3 acid was identified in subsequent non-targeted PFAS analysis, suggesting that both compounds might be formed with an extremely low molar yield that cannot be distinguished from the background levels. PFBA, PFPeA, and PFHxA were the major stable transformation products in Loring soil with molar yields of 1.3 ± 0.5 mol%, 7.0 ± 2.7 mol%, and 5.3 ± 0.7 mol% by day 224, respectively (Figure 5-2B). Low amounts of PFHpA (0.2 ± 0.1 mol%) were also formed. The detection of PFPeA and PFHxA as the most abundant terminal products is consistent with previous studies of 6:2 FTS biotransformation in mixed microbial cultures (i.e., activated sludge,²⁴ sediment,²⁵ wetland slurry,²⁸ landfill leachate²⁹).

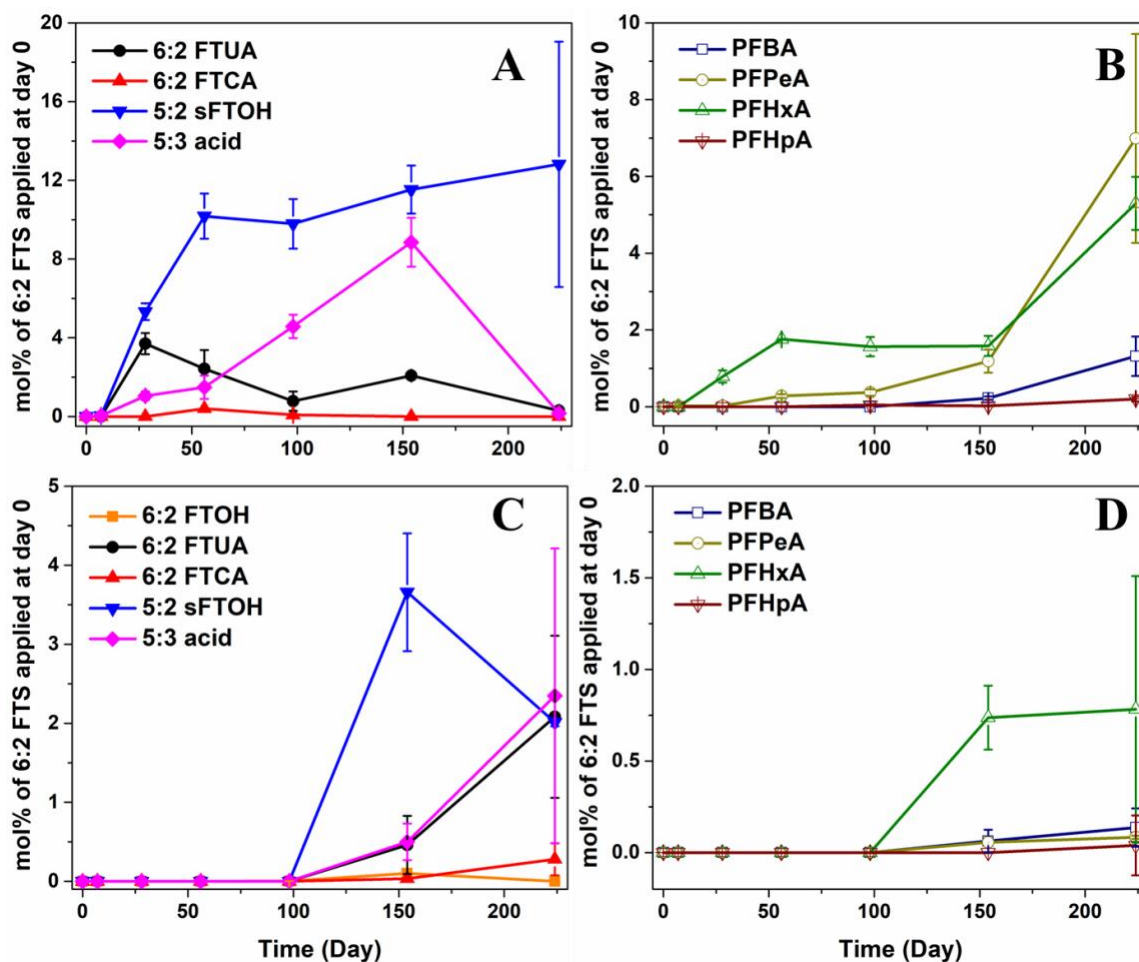


Figure 5-2. Changes in concentrations of per- (Panels A and C) and polyfluorinated (Panels B and D) biotransformation products during 6:2 FTS aerobic biotransformation in Loring (Panels A and B) and Robins (Panels C and D) soil microcosms. Error bars represent the standard deviation of triplicate live treatments. Note that different y-axis scales were used in Panels A-D.

Figures 5-2C and 5-2D show the molar yields of 6:2 FTS biotransformation products in the live treatments of Robins soil microcosms. Also, 6:2 FTUA, 6:2 FTCA, and 5:2 sFTOH were detected in positive controls but not in abiotic controls, indicating that biotransformation of legacy 6:2 FTS occurred in Robins soil (Table D-11). In live treatments, trace amounts of 6:2 FTOH were detected at day 98, which increased to 0.1 ± 0.0 mol% by day 154, while other transformation products were below the LODs until day 154 (Figures 5-2C and 5-2D). At day 224, 6:2 FTS biotransformation in Robins soil yielded 6:2 FTUA (2.1 ± 1.0 mol%), 6:2 FTCA (0.3 ± 0.2 mol%), 5:2 sFTOH (2.0 ± 0.1 mol%), 5:3 acid (2.3 ± 1.9 mol%), PFBA (0.3 ± 0.1 mol%), PFPeA (0.1 ± 0.0 mol%), and PFHxA (0.8 ± 0.7 mol%). Taken together, the total molar yield of all quantified transformation products in Robins soil by day 224 was ca. 8.0 mol%, while it was ca. 27.1 mol%

in Loring soil. These results illustrate that 6:2 FTS was biotransformed in Robins soil at a much slower rate and to a lesser extent than in Loring soil.

5.3.2.3 Comparison of 6:2 FTS biotransformation. To compare 6:2 FTS transformation rates and product formation in different environmental matrices and pure cultures, previous and current studies investigating aerobic biotransformation of 6:2 FTS are summarized in Table D-12. Unlike the biotransformation of FTOHs that has been widely investigated and reported to consistently occur in various environmental matrices,^{26,42–45} relatively limited data are available on 6:2 FTS biotransformation. Furthermore, conflicting results have been obtained from these studies.^{24,25,28,110} Rapid biotransformation of 6:2 FTS was generally achieved by pure bacterial cultures (i.e., *Gordonia* sp. strain NB4-1Y, *Rhodococcus jostii* RHA1, and *Dietzia aurantiaca* J3), with a substantial decrease (i.e., 44-100 mol%) in 6:2 FTS during short incubation periods (<10 days).^{110–112,114} In contrast, relatively slow 6:2 FTS biotransformation was observed in various environmental matrices including activated sludge,²⁴ wetland slurry,²⁸ landfill leachate,^{29,30} and AFFF-impacted soils (the present study), with the exception of a river sediment where a half-life of <5 days was reported.²⁵ 6:2 FTS biotransformation in Robins soil (63.7 mol% remaining after 224 days) was comparable to that in activated sludge (63.7 mol% remaining after 90 days) and constructed wetlands (91.1 mol% remaining after 142 days),^{24,28} and was lower than that in landfill leachate (50 mol% remaining after 90 days; half-life = 86 days).^{29,30} The biotransformation in Loring soil (half-life = 43.3 days), however, was approximately 2-fold faster than in landfill leachate (Table D-12).

In addition to biotransformation rates, large variations in 6:2 FTS transformation products and yields are observed in prior studies (Table D-12). The biotransformation of 6:2 FTS by pure bacterial cultures yielded minimal or negligible amounts of perfluoroalkyl carboxylic acids (PFCAs), whereas 6:2 FTS biotransformation by microbial communities in environmental media consistently resulted in PFCAs formation. Although the molar yields of PFCAs varied among the experimental systems, PFPeA and PFHxA were the most abundant (Table D-12), and PFBA and PFHpA were not consistently detected as 6:2 FTS biotransformation products. Small amounts of PFHpA were only detected in the studies using river sediment,²⁵ pure strain *Rhodococcus jostii* RHA,¹¹² and in the present study. Polyfluorinated products including 6:2 FTOH, 6:2 FTCA, 6:2 FTUA, 5:2 sFTOH, 5:2 ketone and 5:3 acid were commonly reported during 6:2 FTS biotransformation. However, the detection frequency and molar yield of each product varied across

these studies (Table D-12). Taken together, these results suggest that 6:2 FTS biotransformation in different environments and/or by different microbial communities is likely to undergo different pathways.

5.3.2.4 Factors impacting 6:2 FTS biotransformation. *5.3.2.4.1. Sulfur Source.* The presence of more easily assimilated sulfur sources (e.g., sulfate) was reported to potentially inhibit enzymatic desulfonation of 6:2 FTS, the initial step of 6:2 FTS biotransformation.¹¹³ It was shown that rapid 6:2 FTS biotransformation was achieved by pure microbial cultures under sulfur-limiting conditions,^{110-112,114} while the presence of sulfate (10 mM) suppressed the desulfonation process.¹¹² The sulfate present in activated sludge (0.21-0.52 mM),²⁴ landfill leachate (0.32 mM),²⁹ and wetland slurry (8 mM)²⁸ was also assumed by researchers to cause the observed slow 6:2 FTS biotransformation (i.e., ≥ 50 mol% remaining after more than 90 days). There was one exception where 6:2 FTS was biotransformed readily (half-life <5 days) in sediment in the presence of 0.3 mM sulfate.²⁵ However, all the aforementioned studies only reported the background levels (i.e., initial concentration) of sulfate in the environmental media, and did not track the sulfate throughout the experiments. In the present study, sulfate concentrations in Loring and Robins soil microcosms were monitored throughout incubation (Figure D-2). The background levels of sulfate in both soils (<0.12 mM at day 0) were lower than those in previous environmental media studies.^{24,25,28,29} The initial concentration was 3 to 5 times higher in Robins soil than Loring soil (0.10 ± 0.00 mM and 0.02 ± 0.01 mM, respectively). Sulfate in bioactive Loring soil microcosms was rapidly and completely consumed by day 7, whereas sulfate was not nearly depleted (<0.01 mM) until day 98 in Robins soil (Figure D-2). The time point of the initiation of 6:2 FTS biotransformation (e.g., formation of biotransformation products) appeared to coincide with the time point of sulfate depletion in both microcosms (Figures 5-1, 5-2, and D-2; day 7 and day 98 for Loring and Robins microcosms, respectively), indicating that 6:2 FTS biotransformation was favored by the microbial consortium in both soils once sulfur sources were depleted. Therefore, differences in the initial sulfate concentrations and depletion over the incubation period was likely a critical factor resulting in the distinct 6:2 FTS biotransformation behaviors observed between Loring and Robins soil microcosms. Likewise, the rapid 6:2 FTS biotransformation observed in river sediment even in the presence of 0.3 mM sulfate could be explained by rapid sulfate assimilation by the native microbes.²⁵ These findings suggest that the availability of alternate sulfur sources in the

environment may inhibit the desulfonation of 6:2 FTS, and could be a limiting step for 6:2 FTS biotransformation.

5.3.2.4.2. *Microbial community.* The diversity and richness of Loring and Robins soil microbial community was investigated, and differences between the two soils were expressed using the Shannon and Simpson, and Chao1 indices, respectively (Table D-13). Principle coordinate analysis (PCoA) also revealed the distinct differences between the two soil microbial communities (Figure D-3). However, a significant impact of spiked 6:2 FTS and its biotransformation products on the diversity and richness of the two soil microbial communities was not observed ($p > 0.05$, Table D-13). Detailed results and discussion on diversity and richness are described in Appendix D-section S3.

The microbial community composition in Loring and Robins soils was further analyzed on various taxonomic levels. A total of 36 classified phyla in the domain Bacteria and 5 phyla in the domain Archaea were shared. Figure D-4 shows Proteobacteria was the most dominant phylum in Loring and Robins soils (relative abundance >35%). These results corroborate previous studies that identified Proteobacteria as the predominant phylum in surface soils and river sediments that were heavily contaminated by PFAS.¹⁴¹⁻¹⁴³ Additionally, prior studies have observed an obvious increase (12.5-65.7%) in Proteobacteria in wetland slurry and fresh water following exposure to PFAS.^{28,144} These results suggest that Proteobacteria is likely more tolerant of PFAS than other phyla. In this study, two classes of Proteobacteria, Alpha- and Gamma-proteobacteria, were observed in Loring and Robins soils; these microorganisms have been reported to degrade various hydrocarbon compounds,^{145,146} as well as PFAS (e.g., FTOHs, 6:2 FTS).^{113,115,147,148} Another phylum, Actinobacteriota was also observed in all of Loring and Robins soil samples (Figure D-4). Some genera from Actinobacteriota are known as PFAS degraders; for example, *Mycobacterium* is known to degrade 6:2 FTOH,¹⁴⁷ and *Gordonia*, *Rhodococcus*, and *Dietzia* have been shown to transform 6:2 FTS.^{110-112,114} In the current study, *Rhodococcus* was present in Loring and Robins soils (Figure D-5). Taken together with prior work, *Rhodococcus* and/or other strains belonging to the Proteobacteria and Actinobacteriota likely played a role in the 6:2 FTS biotransformation observed in this study.

Desulfobacterota was present in Loring soil at a relative abundance of 1.7-6.5% whereas it was absent in Robins soil (Figure D-4). Many genera in Desulfobacterota have been reported to

desulfonate the organosulfonates.¹⁸² Since the desulfonation is a critical and often a rate-limiting step in 6:2 FTS biotransformation,^{24,29} the distinct difference in the abundance of Desulfobacterota could have contributed to the observed differences in biotransformation rates of 6:2 FTS in Loring and Robins soils. In addition, higher abundances of Bacteroidota ($12.7 \pm 3.4\%$ vs. $0.9 \pm 1.3\%$), Zixibacteria ($3.0 \pm 2.5\%$ vs. 0%), Cyanobacteria ($2.1 \pm 1.5\%$ vs. 0%), Patescibacteria ($1.6 \pm 0.8\%$ vs. 0%), as well as Archaea ($1.2 \pm 0.5\%$ vs. 0%), in Loring soil than Robins soil may partially account for the observed differences in 6:2 FTS biotransformation (Figure D-4). Bacteroidota and Archaea were shown to be associated with diesel- and PFAS-contaminated soils.^{139,146,150} Cyanobacteria species were reported to degrade aromatic hydrocarbons and xenobiotics using various enzymes.¹⁵¹ Patescibacteria was widely detected at sites with organic and metal pollutants,¹⁸³ and was linked to the remediation of aromatic hydrocarbons and heavy metals.¹⁸⁴ Zixibacteria was recently proposed as a new bacterial phylum, and the representative organism in the phylum was reported to be metabolically versatile.¹⁸⁵

The impacts of 6:2 FTS and its biotransformation products on microbial community composition were also investigated by comparing the day 224 samples from live treatments ($\sim 1,700 \mu\text{g/L}$ 6:2 FTS spiked) and from positive controls ($0 \mu\text{g/L}$ 6:2 FTS spiked). At the phylum level, the increase in Myxococcota and Firmicutes were found in both Loring AFB and Robins AFB soil after being exposed to 6:2 FTS (Figure D-4). More discussion about the findings on phylum level is described in Appendix D-section S4. At the genus level, a total of 320 genera were shared, and the Welch t-test with Benjamini-Hochberg false discovery rate (FDR) for multiple test corrections was applied to compare the relative abundance of each genus in live treatments and positive controls. It was found that *Sphingomonas* was the only genus that increased significantly (adjusted $p < 0.05$) in live treatments compared to positive controls in both Loring and Robins soil microcosms. In Loring soil, the relative abundance of *Sphingomonas* was $0.3 \pm 0.0\%$ in live treatments compared to positive controls ($0.2 \pm 0.0\%$); in Robins soil, the relative abundance was $12.0 \pm 3.8\%$ in live treatments compared to positive controls ($5.7 \pm 1.1\%$) (Figure D-5). These results suggest that the genus of *Sphingomonas* likely has higher tolerance to the elevated concentrations of 6:2 FTS and its biotransformation products. Moreover, some species in *Sphingomonas* might play a role in 6:2 FTS biotransformation. Species in *Sphingomonas* are present in various natural environments, and widely known to degrade many kinds of environmental pollutants (e.g., polycyclic aromatic hydrocarbons, chlorinated pesticides).¹⁸⁶⁻¹⁹⁰

Recent studies reported that the relative abundance of *Sphingomonas* increased under PFAS-spiked (e.g., PFOS, 6:2 FTS) conditions.^{28,140}

5.3.3 Identification of novel biotransformation products by LC-HRMS analysis

In the live treatments of Loring and Robins soil microcosms, total mass recovery of 6:2 FTS and transformation products generally decreased with incubation time. For Loring soil, mass recovery decreased from 92.5 ± 5.4 mol% at day 7 to 55.8 ± 4.8 mol% at day 56, then further to 25.7 ± 3.2 mol% at day 154), and for Robins soil, recovery decreased from 98.3 ± 1.1 mol% at day 7 to 71.1 ± 8.1 mol% at day 154 (Figure D-6). However, a similar decrease was not observed in the abiotic controls (Figure D-6). The relatively lower mass recovery observed in live treatments of Loring soil compared with Robins soil can be attributed to the increased extent of 6:2 FTS biotransformation and the associated formation of unknown transformation products. By performing non-targeted LC-HRMS analysis, seven additional compounds were identified as potential biotransformation products of 6:2 FTS (Table D-14). The abundances of these seven products (based on peak areas of extracted ion chromatograms) were substantially higher (> 6-fold) in live treatments than the abiotic and positive controls of Loring and Robins soil microcosms during 6:2 FTS biotransformation (Figures D-7, D-8, and D-9).

As a novel transformation product, 1H-perfluoropentane (C_5HF_{11} , m/z 268.98271) was identified at a highest confidence level 1 (confirmed structure, assigned based on the Schymanski Scale,¹⁷² detailed in Appendix D-section S1). Fragmentation analysis on the MS^2 spectrum (Figure D-10A) demonstrated the presence of its characteristic moieties, including the deprotonated molecule ion (m/z 268.9861) and related ions (e.g., C_2F_5 , m/z 118.9926). The identification was further confirmed by comparison to the chemical standard (Figure D-10B). Another 1H-perfluoroalkane with a shorter carbon chain, 1H-perfluorobutane (C_4HF_9 , m/z 218.98587) was also identified at confidence level 1 by comparison of the MS^2 spectra and fragmentations from microcosm samples and the reference standard (Figure D-11). In addition, ions at m/z 216.98912 and 236.99543 were identified as 1,2,2,3,3,4,4,4-octafluorobutan-1-ol ($C_4H_2F_8O$) at confidence level 2 (probable structure) and $C_7H_2F_8$ (structure shown in Figure D-12B) at confidence level 3 (tentative candidate) based on the MS^2 spectra and fragmentation analysis (Figure D-12). Chemical standards were not commercially available to allow for further structure confirmation.

5.3.4 Biotransformation pathways of 6:2 FTS in AFFF-impacted soil

The proposed biotransformation pathways of 6:2 FTS in Loring and Robins soils, based on the transformation products detected by targeted LC-MS/MS (Figure 5-2) and non-targeted LC-HRMS analyses (Table D-14) are presented in Figure 5-3. The detection of products in LC-MS/MS analysis such as 5:2 sFTOH, 5:3 acid, and PFCAs indicated that pathways reported previously in activated sludge,²⁴ river sediment,²⁵ and landfill leachate,²⁹ also occurred during 6:2 FTS biotransformation by native microbial communities in AFFF-impacted soils. The biotransformation initiated by the microbial desulfonation of 6:2 FTS catalyzed by monooxygenases,^{111,112} resulted in the formation of 6:2 FTOH. Then, 6:2 FTOH was oxidized to 6:2 fluorotelomer aldehyde (6:2 FTAL) by an alcohol dehydrogenase, which was further oxidized to 6:2 FTCA catalyzed by an aldehyde dehydrogenase. Through a dehydrohalogenation reaction, 6:2 FTCA was converted to 6:2 FTUA involving elimination of a hydrogen fluoride (HF). Similar to those previously reported,^{26,50,112} the biotransformation of 6:2 FTOH to 6:2 FTAL, to 6:2 FTCA, and then to 6:2 FTUA was likely a rapid process, so that accumulation of 6:2 FTCA (<0.5 mol%) was minimal (Figure 5-2). The low level of PFHpA formation (Figure 5-2, Tables D-10 and D-11) observed in this study suggests that α -oxidation of 6:2 FTCA might be a minor pathway during 6:2 FTS biotransformation. Although microbial α -oxidation of fluorotelomer compounds (e.g., 6:2 FTOH, 8:2 FTOH) was not previously observed in studies conducted with bacterial culture, activated sludge or soil,^{24,26,43,47,50} the detection of PFHpA in recent 6:2 FTS and 6:2 polyfluoroalkyl phosphates (PAPs) biotransformation studies supports the possibility that microbial α -oxidation of 6:2 FTS to PFHpA occurred.^{25,112,191}

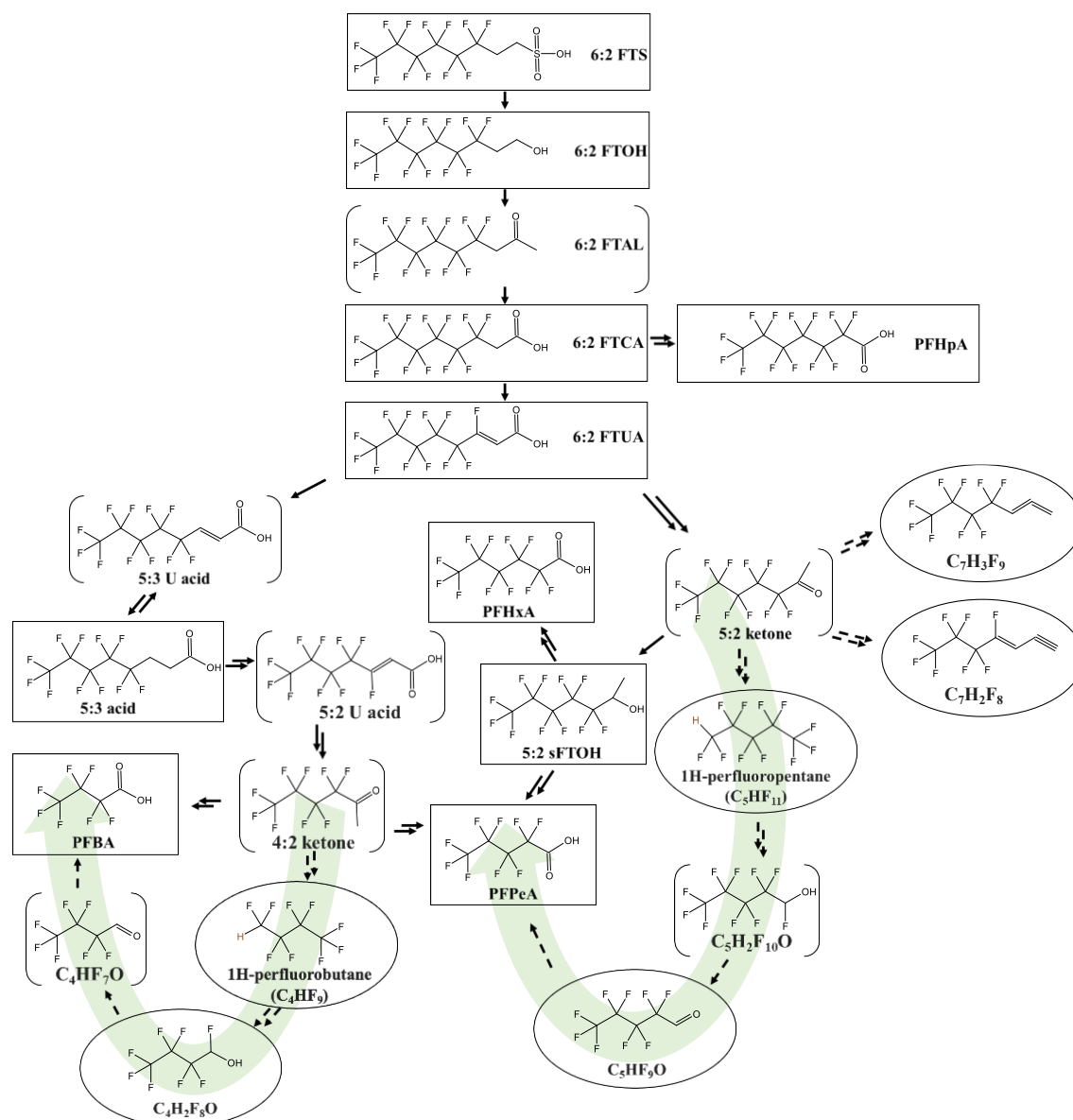


Figure 5-3. Proposed aerobic biotransformation pathways of 6:2 FTS in AFFF-impacted soils. The compounds in the rectangular boxes were detected by LC-MS/MS analysis, and the compounds in the oval boxes were identified using non-targeted LC-HRMS analysis. The compounds in the brackets are proposed transformation products and were not detected in this study. The solid arrows represent the biotransformation steps expected to occur based on the present and previous studies.^{24,25,110} The dashed arrows represent the proposed reactions that may occur. The double arrows represent multiple enzymatic steps involved. The two large, curved arrows in green illustrate the novel “fluorotelomer ketone to PFCA” pathway proposed in this study which elucidate the formation process of PFCAs.

A key branching point for further biotransformation was 6:2 FTUA, after which the pathways diverged. Through multiple enzymatic steps (e.g., defluorination and decarboxylation),^{24,110} 6:2 FTUA can be metabolized to 5:2 ketone. Then, the ketone was converted to 5:2 sFTOH, which is

the precursor to PFPeA and PFHxA via multiple unknown reactions involving the removal of fluorine and carbon atoms.^{24,26} The other transformation pathway for 6:2 FTUA leads to the formation of 5:3 U acid possibly via reductive defluorination.^{26,29,147} Very recently, Yu et al., demonstrated the microbial reductive defluorination of unsaturated PFAS by a mixed microbial culture.¹⁰¹ Further, 5:3 U acid was converted to 5:3 acid through a reduction step facilitated by nicotinamide-adenine dinucleotide phosphate (NADPH), and 5:3 acid could then enter into the “one-carbon removal pathways”, leading to the formation of 5:2 U acid and 4:2 ketone, which are the precursors to PFBA and PFPeA.^{29,111,116}

Although PFCAs have been widely reported as the terminal biotransformation products of fluorotelomer precursors, the specific formation steps have not been elucidated.^{24,43,47,51} Based on the transformation products detected using non-targeted LC-HRMS analysis (Table D-14), and the associated abundances over time during 6:2 FTS biotransformation (Figures D-7, D-8, and D-9), a novel “fluorotelomer ketone to PFCA” pathway is proposed (Figure 5-3). It is hypothesized that the fluorotelomer ketones (i.e., 5:2 ketone and 4:2 ketone) are converted to 1H-perfluoroalkanes (i.e., 1H-perfluoropentane and 1H-perfluorobutane) through multiple enzymatic steps. The structures of both 1H-perfluoroalkanes were confirmed (confidence level 1), and both compounds were formed at a substantially high abundance in the live treatments based on the greater than 6-fold change in peak areas (Figure D-7). The 1H-perfluoroalkanes are then biotransformed to alcohols (i.e., C₄H₂F₈O and C₅H₂F₁₀O) with a fluoride atom replaced by a hydroxyl group (Figure 5-3). The probable structure of 1,2,2,3,3,4,4,4-octafluorobutan-1-ol (confidence level 2) was identified for C₄H₂F₈O in this study. In addition, this compound was confirmed as an intermediate transformation product, based on a 48-fold increase in the peak area at week 14 (relative to day 0) that was followed by a decrease in the abundance at week 32 in Loring soil live treatments (Figure D-8). Subsequently, the two alcohols (i.e., C₄H₂F₈O and C₅H₂F₁₀O) are oxidized by an alcohol dehydrogenase to the corresponding aldehydes (i.e., C₄HF₇O and C₅HF₉O), respectively. With relatively low abundances (peak areas < 3.0E+4) detected (Figure D-8), the C₄HF₇O and C₅HF₉O aldehydes are transient intermediates that are rapidly oxidized by an aldehyde dehydrogenase to PFBA and PFPeA, respectively. Three other products identified in LC-HRMS analysis, C₇H₂F₈, C₇H₃F₉, and ion at *m/z* 292.98316, are suspected to be formed from 5:2 ketone through unknown reduction reactions (Figure 5-3). Based on peak area trends over the incubation, these compounds

are further biotransformed to additional downstream products that are not known at this point (Figure D-9).

5.4 Environmental implications

This study demonstrates that the biotransformation of 6:2 FTS in AFFF-impacted soils is strongly influenced by environmental factors such as the availability of sulfur sources and native microbial community composition. The biotransformation of 6:2 FTS was favored by the microbial consortia only after other easily assimilated sulfur sources (e.g., sulfate) were depleted. Desulfobacterota microorganisms likely promoted 6:2 FTS biotransformation via more efficient desulfonation. Species in the genus *Sphingomonas*, which exhibited higher tolerance to the elevated concentrations of 6:2 FTS and its biotransformation products, are likely to have contributed to 6:2 FTS biotransformation. These results suggest that evaluations of site geochemical and biological attributes are critical towards achieving a better understanding of 6:2 FTS transformation in the field, as well as gaining insights into the management and remediation of AFFF-impacted sites.

By identifying additional 6:2 FTS transformation products that were previously undocumented, a novel “fluorotelomer ketone to PFCA” pathway was proposed to account for the formation of PFCAs from fluorotelomer precursors. Additional studies should address novel compounds such as 1H-perfluoroalkanes (e.g., 1H-perfluoropentane and 1H-perfluorobutane), as the analogues (i.e., 1H-perfluorohexane and 1H-perfluoroheptane) to these compounds were also identified in our work examining biotransformation of a C₈-fluorotelomer precursor.¹⁹² These 1H-perfluoroalkanes are likely unique transformation products that could be present at sites contaminated by fluorotelomer precursors. Future research is needed to assess the prevalence of these compounds at AFFF-impacted sites and to evaluate their potential impacts on ecosystems and human health.

Chapter 6 : Biotransformation of 6:2 Fluorotelomer Sulfonate in Aqueous Film-Forming Foam (AFFF)-impacted Soil under Continuous Flow Conditions

The work in this chapter is being prepared as a manuscript for publication.

6.1 Introduction

Per- and polyfluoroalkyl substances (PFAS) have been extensively used for more than 50 years in a variety of commercial and industrial products,¹ including aqueous film-forming foams (AFFFs) manufactured to effectively extinguish hydrocarbon-based fuel fires.^{8,178} As a result, PFAS contamination is found in surface waters, groundwater, soils, and biota throughout the world,^{54,84,193} and concern over the negative impacts of PFAS contamination on the environmental and human health is growing.^{6,7} Upon release into the environment, the fate of PFAS could be subject to a few processes, such as infiltration, sorption, and abiotic/biotic transformation. Understanding the effects of these processes on the environmental behavior and fate of PFAS could allow for an efficient management and remediation of the contaminated sites.

Microbial transformation of PFAS, primarily the polyfluoroalkyl substances, have been increasingly investigated in recent years. Native microorganisms in various environmental matrices including activated sludge,^{23,24} river sediments,²⁵ and surface soils³¹⁻³⁴ have been reported to biotransform different classes of PFAS (e.g., electrochemical fluorination (ECF)- and fluorotelomerization (FT)-based PFAS) in the laboratory studies. These studies demonstrated that the biotransformation of polyfluoroalkyl substances almost always resulted in the alterations of the non-fluorinated head groups, while partial breakdown of perfluoroalkyl chains could also occur for FT-based PFAS. Accordingly, the biotransformation often forms perfluoroalkyl acids (PFAAs), which are a group of substances of particular concern due to their persistence, toxicity, and bioaccumulation potential.^{14,156,157} In addition, other compounds such as fluorotelomer acids that are more toxic than their PFAA counterparts,^{194,195} could also be formed during the biotransformation of FT-based PFAS.^{25,51} These findings indicate that taking the biotransformation process into account is crucial towards the assessment of the environmental fate of PFAS (especially the polyfluoroalkyl substances), as well as the associated effects on environmental and human health.

Despite increasing knowledge on the biotransformation of PFAS, almost all previous laboratory studies were limited to conduct under well-controlled conditions (e.g., in batch reactors). To the

best of our knowledge, there has been no studies on biotransformation of PFAS in natural porous media under dynamic flow conditions. Incorporation of water flowing into experimental systems is critical to the characterization and quantification of *in situ* PFAS mass transfer and abiotic/biotic transformation processes.

As a commonly reported ingredient in AFFF formulations,^{12,13,74,75,78} and a biotransformation product of other AFFF-related PFAS,^{31,79} 6:2 fluorotelomer sulfonate (6:2 FTS) has been widely detected at AFFF-impacted sites,^{13,14,54–56} with the highest concentrations of 14,600 µg/L and 2,101 µg/kg reported in groundwater and soil, respectively.^{78,83} To date, laboratory studies on the biotransformation of 6:2 FTS have been conducted in the batch reactors, using pure bacterial strains,^{110,112–114} or mixed microbial cultures from various environmental matrices.^{24,25,51,52} These studies have reported wide variations in the 6:2 FTS biotransformation rate and product yields. Environmental factors such as the availability of sulfur source (e.g., sulfate) and microbial community composition were hypothesized and/or demonstrated to contribute to the different biotransformation.^{25,52,112} Yet, it is unknown if other factors relevant to a contaminated site (e.g., dynamic water flowing) will impact the biotransformation of 6:2 FTS.

The objective of the present study is to investigate the fate and transformation of 6:2 FTS in AFFF-impacted sites, under conditions that closely represent the realistic scenario. To this end, surface soil was collected from a former U.S. military base (i.e., an AFFF-impacted site), and was used in one-dimensional column experiments. Two different seepage velocities were applied to evaluate the effects of hydraulic residence time in the porous media on the 6:2 FTS biotransformation. In addition, flow interruptions were conducted to assess if the biotransformation is rate-limited under the experimental column conditions. Last, the 6:2 FTS biotransformation behaviors in the one-dimensional columns were compared to those in our previous microcosms (constructed with same AFFF-impacted soil, see Chapter 5), to better understand the effects of continuous flow conditions on the environmental fate of 6:2 FTS.

6.2 Materials and methods

6.2.1 Chemicals and Materials

The chemical names, acronyms, molecular structures, and suppliers of PFAS targeted in liquid chromatography-tandem mass spectrometry (LC-MS/MS) analysis are provided in the Appendix E, Table E-1. The LC-MS grade water and methanol (>99.9%) were purchased from Honeywell

Burdick & Jackson (Honeywell, Charlotte, NC). All other chemicals used in the present study were reagent grade or higher. For all purposes, ultrapure deionized water (18.2 M Ω cm) from an Evoqua water purification system (Evoqua Water Technologies) was used.

Federal Fine Ottawa sand (30-140 mesh) was obtained from U.S. Silica Company (Berkeley Spring, WV) with an organic carbon (OC) content of <0.1 mg/g, a mean grain size of 0.32 mm and an intrinsic permeability of 4.2×10^{-11} m². An AFFF-impacted soil (hereafter referred to as Loring soil) was collected from the former Loring Air Force Base (Aroostook County, ME). Loring soil has been used in our previous microcosm study on 6:2 FTS biotransformation, in which the soil collection and characterization were described (Chapter 5). Briefly, Loring soil has a moisture content of $24.1 \pm 1.1\%$, and an organic carbon content of $3.5 \pm 0.1\%$. The soil pH (1-part soil: 1-part deionized water) is 7.2 ± 0.2 , and cation exchange capacity (CEC) is 18.7 ± 0.0 meq/100 grams soil. The particle size distribution of Loring soil is $53.1 \pm 3.1\%$ sand, $32.7 \pm 2.3\%$ silt, and $14.2 \pm 0.8\%$ of clay size fractions.

6.2.2 Column design and preparation

A total of four borosilicate glass chromatography column (2.5 cm inner diameter, 15 cm length; Kimble-Chase, Vineland, NJ) were used in this study for investigation of 6:2 FTS biotransformation. Each column was customized with three glass sampling ports that are evenly distributed along the column and sealed with rubber septa (Restek, Bellefonte, PA). All column components were either autoclaved (121 °C, 30 min) or washed in 70% ethanol prior to use. Abiotic and biotic columns were identically packed with mixed Loring soil and Federal Fine sand (1:1, w/w) by alternating the addition of 1-cm porous media with vortexing and manual compression. Following packing, columns were purged with CO₂ gas to facilitate dissolution of entrapped gas, then saturated with sterile synthetic groundwater (see below) in an up-flow mode. Non-reactive tracer tests (20 mM bromide, flow rate = 0.04 mL/min) were completed prior to column experiments. The breakthrough curves of bromide were simulated using the Code for Estimating Equilibrium Transport Parameters from Miscible Displacement Experiments (CFITM) as a part of Studio of Analytical Models (STANMOD) Version 2.2 (available through USDA-ARS U.S. Salinity Laboratory; <http://www.ars.usda.gov>) to determine porosity (n) and aqueous pore volume (PV).

6.2.3 Synthetic groundwater preparation

Synthetic groundwater was prepared according to the recipe previously reported¹³⁶ with modifications to exclude resazurin, L-cysteine, and sodium sulfide due to their potential to be carbon sources for aerobic microorganisms. Synthetic groundwater was prepared in 800 mL batches in a 1000-mL PYREXTM media bottle (Corning Inc., Corning, NY). After autoclaving at 121 °C for 30 min, 680 µL of 6:2 FTS stock solution (2,000 mg/L) prepared in diethylene glycol butyl ether (DGBE) was added into the bottle, yielding a starting 6:2 FTS concentration of 1,700 µg/L. DGBE was used to prepare the 6:2 FTS stock, since it is a primary organic solvent in AFFF formulations, and it was shown to serve as electron donor and carbon source for aerobic microorganisms in previous studies.^{31,37} The synthetic groundwater was then transferred into a 1000-mL PYREXTM Erlenmeyer flask (Corning Inc., Corning, NY) sealed with a rubber stopper, serving as the influent for biotic columns. For preparation of the influent for abiotic columns, additional 1 g/L of sodium azide was added into the synthetic groundwater to prevent microbial growth during column operations (1 g/L was demonstrated as effective in previous microcosm study¹⁹²). In addition, to offset the increase in ionic strength by sodium azide addition, the concentration of bicarbonate in the synthetic groundwater was correspondingly reduced.

6.2.4 Column operation and sampling

Column experiments were initiated by introducing the column influent described above to duplicate abiotic (A1, A2) and biotic columns (B1, B2). The initiation time point was considered as PV = 0. As shown in Figure 6-1, column influent was constantly aerated with sterilized air in the flask, and was delivered to the columns via a peristaltic pump (Gilson Miniplus 3, France) in an up-flow mode. Columns were operated in two phases (Phase I and Phase II), and each phase consisted of a flow interruption during the continuous influent injection. In Phase I (0-33.1 PVs), the influent was introduced to the columns at a flow rate of 5.0 ± 0.1 µL/min, equivalent to a pore-water seepage velocity (v_p) of 3.7 ± 0.2 cm/day and a hydraulic residence time (RT) of 4.1 ± 0.2 days. A 2-day flow interruption was conducted at 11.5 PVs. In Phase II (33.1-58.8 PVs), the flow rate was reduced to 3.2 ± 0.1 µL/min (v_p of 2.4 ± 0.1 cm/day, RT of 6.3 ± 0.3 days), and a longer flow interruption of 7 days was conducted at 47.4 PVs. In sum, all columns were operated for a total of 305 days (136 days for Phase I, and 169 days for Phase II).

Throughout the 305-day operation, the column effluent (A1, A2, B1, B2) dripping out of the effluent tubing was collected in a 15-mL centrifuge tube (Figure 6-1). Effluent samples were used to monitor the column flow rate, and were analyzed for dissolved organic carbon (DOC) concentration (TOC-L CPH, Shimadzu). In addition, 65 μ L of column effluent (A1, A2, B1, B2) was collected from the 3-way valve every PV (Figure 6-1), and immediately mixed with methanol (1,235 μ L) to minimize the potential loss of volatile PFAS. The methanol-diluted sample was then filtered through a 0.2- μ m nylon filter (Corning Inc., Corning, NY), and stored at -20 °C prior to LC-MS/MS analysis. Every four PVs, additional aqueous samples were withdrawn from the biotic column (B1, B2) side-ports (port 1, 2, 3, see Figure 6-1) using a Chemyx Fusion 200 syringe pump (Chemyx Inc., Stafford, TX) and 1-mL syringe (BD Luer-Lok) at a 10% of background flow rate (e.g., 0.5 μ L/min withdrawn rate in Phase I). The withdrawn sample (65 μ L) was also immediately mixed with methanol (1,235 μ L) and stored at -20 °C for further PFAS analysis.

Throughout the experiments, 1.5 mL of side-port samples were also withdrawn during 25.5-27.5 PVs in Phase I, and during 40.6-43.0 PVs and 47.4-48.9 PVs in Phase II following the method described above for the measurements of oxidation-reduction potential (ORP). At the termination of column experiments, all columns were dissected for PFAS extraction to determine the distribution of 6:2 FTS and biotransformation products in the solid phase throughout the columns.

6.2.5. LC-MS/MS Analysis

Target PFAS analytes for LC-MS/MS analysis are listed in Table E-1. The analysis of perfluoroalkyl acids (PFAAs) and polyfluorinated compounds were performed as described previously (Chapter 5). Detection was achieved using a Waters ACQUITY ultra high-performance liquid chromatograph coupled with a Waters Xevo triple quadrupole mass spectrometer (UPLC-MS/MS) (Waters Corporation, Milford, MA). The UPLC was equipped with a Waters ACQUITY UPLC BEH C18 Column (130Å, 1.7 μ m, 2.1 mm X 50 mm). Details on the solvent gradient, instrumental parameters, and the detection limits of target PFAS can be found in the Chapter 5.

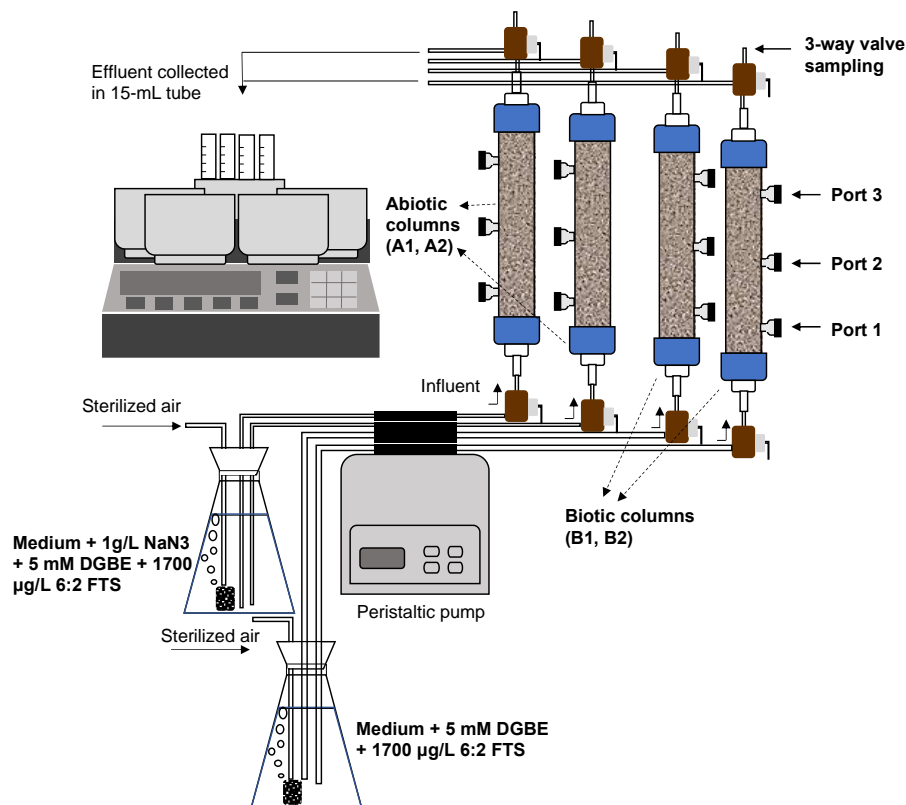


Figure 6-1. Schematic of column experimental set-up.

6.3 Results and discussion

Results from non-reactive tracer tests revealed that four columns (A1, A2, B1, B2) were packed almost identically, with a PV of 28.9 ± 0.3 mL and a porosity of 0.35 ± 0.00 cm³/cm³ (Table E-2). For simplicity, the average PV was used for all columns in subsequent results and discussion, and no relative standard deviation of PV was noted for duplicate abiotic and biotic columns.

Throughout the 305-day column experiments, the consumption of DGBE in biotic columns was monitored by comparing the DOC concentrations in biotic column effluents to abiotic columns (Figure E-1, Appendix E). Lower DOC concentrations were constantly observed in the biotic effluent than abiotic ones (Figure E-1). In addition, ORPs of the biotic column samples collected from influent, effluent, and three side-ports during the operation in Phase I and Phase II were all greater than 450 mV (values reported relative to standard hydrogen electrode) (Table E-3). These results indicated that oxic conditions were maintained in biotic columns throughout the experiments, and DGBE was biodegraded by the aerobic microorganisms in biotic columns.

6.3.1 Biotransformation of 6:2 FTS under dynamic flow conditions

Targeted LC-MS/MS analysis of column effluent samples indicated the production of eight 6:2 FTS biotransformation products in biotic columns that were also observed in the previous microcosm study (Chapter 5). Those transformation products were 6:2 fluorotelomer saturated carboxylic acid (6:2 FTCA), 6:2 fluorotelomer unsaturated carboxylic acid (6:2 FTUA), 5:2 secondary fluorotelomer alcohol (5:2 sFTOH), 5:3 fluorotelomer carboxylic acid (5:3 acid), perfluorobutanoic acid (PFBA), perfluoropentanoic acid (PFPeA), perfluorohexanoic acid (PFHxA), and perfluoroheptanoic acid (PFHpA). In abiotic column effluents, 6:2 FTCA, 6:2 FTUA, and 5:2 sFTOH were below the limits of detection (LODs); small amounts of 5:3 acid, PFBA, PFPeA, PFHxA, and PFHpA were detected as legacy PFAS in Loring soil, without significant increase ($p > 0.05$) throughout the experiments. In contrast, substantially higher concentrations of these eight compounds were detected in the effluents from biotic columns than abiotic columns. The molar yields of all targeted 6:2 FTS biotransformation products in biotic columns were accordingly determined after subtracting their concentrations in abiotic column effluents.

To better depict and understand the biotransformation of 6:2 FTS in the column experiments, the eight transformation products were categorized into three classes: early intermediates (i.e., 6:2 FTCA and 6:2 FTUA), middle intermediates (i.e., 5:2 sFTOH and 5:3 acid), and terminal products (i.e., PFBA, PFPeA, PFHxA, and PFHpA), based on the findings in the prior microcosm study (Table E-4; also in Chapter 5). Briefly, during the 224-day incubation in Loring soil microcosms, low levels of 6:2 FTCA (<0.5 mol%) were formed due to its rapid biotransformation to 6:2 FTUA, which peaked at early-stage of incubation (day 28, 3.7 ± 0.5 mol%). As a major intermediate, 5:2 sFTOH was rapidly produced in the first 56 days (10.2 ± 1.1 mol% at day 56), then leveled off. Another major intermediate, 5:3 acid reached its peak molar yield at 8.9 ± 1.2 mol% by day 154. PFBA, PFPeA, PFHxA, and PFHpA were continuously accumulated until the end of incubation, thus were regarded as terminal products.

6.3.1.1 Biotransformation of 6:2 FTS in Phase I. Column breakthrough results were reported as molar percent (i.e., ratio of molar concentration of 6:2 FTS and biotransformation products in the effluent to the molar concentration of 6:2 FTS spiked in the influent). Throughout the 305-day experiments, the molar percent of 6:2 FTS in abiotic column effluents remained relatively constant

(98.8 ± 10.5 mol%) after the breakthrough (i.e., increased from 1.2 ± 0.0 mol% at 0.5 PVs to 103.8 ± 9.3 mol% at 2.5 PVs), indicating 6:2 FTS was stable in the abiotic columns (Figure 6-2). The observation was also in agreement with the absent formation of 6:2 FTS transformation products in abiotic column effluents. In the biotic columns, however, biotransformation of 6:2 FTS was observed throughout the experiments, as demonstrated by the decrease in 6:2 FTS (Figure 6-2), and the formations of transformation products in the column effluents (Figure 6-3).

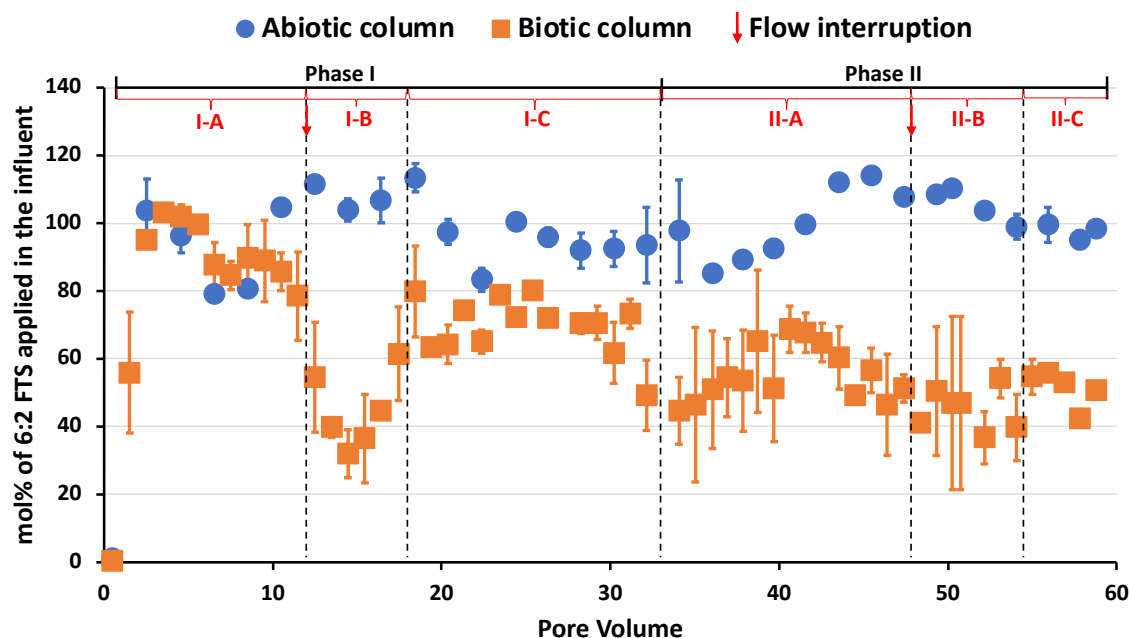


Figure 6-2. Time-course of 6:2 FTS concentration in the effluents from abiotic and biotic columns. Error bars represent the standard deviation of duplicate abiotic and biotic columns.

The biotransformation of 6:2 FTS during the operation of Phase I can be divided into three subphases (Phases I-A, I-B, and I-C; see Figure 6-2 and Figure 6-3). In Phase I-A (0.5-11.5 PVs), the breakthrough of 6:2 FTS was observed during 0.5-2.5 PVs, followed by a slow decrease in 6:2 FTS concentration (Figure 6-2), as well as an increasing formation of biotransformation products especially the early intermediates (6:2 FTCA and 6:2 FTUA) during 2.5-11.5 PVs (Figure 6-3). Specifically, 6:2 FTS in the biotic column effluents decreased from 95.0 ± 0.7 mol% at 2.5 PVs to 84.6 ± 4.2 mol% at 7.5 PVs, further to 78.5 ± 13.0 mol% at 11.5 PVs (Figure 6-2). Correspondingly, the combined molar yields of 6:2 FTCA and 6:2 FTUA increased from 1.9 ± 1.5 mol% at 2.5 PVs to 6.6 ± 5.0 mol% at 7.5 PVs, further to 18.1 ± 4.3 mol% at 11.5 PVs (Figure 6-

3). The increased production of 5:3 acid was also observed (0.1 and 2.4 mol% at 2.5 and 11.5 PVs, respectively). The formation of terminal products (i.e., C₄-C₇ PFCAs) during this subphase was minimal, except PFHxA which was produced with 0.3 ± 0.1 mol% at 11.5 PVs (Figure 6-3). Taken together, these results indicate that the biotransformation of 6:2 FTS was initiated in Phase I-A, and the extent of 6:2 FTS biotransformation was gradually increasing, which might be attributed to the acclimation of native soil microorganisms under tested column conditions.

At 11.5 PVs, a 2-day flow interruption was conducted to all columns. A sharp decrease in 6:2 FTS was observed in the following 3 PVs (e.g., only 32.0 ± 7.1 mol% of 6:2 FTS at 14.5 PVs), followed by a bounce-back to 61.4 ± 13.8 mol% at 17.5 PVs (Figure 6-2). During Phase I-B (11.5-17.5 PVs), a greater formation of terminal products and 5:2 sFTOH was observed than that prior to flow interruption (Figure 6-3). For example, PFBA and PFHpA that were not produced prior to flow interruption, were both formed with an average molar yield of 0.1 ± 0.1 mol% during Phase I-B (Table E-5). Here, an average molar yield of one compound represents the average value of its molar yields measured in all sampling points during a subphase (Table E-5). The formation of 6:2 FTCA and 6:2 FTUA was correspondingly decreased in this subphase, with an average combined molar yield of 8.8 ± 5.3 mol% (Figure 6-3, Table E-5). The results suggest that a greater extent of 6:2 FTS biotransformation likely occurred in Phase I-B following the 2-day flow interruption. In addition, the sharp decrease in 6:2 FTS observed in biotic column effluents following the flow interruption was unlikely caused by rate-limited sorption of 6:2 FTS to the porous media, since similar decrease was not found in abiotic column effluents (Figure 6-2).

During 17.5-33.1 PVs (Phase I-C), 6:2 FTS concentrations remained relatively stable in the biotic column effluents (Figure 6-2). Likewise, the composition of 6:2 FTS biotransformation products in the effluents was comparatively constant, though some fluctuation was observed, for instance, at 30.2 and 32.2 PVs (Figure 6-3). Therefore, 6:2 FTS biotransformation might be at a steady-state in Phase I-C under the tested conditions (i.e., $RT = 4.1 \pm 0.2$ days). Under this steady-state, an average 6:2 FTS concentration of 70.8 ± 11.9 mol% remained in the column effluents, along with average molar yields of 5.2 ± 3.8 mol% for 6:2 FTCA, 5.1 ± 2.5 mol% for 6:2 FTUA, 3.8 ± 3.2 mol% for 5:2 sFTOH, 2.0 ± 1.9 mol% for 5:3 acid, 0.0 ± 0.1 mol% for PFBA, 0.1 ± 0.1 mol% for PFPeA, 0.2 ± 0.2 mol% for PFHxA, and 0.0 ± 0.1 mol% for PFHpA, respectively (Figure 6-3, Table E-5).

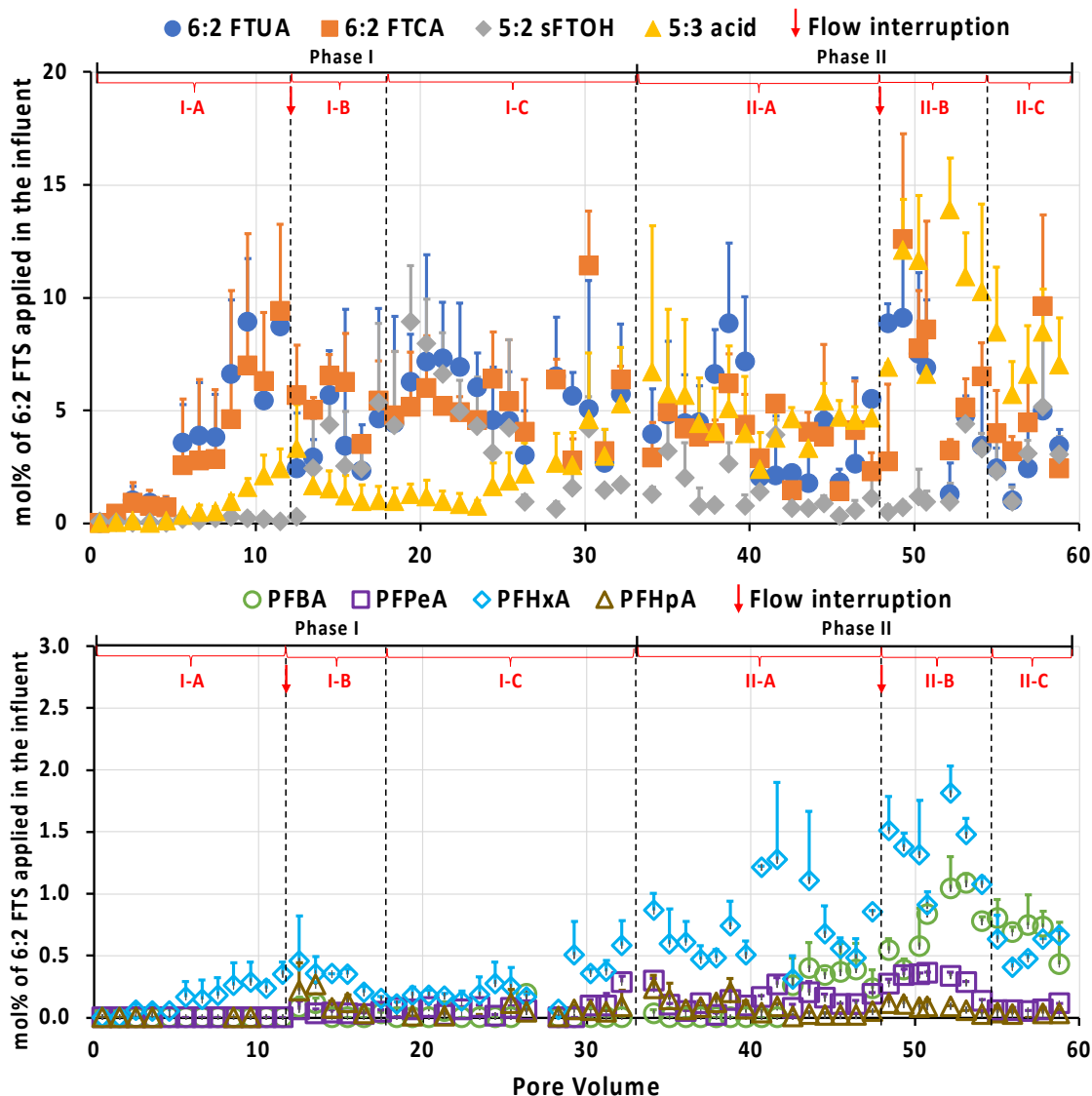


Figure 6-3. Time-courses of the concentrations of biotransformation products during 6:2 FTS biotransformation in biotic columns. Error bars represent the standard deviation of duplicate biotic columns. Note that different y-axis scales were used in top and bottom plots.

6.3.1.2 Biotransformation of 6:2 FTS in Phase II. At 33.1 PVs, the flow rate for influent delivery to all columns was reduced to 3.2 ± 0.1 $\mu\text{L}/\text{min}$. Columns operation then entered Phase II, which can also be divided into three subphases (Phases II-A, II-B, and II-C, see Figure 6-2 and Figure 6-3). A large variation in 6:2 FTS effluent concentrations was first observed from two biotic columns during the several PVs (35.0-39.7 PVs) following the decrease of flow rate (Figure 6-2). An adverse environment (e.g., temporary inadaptation) might be created to the aerobic

microorganisms in one of the biotic columns due to the sudden flow rate reduction. Accordingly, a short-term poor performance of 6:2 FTS biotransformation was observed in that column. After gradual adaption, two biotic columns started to behave similarly at 40.6 PVs (Figure 6-2). Overall, obvious lower concentrations of 6:2 FTS was observed in Phase II-A (33.1-47.4 PVs) than those in Phase I-C (Figure 6-2). In average, 55.4 ± 15.0 mol% of 6:2 FTS remained in the column effluents during Phase II-A (Table E-5), which was much lower than that during Phase I-C (i.e., 70.8 ± 11.9 mol%). Correspondingly, greater amounts of terminal products were formed, with a molar yield of 0.1 ± 0.2 mol% for PFBA, 0.1 ± 0.1 mol% for PFPeA, 0.7 ± 0.4 mol% for PFHxA, and 0.1 ± 0.1 mol% for PFHpA, respectively (Figure 6-3, Table E-5). The molar yield of PFHxA during Phase II-A was more than 3-fold higher than that during Phase I-C. In addition, less of early intermediates was produced during Phase II-A, with an average molar yield of 3.7 ± 2.6 mol% for 6:2 FTCA, and 4.2 ± 2.6 mol% for 6:2 FTUA, respectively (Figure 6-3, Table E-5). As for the two middle intermediates, the production of 5:2 sFTOH decreased from 3.8 ± 3.2 mol% (average molar yield) in Phase I-C to 1.4 ± 1.4 mol% in Phase II-A; while 5:3 acid formation increased from 2.0 ± 1.9 mol% in Phase I-C to 4.7 ± 2.7 mol% in Phase II-A (Figure 6-3, Table E-5). Taken together, these results indicate that a greater extent of 6:2 FTS biotransformation occurred in Phase II-A than Phase I-C. The slower flow rate in Phase II-A rendered soil microorganisms more time (i.e., longer residence time) for 6:2 FTS biotransformation, resulting in a more complete transformation, namely, less formations of early intermediates but greater formations of terminal products (Figure 6-3).

At 47.4 PVs, a longer flow interruption of 7 days was performed to all columns. Immediately after resuming the flow, ORPs of the samples collected from biotic column side-ports were measured to confirm if oxygen was sufficient for microbial growth during the flow interruption. The measurement of 569.5 ± 22.7 mV (values reported relative to standard hydrogen electrode) suggested that oxic condition was predominant during flow interruption (Table E-3). Compared to Phase II-A, in the Phase II-B following the resumption of flow (i.e., 47.4-54.1 PVs), a substantial increase in the production of 6:2 FTS biotransformation products was observed (Figure 6-3), along with the decreased concentration of 6:2 FTS in the effluents (average molar percent of 45.1 ± 17.3 mol%, Figure 6-2). In particular, the molar yields of 5:3 acid (10.4 ± 3.4 mol%), PFBA (0.7 ± 0.3 mol%), PFPeA (0.3 ± 0.1 mol%) and PFHxA (1.4 ± 0.4 mol%) in Phase II-B were all >2-fold greater than those in Phase II-A (Figure 6-3, Table E-5). Even for the early intermediates 6:2 FTCA

and 6:2 FTUA, both were also formed with higher molar yields (6.6 ± 4.0 and 6.0 ± 4.1 mol%, respectively) in Phase II-B (Figure 6-3, Table E-5). These observations indicate that after the 7-day flow interruption, the biotransformation of 6:2 FTS was greatly promoted in Phase II-B, resulting in a greater production of all targeted 6:2 FTS transformation products.

The promoting effect of flow interruption on 6:2 FTS biotransformation appeared to be minimal after 54.1 PVs, as the production of biotransformation products in Phase II-C (54.1-58.8 PVs) returned to the similar levels observed in Phase II-A (Figure 6-3). For example, the combined average molar yield of early intermediates was 7.9 ± 5.2 mol% in Phase II-A, and 7.6 ± 6.0 mol% in Phase II-C, respectively (Table E-5). Also, the combined average molar yield of terminal products was 1.0 ± 0.8 mol% in Phase II-A, and 1.4 ± 0.3 mol% in Phase II-C, respectively (Table E-5). Moreover, similar concentrations of 6:2 FTS in the effluents were observed in the two subphases (55.4 ± 15.0 and 52.3 ± 5.8 mol% averaged in Phase II-A and Phase II-C, respectively) (Figure 6-2). Therefore, the observed concentration of 6:2 FTS and associated biotransformation products in Phase II-A and Phase II-C may represent the steady-state of 6:2 FTS biotransformation under the slower flowing conditions (i.e., $RT = 6.3 \pm 0.3$ days).

6.3.1.3 Effects of flow rate and flow interruption on 6:2 FTS biotransformation. The average molar percent of 6:2 FTS and biotransformation products at different phases during column experiments were summarized in Table E-5. These average molar percent allowed for a better understanding of the effects of flow rate and flow interruption on 6:2 FTS biotransformation. By reducing the flow rate from 5.0 ± 0.1 $\mu\text{L}/\text{min}$ in Phase I to 3.2 ± 0.1 $\mu\text{L}/\text{min}$ in Phase II (i.e., 36% reduction), a more complete 6:2 FTS biotransformation was achieved in Phase II (Table E-5). Specifically, 22-26% lower concentrations of 6:2 FTS were measured in Phases II-A and II-C than those in Phase I-C (Table E-5). Also, much more terminal biotransformation products (C₄-C₇ PFCAs) were produced in Phases II-A (1.0 ± 0.8 mol%) and II-C (1.4 ± 0.3 mol%) than Phase I-C (0.3 ± 0.4 mol%), while less early intermediates were produced in Phases II-A (7.9 ± 5.2 mol%) and II-C (7.6 ± 6.0 mol%) than Phase I-C (10.3 ± 6.3 mol%) (Table E-5).

An apparent promoting effect of flow interruption on 6:2 FTS biotransformation in the several PVs following flow resumption was demonstrated in the present study, as discussed in Sections 3.1.1 and 3.1.2. The concentrations of 6:2 FTS and biotransformation products in the phases prior to and after the flow interruption (e.g., Phase II-A and Phase II-B) were compared (Table E-5).

One point of interest is the promoting effect of either the 2-day flow interruption at 11.5 PVs or the 7-day flow interruption at 47.4 PVs on 6:2 FTS biotransformation lasted approximately 6-7 PVs after the flow resumption (i.e., Phases I-B and II-B) (Figure 6-2 and Figure 6-3). The underlying reason for such lasting effect might be the growing abundances of soil microbial communities during the flow interruption, though more future research and evidence is recommended for confirmation. Regardless, the promoting effect resulted from flow interruption suggest that the 6:2 FTS biotransformation under the investigated column conditions was rate limited by the dynamic flow conditions. The finding was also supported by the observation that more complete 6:2 FTS biotransformation occurred under slower flow rate (i.e., Phase II).

6.3.2 Biotransformation of 6:2 FTS along the flowing path

The biotransformation of 6:2 FTS along the flowing path in the biotic columns were investigated using the samples collected from the three side-ports on the columns (Figure 6-1). The flowing path of synthetic groundwater (i.e., influent) was first at Port 1, then to Port 2, further to Port 3, and finally to 3-way valve sampling location (i.e., effluent). Throughout the 305-day column experiments, a total of 13 sets of side-port samples were collected at different sampling points. To better depict the differences of 6:2 FTS biotransformation along the flowing path, in each subphase (e.g., Phase II-A), the concentrations of 6:2 FTS and biotransformation products measured in each of Ports 1-3 and effluent samples were averaged respectively (Figure 6-4). For example, the average molar percent of 6:2 FTS and biotransformation products at Port 1 in Phase I-C (Figure 6-4) represents the average concentration of each compound in the Port 1 samples collected at three sampling points in Phase I-C (i.e., 24.4, 28.3, and 32.2 PVs). Phases I-A and I-B were not included in Figure 6-4, because an incorrect sampling technique was used initially for side-ports sampling (i.e., needle did not reach to the center of columns) which resulted in the side-port samples collected during Phases I-A and I-B were mostly from the Port itself (i.e., a “dead zone”) instead of the flowing stream.

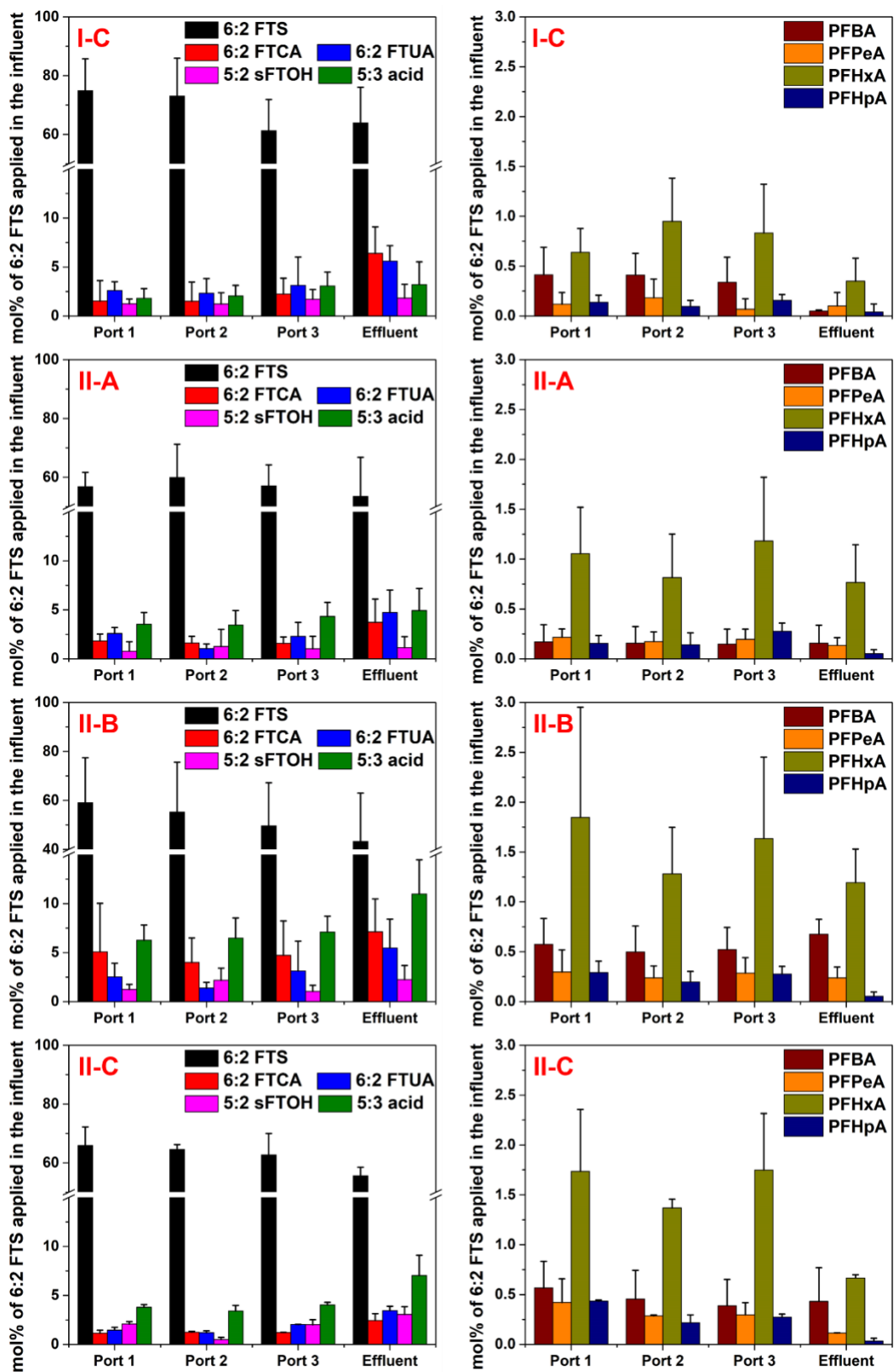


Figure 6-4. The average molar percent of 6:2 FTS and biotransformation products along the flowing path (i.e., Port 1, Port 2, Port 3, and Effluent, See Figure 6-1) in different phases.

In general, a decreasing trend in 6:2 FTS concentration over the flowing path was observed in each subphase (Figure 6-4). For example, average molar percent of 6:2 FTS decreased from 74.9 ± 10.9 mol% at Port 1 to 73.1 ± 12.8 mol% at Port 2, further to 61.3 ± 10.6 mol% at Port 3 during Phase I-C. Likewise, average molar percent of 6:2 FTS at Ports 1-3 and effluent during Phase II-C were 65.9 ± 6.3 , 64.6 ± 1.7 , 62.7 ± 7.3 , and 55.6 ± 2.9 mol%, respectively (Figure 6-4). Correspondingly, increasing trends in the concentrations of early and middle intermediates over the flowing path were observed (Figure 6-4). Take Phase I-C as an example, 6:2 FTCA and 6:2 FTUA gradually increased from 1.5 ± 2.1 and 2.6 ± 0.9 mol% at Port 1, to 6.4 ± 2.7 and 5.6 ± 1.6 mol% in the effluent, respectively (Figure 6-4). Similarly, 5:2 sFTOH and 5:3 acid gradually increased from 1.3 ± 0.5 and 1.8 ± 1.0 mol% at Port 1, to 1.8 ± 1.4 and 3.2 ± 2.3 mol% in the effluent, respectively (Figure 6-4). Overall, a decrease of 14.6%, 5.9%, 26.7%, and 15.6% in 6:2 FTS concentration was determined in the effluent relative to Port 1 in Phases I-C, II-A, II-B, and II-C, respectively. For the formation of early and middle intermediates in these four subphases, increase of 40.3-320.3%, 82.1-136.5%, 45.7-81.1%, and 39.5-85.3% in the effluent relative to Port 1 were observed for 6:2 FTCA, 6:2 FTUA, 5:2 sFTOH, and 5:3 acid, respectively. Taken together, these findings demonstrate that the biotransformation of 6:2 FTS was gradually proceeding along the flowing path under the different tested column conditions (e.g., different flow rates).

However, an increasing trend in the production of terminal products was not observed over the flowing path in each subphase (Figure 6-4). The average molar yields of PFBA, PFPeA, PFHxA, and PFHpA stayed relatively stable among the Ports 1-3 and effluent samples (Figure 6-4). For instance, during Phase II-C, average molar yields of PFHxA at Ports 1-3 and effluent were 1.1 ± 0.5 , 0.8 ± 0.4 , 1.2 ± 0.6 , and 0.8 ± 0.4 mol%, respectively (Figure 6-4). Meanwhile, PFBA, PFPeA, and PFHpA remained at 0.1-0.2, 0.1-0.2, and 0.1-0.3 mol%, respectively, among the Ports 1-3 and effluent samples (Figure 6-4). The relatively stable molar yields of terminal products observed along the flowing path could be attributed to the short RTs that were used in the present column experiments. Although RT was increased to 6.3 ± 0.3 days in Phase II, it was still likely much shorter than that needed for a substantial amount of PFCAs production during 6:2 FTS biotransformation. In prior microcosm study, the molar yields of PFCAs from day 28 to day 154 (e.g., PFHxA ranging from 0.8 ± 0.2 to 1.8 ± 0.0 mol%) were comparable to those in the present column experiment (Table E-4 and Table E-5). Until the incubation at day 224, the molar yield of each PFCA increased substantially compared to day 154; for example, PFHxA increased from 1.6

± 0.3 to 5.3 ± 0.7 mol% by day 224 (Table E-4). The previously proposed “fluorotelomer ketone to PFCA” pathway that led to formation of PFCAs might not be able to be completed in such short RTs (4.1-6.3 days) used in the present study.

There is a surprising finding that 6:2 FTS biotransformation and the associated production of biotransformation products occurred in the first quarter of the column (i.e., from influent injection to Port 1, see Figure 6-1), appeared to represent a significant portion of the overall 6:2 FTS biotransformation throughout the column (Figure 6-4). Although the decrease in 6:2 FTS as well as the increases in early and middle intermediates were observed along the flowing path (discussed above), such decrease or increases were not in proportion to the flowing distance. For example, in Phases I-C, II-A, II-B, and II-C, only 5.9-26.7% more decrease in 6:2 FTS was found in the effluent relative to Port 1 (Figure 6-4), although the distance of Port 1 to effluent was 3-fold longer than that from influent injection to Port 1 (Figure 6-1). Similarly, most of the increases in production of biotransformation products were less than 100% (i.e., 2-fold increase) in the effluent relative to Port 1 (Figure 6-4). These results suggest that the first several steps of 6:2 FTS biotransformation leading to the formation of 6:2 FTCA, 6:2 FTUA, 5:2 sFTOH, or 5:3 acid might be relatively fast, namely, these steps could be completed in 1-2 days (1/4 of RTs) under the tested column conditions. Further biotransformation of those intermediates might explain the lower-than-expected increases in their production along the flowing path.

6.3.3 Comparison of 6:2 FTS biotransformation between microcosm and column experiments

The concentrations of 6:2 FTS and biotransformation products at different time points in prior microcosm study and in different phases of the present column study were summarized in Table E-4 and Table E-5, respectively. In prior microcosm study, the biotransformation of 6:2 FTS in the first 7 days of incubation was minimal, with only 0.1 ± 0.0 mol% of biotransformation products quantified (Table E-4). The biotransformation proceeded on day 28 and day 56, with 64.4 ± 8.9 and 39.2 ± 2.1 mol% of 6:2 FTS remaining in the microcosms, respectively (Table E-4). Further, 6:2 FTS decreased to 29.9 ± 7.6 and 0.2 ± 0.0 mol% on day 98 and day 154, respectively (Table E-4). With the increasing extent of 6:2 FTS biotransformation, the production of quantified biotransformation products was also increased, together with the gradual decrease in the total mass recovery (Table E-4). The decreasing mass recovery was attributed to the increasing formations of

biotransformation products that were not quantified by LC-MS/MS analysis over the incubation. In the present column experiments, the extent of 6:2 FTS biotransformation in different phases can be approximately corresponded to that at a certain time point in the microcosm study, based on the comparisons of molar percent of 6:2 FTS and quantified biotransformation products, as well as the total mass recovery (Table E-4 and Table E-5). Specifically, 6:2 FTS biotransformation during the steady-state under faster flow rate (i.e., Phase I-C, $RT = 4.1 \pm 0.2$ days) might be close to that occurred between day 7 to day 28 in the microcosm study, considering the slightly higher 6:2 FTS concentration and mass recovery in Phase I-C than those at day 28 microcosms (Table E-4 and Table E-5). Similarly, 6:2 FTS biotransformation during Phases II-A and II-C ($RT = 6.3 \pm 0.3$ days) might be close to that occurred between day 28 to 56 in the microcosm study, given the 6:2 FTS concentration and mass recovery in Phases II-A and II-C were higher than those at day 56 microcosms but lower than day 28 microcosms (Table E-4 and Table E-5). A slightly higher mass recovery might be achieved in the columns than microcosms if same extent of 6:2 FTS biotransformation occurred, because the sorption of 6:2 FTS and biotransformation products onto the column glass surface and porous media might be negligible under the continuous flowing conditions (3-4 μM of 6:2 FTS in the influent). At the termination of column experiments, the porous media packed in the biotic columns were dissected and extracted. Only 6:2 FTS, 5:3 acid, PFHxA, and PFHpA were detected above the LODs, with 6:2 FTS concentrations of 0.6-0.8 nM/g dw porous media, and <0.01 nM/g dw porous media for the other three products.

Overall, the RTs in the present column experiments were much shorter than the incubation time needed in the microcosms to achieve an approximately same extent of 6:2 FTS biotransformation. The results indicate that the dynamic flowing condition in the porous media likely promoted the biotransformation of 6:2 FTS, compared to that observed in the microcosms. Previously, similar promoting effects of continuous flow on microbial dechlorination activity was also observed, with a more than 200-fold greater dechlorination rates in columns than those in batch reactors.¹⁹⁶ In addition to the biotransformation rate, biotransformation pathways of 6:2 FTS might also be impacted by flow conditions. First, a greater production of early intermediates 6:2 FTCA and 6:2 FTUA was observed in the columns than microcosms (Table E-4 and Table E-5). The combined molar yield of 6:2 FTCA and 6:2 FTUA in column experiments was 7.6-12.6 mol%, which was much higher than that in the microcosms (<3.7 mol%). Second, further biotransformation of 6:2 FTUA to 5:2 sFTOH was preferred over the transformation of 6:2 FTUA to 5:3 acid in the

microcosms, with a much greater molar yield of 5:2 sFTOH than 5:3 acid during the incubation, especially in first 56 days (Table E-4). However, such preference was not observed in the present column experiments (Figure 6-3); moreover, the reverse preference of conversion to 5:3 acid over the conversion to 5:2 sFTOH was found in Phase II of column experiments (Figure 6-3, Table E-5). Last, PFPeA and PFHxA were the two primary terminal products of 6:2 FTS biotransformation in the prior microcosms (Table E-4). However, PFPeA was not determined as a main terminal product in the columns (<0.3 ml%); instead, PFBA was found to be more abundantly produced (ca. 0.7 mol% in Phases II-B and II-C) (Figure 6-3, Table E-5). These results suggest that a large discrepancy in 6:2 FTS biotransformation (e.g., rate, pathway) might exist between the experimental systems with and without incorporation of dynamic flow conditions. Therefore, only the results from batch experiments using the site materials might not be enough to accurately evaluate the biotransformation of 6:2 FTS at a site where dynamic flowing is present.

6.4 Environmental implications

This study, for the first time, investigated the biotransformation of 6:2 FTS under continuous flow conditions during 305-day column experiments. The biotransformation was demonstrated to be rate limited by the flow condition. Under a slower flow rate, more time was provided to soil microorganisms for a more complete 6:2 FTS biotransformation, resulting in less formation of early intermediates (i.e., 6:2 FTCA and 6:2 FTUA) but greater formation of terminal products (i.e., C₄-C₇ PFCAs). In addition, flow interruption (2-7 days) was found to promote the biotransformation of 6:2 FTS after the resumption of flow, and the promoting effect could last approximately 6-7 PVs. The analysis of samples collected from the side-ports on columns confirmed that 6:2 FTS biotransformation proceeded along the flowing path, with a generally decreasing trend in 6:2 FTS concentration and increasing trends in biotransformation products over the path. These findings indicate that the flow condition is a critical parameter for the assessment of the fate and transformation of 6:2 FTS in natural environment.

By the comparison of 6:2 FTS biotransformation in the present column experiments to that in prior microcosms, continuous flow condition was demonstrated to promote the biotransformation. In other words, the environmental stability of 6:2 FTS under flow conditions is likely substantially lower than that observed in batch reactor experiments using same microbial community. Correspondingly, substantially greater production of 6:2 FTS biotransformation products is

expected under flow condition than those determined in batch reactor experiments during a certain time period. Moreover, the biotransformation pathways of 6:2 FTS in column experiments differed from those observed in batch experiments. Overall, cautions may need to be taken to apply the biotransformation behavior of one PFAS compound obtained in batch reactor experiments for the evaluation of its fate in natural environment where dynamic flowing is present. Given almost all studies on PFAS biotransformation were conducted in batch reactor experiments so far, the findings in the present study highlight the importance and underscore the urgent need of incorporation of system conditions such as hydraulic parameters into experimental systems in the investigation of PFAS biotransformation.

Chapter 7 : Key findings, publications, and recommendations for future work

The studies described herein are intended to enhance the understandings of biotransformation of aqueous film-forming foams (AFFF)-derived polyfluoroalkyl substances by native microbial communities under conditions representative of AFFF-impacted sites. The research focuses on examining the biotransformation rates and pathways of three representative precursors, perfluorooctane sulfonamide (FOSA), 8:2 fluorotelomer alcohol (8:2 FTOH), and 6:2 fluorotelomer sulfonate (6:2 FTS), in the laboratory microcosm and column experiments using multiple AFFF-impacted soils under oxic and anoxic conditions. The findings in this research provide insights into the environmental fate and behavior of these precursors, which can provide crucial knowledge for the management and remediation of hundreds of AFFF-impacted sites.

7.1 Key Findings

7.1.1 Production of PFOS from biotransformation of FOSA in aerobic soils

- The biotransformation of FOSA in natural environment might be soil/site dependent. With a tendency to partitioning to the solid phase, the bioavailability of FOSA to the native microbial community appears to a critical parameter for the evaluation of FOSA biotransformation in soil compartment.
- Microorganisms belonging to Proteobacteria, Actinobacteriota, Chloroflexi, Acidobacteriota, and Planctomycetota might play a role in the biotransformation of FOSA, while Cyanobacteria and Bacteroidota might be relatively more tolerant to FOSA and/or the associated transformation products.
- Evaluations of site geochemical and biological attributes are important towards achieving a better understanding of FOSA biotransformation in the field, as well as gaining insights into the management and remediation of contaminated sites.

7.1.2 Biotransformation of 8:2 FTOH in soil from AFFF-impacted sites under nitrate-, sulfate-, and iron-reducing conditions

- The biotransformation rates and pathways of 8:2 FTOH are highly dependent upon redox conditions. The biotransformation was much slower under sulfate- and iron-reducing conditions than under nitrate-reducing conditions, while the fastest biotransformation was reported under oxic conditions.

- PFCAs, which were found as the terminal products of 8:2 FTOH biotransformation under oxic conditions, were produced with less yield under nitrate-reducing conditions, and were not formed under sulfate- and iron-reducing conditions.
- Biostimulation (e.g., lactate amendment) was shown to increase 8:2 FTOH biotransformation rates and products yields (e.g., PFOA) in the anaerobic microcosms.
- Genera potentially responsible for 8:2 FTOH biotransformation under each redox condition were identified including *Lysobacter*, *Herminiimonas*, and *Ramlibacter* under nitrate-reducing conditions, and *Caldicoprobacter* and *Sedimentibacter* under sulfate- and iron-reducing conditions.

7.1.3 Aerobic biotransformation of 6:2 FTS in soils from two AFFF-impacted sites

- The biotransformation of 6:2 FTS in AFFF-impacted soils is strongly influenced by environmental factors such as the availability of sulfur sources and native microbial community composition.
- The biotransformation of 6:2 FTS was favored by the microbial consortia only after other easily assimilated sulfur sources (e.g., sulfate) were depleted.
- Desulfobacterota microorganisms likely promoted 6:2 FTS biotransformation via more efficient desulfonation. Species in the genus *Sphingomonas*, which exhibited higher tolerance to the elevated concentrations of 6:2 FTS and its biotransformation products, are likely to have contributed to 6:2 FTS biotransformation.
- A novel “fluorotelomer ketone to PFCA” pathway was proposed to account for the formation of PFCAs from fluorotelomer precursors.

7.1.4 Biotransformation of 6:2 FTS in AFFF-impacted soil under continuous flow conditions

- The biotransformation of 6:2 FTS was demonstrated to be rate limited by the flow condition in the one-dimensional columns. Under a slower flow rate, more time was provided to soil microorganisms for a more complete 6:2 FTS biotransformation, resulting in less formation of early intermediates (i.e., 6:2 FTCA and 6:2 FTUA) but greater formation of terminal products (i.e., C₄-C₇ PFCAs).
- Flow interruption (2-7 days) was found to promote the biotransformation of 6:2 FTS after the resumption of flow, and the promoting effect could last approximately 6-7 PVs.

- The biotransformation of 6:2 FTS proceeded along the flowing path, with a generally decreasing trend in 6:2 FTS concentration and increasing trends in biotransformation products over the path.
- Continuous flow condition was demonstrated to promote the biotransformation of 6:2 FTS. That is, the environmental stability of 6:2 FTS under flow conditions is likely substantially lower than that observed in batch reactor experiments using same microbial community.

7.2 Publications and Presentations

The research in this dissertation is the subject of one published manuscript, one manuscript submitted, and three complete manuscripts (revision and submission pending). Portions of this dissertation have been previously included in conference platform and poster presentations.

7.2.1 Publications

- Yan, P.-F.; Dong, S.; Manz, K. E.; Liu, C.; Woodcock, M. J.; Mezzari, M. P.; Abriola, L. M.; Pennell, K. D.; Cápiro, N. L. Biotransformation of 8:2 Fluorotelomer Alcohol in Soil from Aqueous Film-Forming Foams (AFFFs)-Impacted Sites under Nitrate-, Sulfate-, and Iron-Reducing Conditions. *Environ. Sci. Technol.* **2022**. <https://doi.org/10.1021/acs.est.2c03669>.
- Yan, P.-F.; Dong, S.; Manz, K. E.; Liu, C.; Woodcock, M. J.; Mezzari, M. P.; Abriola, L. M.; Pennell, K. D.; Cápiro, N. L. Aerobic Biotransformation of 6:2 Fluorotelomer Sulfonate in Soils from Two Aqueous Film-Forming Foam (AFFF)-Impacted Sites. *Environ. Sci. Technol.* (*Manuscript in review*)
- Yan, P.-F.; Dong, S.; Woodcock, M. J.; Abriola, L. M.; Pennell, K. D.; Cápiro, N. L. Biotransformation of 6:2 Fluorotelomer Sulfonate in Aqueous Film-Forming Foam (AFFF)-impacted Soil under Continuous Flow Conditions. (*Manuscript to be submitted*)
- Yan, P.-F.; Cápiro, N. L. Differences of per- and polyfluoroalkyl substances in aqueous film-forming foams (AFFFs) and AFFF-impacted environment: role of microbial transformation. (*Manuscript in preparation*)
- Yan, P.-F.; Dong, S.; Abriola, L. M.; Pennell, K. D.; Cápiro, N. L. Production of perfluorooctane sulfonate (PFOS) from biotransformation of perfluorooctane sulfonamide (FOSA) in aerobic soils. (*Manuscript in preparation*)

7.2.2 Selected presentations

- Yan, P.-F., Dong, S., Manz, K.E., Woodcock M., Liu C., Pennell, K.D., Cápiro, N.L. Biotransformation of 6:2 fluorotelomer sulfonate in AFFF-impacted soil: microcosm and column experiments (Platform Presentation). *AEESP 2022 Environmental Engineering at the Confluence*. June 28-30 St. Louis, MO
- Yan, P.-F., Dong, S., Manz, K.E., Woodcock M., Liu C., Pennell, K.D., Cápiro, N.L. Biotransformation of 6:2 fluorotelomer sulfonate in AFFF-impacted soil (Poster Presentation). *9th Annual Graduate Engineering Research Showcase*. October 2021, Auburn University, Auburn, AL
- Yan, P.-F., Dong, S., Liu C., Woodcock M., Manz, K.E., Pennell, K.D., Cápiro, N.L. Biotransformation of 6:2 fluorotelomer sulfonate in AFFF-impacted soil under oxic and anoxic conditions (Platform Presentation). *ACS Fall 2021 Resilience of Chemistry*. August 22-26 Atlanta, GA
- Yan, P.-F., Dong, S., Liu C., Manz, K.E., Pennell, K.D., Cápiro, N.L. Anaerobic biotransformation of 8:2 FTOH in soil from AFFF-impacted sites under nitrate-, sulfate-, and iron-reducing conditions (Poster Presentation). *RemTEC Summit Student Program & Poster Presentation Competition*. March 2021.

7.3 Recommendations for Future Research

Based on the observations and findings in this study, the following recommendations are made for future research.

In Chapters 3, 4 and 5, multiple phyla and genera were identified to be potentially responsible for the biotransformation of FOSA, 8:2 FTOH, and 6:2 FTS under oxic or anoxic conditions. For example, genera *Lysobacter*, *Herminiimonas*, and *Ramlibacter* might be responsible for 8:2 FTOH biotransformation under nitrate-reducing conditions, while *Caldicoprobacter* and *Sedimentibacter* might contribute to the biotransformation under sulfate- and iron-reducing conditions. Future investigation with isolated pure cultures is highly recommended to better assess the biotransformation of each precursor with species from correspondingly identified genera.

In Chapters 4 and 5, novel compounds including 1H-perfluoroalkanes (e.g., 1H-perfluorobutane, 1H-perfluoropentane, and 1H-perfluoroheptane) were identified as the

biotransformation products of 8:2 FTOH or 6:2 FTS under various redox conditions. These 1H-perfluoroalkanes are likely unique transformation products that could be present at sites contaminated by fluorotelomer precursors. Future research is needed to assess the prevalence of these compounds at AFFF-impacted sites and to evaluate their potential impacts on ecosystems and human health. Moreover, the environmental fate of these newly identified compounds is not yet understood. Future research is thus recommended to elucidate their potential biotransformation and pathways.

The results presented in Chapter 6 demonstrate that the biotransformation rates and pathways of 6:2 FTS in flow-through one-dimensional columns differed from those observed in batch experiments. The findings highlight the importance of incorporation of system conditions such as hydraulic parameters into experimental systems in the investigation of PFAS biotransformation. Given almost all studies reported so far on PFAS biotransformation were conducted in batch reactor experiments, more future research is needed to assess the biotransformation of PFAS in the laboratory experiments of increasing scale and complexity, for example, in one-dimensional saturated/unsaturated columns, and multi-dimensional systems incorporating unsaturated and saturated zones. Further, field-scale pilot studies are recommended to be performed to provide deeper understandings of PFAS fate and transformation in the systems with realistic complexity.

Reference

- (1) Buck, R. C.; Franklin, J.; Berger, U.; Conder, J. M.; Cousins, I. T.; de Voogt, P.; Jensen, A. A.; Kannan, K.; Mabury, S. A.; van Leeuwen, S. P. Perfluoroalkyl and Polyfluoroalkyl Substances in the Environment: Terminology, Classification, and Origins. *Integr. Environ. Assess. Manag.* **2011**, *7* (4), 513–541. <https://doi.org/10.1002/ieam.258>.
- (2) Lyu, X.; Xiao, F.; Shen, C.; Chen, J.; Park, C. M.; Sun, Y.; Flury, M.; Wang, D. Per- and Polyfluoroalkyl Substances (PFAS) in Subsurface Environments: Occurrence, Fate, Transport, and Research Prospect. *Rev. Geophys.* **2022**, *60* (3), e2021RG000765. <https://doi.org/10.1029/2021RG000765>.
- (3) Xu, B.; Liu, S.; Zhou, J. L.; Zheng, C.; Weifeng, J.; Chen, B.; Zhang, T.; Qiu, W. PFAS and Their Substitutes in Groundwater: Occurrence, Transformation and Remediation. *J. Hazard. Mater.* **2021**, *412*, 125159. <https://doi.org/10.1016/j.jhazmat.2021.125159>.
- (4) Brusseau, M. L.; Anderson, R. H.; Guo, B. PFAS Concentrations in Soils: Background Levels versus Contaminated Sites. *Sci. Total Environ.* **2020**, *740*, 140017. <https://doi.org/10.1016/j.scitotenv.2020.140017>.
- (5) Hu, X. C.; Andrews, D. Q.; Lindstrom, A. B.; Bruton, T. A.; Schaidler, L. A.; Grandjean, P.; Lohmann, R.; Carignan, C. C.; Blum, A.; Balan, S. A.; Higgins, C. P.; Sunderland, E. M. Detection of Poly- and Perfluoroalkyl Substances (PFASs) in U.S. Drinking Water Linked to Industrial Sites, Military Fire Training Areas, and Wastewater Treatment Plants. *Environ. Sci. Technol. Lett.* **2016**, *3* (10), 344–350. <https://doi.org/10.1021/acs.estlett.6b00260>.
- (6) Grandjean, P.; Clapp, R. Perfluorinated Alkyl Substances: Emerging Insights Into Health Risks. *NEW Solut. J. Environ. Occup. Health Policy* **2015**, *25* (2), 147–163. <https://doi.org/10.1177/1048291115590506>.
- (7) Sedlak, M. D.; Benskin, J. P.; Wong, A.; Grace, R.; Greig, D. J. Per- and Polyfluoroalkyl Substances (PFASs) in San Francisco Bay Wildlife: Temporal Trends, Exposure Pathways, and Notable Presence of Precursor Compounds. *Chemosphere* **2017**, *185*, 1217–1226. <https://doi.org/10.1016/j.chemosphere.2017.04.096>.
- (8) Moody, C. A.; Field, J. A. Perfluorinated Surfactants and the Environmental Implications of Their Use in Fire-Fighting Foams. *Environ. Sci. Technol.* **2000**, *34* (18), 3864–3870. <https://doi.org/10.1021/es991359u>.
- (9) Kissa, E. *Fluorinated Surfactants: Synthesis, Properties, Applications*; Surfactant science series; M. Dekker: New York, 1994.
- (10) Moody, C. A.; Field, J. A. Determination of Perfluorocarboxylates in Groundwater Impacted by Fire-Fighting Activity. *Environ. Sci. Technol.* **1999**, *33* (16), 2800–2806. <https://doi.org/10.1021/es981355+>.
- (11) Tuve, R. L.; Jablonski, E. J. Method of Extinguishing Liquid Hydrocarbon Fires. US3258423A, June 28, 1966.
- (12) Place, B. J.; Field, J. A. Identification of Novel Fluorochemicals in Aqueous Film-Forming Foams Used by the US Military. *Environ. Sci. Technol.* **2012**, *46* (13), 7120–7127. <https://doi.org/10.1021/es301465n>.

- (13) Backe, W. J.; Day, T. C.; Field, J. A. Zwitterionic, Cationic, and Anionic Fluorinated Chemicals in Aqueous Film Forming Foam Formulations and Groundwater from U.S. Military Bases by Nonaqueous Large-Volume Injection HPLC-MS/MS. *Environ. Sci. Technol.* **2013**, *47* (10), 5226–5234. <https://doi.org/10.1021/es3034999>.
- (14) Houtz, E. F.; Higgins, C. P.; Field, J. A.; Sedlak, D. L. Persistence of Perfluoroalkyl Acid Precursors in AFFF-Impacted Groundwater and Soil. *Environ. Sci. Technol.* **2013**, *47* (15), 8187–8195. <https://doi.org/10.1021/es4018877>.
- (15) Barzen-Hanson, K. A.; Roberts, S. C.; Choyke, S.; Oetjen, K.; McAlees, A.; Riddell, N.; McCrindle, R.; Ferguson, P. L.; Higgins, C. P.; Field, J. A. Discovery of 40 Classes of Per- and Polyfluoroalkyl Substances in Historical Aqueous Film-Forming Foams (AFFFs) and AFFF-Impacted Groundwater. *Environ. Sci. Technol.* **2017**, *51* (4), 2047–2057. <https://doi.org/10.1021/acs.est.6b05843>.
- (16) Leeson, A.; Thompson, T.; Stroo, H. F.; Anderson, R. H.; Speicher, J.; Mills, M. A.; Willey, J.; Coyle, C.; Ghosh, R.; Lebrón, C.; Patton, C. Identifying and Managing Aqueous Film-Forming Foam-Derived Per- and Polyfluoroalkyl Substances in the Environment. *Environ. Toxicol. Chem.* **2021**, *40* (1), 24–36. <https://doi.org/10.1002/etc.4894>.
- (17) Ruyle, B. J.; Pickard, H. M.; LeBlanc, D. R.; Tokranov, A. K.; Thackray, C. P.; Hu, X. C.; Vecitis, C. D.; Sunderland, E. M. Isolating the AFFF Signature in Coastal Watersheds Using Oxidizable PFAS Precursors and Unexplained Organofluorine. *Environ. Sci. Technol.* **2021**, *55* (6), 3686–3695. <https://doi.org/10.1021/acs.est.0c07296>.
- (18) Hatton, J.; Holton, C.; DiGuseppi, B. Occurrence and Behavior of Per- and Polyfluoroalkyl Substances from Aqueous Film-Forming Foam in Groundwater Systems. *Remediat. J.* **2018**, *28* (2), 89–99. <https://doi.org/10.1002/rem.21552>.
- (19) Liu, J.; Mejia Avendaño, S. Microbial Degradation of Polyfluoroalkyl Chemicals in the Environment: A Review. *Environ. Int.* **2013**, *61*, 98–114. <https://doi.org/10.1016/j.envint.2013.08.022>.
- (20) Choi, Y. J.; Helbling, D. E.; Liu, J.; Olivares, C. I.; Higgins, C. P. Microbial Biotransformation of Aqueous Film-Forming Foam Derived Polyfluoroalkyl Substances. *Sci. Total Environ.* **2022**, *824*, 153711. <https://doi.org/10.1016/j.scitotenv.2022.153711>.
- (21) Parsons, J. R.; Sáez, M.; Dolfing, J.; de Voogt, P. Biodegradation of Perfluorinated Compounds. In *Reviews of Environmental Contamination and Toxicology Vol 196*; Whitacre, D. M., Ed.; Reviews of Environmental Contamination and Toxicology; Springer US: New York, NY, 2008; Vol. 196, pp 53–71. https://doi.org/10.1007/978-0-387-78444-1_2.
- (22) Zhang, W.; Pang, S.; Lin, Z.; Mishra, S.; Bhatt, P.; Chen, S. Biotransformation of Perfluoroalkyl Acid Precursors from Various Environmental Systems: Advances and Perspectives. *Environ. Pollut.* **2021**, *272*, 115908. <https://doi.org/10.1016/j.envpol.2020.115908>.
- (23) Wang, N.; Szostek, B.; Folsom, P. W.; Sulecki, L. M.; Capka, V.; Buck, R. C.; Berti, W. R.; Gannon, J. T. Aerobic Biotransformation of ¹⁴C-Labeled 8-2 Telomer B Alcohol by Activated Sludge from a Domestic Sewage Treatment Plant. *Environ. Sci. Technol.* **2005**, *39* (2), 531–538. <https://doi.org/10.1021/es049466y>.
- (24) Wang, N.; Liu, J.; Buck, R. C.; Korzeniowski, S. H.; Wolstenholme, B. W.; Folsom, P. W.; Sulecki, L. M. 6:2 Fluorotelomer Sulfonate Aerobic Biotransformation in Activated Sludge of

Waste Water Treatment Plants. *Chemosphere* **2011**, 82 (6), 853–858. <https://doi.org/10.1016/j.chemosphere.2010.11.003>.

(25) Zhang, S.; Lu, X.; Wang, N.; Buck, R. C. Biotransformation Potential of 6:2 Fluorotelomer Sulfonate (6:2 FTSA) in Aerobic and Anaerobic Sediment. *Chemosphere* **2016**, 154, 224–230. <https://doi.org/10.1016/j.chemosphere.2016.03.062>.

(26) Liu, J.; Wang, N.; Szostek, B.; Buck, R. C.; Panciroli, P. K.; Folsom, P. W.; Sulecki, L. M.; Bellin, C. A. 6-2 Fluorotelomer Alcohol Aerobic Biodegradation in Soil and Mixed Bacterial Culture. *Chemosphere* **2010**, 78 (4), 437–444. <https://doi.org/10.1016/j.chemosphere.2009.10.044>.

(27) Dinglasan, M. J. A.; Ye, Y.; Edwards, E. A.; Mabury, S. A. Fluorotelomer Alcohol Biodegradation Yields Poly- and Perfluorinated Acids. *Environ. Sci. Technol.* **2004**, 38 (10), 2857–2864. <https://doi.org/10.1021/es0350177>.

(28) Yin, T.; Tran, N. H.; Huiting, C.; He, Y.; Gin, K. Y.-H. Biotransformation of Polyfluoroalkyl Substances by Microbial Consortia from Constructed Wetlands under Aerobic and Anoxic Conditions. *Chemosphere* **2019**, 233, 101–109. <https://doi.org/10.1016/j.chemosphere.2019.05.227>.

(29) Hamid, H.; Li, L. Y.; Grace, J. R. Aerobic Biotransformation of Fluorotelomer Compounds in Landfill Leachate-Sediment. *Sci. Total Environ.* **2020**, 713, 136547. <https://doi.org/10.1016/j.scitotenv.2020.136547>.

(30) Hamid, H.; Li, L. Y.; Grace, J. R. Formation of Perfluorocarboxylic Acids from 6:2 Fluorotelomer Sulfonate (6:2 FTS) in Landfill Leachate: Role of Microbial Communities. *Environ. Pollut.* **2020**, 259, 113835. <https://doi.org/10.1016/j.envpol.2019.113835>.

(31) Harding-Marjanovic, K. C.; Houtz, E. F.; Yi, S.; Field, J. A.; Sedlak, D. L.; Alvarez-Cohen, L. Aerobic Biotransformation of Fluorotelomer Thioether Amido Sulfonate (Lodyne) in AFFF-Amended Microcosms. *Environ. Sci. Technol.* **2015**, 49 (13), 7666–7674. <https://doi.org/10.1021/acs.est.5b01219>.

(32) Mejia-Avenidaño, S.; Vo Duy, S.; Sauvé, S.; Liu, J. Generation of Perfluoroalkyl Acids from Aerobic Biotransformation of Quaternary Ammonium Polyfluoroalkyl Surfactants. *Environ. Sci. Technol.* **2016**, 50 (18), 9923–9932. <https://doi.org/10.1021/acs.est.6b00140>.

(33) Chen, H.; Liu, M.; Munoz, G.; Duy, S. V.; Sauvé, S.; Yao, Y.; Sun, H.; Liu, J. Fast Generation of Perfluoroalkyl Acids from Polyfluoroalkyl Amine Oxides in Aerobic Soils. *Environ. Sci. Technol. Lett.* **2020**, 7 (10), 714–720. <https://doi.org/10.1021/acs.estlett.0c00543>.

(34) Liu, M.; Munoz, G.; Vo Duy, S.; Sauvé, S.; Liu, J. Stability of Nitrogen-Containing Polyfluoroalkyl Substances in Aerobic Soils. *Environ. Sci. Technol.* **2021**, acs.est.0c05811. <https://doi.org/10.1021/acs.est.0c05811>.

(35) Rhoads, K. R.; Janssen, E. M.-L.; Luthy, R. G.; Criddle, C. S. Aerobic Biotransformation and Fate of *N*-Ethyl Perfluorooctane Sulfonamidoethanol (*N*-EtFOSE) in Activated Sludge. *Environ. Sci. Technol.* **2008**, 42 (8), 2873–2878. <https://doi.org/10.1021/es702866c>.

(36) Liu, J.; Zhong, G.; Li, W.; Mejia Avenidaño, S. Isomer-Specific Biotransformation of Perfluoroalkyl Sulfonamide Compounds in Aerobic Soil. *Sci. Total Environ.* **2019**, 651, 766–774. <https://doi.org/10.1016/j.scitotenv.2018.09.214>.

- (37) Yi, S.; Harding-Marjanovic, K. C.; Houtz, E. F.; Gao, Y.; Lawrence, J. E.; Nichiporuk, R. V.; Iavarone, A. T.; Zhuang, W.-Q.; Hansen, M.; Field, J. A.; Sedlak, D. L.; Alvarez-Cohen, L. Biotransformation of AFFF Component 6:2 Fluorotelomer Thioether Amido Sulfonate Generates 6:2 Fluorotelomer Thioether Carboxylate under Sulfate-Reducing Conditions. *Environ. Sci. Technol. Lett.* **2018**, *5* (5), 283–288. <https://doi.org/10.1021/acs.estlett.8b00148>.
- (38) Zhang, S.; Szostek, B.; McCausland, P. K.; Wolstenholme, B. W.; Lu, X.; Wang, N.; Buck, R. C. 6:2 and 8:2 Fluorotelomer Alcohol Anaerobic Biotransformation in Digester Sludge from a WWTP under Methanogenic Conditions. *Environ. Sci. Technol.* **2013**, *47* (9), 4227–4235. <https://doi.org/10.1021/es4000824>.
- (39) Li, F.; Su, Q.; Zhou, Z.; Liao, X.; Zou, J.; Yuan, B.; Sun, W. Anaerobic Biodegradation of 8:2 Fluorotelomer Alcohol in Anaerobic Activated Sludge: Metabolic Products and Pathways. *Chemosphere* **2018**, *200*, 124–132. <https://doi.org/10.1016/j.chemosphere.2018.02.065>.
- (40) Ochoa-Herrera, V.; Field, J. A.; Luna-Velasco, A.; Sierra-Alvarez, R. Microbial Toxicity and Biodegradability of Perfluorooctane Sulfonate (PFOS) and Shorter Chain Perfluoroalkyl and Polyfluoroalkyl Substances (PFASs). *Environ. Sci. Process. Impacts* **2016**, *18* (9), 1236–1246. <https://doi.org/10.1039/C6EM00366D>.
- (41) Zhang, S.; Szostek, B.; McCausland, P. K.; Wolstenholme, B. W.; Lu, X.; Wang, N.; Buck, R. C. 6:2 and 8:2 Fluorotelomer Alcohol Anaerobic Biotransformation in Digester Sludge from a WWTP under Methanogenic Conditions. *Environ. Sci. Technol.* **2013**, *47* (9), 4227–4235. <https://doi.org/10.1021/es4000824>.
- (42) Zhao, L.; Folsom, P. W.; Wolstenholme, B. W.; Sun, H.; Wang, N.; Buck, R. C. 6:2 Fluorotelomer Alcohol Biotransformation in an Aerobic River Sediment System. *Chemosphere* **2013**, *90* (2), 203–209. <https://doi.org/10.1016/j.chemosphere.2012.06.035>.
- (43) Wang, N.; Szostek, B.; Buck, R. C.; Folsom, P. W.; Sulecki, L. M.; Gannon, J. T. 8-2 Fluorotelomer Alcohol Aerobic Soil Biodegradation: Pathways, Metabolites, and Metabolite Yields. *Chemosphere* **2009**, *75* (8), 1089–1096. <https://doi.org/10.1016/j.chemosphere.2009.01.033>.
- (44) Yu, X.; Takabe, Y.; Yamamoto, K.; Matsumura, C.; Nishimura, F. Biodegradation Property of 8:2 Fluorotelomer Alcohol (8:2 FTOH) under Aerobic/Anoxic/Anaerobic Conditions. *J. Water Environ. Technol.* **2016**, *14* (3), 177–190. <https://doi.org/10.2965/jwet.15-056>.
- (45) Zhao, L.; McCausland, P. K.; Folsom, P. W.; Wolstenholme, B. W.; Sun, H.; Wang, N.; Buck, R. C. 6:2 Fluorotelomer Alcohol Aerobic Biotransformation in Activated Sludge from Two Domestic Wastewater Treatment Plants. *Chemosphere* **2013**, *92* (4), 464–470. <https://doi.org/10.1016/j.chemosphere.2013.02.032>.
- (46) Wang, N.; Szostek, B.; Buck, R. C.; Folsom, P. W.; Sulecki, L. M.; Capka, V.; Berti, W. R.; Gannon, J. T. Fluorotelomer Alcohol Biodegradation Direct Evidence That Perfluorinated Carbon Chains Breakdown. *Environ. Sci. Technol.* **2005**, *39* (19), 7516–7528. <https://doi.org/10.1021/es0506760>.
- (47) Liu, J.; Lee, L. S.; Nies, L. F.; Nakatsu, C. H.; Turco, R. F. Biotransformation of 8:2 Fluorotelomer Alcohol in Soil and by Soil Bacteria Isolates. *Environ. Sci. Technol.* **2007**, *41* (23), 8024–8030. <https://doi.org/10.1021/es0708722>.

- (48) Washington, J. W.; Ellington, J. J.; Jenkins, T. M.; Evans, J. J.; Yoo, H.; Hafner, S. C. Degradability of an Acrylate-Linked, Fluorotelomer Polymer in Soil. *Environ. Sci. Technol.* **2009**, *43* (17), 6617–6623. <https://doi.org/10.1021/es9002668>.
- (49) Washington, J. W.; Jenkins, T. M.; Weber, E. J. Identification of Unsaturated and 2H Polyfluorocarboxylate Homologous Series and Their Detection in Environmental Samples and as Polymer Degradation Products. *Environ. Sci. Technol.* **2015**, *49* (22), 13256–13263. <https://doi.org/10.1021/acs.est.5b03379>.
- (50) Liu, J.; Wang, N.; Buck, R. C.; Wolstenholme, B. W.; Folsom, P. W.; Sulecki, L. M.; Bellin, C. A. Aerobic Biodegradation of [14C] 6:2 Fluorotelomer Alcohol in a Flow-through Soil Incubation System. *Chemosphere* **2010**, *80* (7), 716–723. <https://doi.org/10.1016/j.chemosphere.2010.05.027>.
- (51) Hamid, H.; Li, L. Y.; Grace, J. R. Aerobic Biotransformation of Fluorotelomer Compounds in Landfill Leachate-Sediment. *Sci. Total Environ.* **2020**, *713*, 136547. <https://doi.org/10.1016/j.scitotenv.2020.136547>.
- (52) Yin, T.; Tran, N. H.; Huiting, C.; He, Y.; Gin, K. Y.-H. Biotransformation of Polyfluoroalkyl Substances by Microbial Consortia from Constructed Wetlands under Aerobic and Anoxic Conditions. *Chemosphere* **2019**, *233*, 101–109. <https://doi.org/10.1016/j.chemosphere.2019.05.227>.
- (53) Yi, S.; Harding-Marjanovic, K. C.; Houtz, E. F.; Antell, E.; Olivares, C.; Nichiporuk, R. V.; Iavarone, A. T.; Zhuang, W.-Q.; Field, J. A.; Sedlak, D. L.; Alvarez-Cohen, L. Biotransformation of 6:2 Fluorotelomer Thioether Amido Sulfonate in Aqueous Film-Forming Foams under Nitrate-Reducing Conditions. *Environ. Sci. Technol.* **2022**. <https://doi.org/10.1021/acs.est.2c00063>.
- (54) Ahrens, L.; Norström, K.; Viktor, T.; Cousins, A. P.; Josefsson, S. Stockholm Arlanda Airport as a Source of Per- and Polyfluoroalkyl Substances to Water, Sediment and Fish. *Chemosphere* **2015**, *129*, 33–38. <https://doi.org/10.1016/j.chemosphere.2014.03.136>.
- (55) McGuire, M. E.; Schaefer, C.; Richards, T.; Backe, W. J.; Field, J. A.; Houtz, E.; Sedlak, D. L.; Guelfo, J. L.; Wunsch, A.; Higgins, C. P. Evidence of Remediation-Induced Alteration of Subsurface Poly- and Perfluoroalkyl Substance Distribution at a Former Firefighter Training Area. *Environ. Sci. Technol.* **2014**, *48* (12), 6644–6652. <https://doi.org/10.1021/es5006187>.
- (56) Dauchy, X.; Boiteux, V.; Bach, C.; Rosin, C.; Munoz, J.-F. Per- and Polyfluoroalkyl Substances in Firefighting Foam Concentrates and Water Samples Collected near Sites Impacted by the Use of These Foams. *Chemosphere* **2017**, *183*, 53–61. <https://doi.org/10.1016/j.chemosphere.2017.05.056>.
- (57) Nickerson, A.; Maizel, A. C.; Kulkarni, P. R.; Adamson, D. T.; Kornuc, J. J.; Higgins, C. P. Enhanced Extraction of AFFF-Associated PFASs from Source Zone Soils. *Environ. Sci. Technol.* **2020**, *54* (8), 4952–4962. <https://doi.org/10.1021/acs.est.0c00792>.
- (58) Nickerson, A.; Rodowa, A. E.; Adamson, D. T.; Field, J. A.; Kulkarni, P. R.; Kornuc, J. J.; Higgins, C. P. Spatial Trends of Anionic, Zwitterionic, and Cationic PFASs at an AFFF-Impacted Site. *Environ. Sci. Technol.* **2021**, *55* (1), 313–323. <https://doi.org/10.1021/acs.est.0c04473>.
- (59) USEPA. Provisional Health Advisories for Perfluorooctanoic Acid (PFOA) and Perfluorooctane Sulfonate (PFOS). **2009**.

- (60) USEPA. Drinking Water Health Advisory for Perfluorooctane Sulfonate (PFOS). *U. S. Environ. Prot. EPA Off. Water* **2016a**, EPA 822-16-004.
- (61) USEPA. Drinking Water Health Advisory for Perfluorooctanoic Acid (PFOA). *U. S. Environ. Prot. EPA Off. Water* **2016b**, 822-R-16-005.
- (62) Post, G. B. Recent US State and Federal Drinking Water Guidelines for Per- and Polyfluoroalkyl Substances. *Environ. Toxicol. Chem.* **2021**, *40* (3), 550–563. <https://doi.org/10.1002/etc.4863>.
- (63) USEPA. Interim Drinking Water Health Advisory: Perfluorooctane Sulfonic Acid (PFOS) CASRN 1763-23-1. *U. S. Environ. Prot. EPA Off. Water* **2022a**, EPA/822/R-22/004.
- (64) USEPA. Interim Drinking Water Health Advisory: Perfluorooctanoic Acid (PFOA) CASRN 335-67-1. *U. S. Environ. Prot. EPA Off. Water* **2022b**, EPA/822/R-22/003.
- (65) Alsmeyer, Y. W.; Childs, W. V.; Flynn, R. M.; Moore, G. G. I.; Smeltzer, J. C. Electrochemical Fluorination and Its Applications. In *Organofluorine Chemistry: Principles and Commercial Applications*; Banks, R. E., Smart, B. E., Tatlow, J. C., Eds.; Topics in Applied Chemistry; Springer US: Boston, MA, 1994; pp 121–143. https://doi.org/10.1007/978-1-4899-1202-2_5.
- (66) Schaefer, C. E.; Nguyen, D.; Christie, E.; Shea, S.; Higgins, C. P.; Field, J. A. Desorption of Poly- and Perfluoroalkyl Substances from Soil Historically Impacted with Aqueous Film-Forming Foam. *J. Environ. Eng.* **2021**, *147* (2), 06020006. [https://doi.org/10.1061/\(ASCE\)EE.1943-7870.0001846](https://doi.org/10.1061/(ASCE)EE.1943-7870.0001846).
- (67) Maizel, A. C.; Shea, S.; Nickerson, A.; Schaefer, C.; Higgins, C. P. Release of Per- and Polyfluoroalkyl Substances from Aqueous Film-Forming Foam Impacted Soils. *Environ. Sci. Technol.* **2021**. <https://doi.org/10.1021/acs.est.1c02871>.
- (68) D'Agostino, L. A.; Mabury, S. A. Identification of Novel Fluorinated Surfactants in Aqueous Film Forming Foams and Commercial Surfactant Concentrates. *Environ. Sci. Technol.* **2014**, *48* (1), 121–129. <https://doi.org/10.1021/es403729e>.
- (69) Ruyle, B. J.; Thackray, C. P.; McCord, J. P.; Strynar, M. J.; Mauge-Lewis, K. A.; Fenton, S. E.; Sunderland, E. M. Reconstructing the Composition of Per- and Polyfluoroalkyl Substances in Contemporary Aqueous Film-Forming Foams. *Environ. Sci. Technol. Lett.* **2021**, *8* (1), 59–65. <https://doi.org/10.1021/acs.estlett.0c00798>.
- (70) Hamid, H.; Li, L. Y.; Grace, J. R. Review of the Fate and Transformation of Per- and Polyfluoroalkyl Substances (PFASs) in Landfills. *Environ. Pollut.* **2018**, *235*, 74–84. <https://doi.org/10.1016/j.envpol.2017.12.030>.
- (71) Sharifan, H.; Bagheri, M.; Wang, D.; Burken, J. G.; Higgins, C. P.; Liang, Y.; Liu, J.; Schaefer, C. E.; Blotvogel, J. Fate and Transport of Per- and Polyfluoroalkyl Substances (PFASs) in the Vadose Zone. *Sci. Total Environ.* **2021**, *771*, 145427. <https://doi.org/10.1016/j.scitotenv.2021.145427>.
- (72) Zhang, Z.; Sarkar, D.; Biswas, J. K.; Datta, R. Biodegradation of Per- and Polyfluoroalkyl Substances (PFAS): A Review. *Bioresour. Technol.* **2022**, *344*, 126223. <https://doi.org/10.1016/j.biortech.2021.126223>.

- (73) Material Safety Data Sheet for FC-203CF Light Water Brand Aqueous Film Forming Foam, 3M Company, St. Paul, MN, 1997.
- (74) Herzke, D.; Olsson, E.; Posner, S. Perfluoroalkyl and Polyfluoroalkyl Substances (PFASs) in Consumer Products in Norway – A Pilot Study. *Chemosphere* **2012**, *88* (8), 980–987. <https://doi.org/10.1016/j.chemosphere.2012.03.035>.
- (75) Weiner, B.; Yeung, L. W. Y.; Marchington, E. B.; D’Agostino, L. A.; Mabury, S. A. Organic Fluorine Content in Aqueous Film Forming Foams (AFFFs) and Biodegradation of the Foam Component 6 : 2 Fluorotelomermercaptopalkylamido Sulfonate (6 : 2 FTSAS). *Environ. Chem.* **2013**, *10* (6), 486–493. <https://doi.org/10.1071/EN13128>.
- (76) Barzen-Hanson, K. A.; Field, J. A. Discovery and Implications of C₂ and C₃ Perfluoroalkyl Sulfonates in Aqueous Film-Forming Foams and Groundwater. *Environ. Sci. Technol. Lett.* **2015**, *2* (4), 95–99. <https://doi.org/10.1021/acs.estlett.5b00049>.
- (77) Favreau, P.; Poncioni-Rothlisberger, C.; Place, B. J.; Bouchex-Bellomie, H.; Weber, A.; Tremp, J.; Field, J. A.; Kohler, M. Multianalyte Profiling of Per- and Polyfluoroalkyl Substances (PFASs) in Liquid Commercial Products. *Chemosphere* **2017**, *171*, 491–501. <https://doi.org/10.1016/j.chemosphere.2016.11.127>.
- (78) Schultz, M. M.; Barofsky, D. F.; Field, J. A. Quantitative Determination of Fluorotelomer Sulfonates in Groundwater by LC MS/MS. *Environ. Sci. Technol.* **2004**, *38* (6), 1828–1835. <https://doi.org/10.1021/es035031j>.
- (79) Moe, M. K.; Huber, S.; Svenson, J.; Hagenaars, A.; Pabon, M.; Trümper, M.; Berger, U.; Knapen, D.; Herzke, D. The Structure of the Fire Fighting Foam Surfactant Forafac®1157 and Its Biological and Photolytic Transformation Products. *Chemosphere* **2012**, *89* (7), 869–875. <https://doi.org/10.1016/j.chemosphere.2012.05.012>.
- (80) D’Agostino, L. A.; Mabury, S. A. Aerobic Biodegradation of 2 Fluorotelomer Sulfonamide-Based Aqueous Film-Forming Foam Components Produces Perfluoroalkyl Carboxylates. *Environ. Toxicol. Chem.* **2017**, *36* (8), 2012–2021. <https://doi.org/10.1002/etc.3750>.
- (81) Mejia-Avenidaño, S.; Munoz, G.; Vo Duy, S.; Desrosiers, M.; Benoît, P.; Sauv , S.; Liu, J. Novel Fluoroalkylated Surfactants in Soils Following Firefighting Foam Deployment During the Lac-M gantic Railway Accident. *Environ. Sci. Technol.* **2017**, *51* (15), 8313–8323. <https://doi.org/10.1021/acs.est.7b02028>.
- (82) A. Moody, C.; N. Hebert, G.; H. Strauss, S.; A. Field, J. Occurrence and Persistence of Perfluorooctanesulfonate and Other Perfluorinated Surfactants in Groundwater at a Fire-Training Area at Wurtsmith Air Force Base, Michigan, USA. *J. Environ. Monit.* **2003**, *5* (2), 341–345. <https://doi.org/10.1039/B212497A>.
- (83) K rrman, A.; Elgh-Dalgren, K.; Lafossas, C.; M skeland, T.; K rrman, A.; Elgh-Dalgren, K.; Lafossas, C.; M skeland, T. Environmental Levels and Distribution of Structural Isomers of Perfluoroalkyl Acids after Aqueous Fire-Fighting Foam (AFFF) Contamination. *Environ. Chem.* **2011**, *8* (4), 372–380. <https://doi.org/10.1071/EN10145>.
- (84) Filipovic, M.; Woldegiorgis, A.; Norstr m, K.; Bibi, M.; Lindberg, M.;  ster s, A.-H. Historical Usage of Aqueous Film Forming Foam: A Case Study of the Widespread Distribution of Perfluoroalkyl Acids from a Military Airport to Groundwater, Lakes, Soils and Fish. *Chemosphere* **2015**, *129*, 39–45. <https://doi.org/10.1016/j.chemosphere.2014.09.005>.

- (85) Bräunig, J.; Baduel, C.; Heffernan, A.; Rotander, A.; Donaldson, E.; Mueller, J. F. Fate and Redistribution of Perfluoroalkyl Acids through AFFF-Impacted Groundwater. *Sci. Total Environ.* **2017**, *596–597*, 360–368. <https://doi.org/10.1016/j.scitotenv.2017.04.095>.
- (86) Dauchy, X.; Boiteux, V.; Colin, A.; Hémard, J.; Bach, C.; Rosin, C.; Munoz, J.-F. Deep Seepage of Per- and Polyfluoroalkyl Substances through the Soil of a Firefighter Training Site and Subsequent Groundwater Contamination. *Chemosphere* **2019**, *214*, 729–737. <https://doi.org/10.1016/j.chemosphere.2018.10.003>.
- (87) Weber, A. K.; Barber, L. B.; LeBlanc, D. R.; Sunderland, E. M.; Vecitis, C. D. Geochemical and Hydrologic Factors Controlling Subsurface Transport of Poly- and Perfluoroalkyl Substances, Cape Cod, Massachusetts. *Environ. Sci. Technol.* **2017**, *51* (8), 4269–4279. <https://doi.org/10.1021/acs.est.6b05573>.
- (88) Martin, D.; Munoz, G.; Mejia-Avenidaño, S.; Duy, S. V.; Yao, Y.; Volchek, K.; Brown, C. E.; Liu, J.; Sauv e, S. Zwitterionic, Cationic, and Anionic Perfluoroalkyl and Polyfluoroalkyl Substances Integrated into Total Oxidizable Precursor Assay of Contaminated Groundwater. *Talanta* **2019**, *195*, 533–542. <https://doi.org/10.1016/j.talanta.2018.11.093>.
- (89) Reinikainen, J.; Perkola, N.;  yst o, L.; Sorvari, J. The Occurrence, Distribution, and Risks of PFAS at AFFF-Impacted Sites in Finland. *Sci. Total Environ.* **2022**, *829*, 154237. <https://doi.org/10.1016/j.scitotenv.2022.154237>.
- (90) Moody, C. A.; Martin, J. W.; Kwan, W. C.; Muir, D. C. G.; Mabury, S. A. Monitoring Perfluorinated Surfactants in Biota and Surface Water Samples Following an Accidental Release of Fire-Fighting Foam into Etobicoke Creek. *Environ. Sci. Technol.* **2002**, *36* (4), 545–551. <https://doi.org/10.1021/es011001+>.
- (91) Strynar, M. J.; Lindstrom, A. B.; Nakayama, S. F.; Egeghy, P. P.; Helfant, L. J. Pilot Scale Application of a Method for the Analysis of Perfluorinated Compounds in Surface Soils. *Chemosphere* **2012**, *86* (3), 252–257. <https://doi.org/10.1016/j.chemosphere.2011.09.036>.
- (92) Rankin, K.; Mabury, S. A.; Jenkins, T. M.; Washington, J. W. A North American and Global Survey of Perfluoroalkyl Substances in Surface Soils: Distribution Patterns and Mode of Occurrence. *Chemosphere* **2016**, *161*, 333–341. <https://doi.org/10.1016/j.chemosphere.2016.06.109>.
- (93) Washington, J. W.; Rankin, K.; Libelo, E. L.; Lynch, D. G.; Cyterski, M. Determining Global Background Soil PFAS Loads and the Fluorotelomer-Based Polymer Degradation Rates That Can Account for These Loads. *Sci. Total Environ.* **2019**, *651*, 2444–2449. <https://doi.org/10.1016/j.scitotenv.2018.10.071>.
- (94) Bräunig, J.; Baduel, C.; Barnes, C. M.; Mueller, J. F. Leaching and Bioavailability of Selected Perfluoroalkyl Acids (PFAAs) from Soil Contaminated by Firefighting Activities. *Sci. Total Environ.* **2019**, *646*, 471–479. <https://doi.org/10.1016/j.scitotenv.2018.07.231>.
- (95) Skaar, J. S.; R ader, E. M.; Lyche, J. L.; Ahrens, L.; Kallenborn, R. Elucidation of Contamination Sources for Poly- and Perfluoroalkyl Substances (PFASs) on Svalbard (Norwegian Arctic). *Environ. Sci. Pollut. Res.* **2019**, *26* (8), 7356–7363. <https://doi.org/10.1007/s11356-018-2162-4>.

- (96) Hunter Anderson, R.; Adamson, D. T.; Stroo, H. F. Partitioning of Poly- and Perfluoroalkyl Substances from Soil to Groundwater within Aqueous Film-Forming Foam Source Zones. *J. Contam. Hydrol.* **2019**, *220*, 59–65. <https://doi.org/10.1016/j.jconhyd.2018.11.011>.
- (97) Awad, E.; Zhang, X.; Bhavsar, S. P.; Petro, S.; Crozier, P. W.; Reiner, E. J.; Fletcher, R.; Tittlemier, S. A.; Braekevelt, E. Long-Term Environmental Fate of Perfluorinated Compounds after Accidental Release at Toronto Airport. *Environ. Sci. Technol.* **2011**, *45* (19), 8081–8089. <https://doi.org/10.1021/es2001985>.
- (98) Munoz, G.; Duy, S. V.; Labadie, P.; Botta, F.; Budzinski, H.; Lestremau, F.; Liu, J.; Sauvé, S. Analysis of Zwitterionic, Cationic, and Anionic Poly- and Perfluoroalkyl Surfactants in Sediments by Liquid Chromatography Polarity-Switching Electrospray Ionization Coupled to High Resolution Mass Spectrometry. *Talanta* **2016**, *152*, 447–456. <https://doi.org/10.1016/j.talanta.2016.02.021>.
- (99) Munoz, G.; Desrosiers, M.; Duy, S. V.; Labadie, P.; Budzinski, H.; Liu, J.; Sauvé, S. Environmental Occurrence of Perfluoroalkyl Acids and Novel Fluorotelomer Surfactants in the Freshwater Fish *Catostomus commersonii* and Sediments Following Firefighting Foam Deployment at the Lac-Mégantic Railway Accident. *Environ. Sci. Technol.* **2017**, *51* (3), 1231–1240. <https://doi.org/10.1021/acs.est.6b05432>.
- (100) Huang, S.; Jaffé, P. R. Defluorination of Perfluorooctanoic Acid (PFOA) and Perfluorooctane Sulfonate (PFOS) by *Acidimicrobium* Sp. Strain A6. *Environ. Sci. Technol.* **2019**, *53* (19), 11410–11419. <https://doi.org/10.1021/acs.est.9b04047>.
- (101) Yu, Y.; Zhang, K.; Li, Z.; Ren, C.; Chen, J.; Lin, Y.-H.; Liu, J.; Men, Y. Microbial Cleavage of C–F Bonds in Two C₆ Per- and Polyfluorinated Compounds via Reductive Defluorination. *Environ. Sci. Technol.* **2020**, *54* (22), 14393–14402. <https://doi.org/10.1021/acs.est.0c04483>.
- (102) Yu, Y.; Che, S.; Ren, C.; Jin, B.; Tian, Z.; Liu, J.; Men, Y. Microbial Defluorination of Unsaturated Per- and Polyfluorinated Carboxylic Acids under Anaerobic and Aerobic Conditions: A Structure Specificity Study. *Environ. Sci. Technol.* **2022**. <https://doi.org/10.1021/acs.est.1c05509>.
- (103) Mejia Avendaño, S.; Liu, J. Production of PFOS from Aerobic Soil Biotransformation of Two Perfluoroalkyl Sulfonamide Derivatives. *Chemosphere* **2015**, *119*, 1084–1090. <https://doi.org/10.1016/j.chemosphere.2014.09.059>.
- (104) Zhang, L.; Lee, L. S.; Niu, J.; Liu, J. Kinetic Analysis of Aerobic Biotransformation Pathways of a Perfluorooctane Sulfonate (PFOS) Precursor in Distinctly Different Soils. *Environ. Pollut.* **2017**, *229*, 159–167. <https://doi.org/10.1016/j.envpol.2017.05.074>.
- (105) Yin, T.; Te, S. H.; Reinhard, M.; Yang, Y.; Chen, H.; He, Y.; Gin, K. Y.-H. Biotransformation of Sulfloramid (N-Ethyl Perfluorooctane Sulfonamide) and Dynamics of Associated Rhizospheric Microbial Community in Microcosms of Wetland Plants. *Chemosphere* **2018**, *211*, 379–389. <https://doi.org/10.1016/j.chemosphere.2018.07.157>.
- (106) Shaw, D. M. J.; Munoz, G.; Bottos, E. M.; Duy, S. V.; Sauvé, S.; Liu, J.; Van Hamme, J. D. Degradation and Defluorination of 6:2 Fluorotelomer Sulfonamidoalkyl Betaine and 6:2 Fluorotelomer Sulfonate by *Gordonia* Sp. Strain NB4-1Y under Sulfur-Limiting Conditions. *Sci. Total Environ.* **2019**, *647*, 690–698. <https://doi.org/10.1016/j.scitotenv.2018.08.012>.

- (107) Olivares, C. I.; Yi, S.; Cook, E. K.; Choi, Y. J.; Montagnolli, R.; Byrne, A.; Higgins, C. P.; Sedlak, D. L.; Alvarez-Cohen, L. Aerobic BTEX Biodegradation Increases Yield of Perfluoroalkyl Carboxylic Acids from Biotransformation of a Polyfluoroalkyl Surfactant, 6:2 FtTAoS. *Environ. Sci. Process. Impacts* **2022**, *24* (3), 439–446. <https://doi.org/10.1039/D1EM00494H>.
- (108) Li, R.; Munoz, G.; Liu, Y.; Sauvé, S.; Ghoshal, S.; Liu, J. Transformation of Novel Polyfluoroalkyl Substances (PFASs) as Co-Contaminants during Biopile Remediation of Petroleum Hydrocarbons. *J. Hazard. Mater.* **2019**, *362*, 140–147. <https://doi.org/10.1016/j.jhazmat.2018.09.021>.
- (109) Houtz, E.; Wang, M.; Park, J.-S. Identification and Fate of Aqueous Film Forming Foam Derived Per- and Polyfluoroalkyl Substances in a Wastewater Treatment Plant. *Environ. Sci. Technol.* **2018**, *52* (22), 13212–13221. <https://doi.org/10.1021/acs.est.8b04028>.
- (110) Shaw, D. M. J.; Munoz, G.; Bottos, E. M.; Duy, S. V.; Sauvé, S.; Liu, J.; Van Hamme, J. D. Degradation and Defluorination of 6:2 Fluorotelomer Sulfonamidoalkyl Betaine and 6:2 Fluorotelomer Sulfonate by *Gordonia* Sp. Strain NB4-1Y under Sulfur-Limiting Conditions. *Sci. Total Environ.* **2019**, *647*, 690–698. <https://doi.org/10.1016/j.scitotenv.2018.08.012>.
- (111) Van Hamme, J. D.; Bottos, E. M.; Bilbey, N. J.; Brewer, S. E. Genomic and Proteomic Characterization of *Gordonia* Sp. NB4-1Y in Relation to 6:2 Fluorotelomer Sulfonate Biodegradation. *Microbiology* **2013**, *159* (Pt_8), 1618–1628. <https://doi.org/10.1099/mic.0.068932-0>.
- (112) Yang, S.-H.; Shi, Y.; Strynar, M.; Chu, K.-H. Desulfonation and Defluorination of 6:2 Fluorotelomer Sulfonic Acid (6:2 FTSA) by *Rhodococcus Jostii* RHA1: Carbon and Sulfur Sources, Enzymes, and Pathways. *J. Hazard. Mater.* **2022**, *423*, 127052. <https://doi.org/10.1016/j.jhazmat.2021.127052>.
- (113) Key, B. D.; Howell, R. D.; Criddle, C. S. Defluorination of Organofluorine Sulfur Compounds by *Pseudomonas* Sp. Strain D2. *Environ. Sci. Technol.* **1998**, *32* (15), 2283–2287. <https://doi.org/10.1021/es9800129>.
- (114) Méndez, V.; Holland, S.; Bhardwaj, S.; McDonald, J.; Khan, S.; O’Carroll, D.; Pickford, R.; Richards, S.; O’Farrell, C.; Coleman, N.; Lee, M.; Manefield, M. J. Aerobic Biotransformation of 6:2 Fluorotelomer Sulfonate by *Dietzia Aurantiaca* J3 under Sulfur-Limiting Conditions. *Sci. Total Environ.* **2022**, *829*, 154587. <https://doi.org/10.1016/j.scitotenv.2022.154587>.
- (115) Kim, M. H.; Wang, N.; McDonald, T.; Chu, K.-H. Biodefluorination and Biotransformation of Fluorotelomer Alcohols by Two Alkane-Degrading *Pseudomonas* Strains. *Biotechnol. Bioeng.* **2012**, *109* (12), 3041–3048. <https://doi.org/10.1002/bit.24561>.
- (116) Wang, N.; Buck, R. C.; Szostek, B.; Sulecki, L. M.; Wolstenholme, B. W. 5:3 Polyfluorinated Acid Aerobic Biotransformation in Activated Sludge via Novel “One-Carbon Removal Pathways.” *Chemosphere* **2012**, *87* (5), 527–534. <https://doi.org/10.1016/j.chemosphere.2011.12.056>.
- (117) Lange, C. C. Anaerobic Biotransformation of N-Methyl Perfluorobutanesulfonamido Ethanol and N-Ethyl Perfluorooctanesulfonamido Ethanol. *Environ. Toxicol. Chem.* **2018**, *37* (3), 768–779. <https://doi.org/10.1002/etc.4014>.
- (118) Giesy, J. P.; Kannan, K. Global Distribution of Perfluorooctane Sulfonate in Wildlife. *Environ. Sci. Technol.* **2001**, *35* (7), 1339–1342. <https://doi.org/10.1021/es001834k>.

- (119) Olsen, G. W.; Church, T. R.; Miller, J. P.; Burris, J. M.; Hansen, K. J.; Lundberg, J. K.; Armitage, J. B.; Herron, R. M.; Medhdizadehkashi, Z.; Nobiletti, J. B.; O'Neill, E. M.; Mandel, J. H.; Zobel, L. R. Perfluorooctanesulfonate and Other Fluorochemicals in the Serum of American Red Cross Adult Blood Donors. *Environ. Health Perspect.* **2003**, *111* (16), 1892–1901.
- (120) Paul, A. G.; Jones, K. C.; Sweetman, A. J. A First Global Production, Emission, and Environmental Inventory For Perfluorooctane Sulfonate. *Environ. Sci. Technol.* **2009**, *43* (2), 386–392. <https://doi.org/10.1021/es802216n>.
- (121) *Perfluoroalkyl Sulfonates; Significant New Use Rule*. Federal Register. <https://www.federalregister.gov/documents/2002/12/09/02-31011/perfluoroalkyl-sulfonates-significant-new-use-rule> (accessed 2022-09-13).
- (122) Smith, R. Directive 2006/123/EC of the European Parliament and of the Council of 12 December 2006. In *Core EU Legislation*; Macmillan Education UK: London, 2015; pp 269–287. https://doi.org/10.1007/978-1-137-54482-7_26.
- (123) Löfstedt Gilljam, J.; Leonel, J.; Cousins, I. T.; Benskin, J. P. Is Ongoing Sulfluramid Use in South America a Significant Source of Perfluorooctanesulfonate (PFOS)? Production Inventories, Environmental Fate, and Local Occurrence. *Environ. Sci. Technol.* **2016**, *50* (2), 653–659. <https://doi.org/10.1021/acs.est.5b04544>.
- (124) Martin, J. W.; Ellis, D. A.; Mabury, S. A.; Hurley, M. D.; Wallington, T. J. Atmospheric Chemistry of Perfluoroalkanesulfonamides: Kinetic and Product Studies of the OH Radical and Cl Atom Initiated Oxidation of N-Ethyl Perfluorobutanesulfonamide. *Environ. Sci. Technol.* **2006**, *40* (3), 864–872. <https://doi.org/10.1021/es051362f>.
- (125) Benskin, J. P.; Holt, A.; Martin, J. W. Isomer-Specific Biotransformation Rates of a Perfluorooctane Sulfonate (PFOS)-Precursor by Cytochrome P450 Isozymes and Human Liver Microsomes. *Environ. Sci. Technol.* **2009**, *43* (22), 8566–8572. <https://doi.org/10.1021/es901915f>.
- (126) Martin, J. W.; Asher, B. J.; Beesoon, S.; Benskin, J. P.; Ross, M. S. PFOS or PreFOS? Are Perfluorooctane Sulfonate Precursors (PreFOS) Important Determinants of Human and Environmental Perfluorooctane Sulfonate (PFOS) Exposure? *J. Environ. Monit.* **2010**, *12* (11), 1979–2004. <https://doi.org/10.1039/C0EM00295J>.
- (127) Fromme, H.; Tittlemier, S. A.; Völkel, W.; Wilhelm, M.; Twardella, D. Perfluorinated Compounds – Exposure Assessment for the General Population in Western Countries. *Int. J. Hyg. Environ. Health* **2009**, *212* (3), 239–270. <https://doi.org/10.1016/j.ijheh.2008.04.007>.
- (128) Benskin, J. P.; Ikonou, M. G.; Gobas, F. A. P. C.; Begley, T. H.; Woudneh, M. B.; Cosgrove, J. R. Biodegradation of N-Ethyl Perfluorooctane Sulfonamido Ethanol (EtFOSE) and EtFOSE-Based Phosphate Diester (SAmPAP Diester) in Marine Sediments. *Environ. Sci. Technol.* **2013**, *47* (3), 1381–1389. <https://doi.org/10.1021/es304336r>.
- (129) Pan, C.-G.; Zhao, J.-L.; Liu, Y.-S.; Zhang, Q.-Q.; Chen, Z.-F.; Lai, H.-J.; Peng, F.-J.; Liu, S.-S.; Ying, G.-G. Bioaccumulation and Risk Assessment of Per- and Polyfluoroalkyl Substances in Wild Freshwater Fish from Rivers in the Pearl River Delta Region, South China. *Ecotoxicol. Environ. Saf.* **2014**, *107*, 192–199. <https://doi.org/10.1016/j.ecoenv.2014.05.031>.
- (130) Olufsen, M.; Arukwe, A. Endocrine, Biotransformation, and Oxidative Stress Responses in Salmon Hepatocytes Exposed to Chemically Induced Hypoxia and Perfluorooctane

Sulfonamide (PFOSA), given Singly or in Combination. *Environ. Sci. Pollut. Res.* **2015**, *22* (22), 17350–17366. <https://doi.org/10.1007/s11356-014-3847-y>.

(131) Bonfeld-Jørgensen, E. C.; Long, M.; Fredslund, S. O.; Bossi, R.; Olsen, J. Breast Cancer Risk after Exposure to Perfluorinated Compounds in Danish Women: A Case–Control Study Nested in the Danish National Birth Cohort. *Cancer Causes Control* **2014**, *25* (11), 1439–1448. <https://doi.org/10.1007/s10552-014-0446-7>.

(132) Slotkin, T. A.; MacKillop, E. A.; Melnick, R. L.; Thayer, K. A.; Seidler, F. J. Developmental Neurotoxicity of Perfluorinated Chemicals Modeled in Vitro. *Environ. Health Perspect.* **2008**, *116* (6), 716–722. <https://doi.org/10.1289/ehp.11253>.

(133) Murakami, M.; Nishikoori, H.; Sakai, H.; Oguma, K.; Takada, H.; Takizawa, S. Formation of Perfluorinated Surfactants from Precursors by Indigenous Microorganisms in Groundwater. *Chemosphere* **2013**, *93* (1), 140–145. <https://doi.org/10.1016/j.chemosphere.2013.05.010>.

(134) Zhao, S.; Zhou, T.; Wang, B.; Zhu, L.; Chen, M.; Li, D.; Yang, L. Different Biotransformation Behaviors of Perfluorooctane Sulfonamide in Wheat (*Triticum Aestivum* L.) from Earthworms (*Eisenia Fetida*). *J. Hazard. Mater.* **2018**, *346*, 191–198. <https://doi.org/10.1016/j.jhazmat.2017.12.018>.

(135) Yan, P.-F.; Dong, S.; Manz, K. E.; Liu, C.; Woodcock, M. J.; Mezzari, M. P.; Abriola, L. M.; Pennell, K. D.; Cápiro, N. L. Biotransformation of 8:2 Fluorotelomer Alcohol in Soil from Aqueous Film-Forming Foams (AFFFs)-Impacted Sites under Nitrate-, Sulfate-, and Iron-Reducing Conditions. *Environ. Sci. Technol.* **2022**, *56* (19), 13728–13739. <https://doi.org/10.1021/acs.est.2c03669>.

(136) Löffler, F. E.; Sanford, R. A.; Ritalahti, K. M. Enrichment, Cultivation, and Detection of Reductively Dechlorinating Bacteria. In *Methods in Enzymology*; Environmental Microbiology; Academic Press, 2005; Vol. 397, pp 77–111. [https://doi.org/10.1016/S0076-6879\(05\)97005-5](https://doi.org/10.1016/S0076-6879(05)97005-5).

(137) Anderson, R. H.; Long, G. C.; Porter, R. C.; Anderson, J. K. Occurrence of Select Perfluoroalkyl Substances at U.S. Air Force Aqueous Film-Forming Foam Release Sites Other than Fire-Training Areas: Field-Validation of Critical Fate and Transport Properties. *Chemosphere* **2016**, *150*, 678–685. <https://doi.org/10.1016/j.chemosphere.2016.01.014>.

(138) Whittaker, R. H. Evolution and Measurement of Species Diversity. *TAXON* **1972**, *21* (2–3), 213–251. <https://doi.org/10.2307/1218190>.

(139) Zhang, S.; Merino, N.; Wang, N.; Ruan, T.; Lu, X. Impact of 6:2 Fluorotelomer Alcohol Aerobic Biotransformation on a Sediment Microbial Community. *Sci. Total Environ.* **2017**, *575*, 1361–1368. <https://doi.org/10.1016/j.scitotenv.2016.09.214>.

(140) Qiao, W.; Xie, Z.; Zhang, Y.; Liu, X.; Xie, S.; Huang, J.; Yu, L. Perfluoroalkyl Substances (PFASs) Influence the Structure and Function of Soil Bacterial Community: Greenhouse Experiment. *Sci. Total Environ.* **2018**, *642*, 1118–1126. <https://doi.org/10.1016/j.scitotenv.2018.06.113>.

(141) Sun, Y.; Wang, T.; Peng, X.; Wang, P.; Lu, Y. Bacterial Community Compositions in Sediment Polluted by Perfluoroalkyl Acids (PFAAs) Using Illumina High-Throughput Sequencing. *Environ. Sci. Pollut. Res.* **2016**, *23* (11), 10556–10565. <https://doi.org/10.1007/s11356-016-6055-0>.

- (142) Bao, Y.; Li, B.; Xie, S.; Huang, J. Vertical Profiles of Microbial Communities in Perfluoroalkyl Substance-Contaminated Soils. *Ann. Microbiol.* **2018**, *68* (6), 399–408. <https://doi.org/10.1007/s13213-018-1346-y>.
- (143) Li, B.; Bao, Y.; Xu, Y.; Xie, S.; Huang, J. Vertical Distribution of Microbial Communities in Soils Contaminated by Chromium and Perfluoroalkyl Substances. *Sci. Total Environ.* **2017**, *599–600*, 156–164. <https://doi.org/10.1016/j.scitotenv.2017.04.241>.
- (144) Zhang, D.; Zhang, W.; Liang, Y. Bacterial Community in a Freshwater Pond Responding to the Presence of Perfluorooctanoic Acid (PFOA). *Environ. Technol.* **2020**, *41* (27), 3646–3656. <https://doi.org/10.1080/09593330.2019.1616828>.
- (145) van Beilen, J. B.; Funhoff, E. G. Alkane Hydroxylases Involved in Microbial Alkane Degradation. *Appl. Microbiol. Biotechnol.* **2007**, *74* (1), 13–21. <https://doi.org/10.1007/s00253-006-0748-0>.
- (146) Sutton, N. B.; Maphosa, F.; Morillo, J. A.; Abu Al-Soud, W.; Langenhoff, A. A. M.; Grotenhuis, T.; Rijnaarts, H. H. M.; Smidt, H. Impact of Long-Term Diesel Contamination on Soil Microbial Community Structure. *Appl. Environ. Microbiol.* **2013**, *79* (2), 619–630. <https://doi.org/10.1128/AEM.02747-12>.
- (147) Kim, M. H.; Wang, N.; Chu, K. H. 6:2 Fluorotelomer Alcohol (6:2 FTOH) Biodegradation by Multiple Microbial Species under Different Physiological Conditions. *Appl. Microbiol. Biotechnol.* **2014**, *98* (4), 1831–1840. <https://doi.org/10.1007/s00253-013-5131-3>.
- (148) Lewis, M.; Kim, M.-H.; Wang, N.; Chu, K.-H. Engineering Artificial Communities for Enhanced FTOH Degradation. *Sci. Total Environ.* **2016**, *572*, 935–942. <https://doi.org/10.1016/j.scitotenv.2016.07.223>.
- (149) Krzmarzick, M. J.; Crary, B. B.; Harding, J. J.; Oyerinde, O. O.; Leri, A. C.; Myneni, S. C. B.; Novak, P. J. Natural Niche for Organohalide-Respiring Chloroflexi. *Appl. Environ. Microbiol.* **2012**, *78* (2), 393–401. <https://doi.org/10.1128/AEM.06510-11>.
- (150) Yu, X.; Nishimura, F.; Hidaka, T. Effects of Microbial Activity on Perfluorinated Carboxylic Acids (PFCAs) Generation during Aerobic Biotransformation of Fluorotelomer Alcohols in Activated Sludge. *Sci. Total Environ.* **2018**, *610–611*, 776–785. <https://doi.org/10.1016/j.scitotenv.2017.08.075>.
- (151) Touliabah, H. E.-S.; El-Sheekh, M. M.; Ismail, M. M.; El-Kassas, H. A Review of Microalgae- and Cyanobacteria-Based Biodegradation of Organic Pollutants. *Molecules* **2022**, *27* (3), 1141. <https://doi.org/10.3390/molecules27031141>.
- (152) Sei, K.; Miyagaki, K.; Kakinoki, T.; Fukugasako, K.; Inoue, D.; Ike, M. Isolation and Characterization of Bacterial Strains That Have High Ability to Degrade 1,4-Dioxane as a Sole Carbon and Energy Source. *Biodegradation* **2013**, *24* (5), 665–674. <https://doi.org/10.1007/s10532-012-9614-1>.
- (153) Moosvi, S. A.; Pacheco, C. C.; McDonald, I. R.; De Marco, P.; Pearce, D. A.; Kelly, D. P.; Wood, A. P. Isolation and Properties of Methanesulfonate-Degrading *Afipia Felis* from Antarctica and Comparison with Other Strains of *A. Felis*. *Environ. Microbiol.* **2005**, *7* (1), 22–33. <https://doi.org/10.1111/j.1462-2920.2004.00661.x>.

- (154) Zhang, P.; Hozalski, R. M.; Leach, L. H.; Camper, A. K.; Goslan, E. H.; Parsons, S. A.; Xie, Y. F.; LaPara, T. M. Isolation and Characterization of Haloacetic Acid-Degrading *Afipia* Spp. from Drinking Water. *FEMS Microbiol. Lett.* **2009**, *297* (2), 203–208. <https://doi.org/10.1111/j.1574-6968.2009.01687.x>.
- (155) A. Moody, C.; N. Hebert, G.; H. Strauss, S.; A. Field, J. Occurrence and Persistence of Perfluorooctanesulfonate and Other Perfluorinated Surfactants in Groundwater at a Fire-Training Area at Wurtsmith Air Force Base, Michigan, USA. *J. Environ. Monit.* **2003**, *5* (2), 341–345. <https://doi.org/10.1039/B212497A>.
- (156) Awad, E.; Zhang, X.; Bhavsar, S. P.; Petro, S.; Crozier, P. W.; Reiner, E. J.; Fletcher, R.; Tittlemier, S. A.; Braekevelt, E. Long-Term Environmental Fate of Perfluorinated Compounds after Accidental Release at Toronto Airport. *Environ. Sci. Technol.* **2011**, *45* (19), 8081–8089. <https://doi.org/10.1021/es2001985>.
- (157) Nelson Jessica W.; Hatch Elizabeth E.; Webster Thomas F. Exposure to Polyfluoroalkyl Chemicals and Cholesterol, Body Weight, and Insulin Resistance in the General U.S. Population. *Environ. Health Perspect.* **2010**, *118* (2), 197–202. <https://doi.org/10.1289/ehp.0901165>.
- (158) Kim, M. H.; Wang, N.; McDonald, T.; Chu, K.-H. Biodefluorination and Biotransformation of Fluorotelomer Alcohols by Two Alkane-Degrading *Pseudomonas* Strains. *Biotechnol. Bioeng.* **2012**, *109* (12), 3041–3048. <https://doi.org/10.1002/bit.24561>.
- (159) Favreau, P.; Poncioni-Rothlisberger, C.; Place, B. J.; Bouchex-Bellomie, H.; Weber, A.; Tremp, J.; Field, J. A.; Kohler, M. Multianalyte Profiling of Per- and Polyfluoroalkyl Substances (PFASs) in Liquid Commercial Products. *Chemosphere* **2017**, *171*, 491–501. <https://doi.org/10.1016/j.chemosphere.2016.11.127>.
- (160) Higgins, C.; Field, J.; Deeb, R.; Conder, J. *FAQs Regarding PFASs Associated with AFFF Use at U.S. Military Sites*; Environmental Security Technology Certification Program Alexandria United States, 2017.
- (161) Keränen, J.; Ahkola, H.; Knuutinen, J.; Herve, S.; Reinikainen, M.; Koistinen, J. Formation of PFOA from 8:2 FTOH in Closed-Bottle Experiments with Brackish Water. *Environ. Sci. Pollut. Res.* **2013**, *20* (11), 8001–8012. <https://doi.org/10.1007/s11356-013-1975-4>.
- (162) Sáez, M.; de Voogt, P.; Parsons, J. R. Persistence of Perfluoroalkylated Substances in Closed Bottle Tests with Municipal Sewage Sludge. *Environ. Sci. Pollut. Res.* **2008**, *15* (6), 472–477. <https://doi.org/10.1007/s11356-008-0020-5>.
- (163) Harding-Marjanovic, K. C.; Yi, S.; Weathers, T. S.; Sharp, J. O.; Sedlak, D. L.; Alvarez-Cohen, L. Effects of Aqueous Film-Forming Foams (AFFFs) on Trichloroethene (TCE) Dechlorination by a Dehalococoides Mccartyi-Containing Microbial Community. *Environ. Sci. Technol.* **2016**, *50* (7), 3352–3361. <https://doi.org/10.1021/acs.est.5b04773>.
- (164) McCord, J.; Newton, S.; Strynar, M. Validation of Quantitative Measurements and Semi-Quantitative Estimates of Emerging Perfluoroethercarboxylic Acids (PFECAs) and Hexafluoropropylene Oxide Acids (HFPOAs). *J. Chromatogr. A* **2018**, *1551*, 52–58. <https://doi.org/10.1016/j.chroma.2018.03.047>.
- (165) Szostek, B.; Prickett, K. B.; Buck, R. C. Determination of Fluorotelomer Alcohols by Liquid Chromatography/Tandem Mass Spectrometry in Water. *Rapid Commun. Mass Spectrom.* **2006**, *20* (19), 2837–2844. <https://doi.org/10.1002/rcm.2667>.

- (166) Thompson, L. R.; Sanders, J. G.; McDonald, D.; Amir, A.; Ladau, J.; Locey, K. J.; Prill, R. J.; Tripathi, A.; Gibbons, S. M.; Ackermann, G.; Navas-Molina, J. A.; Janssen, S.; Kopylova, E.; Vázquez-Baeza, Y.; González, A.; Morton, J. T.; Mirarab, S.; Zech Xu, Z.; Jiang, L.; Haroon, M. F.; Kanbar, J.; Zhu, Q.; Jin Song, S.; Kosciulek, T.; Bokulich, N. A.; Lefler, J.; Brislawn, C. J.; Humphrey, G.; Owens, S. M.; Hampton-Marcell, J.; Berg-Lyons, D.; McKenzie, V.; Fierer, N.; Fuhrman, J. A.; Clauset, A.; Stevens, R. L.; Shade, A.; Pollard, K. S.; Goodwin, K. D.; Jansson, J. K.; Gilbert, J. A.; Knight, R. A Communal Catalogue Reveals Earth's Multiscale Microbial Diversity. *Nature* **2017**, *551* (7681), 457–463. <https://doi.org/10.1038/nature24621>.
- (167) Edgar, R. C. Search and Clustering Orders of Magnitude Faster than BLAST. *Bioinformatics* **2010**, *26* (19), 2460–2461. <https://doi.org/10.1093/bioinformatics/btq461>.
- (168) Edgar, R. C. UPARSE: Highly Accurate OTU Sequences from Microbial Amplicon Reads. *Nat. Methods* **2013**, *10* (10), 996–998. <https://doi.org/10.1038/nmeth.2604>.
- (169) Quast, C.; Pruesse, E.; Yilmaz, P.; Gerken, J.; Schweer, T.; Yarza, P.; Peplies, J.; Glöckner, F. O. The SILVA Ribosomal RNA Gene Database Project: Improved Data Processing and Web-Based Tools. *Nucleic Acids Res.* **2013**, *41* (Database issue), D590–596. <https://doi.org/10.1093/nar/gks1219>.
- (170) Koch, V.; Knaup, W.; Fiebig, S.; Geffke, T.; Schulze, D. Biodegradation Kinetic and Estimated Half-Life of a Clariant Fluorotelomer-Based Acrylate Polymer—Results from a Test on Aerobic Transformation in Soil. *Reprod. Toxicol.* **2009**, *3–4* (27), 420–421. <https://doi.org/10.1016/j.reprotox.2008.11.068>.
- (171) Liu, J.; Lee, L. S. Solubility and Sorption by Soils of 8:2 Fluorotelomer Alcohol in Water and Cosolvent Systems. *Environ. Sci. Technol.* **2005**, *39* (19), 7535–7540. <https://doi.org/10.1021/es051125c>.
- (172) Schymanski, E. L.; Jeon, J.; Gulde, R.; Fenner, K.; Ruff, M.; Singer, H. P.; Hollender, J. Identifying Small Molecules via High Resolution Mass Spectrometry: Communicating Confidence. *Environ. Sci. Technol.* **2014**, *48* (4), 2097–2098. <https://doi.org/10.1021/es5002105>.
- (173) Ramette, A. Multivariate Analyses in Microbial Ecology: Multivariate Analyses in Microbial Ecology. *FEMS Microbiol. Ecol.* **2007**, *62* (2), 142–160. <https://doi.org/10.1111/j.1574-6941.2007.00375.x>.
- (174) Lovley, D. R.; Roden, E. E.; Phillips, E. J. P.; Woodward, J. C. Enzymatic Iron and Uranium Reduction by Sulfate-Reducing Bacteria. *Mar. Geol.* **1993**, *113* (1), 41–53. [https://doi.org/10.1016/0025-3227\(93\)90148-O](https://doi.org/10.1016/0025-3227(93)90148-O).
- (175) Tebo, B. M.; Obratsova, A. Y. Sulfate-Reducing Bacterium Grows with Cr(VI), U(VI), Mn(IV), and Fe(III) as Electron Acceptors. *FEMS Microbiol. Lett.* **1998**, *162* (1), 193–199. <https://doi.org/10.1111/j.1574-6968.1998.tb12998.x>.
- (176) Krzmarzick, M. J.; Miller, H. R.; Yan, T.; Novak, P. J. Novel Firmicutes Group Implicated in the Dechlorination of Two Chlorinated Xanthenes, Analogues of Natural Organochlorines. *Appl. Environ. Microbiol.* **2014**, *80* (3), 1210–1218. <https://doi.org/10.1128/AEM.03472-13>.
- (177) Sanford, R. A.; Cole, J. R.; Tiedje, J. M. Characterization and Description of Anaeromyxobacter Dehalogenans Gen. Nov., Sp. Nov., an Aryl-Halorespiring Facultative Anaerobic Myxobacterium. *Appl. Environ. Microbiol.* **2002**, *68* (2), 893–900. <https://doi.org/10.1128/AEM.68.2.893-900.2002>.

- (178) Moody, C. A.; Field, J. A. Determination of Perfluorocarboxylates in Groundwater Impacted by Fire-Fighting Activity. *Environ. Sci. Technol.* **1999**, *33* (16), 2800–2806. <https://doi.org/10.1021/es981355+>.
- (179) Baduel, C.; Paxman, C. J.; Mueller, J. F. Perfluoroalkyl Substances in a Firefighting Training Ground (FTG), Distribution and Potential Future Release. *J. Hazard. Mater.* **2015**, *296*, 46–53. <https://doi.org/10.1016/j.jhazmat.2015.03.007>.
- (180) Rognes, T.; Flouri, T.; Nichols, B.; Quince, C.; Mahé, F. VSEARCH: A Versatile Open Source Tool for Metagenomics. *PeerJ* **2016**, *4*, e2584. <https://doi.org/10.7717/peerj.2584>.
- (181) Amir, A.; McDonald, D.; Navas-Molina, J. A.; Kopylova, E.; Morton, J. T.; Zech Xu, Z.; Kightley, E. P.; Thompson, L. R.; Hyde, E. R.; Gonzalez, A.; Knight, R. Deblur Rapidly Resolves Single-Nucleotide Community Sequence Patterns. *mSystems* **2017**, *2* (2), e00191-16. <https://doi.org/10.1128/mSystems.00191-16>.
- (182) Cook, A. M.; Laue, H.; Junker, F. Microbial Desulfonation. *FEMS Microbiol. Rev.* **1998**, *22* (5), 399–419. <https://doi.org/10.1111/j.1574-6976.1998.tb00378.x>.
- (183) Tripathi, S.; Purchase, D.; Al-Rashed, S.; Chandra, R. Microbial Community Dynamics and Their Relationships with Organic and Metal Pollutants of Sugarcane Molasses-Based Distillery Wastewater Sludge. *Environ. Pollut.* **2022**, *292*, 118267. <https://doi.org/10.1016/j.envpol.2021.118267>.
- (184) Cao, X.; Cui, X.; Xie, M.; Zhao, R.; Xu, L.; Ni, S.; Cui, Z. Amendments and Bioaugmentation Enhanced Phytoremediation and Micro-Ecology for PAHs and Heavy Metals Co-Contaminated Soils. *J. Hazard. Mater.* **2022**, *426*, 128096. <https://doi.org/10.1016/j.jhazmat.2021.128096>.
- (185) Castelle, C. J.; Hug, L. A.; Wrighton, K. C.; Thomas, B. C.; Williams, K. H.; Wu, D.; Tringe, S. G.; Singer, S. W.; Eisen, J. A.; Banfield, J. F. Extraordinary Phylogenetic Diversity and Metabolic Versatility in Aquifer Sediment. *Nat. Commun.* **2013**, *4*, 2120. <https://doi.org/10.1038/ncomms3120>.
- (186) Bhatt, P.; Huang, Y.; Rene, E. R.; Kumar, A. J.; Chen, S. Mechanism of Allethrin Biodegradation by a Newly Isolated *Sphingomonas Trueperi* Strain CW3 from Wastewater Sludge. *Bioresour. Technol.* **2020**, *305*, 123074. <https://doi.org/10.1016/j.biortech.2020.123074>.
- (187) Nagata, Y.; Miyauchi, K.; Takagi, M. Complete Analysis of Genes and Enzymes for γ -Hexachlorocyclohexane Degradation in *Sphingomonas Paucimobilis* UT26. *J. Ind. Microbiol. Biotechnol.* **1999**, *23* (4–5), 380–390. <https://doi.org/10.1038/sj.jim.2900736>.
- (188) Zhang, J.; Gan, W.; Zhao, R.; Yu, K.; Lei, H.; Li, R.; Li, X.; Li, B. Chloramphenicol Biodegradation by Enriched Bacterial Consortia and Isolated Strain *Sphingomonas* Sp. CL5.1: The Reconstruction of a Novel Biodegradation Pathway. *Water Res.* **2020**, *187*, 116397. <https://doi.org/10.1016/j.watres.2020.116397>.
- (189) Zhou, L.; Li, H.; Zhang, Y.; Han, S.; Xu, H. *Sphingomonas* from Petroleum-Contaminated Soils in Shenfu, China and Their PAHs Degradation Abilities. *Braz. J. Microbiol.* **2016**, *47* (2), 271–278. <https://doi.org/10.1016/j.bjm.2016.01.001>.
- (190) Premnath, N.; Mohanrasu, K.; Guru Raj Rao, R.; Dinesh, G. H.; Prakash, G. S.; Ananthi, V.; Ponnuchamy, K.; Muthusamy, G.; Arun, A. A Crucial Review on Polycyclic Aromatic

Hydrocarbons - Environmental Occurrence and Strategies for Microbial Degradation. *Chemosphere* **2021**, *280*, 130608. <https://doi.org/10.1016/j.chemosphere.2021.130608>.

(191) Lee, H.; D'eon, J.; Mabury, S. A. Biodegradation of Polyfluoroalkyl Phosphates as a Source of Perfluorinated Acids to the Environment. *Environ. Sci. Technol.* **2010**, *44* (9), 3305–3310. <https://doi.org/10.1021/es9028183>.

(192) Yan, P.-F.; Dong, S.; Manz, K. E.; Liu, C.; Woodcock, M. J.; Mezzari, M. P.; Abriola, L. M.; Pennell, K. D.; Cápiro, N. L. Biotransformation of 8:2 Fluorotelomer Alcohol in Soil from Aqueous Film-Forming Foams (AFFFs)-Impacted Sites under Nitrate-, Sulfate-, and Iron-Reducing Conditions. *Environ. Sci. Technol.* **2022**. <https://doi.org/10.1021/acs.est.2c03669>.

(193) Prevedouros, K.; Cousins, I. T.; Buck, R. C.; Korzeniowski, S. H. Sources, Fate and Transport of Perfluorocarboxylates. *Environ. Sci. Technol.* **2006**, *40* (1), 32–44. <https://doi.org/10.1021/es0512475>.

(194) Mitchell, R. J.; Myers, A. L.; Mabury, S. A.; Solomon, K. R.; Sibley, P. K. Toxicity of Fluorotelomer Carboxylic Acids to the Algae *Pseudokirchneriella Subcapitata* and *Chlorella Vulgaris*, and the Amphipod *Hyalella Azteca*. *Ecotoxicol. Environ. Saf.* **2011**, *74* (8), 2260–2267. <https://doi.org/10.1016/j.ecoenv.2011.07.034>.

(195) Phillips, M. M. (MacDonald); Dinglasan-Panlilio, M. J. A.; Mabury, S. A.; Solomon, K. R.; Sibley, P. K. Fluorotelomer Acids Are More Toxic than Perfluorinated Acids. *Environ. Sci. Technol.* **2007**, *41* (20), 7159–7163. <https://doi.org/10.1021/es070734c>.

(196) Schaefer, C. E.; Condee, C. W.; Vainberg, S.; Steffan, R. J. Bioaugmentation for Chlorinated Ethenes Using *Dehalococcoides* Sp.: Comparison between Batch and Column Experiments. *Chemosphere* **2009**, *75* (2), 141–148. <https://doi.org/10.1016/j.chemosphere.2008.12.041>.

(197) Staff, S. S. Keys to Soil Taxonomy, 12th Edn Washington. *DC Nat. Resour. Conserv. Serv. U. S. Dep. Agric. Sch.* **2014**.

(198) Costanza, J. Degradation of Tetrachloroethylene and Trichloroethylene under Thermal Remediation Conditions. **2005**.

(199) Aggrawal, M. Determination of Inorganic Anions in Drinking Water Using a Compact Ion Chromatography System. **8**.

(200) Williams, A. J.; Grulke, C. M.; Edwards, J.; McEachran, A. D.; Mansouri, K.; Baker, N. C.; Patlewicz, G.; Shah, I.; Wambaugh, J. F.; Judson, R. S.; Richard, A. M. The CompTox Chemistry Dashboard: A Community Data Resource for Environmental Chemistry. *J. Cheminformatics* **2017**, *9* (1), 61. <https://doi.org/10.1186/s13321-017-0247-6>.

(201) Schymanski, E. L.; Jeon, J.; Gulde, R.; Fenner, K.; Ruff, M.; Singer, H. P.; Hollender, J. Identifying Small Molecules via High Resolution Mass Spectrometry: Communicating Confidence. *Environ. Sci. Technol.* **2014**, *48* (4), 2097–2098. <https://doi.org/10.1021/es5002105>.

(202) Stumm, W.; Lee, G. F. Oxygenation of Ferrous Iron. *Ind. Eng. Chem.* **1961**, *53* (2), 143–146. <https://doi.org/10.1021/ie50614a030>.

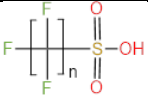
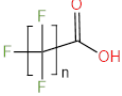
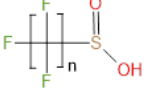

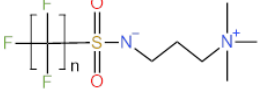
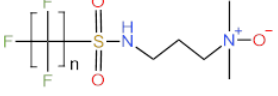
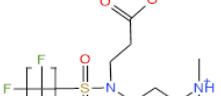
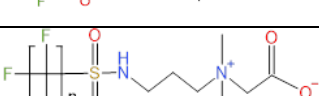
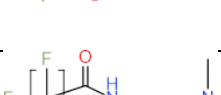
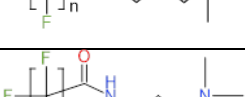
(203) Sepulvado, J. G.; Blaine, A. C.; Hundal, L. S.; Higgins, C. P. Occurrence and Fate of Perfluorochemicals in Soil Following the Land Application of Municipal Biosolids. *Environ. Sci. Technol.* **2011**, *45* (19), 8106–8112. <https://doi.org/10.1021/es103903d>.

- (204) Wang, Z.; MacLeod, M.; Cousins, I. T.; Scheringer, M.; Hungerbühler, K. Using COSMOtherm to Predict Physicochemical Properties of Poly- and Perfluorinated Alkyl Substances (PFASs). *Environ. Chem.* **2011**, 8 (4), 389. <https://doi.org/10.1071/EN10143>.
- (205) Wishart, D. S.; Tian, S.; Allen, D.; Oler, E.; Peters, H.; Lui, V. W.; Gautam, V.; Djoumbou-Feunang, Y.; Greiner, R.; Metz, T. O. BioTransformer 3.0—a Web Server for Accurately Predicting Metabolic Transformation Products. *Nucleic Acids Res.* **2022**, gkac313. <https://doi.org/10.1093/nar/gkac313>.

Appendices

Appendix A. Supporting Information for Chapter 2: Literature review on per- and polyfluoroalkyl substances in aqueous film-forming foams (AFFFs) and AFFF-impacted environment

Table A-1. PFAS class acronym, class name, structure of the class, and the example of acronym of one analogue.

Class acronym	Class name	Structure	Example of compound acronym
Perfluoroalkyl acids (PFAAs)			
PFSA	Perfluoroalkane sulfonic acids		PFOS (n=8)
PFCA	Perfluoroalkyl carboxylic acid		PFOA (n=7)
PFSAi	Perfluoroalkanesulfinate		PFOSi (n=8)
Primary ECF-based precursors			
AmPr-FASA	N-dimethyl ammonio propyl perfluoroalkane sulfonamide		AmPr-FOSA (n=8)
TAmPr-FASA	N-trimethyl ammonio propyl perfluoroalkane sulfonamide		TAmPr-FOSA (n=8)
OAmPr-FASA	N-oxide dimethyl ammonio propyl perfluoroalkane sulfonamide		OAmPr-FOSA (n=8)
AmPr-FASA-PrA	N-dimethyl ammonio propyl perfluoroalkane sulfonamido propanoic acid		AmPr-FOSA-PrA (n=8)
CMe-AmPr-FASA	N-carboxy methyl dimethyl ammonio propyl perfluoroalkane sulfonamide		CMe-AmPr-FOSA (n=8)
AmPr-FAAd	N-dimethylammonio propyl perfluoroalkane amide		AmPr-FOAA (n=7)
TAmPr-FAAd	N-trimethyl ammonio propyl perfluoroalkane amide		TAmPr-FOAA (n=7)

OAmPr-FAAd	N-oxide dimethyl ammonio propyl perfluoroalkane amide		OAmPr-FOAA (n=7)
CMe-AmPr-FAAd	N-carboxy methyl dimethyl ammonio propyl perfluoroalkane amide		CMe-AmPr-FOAA (n=7)
Secondary ECF-based precursors			
FASA	Perfluoroalkane sulfonamide		FOSA (n=8)
MeFASA	N-methyl perfluoroalkane sulfonamide		MeFOSA (n=8)
EtFASA	N-ethyl perfluoroalkane sulfonamide		EtFOSA (n=8)
FASAA	Perfluoroalkane sulfonamido acetic acid		FOSAA (n=8)
MeFASAA	N-methyl perfluoroalkane sulfonamido acetic acid		MeFOSAA (n=8)
EtFASAA	N-ethyl perfluoroalkane sulfonamido acetic acid		EtFOSAA (n=8)
Primary FT-based precursors			
n:2 FTAB	Fluorotelomer sulfonamide alkylbetaine		6:2 FTAB (n=6)
n:2 FtTAoS	Fluorotelomer thioether amido sulfonate		6:2 FtTAoS (n=6)
n:2 FtSaAm	Fluorotelomer sulfonamide amine		6:2 FtSaAm (n=6)
n:2 FtTHN+	Fluorotelomer thiohydroxyl ammonium		6:2 FtTHN+ (n=6)
n:3 FTB	Fluorotelomer betain		7:3 FTB (n=7)

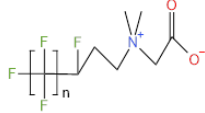
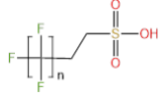
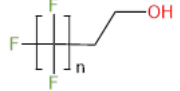
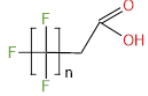
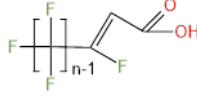
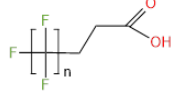
n:1:2 FTB	Fluorotelomer betain		7:1:2 FTB (n=7)
Secondary FT-based precursors			
n:2 FTS	Fluorotelomer sulfonate		6:2 FTS (n=6)
n:2 FTOH	Fluorotelomer alcohol		6:2 FTOH (n=6)
n:2 FTCA	Fluorotelomer saturated carboxylic acid		6:2 FTCA (n=6)
n:2 FTUA	Fluorotelomer unsaturated carboxylic acid		6:2 FTUA (n=6)
n:3 acid	Fluorotelomer acid		7:3 acid (n=7)

Table A-2. Summary statistics of the concentration of selected PFAS previously reported in the surface water samples (n=204) collected from AFFF-impacted sites. C4-C11 PFCAs, C4, C6-C8, C10 PFSAs, and polyfluorinated compounds that were prevalently detected are included in the table. Other polyfluorinated compounds such as newly identified precursors in AFFF formulations (e.g., AmPr-FASAs) with <10 concentrations reported are not included.

PFAS	Detection Frequency	Concentration range (ng/L)	Mean (ng/L)	Median (ng/L)
PFBA	60/99 (60.6%)	0.53-899	175	24
PFPeA	79/109 (72.5%)	0.15-4,120	393	19
PFHxA	91/123 (74.0%)	0.21-6,500	626	22
PFHpA	110/136 (80.9%)	0.31-1,340	122	10
PFOA	180/204 (88.2%)	0.31-11,300	446	32
PFNA	98/136 (72.1%)	0.18-3,290	109	4.4
PFDA	56/136 (41.2%)	0.17-130	15	5.6
PFUnA	28/131 (21.4%)	0.33-547	56	6.0
PFBS	73/109 (67.0%)	0.11-3,500	394	13
PFHxS	150/204 (73.5%)	0.14-134,000	3,726	46
PFHpS	42/88 (47.7%)	0.30-3,200	567	61
PFOS	172/204 (84.3%)	0.35-2,210,000	36,393	140
PFDS	5/125 (4%)	0.67-8.0	3.7	3.6
4:2 FTS	7/88 (8.0%)	0.7-15.9	6.6	5.0
6:2 FTS	57/94 (60.6%)	0.11-10,200	810	28
8:2 FTS	23/88 (26.1%)	0.16-249	45	22
FOSA	43/125 (34.4%)	0.11-139	9.3	1.8
6:2 FTAB	11/16 (68.8%)	59-17,874	2,189	426

Table A-3. Summary statistics of the concentration of selected PFAS previously reported in the surface soil samples (n=274) collected from AFFF-impacted sites. C4-C14 PFCAs, C3-C10 PFSAs, and polyfluorinated compounds that were prevalently detected are included in the table. Other polyfluorinated compounds such as newly identified precursors in AFFF formulations (e.g., AmPr-FASAs) with <10 concentrations reported are not included.

PFAS	Detection Frequency	Concentration range (µg/kg)	Mean (µg/kg)	Median (µg/kg)
PFBA	137/213 (64.3%)	0.07-456	18	2.3
PFPeA	143/223 (64.1%)	0.14-1,421	49	5.9
PFHxA	183/268 (68.3%)	0.07-2,761	66	6.0
PFHpA	144/223 (64.6%)	0.06-323	11	2.4
PFOA	206/274 (75.2%)	0.05-11,484	115	4.0
PFNA	125/223 (56.1%)	0.03-59	6.3	2.2
PFDA	92/223 (41.3%)	0.02-252	9.7	1.0
PFUnA	62/162 (38.3%)	0.02-130	13	0.8
PFDoA	56/162 (34.6%)	0.03-155	11	1.3
PFTTrA	49/160 (30.6%)	0.02-263	19	0.3
PFTeA	32/158 (20.3%)	0.02-82	9.2	0.7
PFPrS	4/10 (40.0%)	0.2-29	7.5	0.4
PFBS	94/223 (42.2%)	0.02-1,672	51	1.3
PFPeS	5/10 (50.0%)	0.01-66	17	0.9
PFHxS	219/268 (81.7%)	0.01-23,875	288	8.0
PFHpS	60/148 (40.5%)	0.01-2,494	61	2.5
PFOS	249/274 (90.9%)	0.03-55,197	1,485	78
PFNS	9/10 (90.0%)	0.01-8,900	1,041	1.9
PFDS	100/209 (47.8%)	0.02-5,700	70	1.4
4:2 FTS	36/132 (27.3%)	0.01-126	3.8	0.1
6:2 FTS	130/160 (81.3%)	0.03-6,200	256	40
8:2 FTS	101/148 (68.2%)	0.05-4,073	156	14
10:2 FTS	3/10 (30.0%)	0.3-0.4	0.3	0.4
6:2 FTUA	27/105 (25.7%)	0.04-25	1.4	0.3
8:2 FTUA	30/105 (28.6%)	0.03-53	2.1	0.1
10:2 FTUA	3/77 (3.9%)	0.7-23	13	16
5:3 acid	29/95 (30.5%)	0.3-16	3.1	1.5

7:3 acid	28/28 (100%)	0.2-15	1.6	0.4
FHxSA	18/26 (69.2%)	1.1-1,800	360	12
FOSA	97/148 (65.5%)	0.01-3,400	110	3
FOSAA	10/105 (9.5%)	0.01-0.8	0.2	0.02
EtFOSA	17/132 (12.9%)	0.02-0.7	0.1	0.04
6:2 FTAB	81/117 (69.2%)	1.7-631,338	12,975	494
6:2 FtSaAm	19/83 (22.9%)	8-7,074	727	116

Table A-4. Summary statistics of the concentration of selected PFAS previously reported in the subsurface soil samples (n=169) collected from AFFF-impacted sites. C4-C11 PFCAs, C3-C10 PFSAs, and polyfluorinated compounds that were prevalently detected are included in the table. Other polyfluorinated compounds such as newly identified precursors in AFFF formulations (e.g., AmPr-FASAs) with <10 concentrations reported are not included.

PFAS	Detection Frequency	Concentration range (µg/kg)	Mean (µg/kg)	Median (µg/kg)
PFBA	45/153 (29.4%)	1.2-52	11	5.0
PFPeA	99/153 (64.7%)	0.1-142	14	7.0
PFHxA	120/153 (78.4%)	0.4-297	31	11
PFHpA	96/153 (62.7%)	0.2-38	6.2	3.0
PFOA	114/169 (67.5%)	0.2-536	43	8.4
PFNA	39/153 (25.5%)	0.1-4.2	1.2	1.0
PFDA	34/153 (22.2%)	0.3-6.0	1.1	0.7
PFUnA	15/137 (10.9%)	0.02-5.0	0.5	0.1
PFPrS	26/47 (55.3%)	0.05-16	2.5	1.5
PFBS	100/153 (65.4%)	0.02-1,105	42	5.0
PFPeS	45/47 (95.7%)	0.08-51	6.4	2.8
PFHxS	127/153 (83.0%)	0.7-947	84	25
PFHpS	75/137 (54.7%)	0.07-51	6.0	3.5
PFOS	135/169 (79.9%)	0.03-3,960	231	80
PFNS	29/47 (61.7%)	0.07-14	1.4	0.4
PFDS	25/153 (16.3%)	0.02-52	7.8	2.1
4:2 FTS	15/127 (11.8%)	0.6-5.7	2.4	2.1
6:2 FTS	106/137 (77.4%)	0.4-370	49	27
8:2 FTS	61/137 (44.5%)	0.07-198	26	10
FHxSA	49/57 (86.0%)	0.6-110	22	17
FOSA	52/137 (38.0%)	0.06-138	17	5.8
MeFOSAA	12/127 (9.4%)	0.05-3.4	1.1	0.5
6:2 FTAB	54/111 (48.6%)	4.0-11,699	1,847	280

Table A-5. Summary statistics of the concentration of selected PFAS previously reported in the sediment samples (n=78) collected from AFFF-impacted sites. C4-C13 PFCAs, C4, C6-C8, C10 PFSA, and polyfluorinated compounds that were prevalently detected are included in the table. Other polyfluorinated compounds such as newly identified precursors in AFFF formulations (e.g., AmPr-FASAs) with <10 concentrations reported are not included.

PFAS	Detection Frequency	Concentration range (µg/kg)	Mean (µg/kg)	Median (µg/kg)
PFBA	14/42 (33.3%)	0.05-0.9	0.2	0.1
PFPeA	15/51 (29.4%)	0.00-2.5	0.6	0.5
PFHxA	15/51 (29.4%)	0.00-3.4	0.8	0.7
PFHpA	15/78 (19.2%)	0.00-1.4	0.3	0.2
PFOA	35/78 (44.9%)	0.01-2.3	0.2	0.1
PFNA	9/78 (11.5%)	0.01-21.7	3.4	0.1
PFDA	19/78 (24.4%)	0.00-1.4	0.2	0.1
PFUnA	27/78 (34.6%)	0.00-81	8.8	0.3
PFDoA	19/78 (24.4%)	0.00-5.7	0.8	0.3
PFTTrA	23/70 (32.9%)	0.06-235	13.2	0.6
PFBS	4/51 (7.8%)	0.01-0.5	0.2	0.2
PFHxS	19/78 (24.4%)	0.00-3.0	0.9	0.7
PFHpS	2/34 (5.9%)	0.2-0.5	0.3	0.3
PFOS	50/78 (64.1%)	0.00-88	15	1.1
PFDS	26/78 (33.3%)	0.01-1.7	0.4	0.2
6:2 FTS	24/51 (47.1%)	0.00-23	4.3	0.5
8:2 FTS	14/39 (35.9%)	0.00-34.3	3.4	0.1
FOSA	22/69 (31.9%)	0.01-2.8	0.3	0.1
8:2 FTAB	11/16 (68.8%)	0.02-4.5	0.9	0.1
10:2 FTAB	10/16 (62.5%)	0.01-7.6	1.1	0.1

Appendix B. Supporting Information for Chapter 3: Production of perfluorooctane sulfonate (PFOS) from biotransformation of perfluorooctane sulfonamide (FOSA) in aerobic soils

Table B-1. Physical and chemical properties of Loring and Hudson soils.

	Loring soil	Hudson soil
Sand, Silt, Clay (%)	53.1 ± 3.1, 32.7 ± 2.3, 14.2 ± 0.8	15.6 ± 3.1, 68.3 ± 1.7, 16.1 ± 1.4
USDA Textual Class	Loam/Sandy Loam	Silt Loam
CEC (meq/100 grams)	18.7 ± 0.0	14.7 ± 1.1
Organic Carbon (%)	3.5 ± 0.1	1.1 ± 0.0
Moisture Content (%)	24.1 ± 1.1	13.8 ± 0.6
pH (1-part soil: 1-part deionized water)	7.2 ± 0.2	6.5 ± 0.0

Table B-2. Targeted mass inclusion list used in LC-MS analysis.

Compound	Formula	m/z	RT (min)	Window (min)	HCD Collision Energy (%)
FOSA	C8HF17NO2S	497.9462	12.4	1	40
FHxSA	C6HF13NO2S	397.9526	10.59	1	40
PFOS	C8F17SO3	498.9302	10.3	2	50
PFHpS	C7F15SO3	448.9334	9.8	2	60
PFHxS	C6F13SO3	398.9366	9.2	2	40
PFPeS	C5F11SO3	348.9398	8.39	1	50
PFBS	C4F9SO3	298.943	6.7	1.5	50
PFBA	C4HF7O2	212.9792	1.6	0.5	30
PFPeA	C5F9O2	262.976	2.9	1	14
PFHxA	C6F11O2	312.9728	7	1	14
PFHpA	C7F13O2	362.9696	8.3	1	14
PFOA	C8F15O2	412.9664	9.04	2	14

Table B-3. Limits of detection (LODs) and limits of quantification (LOQs) of targeted PFAS.

Analytes	LOD ^a (ng/mL)	LOQ (ng/mL)
PFBA	0.01	0.01
PFPeA	0.01	0.03
PFHxA	0.01	0.04
PFHpA	0.01	0.01
PFOA	0.01	0.01
PFBS	0.02	0.07
PFPeS	0.01	0.01
PFHxS	0.01	0.01
PFHpS	0.01	0.01
PFOS	0.01	0.01
FHxSA	0.01	0.01
FOSA	0.01	0.01

^aLODs and LOQs were calculated based on the signal-to-noise ratio (S/N), with a S/N of 3 for LOD and 10 for LOQ, respectively.

Table B-4. Changes in the mass (nmole) of FOSA and PFOS in Loring soil microcosms.

Time	FOSA			PFOS		
	Live treatment	Abiotic control	Positive control	Live treatment	Abiotic control	Positive control
Day 0	24.2 ± 1.2	17.0 ± 0.1	0.6 ± 0.0	47.1 ± 0.4	47.3 ± 0.1	47.5 ± 1.4
Day 28	22.4 ± 0.2	16.1 ± 0.3	0.6 ± 0.0	52.1 ± 0.4	53.7 ± 0.8	57.2 ± 0.4
Day 56	24.5 ± 0.5	19.0 ± 0.3	0.8 ± 0.1	57.9 ± 0.6	57.5 ± 2.2	57.2 ± 0.1
Day 98	18.9 ± 0.9	15.1 ± 1.1	0.6 ± 0.0	55.0 ± 0.6	54.1 ± 2.7	53.3 ± 1.6
Day 154	17.2 ± 0.9	15.2 ± 0.2	0.7 ± 0.1	52.5 ± 0.8	47.0 ± 0.0	46.3 ± 0.2
Day 224	15.6 ± 1.1	16.3 ± 0.4	0.6 ± 0.0	55.9 ± 2.7	49.7 ± 1.1	50.7 ± 0.4
Day 308	13.3 ± 0.7	14.9 ± 0.5	0.6 ± 0.1	51.5 ± 1.3	47.5 ± 1.2	46.3 ± 1.5

Table B-5. Partitioning of FOSA and PFOS in aqueous and solid phases of Loring and Hudson live treatments (percentage (%) of mass in each phase relative to the total mass).

Time	Loring-live treatments				Hudson-live treatments			
	FOSA		PFOS		FOSA		PFOS	
	Aqueous	Solid	Aqueous	Solid	Aqueous	Solid	Aqueous	Solid
Day 28	9.4 ± 0.6	90.6 ± 0.6	30.4 ± 3.0	69.6 ± 3.0	30.4 ± 1.3	69.6 ± 1.3	60.5 ± 1.2	39.5 ± 1.2
Day 56	8.6 ± 0.2	91.4 ± 0.2	26.2 ± 3.2	73.8 ± 3.2	23.5 ± 1.0	76.5 ± 1.0	53.9 ± 2.4	46.1 ± 2.4
Day 98	11.4 ± 0.5	88.6 ± 0.5	29.4 ± 0.9	70.6 ± 0.9	28.4 ± 1.8	71.6 ± 1.8	51.8 ± 6.3	48.2 ± 6.3
Day 154	9.5 ± 1.2	90.5 ± 1.2	26.4 ± 2.0	73.6 ± 2.0	28.9 ± 1.5	71.1 ± 1.5	49.6 ± 2.7	50.4 ± 2.7
Day 224	9.4 ± 0.5	90.6 ± 0.5	25.1 ± 1.5	74.9 ± 1.5	21.2 ± 4.1	78.8 ± 4.1	44.9 ± 1.5	55.1 ± 1.5
Day 308	8.2 ± 0.5	91.8 ± 0.5	21.3 ± 1.6	78.7 ± 1.6	17.3 ± 7.5	82.7 ± 7.5	43.6 ± 5.3	56.4 ± 5.3

Table B-6. Microbial richness and diversity in Loring and Hudson soils.

Soil type	FOSA (µg/L)	Sampling time	Mapped reads	OTUs	Chao1	Shannon	Simpson																																																																																																	
Loring AFB soil	0	Day 0	6490	687	1019.8 ± 30.8	5.85 ± 0.07	0.99 ± 0.00																																																																																																	
	0	Day 0	6403	651				0	Day 154	6945	267	422.8 ± 0.5	3.67 ± 0.01	0.91 ± 0.01	0	Day 154	7194	283	85	Day 154	6742	267	524.5 ± 95.1	3.69 ± 0.14	0.92 ± 0.01	85	Day 154	6283	280	0	Day 308	5300	280	419.9 ± 6.3	3.98 ± 0.14	0.92 ± 0.02	0	Day 308	6354	276	85	Day 308	6430	251	408.9 ± 34.6	3.75 ± 0.18	0.92 ± 0.02	85	Day 308	6272	233	Hudson AFB soil	0	Day 0	4606	393	586.6 ± 35.6	4.87 ± 0.05	0.98 ± 0.00	0	Day 0	5254	388	0	Day 154	6230	206	256.6 ± 54.6	3.65 ± 0.08	0.94 ± 0.00	0	Day 154	8298	150	85	Day 154	6111	161	254.2 ± 1.3	3.34 ± 0.04	0.91 ± 0.01	85	Day 154	6225	171	0	Day 308	6073	226	297.6 ± 25.5	3.66 ± 0.12	0.93 ± 0.01	0	Day 308	6590	162	85	Day 308	6649	158	219.1 ± 2.9	3.54 ± 0.08	0.92 ± 0.02	85
	0	Day 154	6945	267	422.8 ± 0.5	3.67 ± 0.01	0.91 ± 0.01																																																																																																	
	0	Day 154	7194	283				85	Day 154	6742	267	524.5 ± 95.1	3.69 ± 0.14	0.92 ± 0.01	85	Day 154	6283	280	0	Day 308	5300	280	419.9 ± 6.3	3.98 ± 0.14	0.92 ± 0.02	0	Day 308	6354	276	85	Day 308	6430	251	408.9 ± 34.6	3.75 ± 0.18	0.92 ± 0.02	85	Day 308	6272	233	Hudson AFB soil	0	Day 0	4606	393	586.6 ± 35.6	4.87 ± 0.05	0.98 ± 0.00	0	Day 0	5254		388	0	Day 154	6230	206	256.6 ± 54.6	3.65 ± 0.08	0.94 ± 0.00	0	Day 154	8298	150	85	Day 154	6111	161	254.2 ± 1.3	3.34 ± 0.04	0.91 ± 0.01	85	Day 154	6225	171	0	Day 308	6073	226	297.6 ± 25.5	3.66 ± 0.12	0.93 ± 0.01	0	Day 308	6590	162	85	Day 308	6649	158	219.1 ± 2.9	3.54 ± 0.08	0.92 ± 0.02	85	Day 308	5761	166							
	85	Day 154	6742	267	524.5 ± 95.1	3.69 ± 0.14	0.92 ± 0.01																																																																																																	
	85	Day 154	6283	280				0	Day 308	5300	280	419.9 ± 6.3	3.98 ± 0.14	0.92 ± 0.02	0	Day 308	6354	276	85	Day 308	6430	251	408.9 ± 34.6	3.75 ± 0.18	0.92 ± 0.02	85	Day 308	6272	233	Hudson AFB soil	0	Day 0	4606	393	586.6 ± 35.6	4.87 ± 0.05	0.98 ± 0.00	0	Day 0	5254		388	0	Day 154	6230	206	256.6 ± 54.6	3.65 ± 0.08	0.94 ± 0.00	0	Day 154		8298	150	85	Day 154	6111	161	254.2 ± 1.3	3.34 ± 0.04	0.91 ± 0.01	85	Day 154	6225	171	0	Day 308	6073	226	297.6 ± 25.5	3.66 ± 0.12	0.93 ± 0.01	0	Day 308	6590	162	85	Day 308	6649	158	219.1 ± 2.9	3.54 ± 0.08	0.92 ± 0.02	85	Day 308	5761	166																	
	0	Day 308	5300	280	419.9 ± 6.3	3.98 ± 0.14	0.92 ± 0.02																																																																																																	
	0	Day 308	6354	276				85	Day 308	6430	251	408.9 ± 34.6	3.75 ± 0.18	0.92 ± 0.02	85	Day 308	6272	233	Hudson AFB soil	0	Day 0	4606	393	586.6 ± 35.6	4.87 ± 0.05	0.98 ± 0.00	0	Day 0	5254		388	0	Day 154	6230	206	256.6 ± 54.6	3.65 ± 0.08	0.94 ± 0.00	0	Day 154		8298	150	85	Day 154	6111	161	254.2 ± 1.3	3.34 ± 0.04	0.91 ± 0.01	85		Day 154	6225	171	0	Day 308	6073	226	297.6 ± 25.5	3.66 ± 0.12	0.93 ± 0.01	0	Day 308	6590	162	85	Day 308	6649	158	219.1 ± 2.9	3.54 ± 0.08	0.92 ± 0.02	85	Day 308	5761	166																											
	85	Day 308	6430	251	408.9 ± 34.6	3.75 ± 0.18	0.92 ± 0.02																																																																																																	
	85	Day 308	6272	233				Hudson AFB soil	0	Day 0	4606	393	586.6 ± 35.6	4.87 ± 0.05	0.98 ± 0.00	0	Day 0	5254		388	0	Day 154	6230	206	256.6 ± 54.6	3.65 ± 0.08	0.94 ± 0.00	0	Day 154		8298	150	85	Day 154	6111	161	254.2 ± 1.3	3.34 ± 0.04	0.91 ± 0.01	85		Day 154	6225	171	0	Day 308	6073	226	297.6 ± 25.5	3.66 ± 0.12	0.93 ± 0.01		0	Day 308	6590	162	85	Day 308	6649	158	219.1 ± 2.9	3.54 ± 0.08	0.92 ± 0.02	85	Day 308	5761	166																																					
Hudson AFB soil	0	Day 0	4606	393	586.6 ± 35.6	4.87 ± 0.05	0.98 ± 0.00																																																																																																	
	0	Day 0	5254	388					0	Day 154	6230	206	256.6 ± 54.6	3.65 ± 0.08	0.94 ± 0.00	0	Day 154	8298		150	85	Day 154	6111	161	254.2 ± 1.3	3.34 ± 0.04	0.91 ± 0.01	85	Day 154		6225	171	0	Day 308	6073	226	297.6 ± 25.5	3.66 ± 0.12	0.93 ± 0.01	0		Day 308	6590	162	85	Day 308	6649	158	219.1 ± 2.9	3.54 ± 0.08	0.92 ± 0.02	85	Day 308	5761	166																																																	
	0	Day 154	6230	206	256.6 ± 54.6	3.65 ± 0.08	0.94 ± 0.00																																																																																																	
	0	Day 154	8298	150					85	Day 154	6111	161	254.2 ± 1.3	3.34 ± 0.04	0.91 ± 0.01	85	Day 154	6225		171	0	Day 308	6073	226	297.6 ± 25.5	3.66 ± 0.12	0.93 ± 0.01	0	Day 308		6590	162	85	Day 308	6649	158	219.1 ± 2.9	3.54 ± 0.08	0.92 ± 0.02	85	Day 308	5761	166																																																													
	85	Day 154	6111	161	254.2 ± 1.3	3.34 ± 0.04	0.91 ± 0.01																																																																																																	
	85	Day 154	6225	171					0	Day 308	6073	226	297.6 ± 25.5	3.66 ± 0.12	0.93 ± 0.01	0	Day 308	6590		162	85	Day 308	6649	158	219.1 ± 2.9	3.54 ± 0.08	0.92 ± 0.02	85	Day 308	5761	166																																																																									
	0	Day 308	6073	226	297.6 ± 25.5	3.66 ± 0.12	0.93 ± 0.01																																																																																																	
	0	Day 308	6590	162					85	Day 308	6649	158	219.1 ± 2.9	3.54 ± 0.08	0.92 ± 0.02	85	Day 308	5761	166																																																																																					
	85	Day 308	6649	158	219.1 ± 2.9	3.54 ± 0.08	0.92 ± 0.02																																																																																																	
	85	Day 308	5761	166																																																																																																				

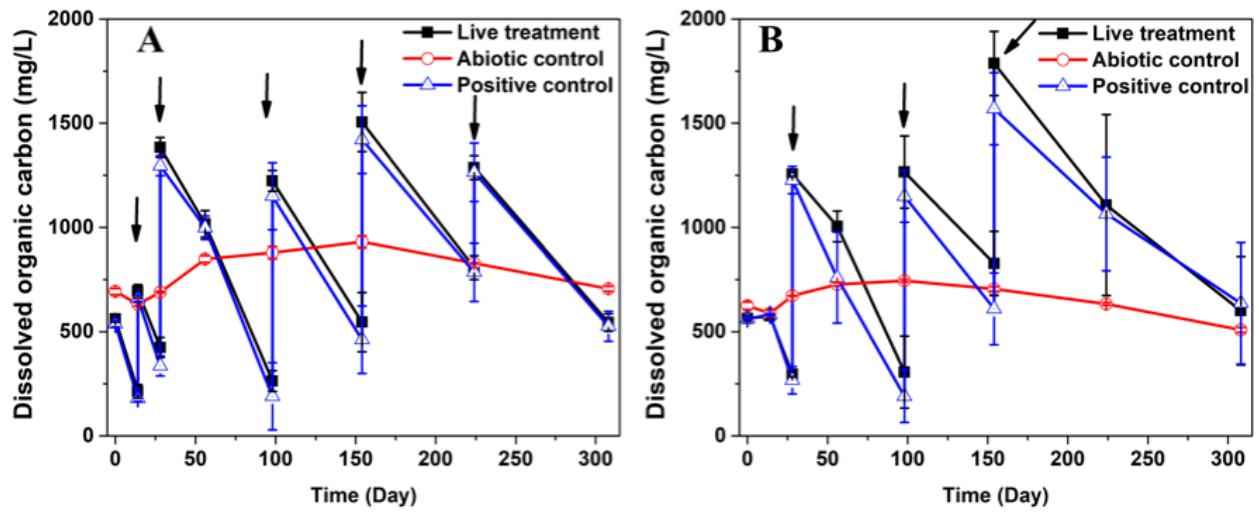


Figure B-1. Concentrations of dissolved organic carbon in Loring (Panel A) and Hudson (Panel B) soil microcosms. Solid arrows represent the amendment of 5 mM or 10 mM DGBE to live treatment and positive control microcosms. Error bars represent the standard deviation of triplicate live treatment microcosms, and of duplicate control microcosms.

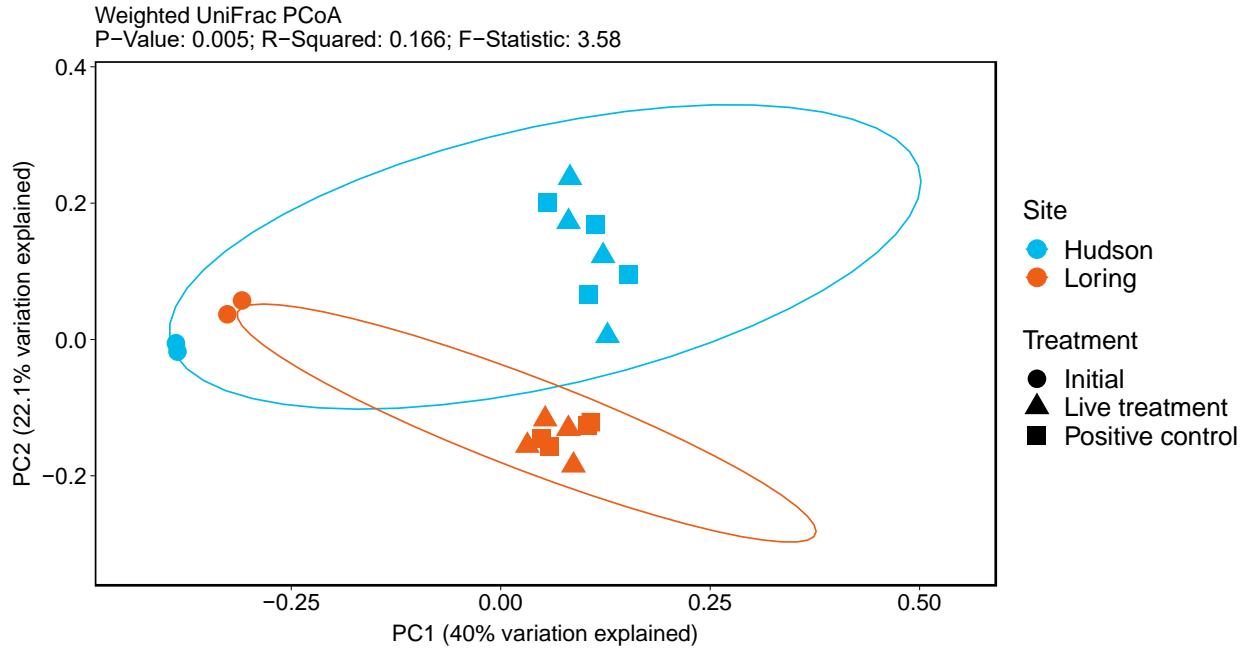


Figure B-2. Principal coordinate analysis (PCoA) plot of phylogenetic microbial community changes among the treatments from Loring and Hudson soil microcosms, as described by weighted UniFrac distance matrices. The PC1 and PC2 axes explain 40% and 22.1% of the variation, respectively.

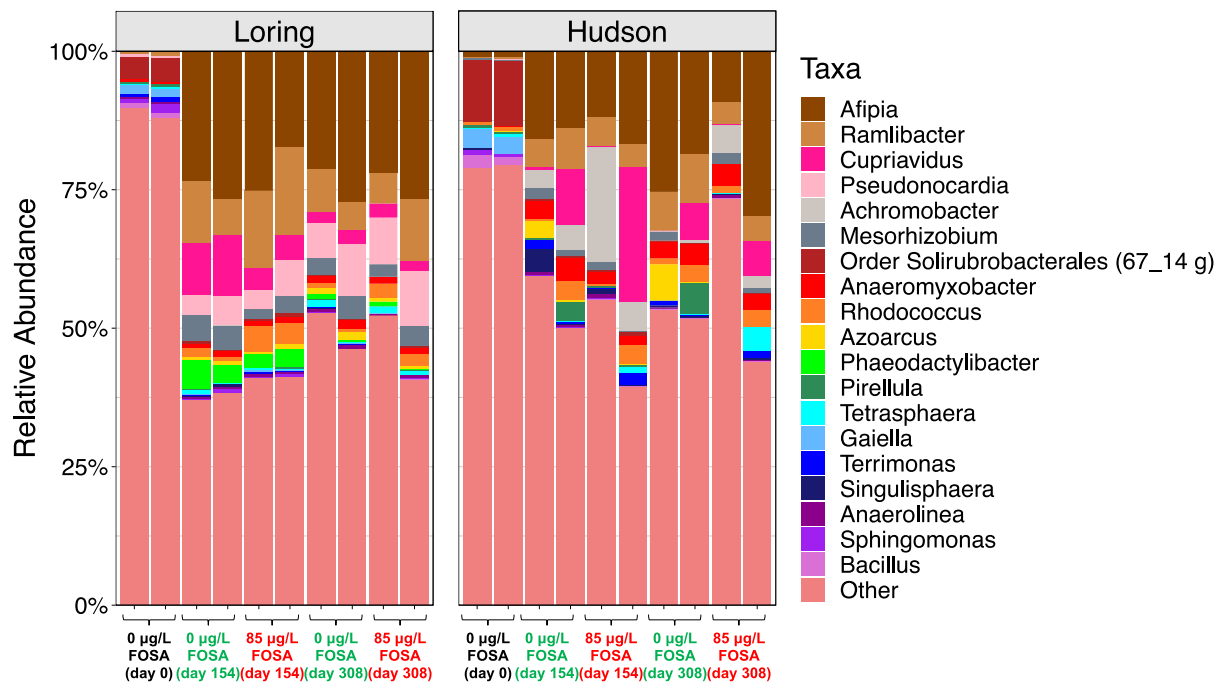


Figure B-3. The relative abundance of microbial community composition at the genus level in Loring (left) and Hudson (right) soil microcosms.

Appendix C. Supporting Information for Chapter 4: Biotransformation of 8:2 Fluorotelomer Alcohol in Soil from Aqueous Film-Forming Foams (AFFFs)-impacted Sites under Nitrate-, Sulfate-, and Iron-reducing Conditions

C-S1. Materials and Methods

Chemicals and standards

The chemical names, acronyms, molecular structures, and suppliers of target PFAS for liquid chromatography tandem mass spectrometry (LC-MS/MS) quantitative analysis are listed in Table C-2. 1H-perfluoroheptane (97%) was purchased from Synquest Laboratories (Alachua, FL). The LC-MS grade water and methanol (>99.9%) used for mobile phase was purchased from Honeywell Burdick & Jackson (Honeywell, Charlotte, NC). All other chemicals used in this study were reagent grade or higher. For all purposes, ultrapure deionized water (18.2 M Ω cm) from Evoqua water purification system (Evoqua Water Technologies) was used.

Soil collection, characterization, and Microcosm preparation

The soil used in microcosms was collected from an AFFF-contaminated location at the former Loring Air Force Base (Limestone, ME). The soil was collected at depths ranging from 0.5 to 5 ft with a hand auger and transported to the laboratory in an ice filled cooler and stored upon arrival at 4 °C. Prior to use, the soil was sieved through a 10-mesh sieve.

The soil at the closest mapped location in Aroostook County, ME, where Loring soil was collected is classified as a *fine-loamy, mixed, superactive, nonacid, frigid Aeric Endoaquepts of the Easton series*.¹⁹⁷ The moisture content of Loring soil was determined as $24.1 \pm 1.1\%$ by weight loss after placement in oven set to 105 °C for 12 hours. The organic carbon content was determined to be $3.5 \pm 0.1\%$ using a total organic carbon analyzer (TOC-L CPH and SSM-5000A, Shimadzu). The pH, CEC, and soil particle size distribution were determined at the Soil, Forage, & Water Testing Laboratory (Auburn, AL). The soil pH (1-part soil: 1-part deionized water) was 7.2 ± 0.2 , while the CEC was 18.7 ± 0.0 meq/100 grams soil. The particle size distribution of Loring soil is $53.1 \pm 3.1\%$ sand, $32.7 \pm 2.3\%$ silt, and $14.2 \pm 0.8\%$ of clay size fractions.

For microcosm preparation, to minimize the loss of volatile 8:2 FTOH and transformation products, a closed-system using Wheaton glass serum bottles, crimp-sealed with butyl rubber septa and aluminum caps was adopted for microcosms set-up. In each reactor (i.e., 60-mL serum bottle), 30 mL of 30 mM bicarbonate-buffered growth medium and 3 g (dry weight) of Loring soil were added. The medium was prepared according to the recipe reported by Löffler et al.¹³⁶ Microcosms were prepared in the anaerobic glove box (Coy Laboratory Products, Inc., Grass Lake, MI) and an oxygen-free N₂/CO₂ headspace was maintained in all microcosms throughout the experiments.

Organic and inorganic content analysis

Conversion of Fe(III) to Fe(II) was determined by the ferrozine assay in iron-reducing microcosms.¹⁹⁸ Briefly, 100 μ L of well-mixed slurry collected from the bottle was immediately mixed with 900 μ L of 0.1 M HCl in a 1.7-mL microcentrifuge tube, to extract Fe(II) from the solid phase and stabilize Fe(II) in the sample (pH < 2). After equilibrating for 1 h, the sample was centrifuged and analyzed by the ferrozine colorimetric assay using a UV-Vis spectrophotometer at 562 nm.

The collected well-mixed slurry was centrifuged at 15,000 rpm for 10 min, and the supernatant was used for other analyses. Specifically, the concentrations of lactate, propionate, and acetate in the aqueous phase were analyzed by a high-performance liquid chromatography (HPLC, Agilent Technologies 1260 Infinity series, CA), equipped with a Bio-Rad Aminex HPX-87H column (300 mm × 7.8 mm). The mobile phase was 5 mM sulfuric acid at a flow rate of 1.0 mL/min, and the column was maintained at 35 °C. The consumption of DGBE was determined by measuring the dissolved organic carbon concentration using a total organic carbon (TOC) analyzer (TOC-L CPH, Shimadzu). Ions including SO₄²⁻, NO₃⁻, and F⁻ were analyzed using a Thermo Scientific™ Dionex™ Aquion™ ion chromatography (IC) system equipped with an IonPac™ AS22 column (4 × 250 mm) and IonPac™ AG22 guard column (4 × 50 mm). The eluent was 4.5 mM sodium carbonate and 1.4 mM sodium bicarbonate at a flow rate of 1.2 mL/min.

Quantification of the fluoride ion was also attempted with samples from the microcosms for the assessment of the extent of defluorination of 8:2 FTOH under each redox condition. The estimated limit of detection (LOD) and limit of quantitation (LOQ) of the analytical method for fluoride were 0.013 mg/L and 0.044 mg/L, respectively.¹⁹⁹ However, the high amounts of chloride (>1000 mg/L) present in the sample matrix (due to the mineral salt medium¹³⁶) required the dilutions for analysis, increasing the LOD and LOQ of the method by at least 5-fold. As the concentration of 8:2 FTOH spiked initially into the microcosms was ~170 µg/L (i.e., ~0.37 µM), it would have produced ~13.9 µg/L of fluoride if two fluoride ions were released from each 8:2 FTOH molecule (e.g., 7:2 sFTOH or PFOA as transformation product). Even if 8:2 FTOH underwent complete defluorination, the resulting fluoride concentration would have been ~111.4 µg/L. Therefore, the fluoride released by the biotransformation of 8:2 FTOH under nitrate-, sulfate-, or iron-reducing conditions, if any, would be lower or near the LOD and LOQ of the method. No distinguishable increase of fluoride was observed in any sample collected from ED or NA treatment, compared to that from abiotic and positive controls.

Non-targeted LC-HRMS Analysis

Pooled samples were injected in triplicate with a 10 µL injection volume on a Thermo QExactive HF-X Orbitrap MS equipped with a Vanquish ultra-high-performance liquid chromatograph (UHPLC-Orbitrap). Sample components were separated on a Thermo Hypersil Gold Vanquish C18 column (50 mm X 2.1 mm x 1.9 µm) at a constant temperature of 60 °C with a solvent gradient consisting of two mobile phases, A and B. PFAS were eluted from the column at a constant flow rate of 0.4 mL/min using a mobile phase gradient as follows: equilibration with 10% B for 1 minute, followed by a gradient ramp from 10% B to 100% B over 4 minutes and held for 2 minutes, and back to 10 % B over 1 minute and held for 2 minutes (total run time 11 minutes, data collected from 0.6 to 9 minutes). The MS was operated in full scan dd-MS² mode (stepped 15 and 55 NCE) with an inclusion list for 21 PFAS. Ionization was performed in negative mode with an ionization window of 1.0 *m/z*, sheath gas flow rate of 40, auxiliary gas flow rate of 10, sweep gas flow rate of 2, spray voltage of 2.7 kV, 310 °C capillary temperature, funnel RF level of 35, and 320 °C auxiliary gas heater temperature. For the full-scan, the Orbitrap was operated with a resolution of 120,000, automatic gain control (AGC) of 3x10⁶, and maximum dwell time of 100ms. For dd-MS², the Orbitrap was operated with a resolution of 15,000, AGC of 2x10⁵, and maximum dwell time of 400ms. MS² fragmentation was performed in the HCD collision cell filled with N₂ (produced by a Peak Scientific Nitrogen Generator, Genius NM32LA). The data files were saved in the .RAW file format and analyzed in Thermo Compound Discoverer (CD) 3.2 software. The data processing workflow used in CD 3.2 is displayed in Figure C-17. Spectral libraries and mass

lists were used to identify 8:2 FTOH transformation byproducts. The libraries included Thermo mzCloud, ChemSpider, and an in-house MS² mass spectral library containing 40 PFAS compounds. The mass lists included 74 hypothesized potential 8:2 FTOH transformation products and 8,142 fluorinated compounds from the EPA's ToxCast/CompTox database.²⁰⁰ A final list containing a total of about 14,000 features was exported to Microsoft Excel after processing the raw data. We developed a R script to facilitate the selection of features of interest based on the peak intensity comparison between samples from an individual treatment over time, and between samples from the live-spiked treatments and abiotic/positive controls at each sampling point.

Confidence scores of the features detected were assigned based on the Schymanski Scale to evaluate the certainty of the structure identification.²⁰¹ Briefly, the highest confidence level 1 (confirmed structure) represents the proposed structure was confirmed via the comparison of the appropriate measurement of a reference standard. Level 2 (probable structure) was achieved when the MS² spectrum and fragmentation have been reported previously for a compound of interest and the spectrum-structure match is unambiguous, or when the structure of the compound could be determined unambiguously by MS² fragmentation analysis. Level 3 (tentative candidate) was assigned when the MS² spectrum and fragmentation were informative for possible structures, but the information was insufficient for one exact structure only. When the MS² fragmentation data was not available while a molecular formula can be assigned unambiguously based on the spectral information, level 4 (unequivocal molecular formula) was assigned.

Targeted GC-HRMS Analysis

The headspace samples (i.e., C₁₈ cartridge eluent), aqueous samples, and soil methanol extracts from nitrate-reducing microcosms were analyzed for 1H-perfluoroheptane using a high-resolution Thermo Q Exactive Orbitrap MS equipped with a Thermo Trace 1300 GC and a TriPlus RSH Autosampler. Helium (99.9999% purity) and nitrogen (99.999% purity) were used as the carrier and c-trap gases, respectively. Sample extracts (3.5 µL) were injected into a 100°C split/splitless inlet operated in split-less mode. Analytes were separated on a Restek Rxi-200 column (105 m x 250 µm inner diameter x 0.25 µm film thickness) column with a 1 mL/min carrier gas flow rate. The transfer line was maintained at 200°C while the oven temperature ramp began at 30°C for 25 min and increased 30°C/min to 220°C, which was held for 1 min, with a 32 min total run time. The source temperature was 150°C and the MS scan range was 50 to 400 m/z. 1H-Perfluoroheptane eluted at 18.10 min. The instrument was operated in electron ionization (EI) mode (70 eV). Data were collected with 60,000 resolution and 1 × 10⁶ automatic gain control. The extracted ion chromatogram (XIC) was used for quantification using the most abundant peak in the mass spectrum (m/z 68.9947). Analyte identity was confirmed using the two confirming ions ratios and retention time (m/z 130.9915, 118.9915). The detection limit was 1,954 ng L⁻¹.

C-S2. Establishment of nitrate-, sulfate-, and iron-reducing microcosms

Throughout the experiments, anaerobic conditions were strictly maintained in all microcosms, as demonstrated by the colorless appearance of the resazurin indicator. In the microcosms under each redox condition, carbon sources and electron donors (i.e., lactate and/or DGBE), and electron acceptors (i.e., NO_3^- , SO_4^{2-} , or Fe(III)/Fe(II)) were monitored to confirm the corresponding microbial activity during incubation period (Figures C1, C-2, and C-3). At certain time points, the amendment of nitrate, sulfate, lactate, or DGBE was made to appropriate microcosms to ensure the presence of sufficient electron acceptor, electron donor, or carbon source (Figures C1, C-2, and C-3).

The establishment of nitrate-, sulfate-, or iron(III)-reducing conditions in the corresponding biologically-active microcosms (i.e., all treatments except abiotic control) were confirmed by the following observations: (1) the decrease in NO_3^- or SO_4^{2-} in nitrate- or sulfate-reducing microcosms; (2) the increase in Fe(II) in iron-reducing microcosms; (3) the conversion of lactate to acetate and propionate, followed by the consumption of latter byproducts in ED treatments and positive controls; (4) the consumption of DGBE, as indicated by decrease in TOC in NA treatments. None of the observations (1) to (4) was found in the abiotic controls, indicating the abiotic conditions were maintained throughout the incubation period in each batch of experiment (Figures C1, C-2, and C-3). Greater extents of carbon source, electron donor and acceptor consumption were measured in ED treatment and positive control under nitrate-reducing conditions than that in all other biologically-active microcosms (i.e., NA treatment under nitrate-reducing, and sulfate-, iron-reducing microcosms). A total of 11 amendments of 40 mM nitrate and 8 amendments of 20 mM lactate were made to ED treatment or positive control under nitrate-reducing conditions, whereas no more than 2 amendments of electron donor or acceptor were made to others (Figures C1, C-2, and C-3). These indicated that the amendment of lactate, additional electron donor and carbon source greatly increased the growth rate of nitrate-reducing microorganisms, however, only slight or no enhancement of the growth was observed in sulfate-, and iron-reducing microorganisms. Although the continuously steady increase in Fe(II) was not observed in biologically-active microcosms, compared to abiotic controls, the formation of Fe(II) from Fe(III) reduction was apparent, and the consumption of lactate and/or DGBE in the situation of sufficient supply of electron acceptor (i.e., 100 mM goethite) was observed (Figure C-3). The active iron-reducing activities were thus confirmed. Fe(II) did not continuously increase, likely due to the pH of the aqueous phase in the microcosms (>7.5 during the most of incubation period, Figure C-3), and the precipitation of ferrous hydroxide (solubility product $K_{sp} = 8.0\text{E-}16$, ferrous hydroxide started to precipitate at $\text{pH} = 7.5$ in 10 mM Fe(II) solution) occurred.²⁰² The well-mixed slurry sample was used in the present study to extract Fe(II) from the solid phase, however, the ferrous hydroxide precipitates might not be evenly and/or efficiently extracted.

C-S3. Background levels of legacy PFAS in Loring AFB soil

Table C-8 shows the background levels of legacy PFAS in Loring soils according to the measurements of day 0 samples from all microcosms (8:2 FTOH background levels only from positive control microcosms). None of 8:2 FTOH, 8:2 FTUA, 8:2 FTCA, 7:2 sFTOH was detected in day 0 samples, indicating that AFFF-contaminated Loring AFB soil did not contain a detectable concentration of these polyfluorinated compounds. However, 7:3 acid was detected in the Loring AFB soil (0.034 ± 0.011 nmole/g dw, Table C-8). Since 7:3 acid is not known to be manufactured but is almost exclusively formed by the biotransformation of fluorotelomer compounds (e.g., 8:2 FTOH etc.),⁵¹ its presence in day 0 samples indicated the *in-situ* biotransformation of AFFF-based fluorotelomer precursors likely occurred in the Loring AFB soil before the soil was collected and transported to the lab. PFOS was present at higher concentration in Loring AFB soil than any other PFAAs targeted in this study, with around 3.4 nmole/g dw. PFHxS was also detected with a concentration of 0.018 ± 0.002 nmole/g dw while the other PFSAAs were below the detection limits (Table C-8). The contamination of PFOS and PFHxS is consistent with the historical applications of 3M AFFF formulation at the Loring AFB.¹³ Among PFCAs, short-chain congeners (i.e., PFBA, PFPeA, PFHxA) were detected with higher concentrations than longer-chain congeners including PFOA (Table C-8), a preponderance of which was found in previous soil surveys.^{92,203} The plausible explanation is that certain amounts of fluorotelomer-based AFFFs (e.g., Ansul and National Foam AFFF) were also used in the Loring AFB.¹⁴ It was further supported by the detection of one fluorotelomer precursor, 6:2 fluorotelomer sulfonate in Loring AFB soil (unpublished work). The higher abundance of short-chain PFCAs likely resulted from the transformation of those fluorotelomer-based precursors.^{14,31}

Table C-1. Experimental set-up of 8:2 FTOH biotransformation microcosms under nitrate-, sulfate-, and iron-reducing conditions

Treatment	Components			
	Spiked 8:2 FTOH ^a	Carbon source & electron donor ^b	Electron acceptor ^c	Other ^d
ED treatment ^e	Yes	Lactate + DGBE	NO ₃ ⁻ /SO ₄ ²⁻ / Fe ³⁺	/
NA treatment ^f	Yes	DGBE	NO ₃ ⁻ /SO ₄ ²⁻ / Fe ³⁺	/
Abiotic control	Yes	Lactate + DGBE	NO ₃ ⁻ /SO ₄ ²⁻ / Fe ³⁺	NaN ₃
Positive control	No	Lactate + DGBE	NO ₃ ⁻ /SO ₄ ²⁻ / Fe ³⁺	/

^a The initial concentration of 8:2 FTOH spiked into the microcosms was ~ 170 µg/L.

^b The carbon source & electron donor(s) were added into the microcosms with initial concentrations of 20 mM lactate and/or 5 mM DGBE.

^c Goethite (100mM, mineral of iron (III) oxide-hydroxide), 20 mM of sodium sulfate or 20 mM of sodium nitrate was added as the electron acceptor in iron-reducing, sulfate-reducing, and nitrate-reducing microcosms, respectively.

^d One gram per liter sodium azide was added to inhibit the microbial activity.

^e ED represents electron donor.

^f NA represents natural attenuation.

Table C-2. Chemical names, acronyms, molecular structures, and suppliers of target poly- and perfluoroalkyl substances (PFAS) for LC-MS/MS quantitative analysis.

Chemical name	Acronym	Molecular structure	Supplier
8:2 fluorotelomer alcohol	8:2 FTOH	$F(CF_2)_8CH_2CH_2OH$	Sigma-Aldrich (St. Louis, USA); Wellington Laboratories (Ontario, Canada)
8:2 fluorotelomer saturated carboxylic acid	8:2 FTCA	$F(CF_2)_8CH_2COOH$	Wellington Laboratories
8:2 fluorotelomer unsaturated carboxylic acid	8:2 FTUA	$F(CF_2)_7CF=CHCOOH$	Wellington Laboratories
7:2 secondary fluorotelomer alcohol	7:2 sFTOH	$F(CF_2)_7CH(OH)CH_3$	Wellington Laboratories
7:3 fluorotelomer carboxylic acid	7:3 acid	$F(CF_2)_7CH_2CH_2COOH$	Wellington Laboratories
Perfluorobutanoic acid	PFBA	$F(CF_2)_3COOH$	
Perfluoropentanoic acid	PFPeA	$F(CF_2)_4COOH$	
Perfluorohexanoic acid	PFHxA	$F(CF_2)_5COOH$	
Perfluoroheptanoic acid	PFHpA	$F(CF_2)_6COOH$	
Perfluorooctanoic acid	PFOA	$F(CF_2)_7COOH$	
Perfluorononanoic acid	PFNA	$F(CF_2)_8COOH$	
Perfluorodecanoic acid	PFDA	$F(CF_2)_9COOH$	PFAC-MXC stock, Wellington Laboratories
Perfluoroundecanoic acid	PFUnA	$F(CF_2)_{10}COOH$	
Perfluorododecanoic acid	PFDoA	$F(CF_2)_{11}COOH$	
Perfluorobutanesulfonic acid	PFBS	$F(CF_2)_4SO_3H$	
Perfluoropentanesulfonic acid	PFPeS	$F(CF_2)_5SO_3H$	
Perfluorohexanesulfonic acid	PFHxS	$F(CF_2)_6SO_3H$	
Perfluoroheptanesulfonic acid	PFHpS	$F(CF_2)_7SO_3H$	
Perfluorooctanesulfonic acid	PFOS	$F(CF_2)_8SO_3H$	

Table C-3. Instrument conditions and LC gradient used for the detection and quantification of 8:2 FTOH and its polyfluorinated transformation products by UPLC-MS/MS.

LC conditions			
LC system:	Waters ACQUITY UPLC I-Class fitted with PFC kit		
Column:	Waters BEH C-18 column (1.7 μ m dia., 2.1 \times 50 mm)		
Column temp:	30 $^{\circ}$ C		
Sample temp:	10 $^{\circ}$ C		
Injection volume:	50 μ L		
Mobile phase A:	Water		
Mobile phase B:	Methanol		
LC gradient			
Time (min)	Flow rate (mL/min)	% A	% B
0	0.25	50	50
2	0.25	10	90
4	0.25	0	100
6	0.25	0	100
7	0.25	50	50
10	0.25	50	50
MS conditions			
MS system:	Waters Xevo TQ-S		
Ionization mode:	ESI-		
Capillary voltage:	1.50 kV		
Desolvation temp:	350 $^{\circ}$ C		
Desolvation gas flow:	750 L/hr		
Source temp:	120 $^{\circ}$ C		
Cone gas flow:	50 L/hr		

Table C-4. Multiple reaction monitoring (MRM) parameters used for the detection and quantification of 8:2 FTOH and its polyfluorinated transformation products by UPLC-MS/MS.

Compound	Molecular Ion (m/z)	Cone Voltage (V)	Collision Energy (V)	Quant. Ion (m/z)	Cone Voltage (V)	Collision Energy (V)	Confirmation Ion (m/z)
8:2 FTOH	462.97	14	12	402.99	18	18	354.97
8:2 FTUA	456.97	30	8	393.08	30	44	119.04
8:2 FTCA	476.90	36	6	413.50	26	14	393.18
7:2 sFTOH	393.03	40	14	219.07			
7:3 Acid	440.97	44	12	337.13	44	20	317.09

Table C-5. Instrument conditions and LC gradient used for the detection and quantification of PFAAs by UPLC-MS/MS.

LC conditions			
LC system:	Waters ACQUITY UPLC I-Class fitted with PFC kit		
Column:	Waters BEH C-18 column (1.7 μ m dia., 2.1 \times 50 mm)		
Column temp:	50 $^{\circ}$ C		
Sample temp:	10 $^{\circ}$ C		
Injection volume:	10 μ L		
Mobile phase A:	95:5 Water:methanol + 2 mM ammonium acetate		
Mobile phase B:	Methanol + 2 mM ammonium acetate		
LC gradient			
Time (min)	Flow rate (mL/min)	% A	% B
0	0.4	90	10
1	0.4	90	10
5	0.4	15	85
5.1	0.4	0	100
7	0.4	0	100
7.5	0.4	90	10
10	0.4	90	10
MS conditions			
MS system:	Waters Xevo TQ-S		
Ionization mode:	ESI-		
Capillary voltage:	1.50 kV		
Desolvation temp:	350 $^{\circ}$ C		
Desolvation gas flow:	650 L/hr		
Source temp:	150 $^{\circ}$ C		
Cone gas flow:	50 L/hr		

Table C-6. Multiple reaction monitoring (MRM) parameters used for the detection and quantification of PFAAs by UPLC-MS/MS.

Compound	Molecular Ion (m/z)	Cone Voltage (V)	Collision Energy (V)	Quant. Ion (m/z)	Cone Voltage (V)	Collision Energy (V)	Confirmation Ion (m/z)
PFBA	212.93	12	5	169.09			
PFPeA	262.95	4	4	219.09			
PFBS	298.95	6	28	98.99	6	32	79.99
PFHxA	312.94	4	4	269.12	4	20	119.02
PFPeS	349.00	15	32	99.00	15	32	80
PFHpA	362.90	12	8	319.14	12	16	169.08
PFHxS	398.90	68	32	98.99	68	36	79.98
PFOA	412.93	2	8	369.12	2	16	169.03
PFNA	462.89	6	9	419.16	6	15	219.1
PFOS	498.83	30	40	99.01	30	44	80
PFDA	512.85	6	10	469.00	6	16	219
PFNS	549.00	10	43	99.00	10	43	80
PFUnA	563.03	8	8	519.08	8	14	269
PFDS	599.03	2	48	99.02	2	55	79.97

Table C-7. Limits of detection (LODs) and limits of quantification (LOQs) of target PFAS.

Analytes	LOD ^a (ng/mL)	LOQ ^b (ng/mL)
8:2 FTOH ^c	0.56	6.10
8:2 FTCA	0.02	0.09
8:2 FTUA	0.02	0.03
7:2 sFTOH ^c	0.17	1.20
7:3 acid	0.02	0.03
PFBA	0.01	0.05
PFPeA	0.01	0.05
PFHxA	0.01	0.05
PFHpA	0.01	0.05
PFOA	0.01	0.05
PFNA	0.01	0.05
PFDA	0.01	0.05
PFUnA	0.01	0.05
PFDoA	0.01	0.05
PFBS	0.01	0.05
PFPeS	0.01	0.05
PFHxS	0.01	0.05
PFHpS	0.01	0.05
PFOS	0.01	0.05

^aLODs are determined based on EPA Method 537.1

^bLOQs are determined with the Lowest Concentration Minimum Reporting Level (LCMRL) Calculator distributed by EPA.

^cThe LODs and LOQs for 8:2 FTOH and 7:2 sFTOH were run-dependent, and the values reported here were the highest levels during the analysis of all microcosm samples.

Table C-8. Concentrations (nanomole per gram soil/dry weight) of individual PFAS in Loring AFB soil.

Category	PFAS	Loring AFB soil
Polyfluorinated compounds	8:2 FTOH	N.D.
	8:2 FTCA	N.D.
	8:2 FTUA	N.D.
	7:2 sFTOH	N.D.
	7:3 acid	0.034 ± 0.011
PFCAs	PFBA	0.031 ± 0.005
	PFPeA	0.048 ± 0.009
	PFHxA	0.032 ± 0.005
	PFHpA	0.011 ± 0.003
	PFOA	0.026 ± 0.005
	PFNA	0.012 ± 0.003
	PFDA	0.007 ± 0.002
	PFUnA	0.012 ± 0.004
	PFDoA	N.D.
PFSAs	PFBS	N.D.
	PFPeS	N.D.
	PFHxS	0.018 ± 0.002
	PFHpS	N.D.
	PFOS	3.412 ± 0.348

N.D.: analyte not detected in the sample.

Table C-9. Potential biotransformation products of 8:2 FTOH identified by LC-HRMS analysis

Abbreviated name	Formula	Mass (<i>m/z</i>)	Mass error [ppm]	Level of confidence ^a	Identified in microcosms
1H-perfluoroheptane	C ₇ HF ₁₅	368.9764	0.14	1	
3-OH-7:3 acid	C ₁₀ H ₅ F ₁₅ O ₃	456.9930	0.36	2	Nitrate-reducing (ED & NA)
7:3 U acid	C ₁₀ H ₃ F ₁₅ O ₂	438.9822	0.24	3	
7:3 U amide	C ₁₀ H ₄ F ₁₅ NO	437.9975	-0.05	4	
3-F-7:3 acid	C ₁₀ H ₄ F ₁₆ O ₂	458.9885	0.67	3	Sulfate-reducing (ED & NA), iron-reducing (ED)

^aThe level of confidence of each identified biotransformation product was assigned using a scheme reported by Schymanski et al.²⁰¹

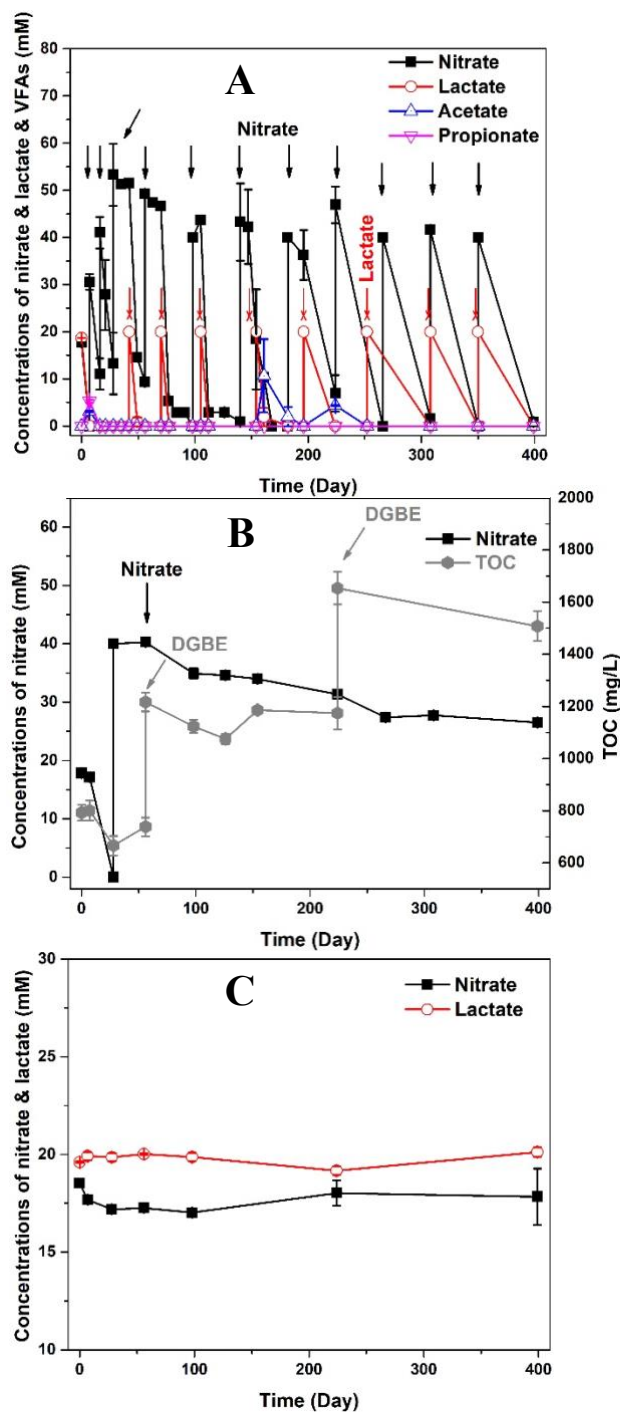


Figure C-1. Concentrations of nitrate and organic acids in ED treatment/positive control (Panel A); concentrations of nitrate and total organic carbon (TOC) in NA treatment (Panel B); concentrations of nitrate and lactate in abiotic control (Panel C). The black, red, and gray arrows represent the individual amendments of 40 mM nitrate, 20 mM lactate, and 5 mM DGBE to the microcosms, respectively. Note that a total of 11 nitrate and 8 lactate amendments were made to ED treatment/positive control due to the rapid depletion of both electron donor and acceptor. Error bars represent the standard deviation of triplicate ED/NA microcosms, and of duplicate control microcosms.

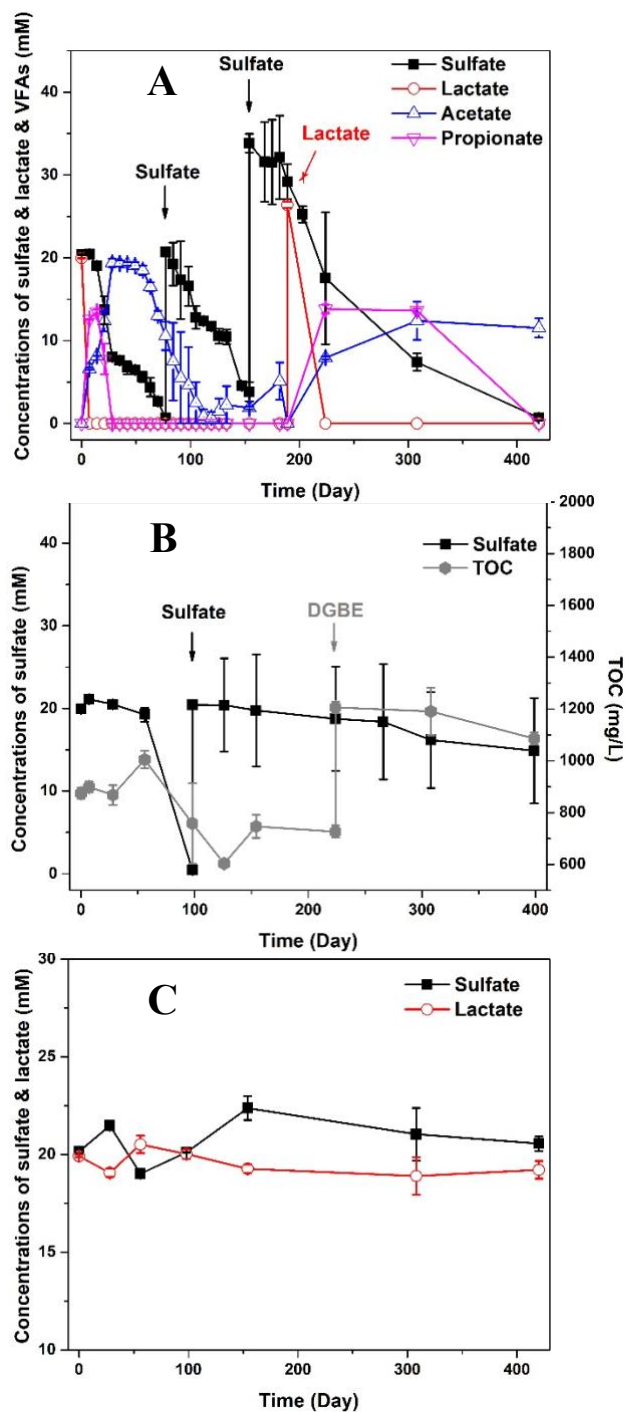


Figure C-2. Concentrations of sulfate and organic acids in ED treatment/positive control (Panel A); concentrations of sulfate and total organic carbon (TOC) in NA treatment (Panel B); concentrations of sulfate and lactate in abiotic control (Panel C). The black, red, and gray arrows represent the individual amendments of 20 mM sulfate, 20 mM lactate, and 5 mM DGBE to the microcosms, respectively. Error bars represent the standard deviation of triplicate ED/NA microcosms, and of duplicate control microcosms.

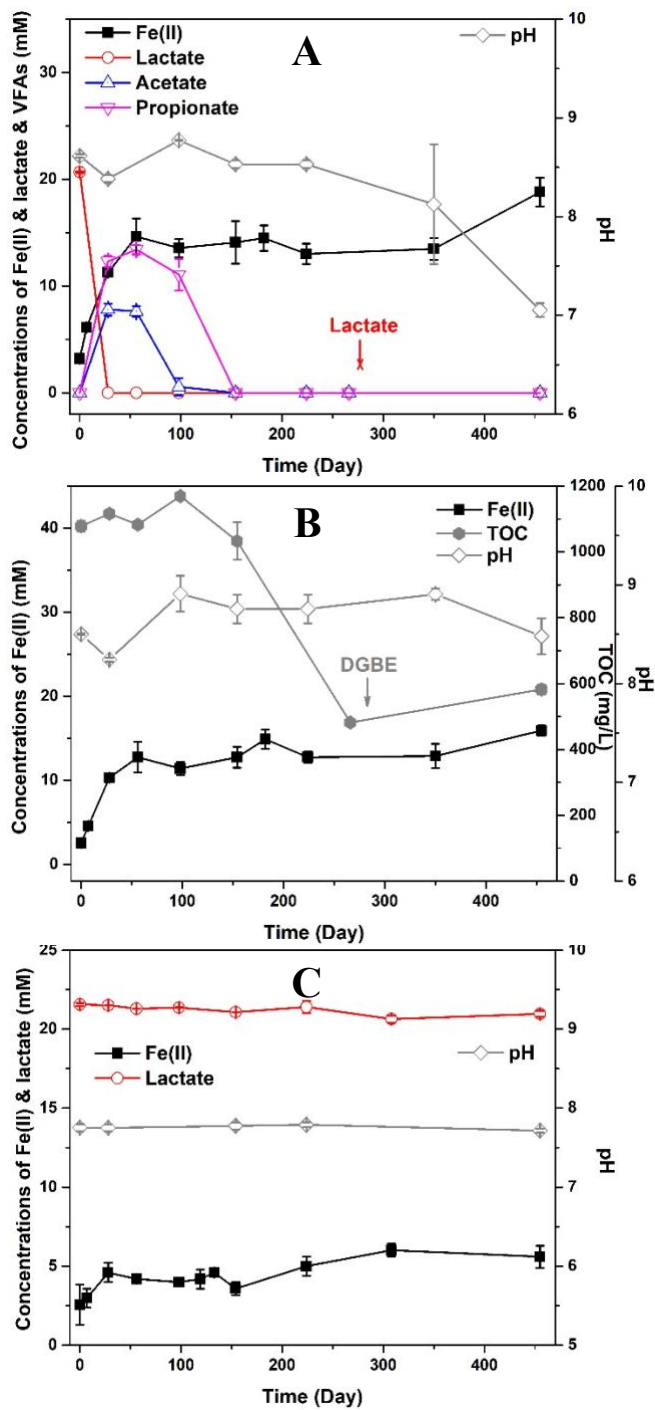


Figure C-3. Concentrations of Fe(II) and organic acids in ED treatment/positive control (Panel A); concentrations of Fe(II) and total organic carbon (TOC) in NA treatment (Panel B); concentrations of Fe(II) and lactate in abiotic control (Panel C). The red, and gray arrows represent the individual amendments of 20 mM lactate, and 5 mM DGBE to the microcosms, respectively. Note that the time variation of pH in each treatment was also plotted in respective Panel. Error bars represent the standard deviation of triplicate ED/NA microcosms, and of duplicate control microcosms.

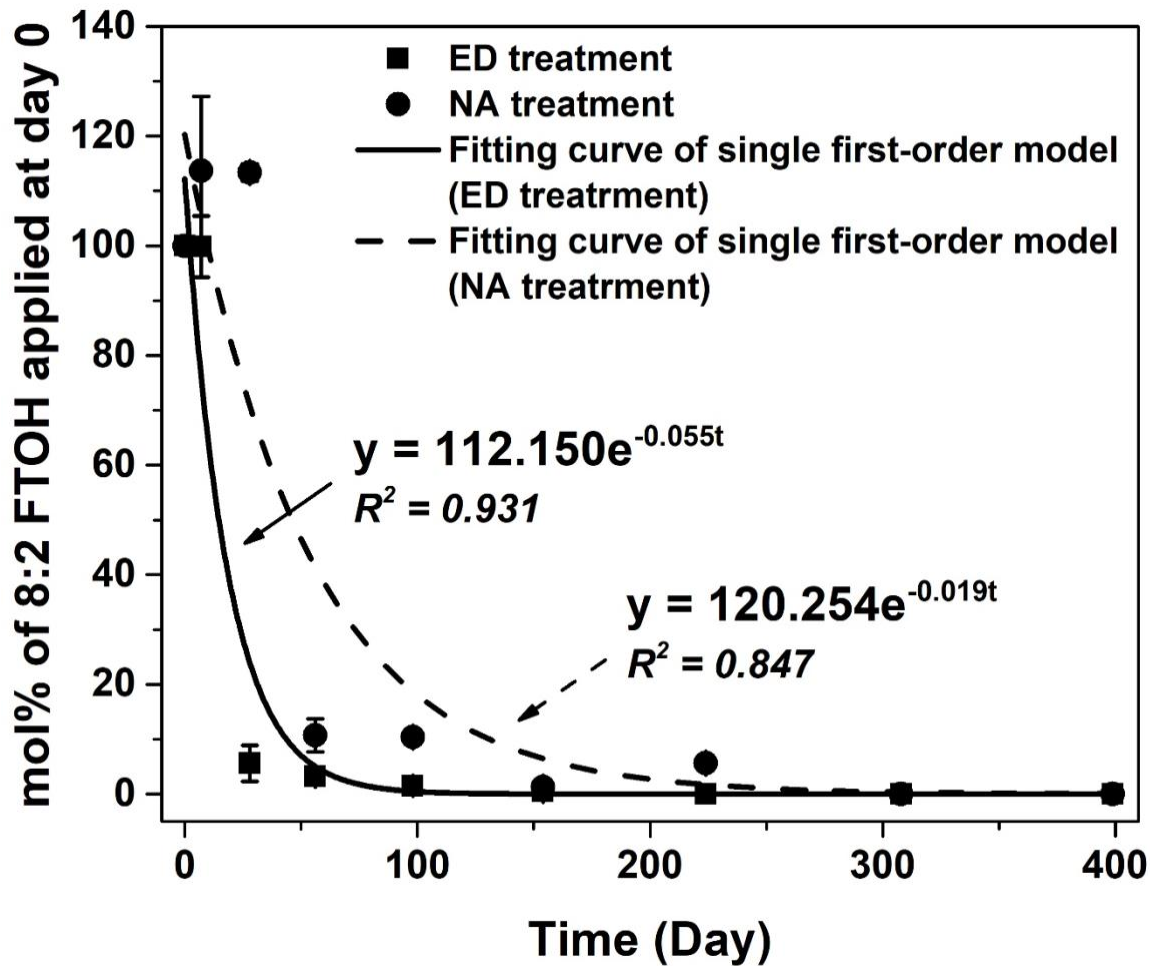


Figure C-4. Changes in molar ratio of residual 8:2 FTOH, and the fitting curves of single first-order kinetic models in ED and NA treatment under nitrate-reducing condition.

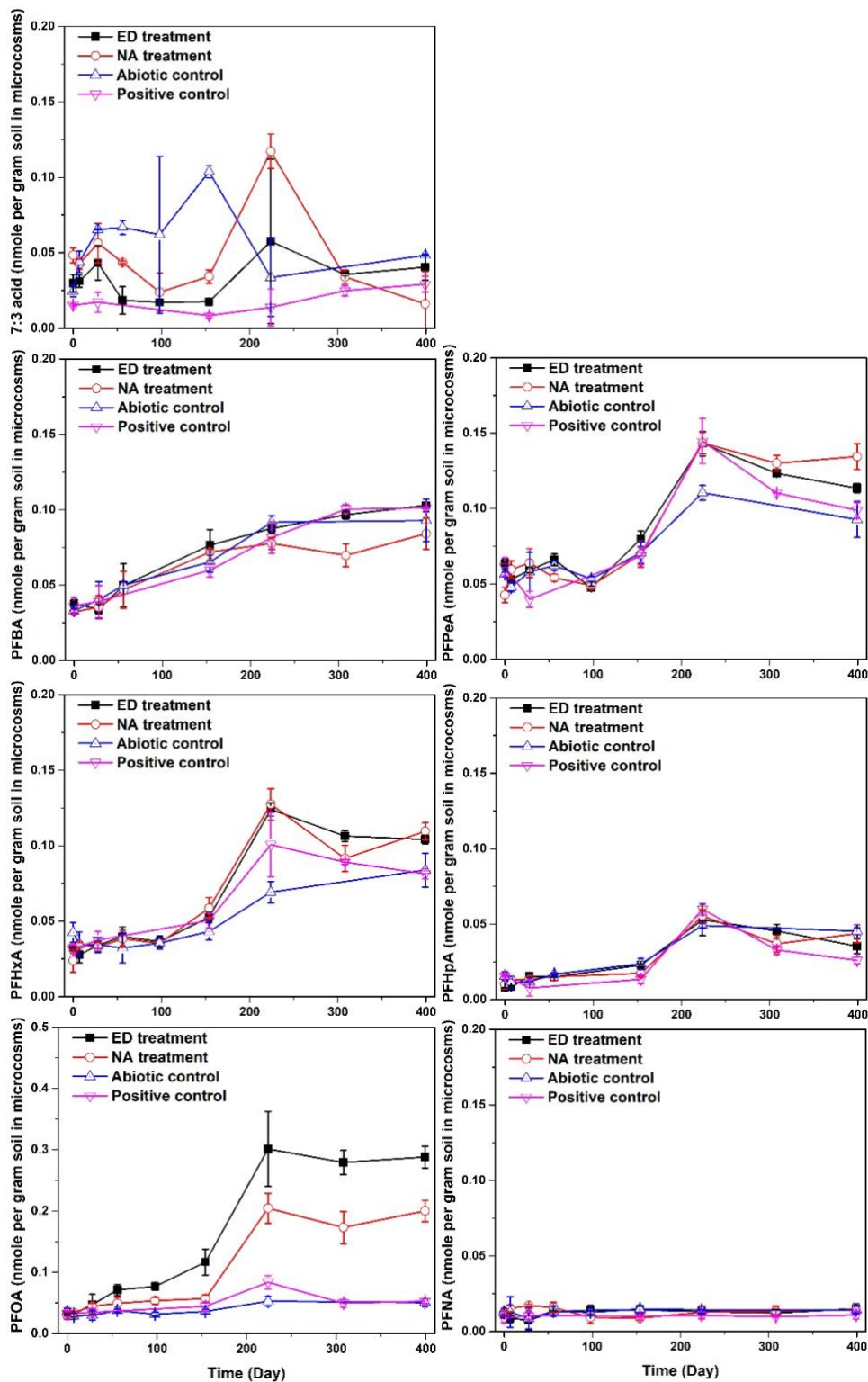


Figure C-5. Changes in the concentrations (nanomole per gram soil/dry weight) of 7:3 acid, and C4-C9 PFCAs in ED, NA treatment, abiotic controls, and positive controls under nitrate-reducing condition throughout the experiments. Note that the y-axis scales in PFOA plot is larger than the scales in other plots.

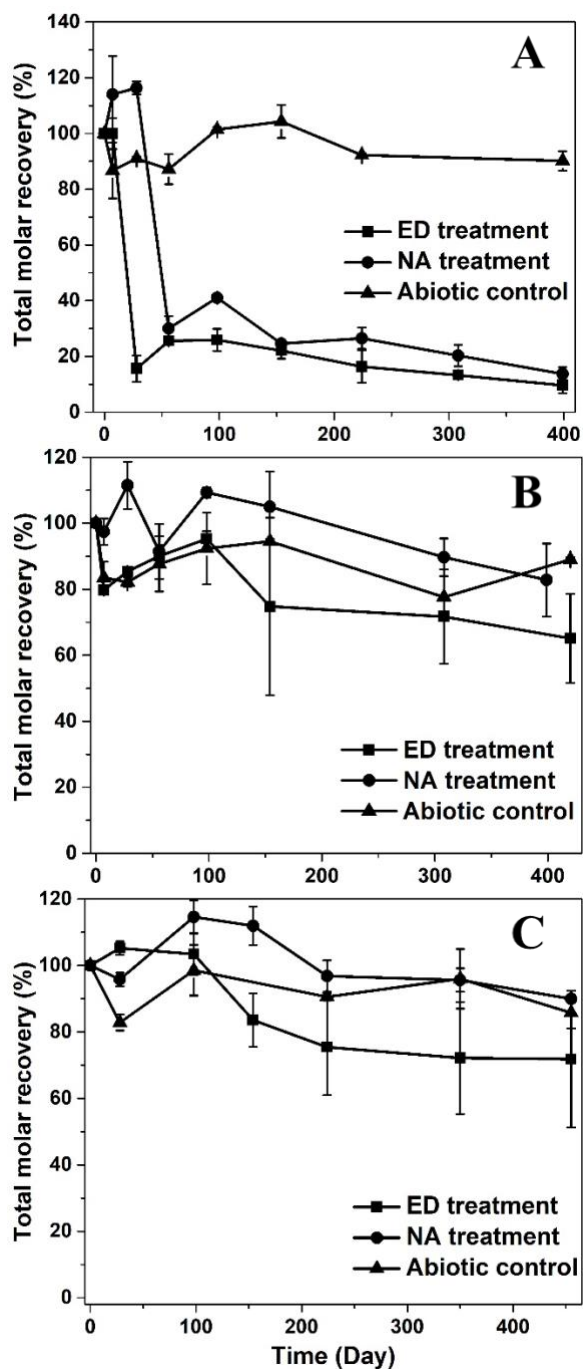


Figure C-6. The total molar recoveries (8:2 FTOH and quantifiable biotransformation products) during 8:2 FTOH biotransformation in ED, NA treatment, and abiotic controls under nitrate-reducing conditions (Panel A), sulfate-reducing conditions (Panel B), iron-reducing conditions (Panel C).

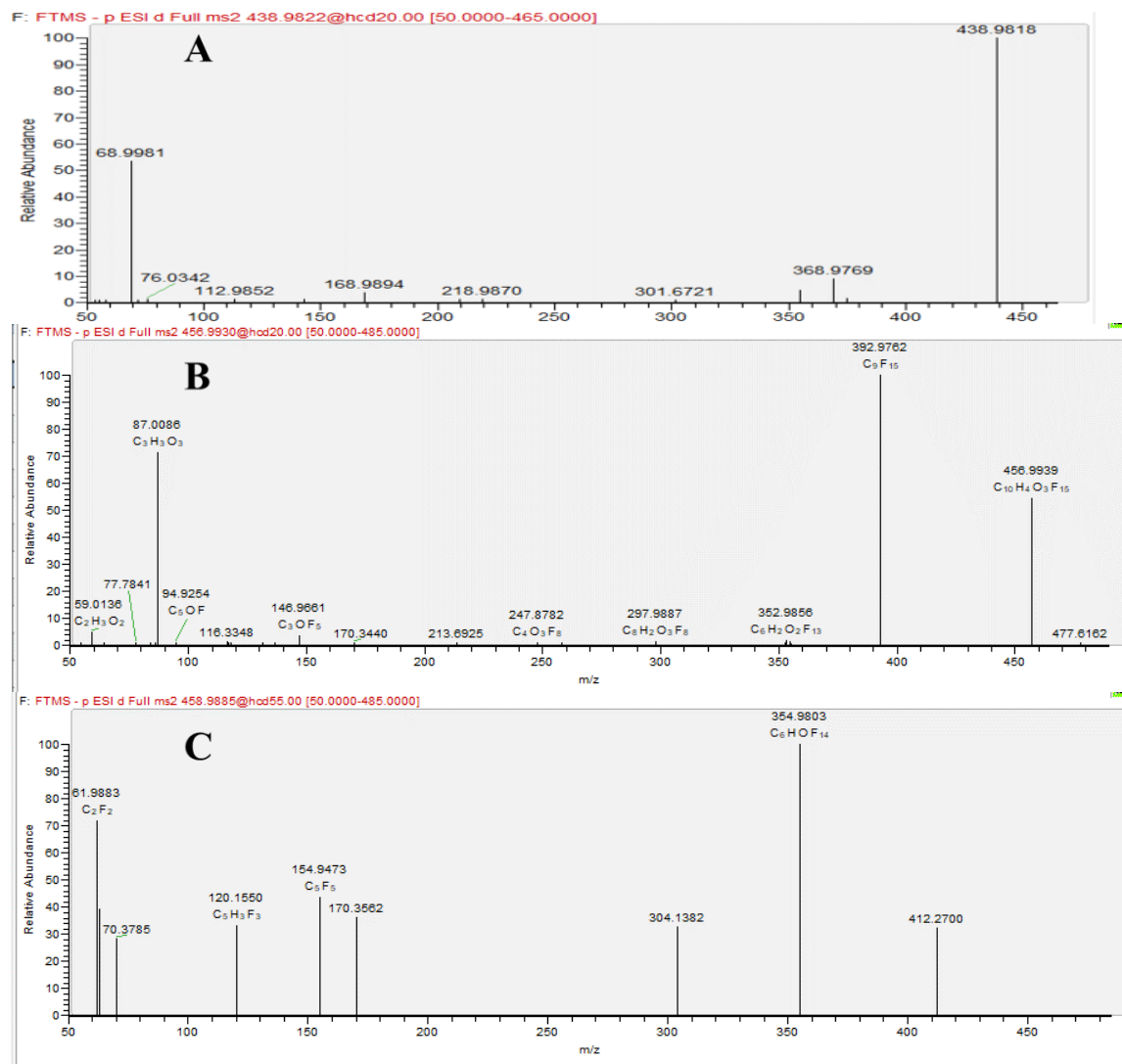


Figure C-7. The MS2 spectra of potential biotransformation products identified in the ED and/or NA treatments under nitrate, sulfate-, or iron-reducing conditions. Panel A, 7:3 U acid (F(CF₂)₇CH=CHCOOH, *m/z* 438.9822); Panel B, 3-OH-7:3 acid (F(CF₂)₇CHOHCH₂COOH, *m/z* 456.9930); Panel C, 3-F-7:3 acid (F(CF₂)₇CFHCH₂COOH, *m/z* 458.9885).

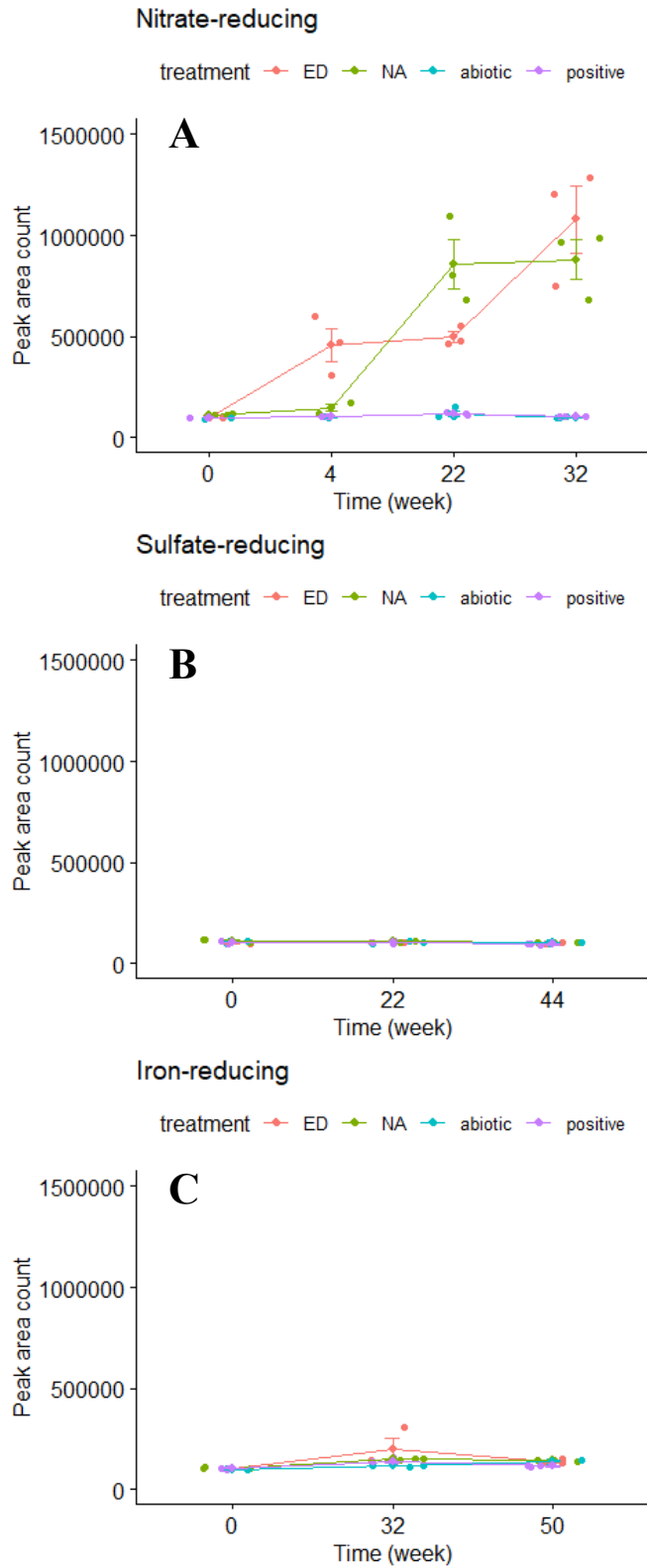


Figure C-8. The time trend of 7:3 U acid during 8:2 FTOH biotransformation in each treatment under (A) nitrate-reducing; (B) sulfate-reducing; and (C) iron-reducing conditions based on peak areas of extracted ion chromatograms.

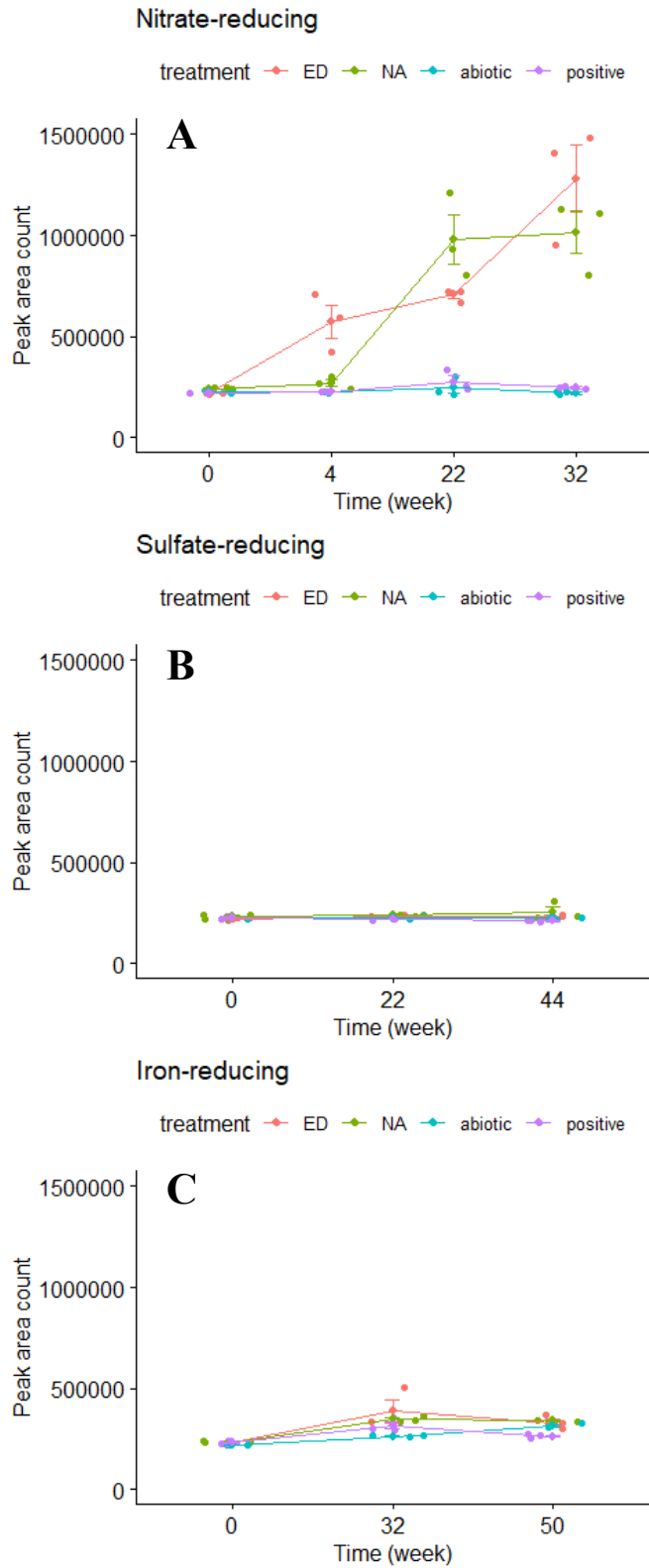


Figure C-9. The time trend of 3-OH-7:3 acid during 8:2 FTOH biotransformation in each treatment under (A) nitrate-reducing; (B) sulfate-reducing; and (C) iron-reducing conditions based on peak areas of extracted ion chromatograms.

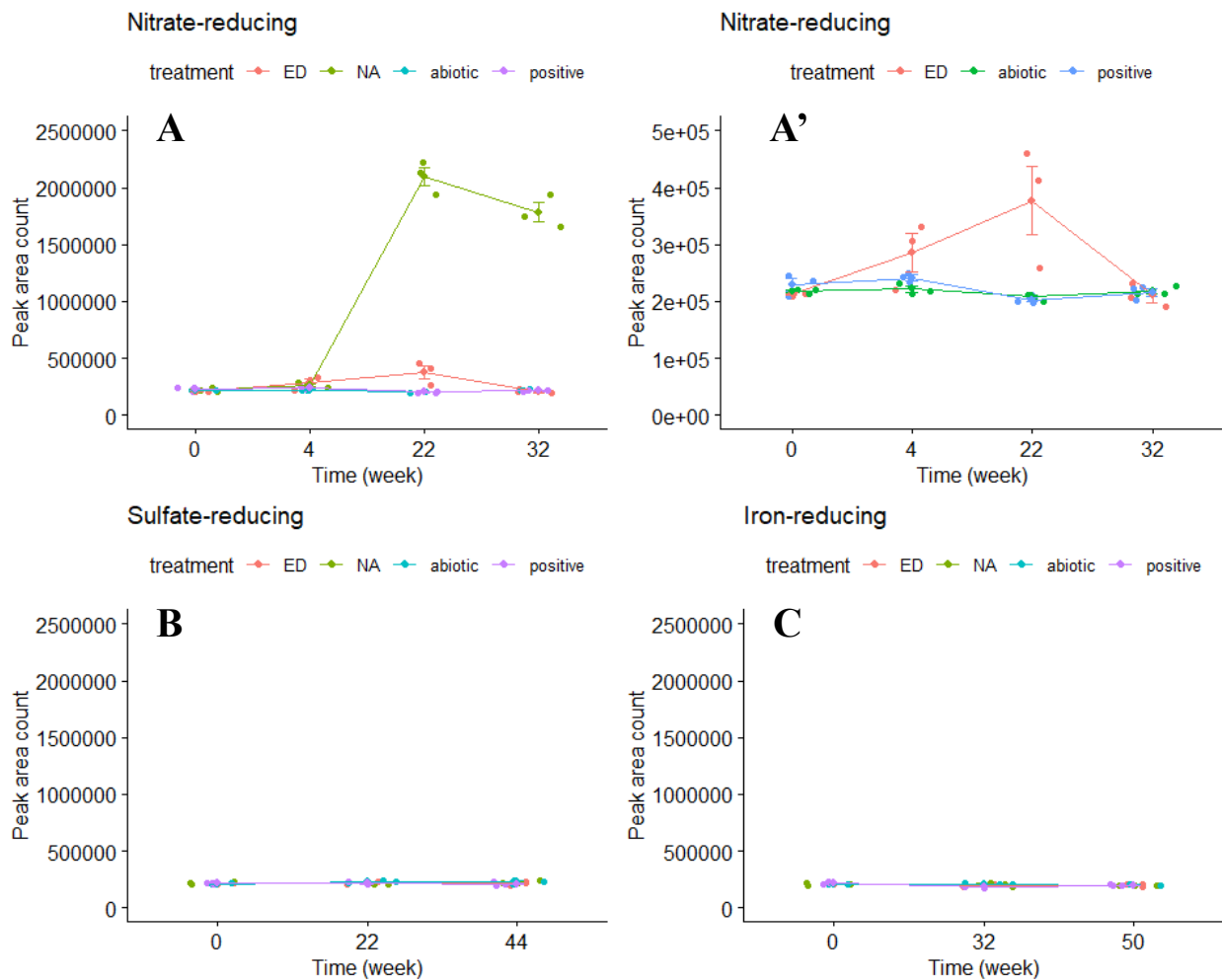


Figure C-10. The time trend of 7:3 U amide during 8:2 FTOH biotransformation in each treatment under (A) nitrate-reducing; (B) sulfate-reducing; and (C) iron-reducing conditions based on peak areas of extracted ion chromatograms. Note Panel A' is the zoom view of Panel A, excluding the NA treatment with a smaller y-axis scale, to illustrate the different time trends between the ED treatment and two controls.

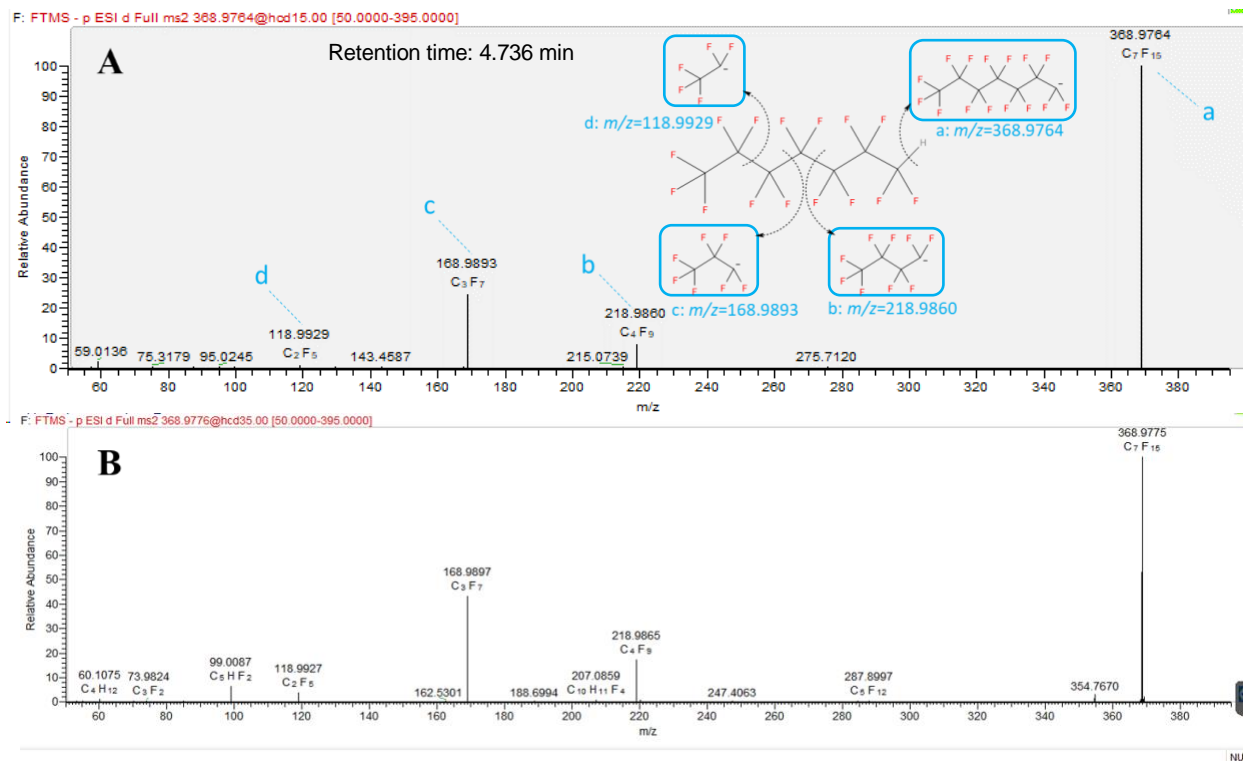


Figure C-11. The MS2 spectra of a novel biotransformation product identified as 1H-perfluoroheptane (m/z 368.9764). Panel A is the spectrum of samples collected from 8:2 FTOH nitrate-reducing microcosms. Panel B is the spectrum of 1 ppb 1H-perfluoroheptane standard.

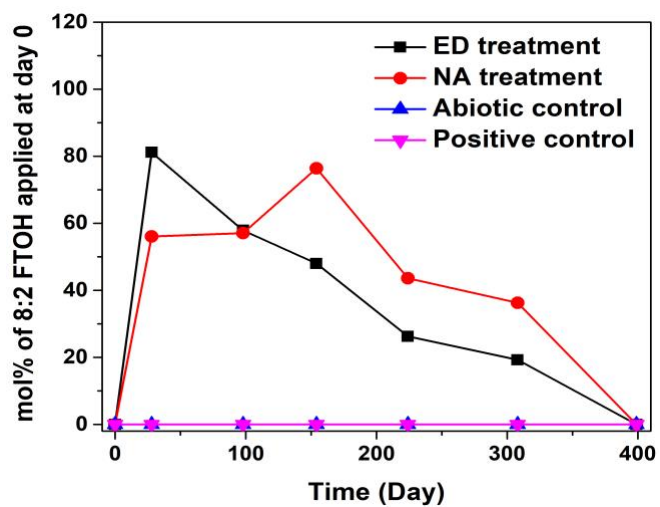


Figure C-12. The molar yields of 1H-perfluoroheptane during 8:2 FTOH biotransformation in each treatment under nitrate-reducing conditions, based on the GC-HRMS quantification results.

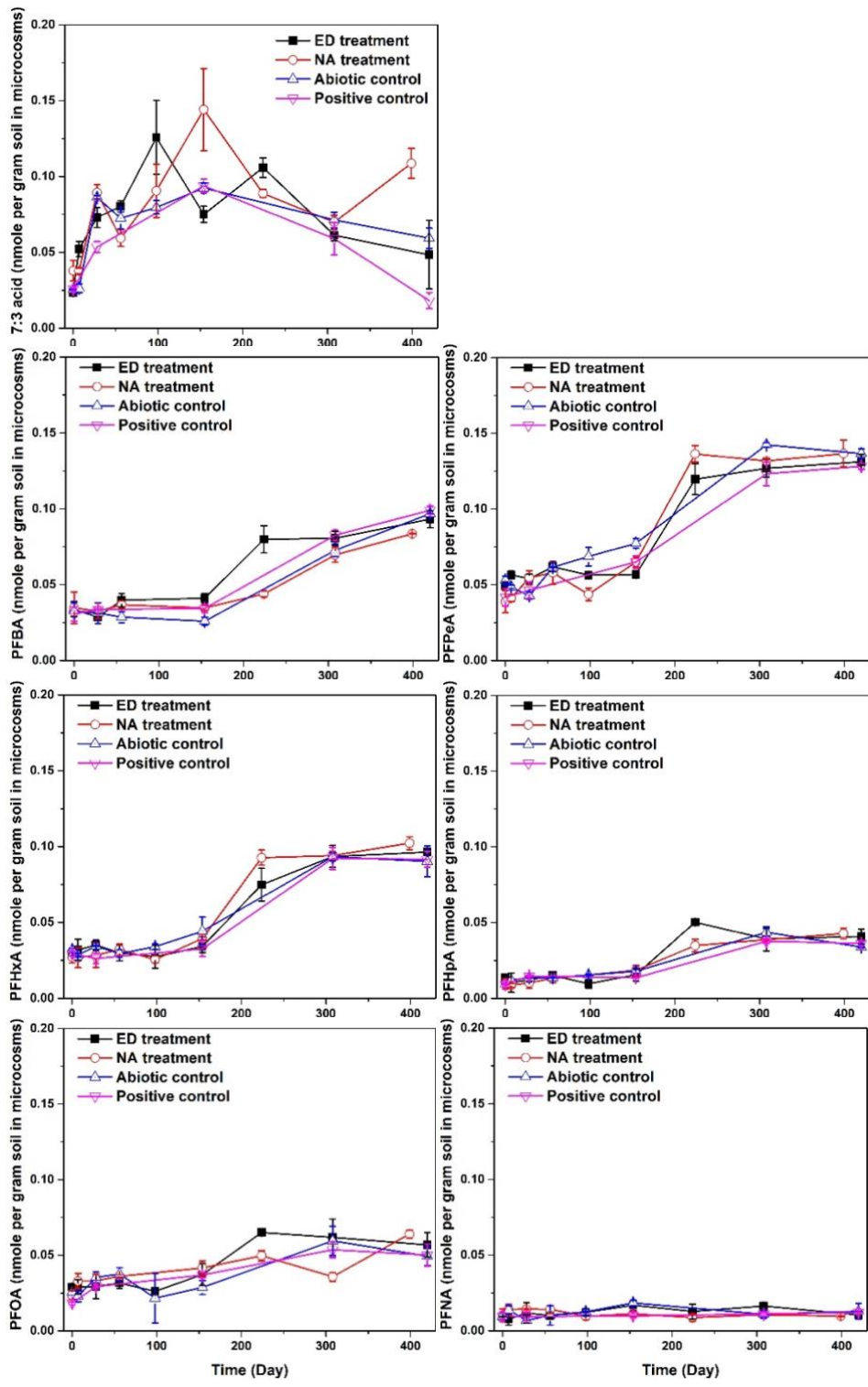


Figure C-13. Changes in the concentrations (nanomole per gram soil/dry weight) of 7:3 acid, and C4-C9 PFCAs in ED, NA treatment, abiotic controls, and positive controls under sulfate-reducing condition throughout the experiments.

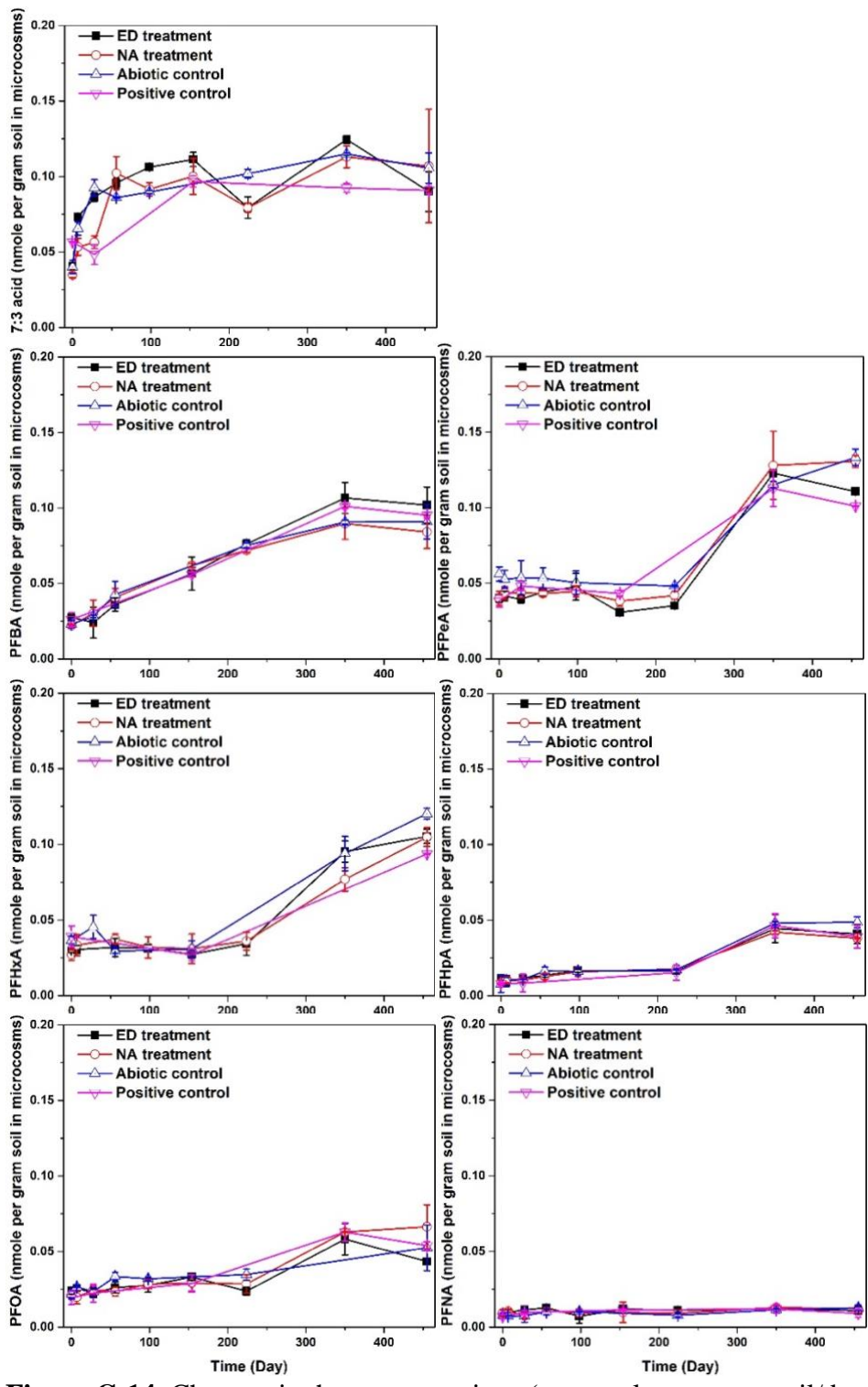


Figure C-14. Changes in the concentrations (nanomole per gram soil/dry weight) of 7:3 acid, and C4-C9 PFCA in ED, NA treatment, abiotic controls, and positive controls under iron-reducing condition throughout the experiments.

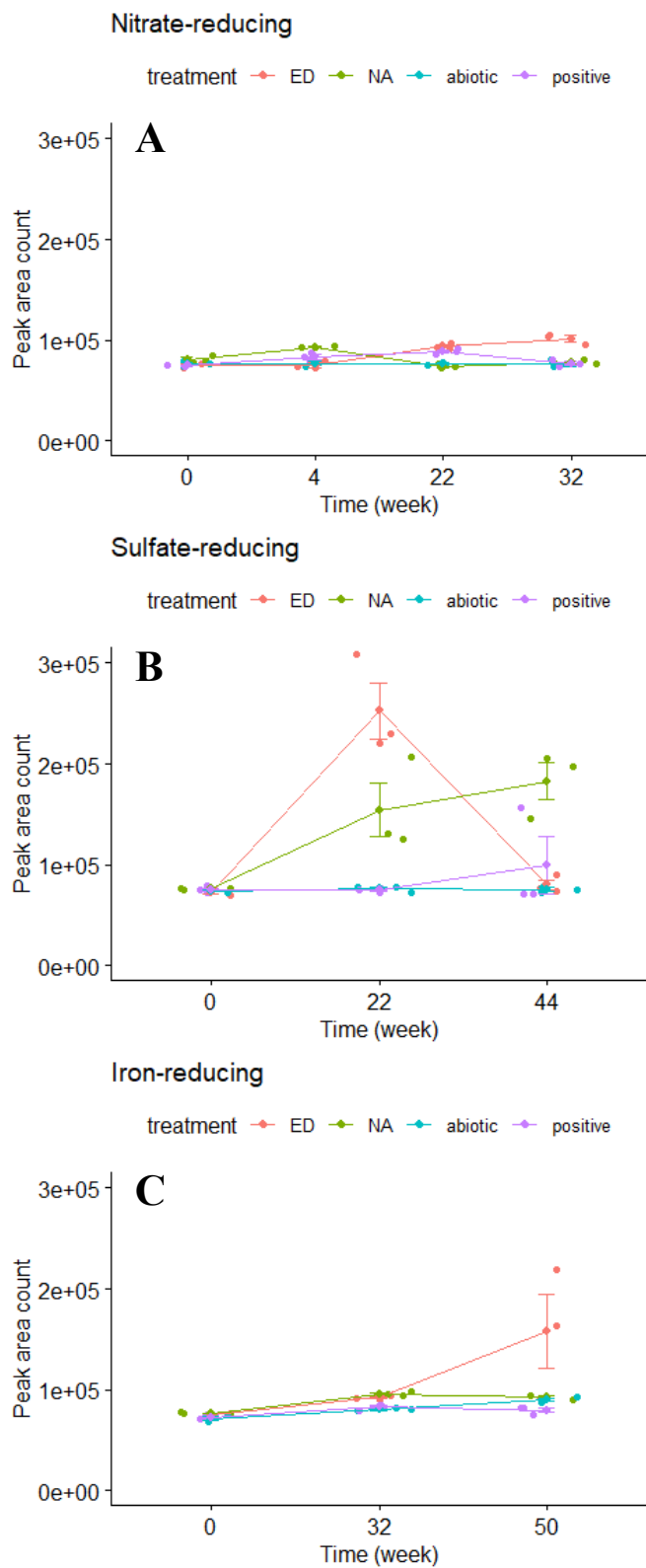


Figure C-15. The time trend of 3-F-7:3 acid during 8:2 FTOH biotransformation in each treatment under (A) nitrate-reducing; (B) sulfate-reducing; and (C) iron-reducing conditions based on peak areas of extracted ion chromatograms.

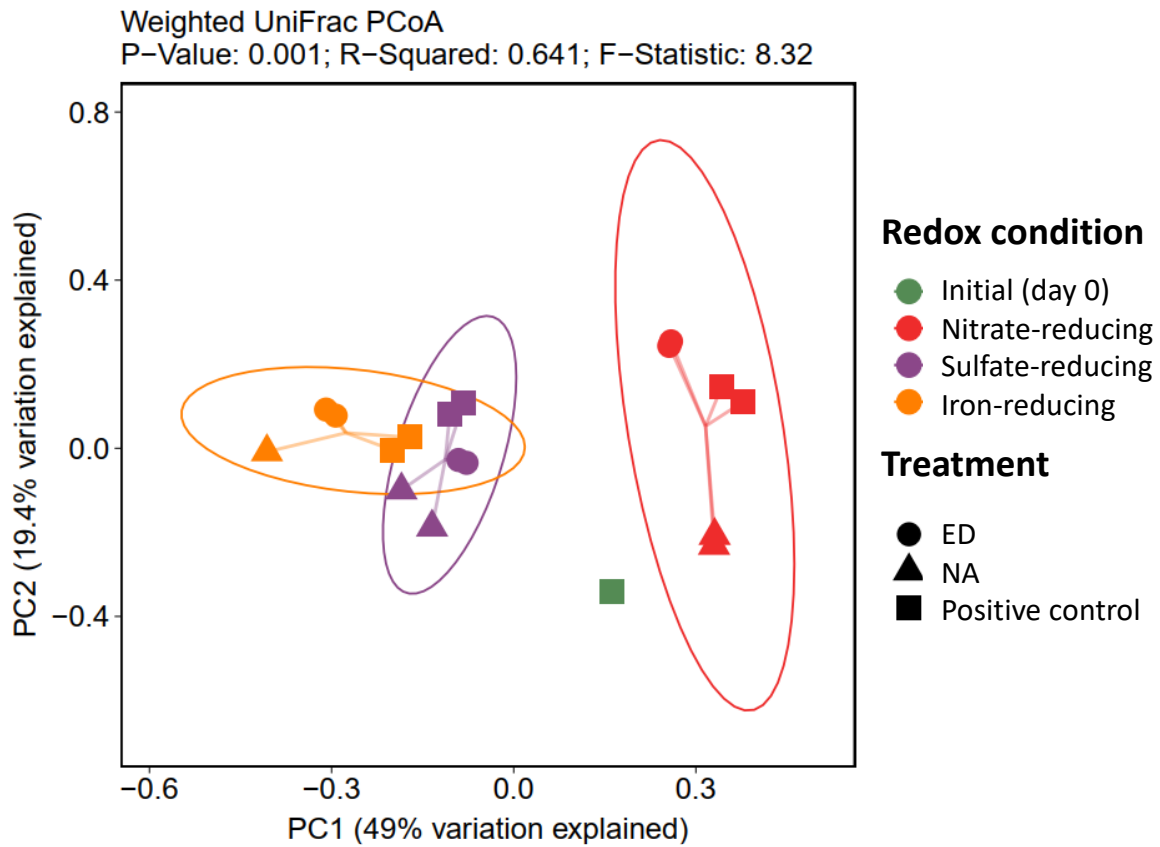


Figure C-16. Principal coordinate analysis (PCoA) plot of phylogenetic microbial community changes among the microcosms under different redox conditions, as described by weighted UniFrac distance matrices.

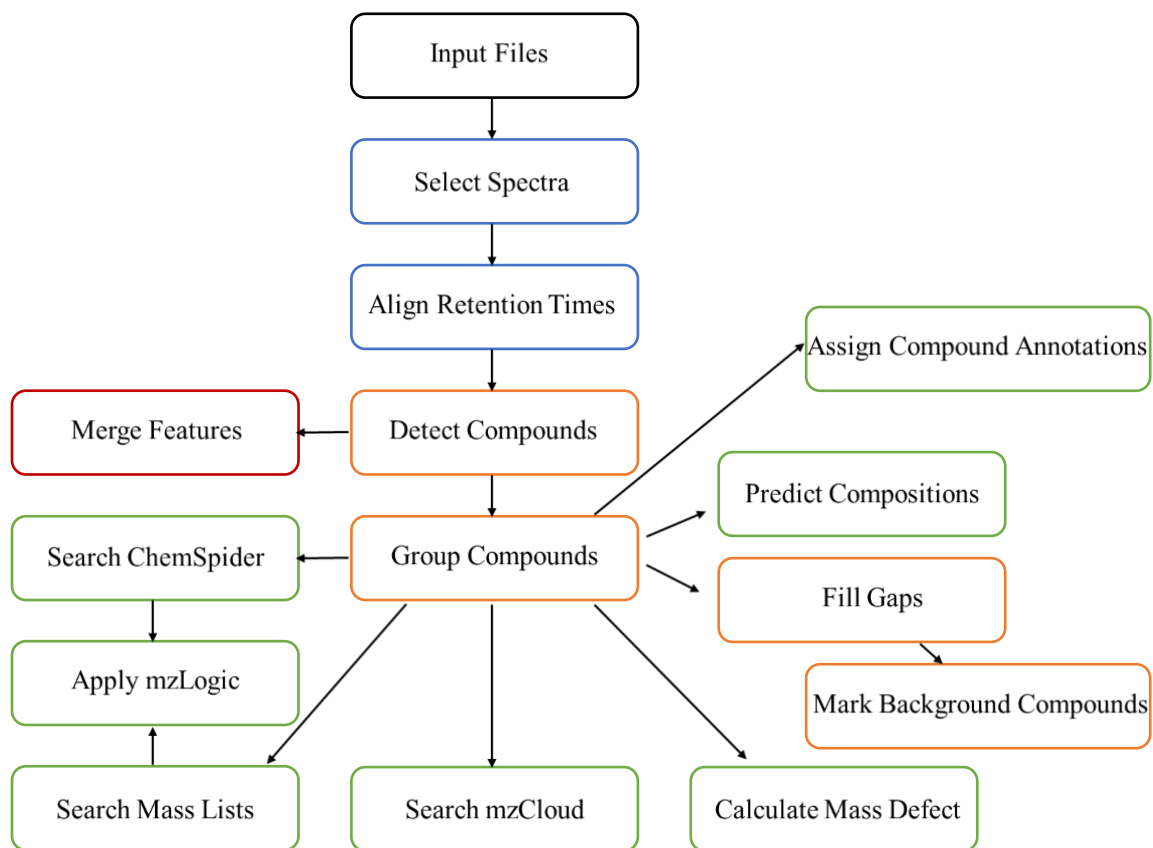


Figure C-17. Compound Discoverer Workflow.

Appendix D. Supporting Information for Chapter 5: Aerobic Biotransformation of 6:2 Fluorotelomer Sulfonate in Soils from Two Aqueous Film-Forming Foam (AFFF)-Impacted Sites

D-S1. Materials and Methods

Soil collection, characterization, and Microcosm preparation

AFFF-impacted soils used in this study were collected from two military sites: the former Loring Air Force Base (Aroostook County, ME) and Robins Air Force Base (Houston County, GA). The soils were collected at depths ranging from 0.5 to 5 ft with a hand auger or shovel, and transported to the laboratory in an ice filled cooler and stored upon arrival at 4 °C. Prior to use, the soil was sieved through a 10-mesh sieve.

Loring and Robins soils were characterized for moisture content, organic matter content, pH, cation exchange capacity (CEC), and soil particle size distribution (Table D-2). The moisture content was determined by weight loss after placement in oven set to 105 °C for 12 hours, and organic matter content was analyzed using a total organic carbon analyzer (TOC-L CPH and SSM-5000A, Shimadzu). The pH, CEC, and soil particle size distribution were quantified by the Soil, Forage, & Water Testing Laboratory (Auburn, AL). The soil particle size distribution was determined by a hydrometer.

Microcosms were prepared in 60-mL Wheaton glass serum bottles under ambient conditions (Table D-3). In each bottle, 3 g (dry weight) of Loring AFB or Robins AFB soil and 30 mL of synthetic groundwater (i.e., 30 mM bicarbonate-buffered growth medium) were added. The medium was prepared according to the recipe reported by Löffler et al.¹³⁶ with modifications to allow for aerobic microbial processes, namely resazurin, L-cysteine, and sodium sulfide were omitted due to the potential to serve as carbon sources under oxic conditions. For live treatment microcosms, each bottle was dosed with 25.5 µL of a 2 g/L 6:2 FTS stock solution prepared in diethylene glycol butyl ether (DGBE) to yield a starting concentration of ~1,700 µg/L, which was far below its predicted aqueous solubility.²⁰⁴ DGBE was used to prepare the stock because it is not only the primary organic solvent in AFFF formulations, but also has been shown to serve as the electron donor and carbon source in prior microcosm studies^{31,37}. Abiotic control microcosms were prepared similarly to the live treatment, except additional 1 g/L of sodium azide was added to prevent microbial growth during incubation (1g/L was demonstrated as effective in the preliminary experiments). In the positive control microcosms, only 25.5 µL of DGBE (no 6:2 FTS) was added into the bottles, and the rest of the procedures were identical as the live treatment.

Non-targeted LC-HRMS Analysis

Pooled samples were injected in triplicate with a 10 µL injection volume on a Thermo QExactive HF-X Orbitrap MS equipped with a Vanquish ultra-high-performance liquid chromatograph (UHPLC-Orbitrap). Sample components were separated on a Thermo Hypersil Gold Vanquish C18 column (50 mm × 2.1 mm × 1.9 µm) at a constant temperature of 60 °C with a solvent gradient consisting of two mobile phases, A (water) and B (methanol). PFAS were eluted from the column at a constant flow rate of 0.4 mL/min using a mobile phase gradient as follows: equilibration with 10% B for 1 minute, followed by a gradient ramp from 10% B to 100% B over 4 minutes and held for 2 minutes, and back to 10 % B over 1 minute and held for 2 minutes (total

run time 11 minutes, data collected from 0.6 to 9 minutes). The MS was operated in full scan dd-MS² mode (stepped 15 and 55 NCE) with an inclusion list for 21 PFAS. Ionization was performed in negative mode with an ionization window of 1.0 *m/z*, sheath gas flow rate of 40, auxiliary gas flow rate of 10, sweep gas flow rate of 2, spray voltage of 2.7 kV, 310 °C capillary temperature, funnel RF level of 35, and 320 °C auxiliary gas heater temperature. For the full-scan, the Orbitrap was operated with a resolution of 120,000, automatic gain control (AGC) of 3x10⁶, and maximum dwell time of 100ms. For dd-MS², the Orbitrap was operated with a resolution of 15,000, AGC of 2x10⁵, and maximum dwell time of 400ms. MS² fragmentation was performed in the HCD collision cell filled with N₂ (produced by a Peak Scientific Nitrogen Generator, Genius NM32LA). The data files were saved in the .RAW file format and analyzed in Thermo Compound Discoverer (CD) 3.2 software. The data processing workflow used in CD 3.2 is displayed in Figure D-13. Spectral libraries and mass lists were used to identify 6:2 FTS transformation byproducts. The libraries included Thermo mzCloud, ChemSpider, and an in-house MS² mass spectral library containing 40 PFAS compounds. The mass lists included 46 hypothesized potential 6:2 FTS transformation products, transformation products predicted by BioTransformer 3.0, and 8,142 fluorinated compounds from the EPA's ToxCast/CompTox database.^{200,205} A final list containing a total of 705 features was exported to Microsoft Excel after processing the raw data. We developed a R script to facilitate the selection of features of interest based on the peak intensity comparison between samples from an individual treatment over time, and between samples from the live-spiked treatments and abiotic/positive controls at each sampling point.

Confidence scores of the features detected were assigned based on the Schymanski Scale to evaluate the certainty of the structure identification.²⁰¹ Briefly, the highest confidence level 1 (confirmed structure) represents the proposed structure was confirmed via the comparison of the appropriate measurement of a reference standard. Level 2 (probable structure) was achieved when the MS² spectrum and fragmentation have been reported previously for a compound of interest and the spectrum-structure match is unambiguous, or when the structure of the compound could be determined unambiguously by MS² fragmentation analysis. Level 3 (tentative candidate) was assigned when the MS² spectrum and fragmentation were informative for possible structures, but the information was insufficient for one exact structure only. When the MS² fragmentation data was not available while a molecular formula can be assigned unambiguously based on the spectral information, level 4 (unequivocal molecular formula) was assigned.

D-S2. Background levels of 6:2 FTS and its potential transformation products in Loring and Robins soils.

Based on previous 6:2 FTS biotransformation studies^{24,25,28} and the commercial availability of authentic standards, a total of 11 PFAS compounds including 6:2 FTS and its potential transformation products were quantitatively analyzed throughout the experiments. Table D-9 shows the background levels of these compounds in Loring and Robins soils based on the measurements of day 0 samples from all microcosms (6:2 FTS background levels only from positive control microcosms). 6:2 FTS, which has been widely detected in soil and groundwater samples at AFFF-impacted sites,^{12,78} was detected in both soils, with about 10-fold higher concentrations in Robins soil than Loring soil. Since 6:2 FTS was reported as a transformation product of the major ingredients (e.g., fluorotelomer thioamido sulfonates, fluorotelomer sulfonamide betains and amines) in several AFFF formulations (e.g., Ansul and National Foam AFFF),^{14,31} the higher background levels of 6:2 FTS detected in Robins soil were likely due to more historical applications of these fluorotelomer-based AFFFs at the sites.

Two polyfluorinated compounds, 5:3 acid and 3:3 acid, were also detected in the Loring and Robins soils (Table D-9). However, both compounds are not known to be manufactured but are almost exclusively formed by the biotransformation of fluorotelomer compounds (e.g., 6:2 FTS and 6:2 FTOH).²⁹ The presence of these compounds implied that the on-site biotransformation of AFFF-derived fluorotelomer precursors was likely occurring in the two AFFF-impacted sites where the soils were sampled. Among the C4-C7 PFCAs, PFHxA was detected in Robins soil with the highest concentration (0.291 ± 0.039 nmole/g dw), which was around 8-fold higher than PFHxA in Loring soil (0.036 ± 0.005 nmole/g dw) (Table D-9). The concentration of each target PFCA in Loring soil was lower than that in Robins soil, which might be due to more and/or greater extent of on-site biotransformation of fluorotelomer-based precursors in Robins soil that partially resulted in the formation of PFCAs.^{31,110}

D-S3. Diversity and richness of microbial community.

The mapped reads of 16S rRNA gene amplicons from Loring and Robins soil microcosms varied in the range of 1,878 to 18,059 (Table D-13). To facilitate the comparison of diversity and richness of microbial community, the number of reads in all samples was rarefied to an identical sequencing depth (1,878), which was within the plateau range of the rarefaction curves, indicating that the sequencing depth was reasonable. The quality-filtered reads were clustered into operational taxonomic units (OTUs) at a 97% similarity level. The number of OTUs in all the samples ranged from 25 to 554 (Table D-13).

Alpha diversity, defined as the mean diversity of species in a community,¹³⁸ was estimated using the Shannon and Simpson indices. Species richness, the number of species or OTUs present in a community, was estimated using richness index Chao1. These indices of the microbial communities in Loring and Robins soil samples were shown in Table D-13. The overall diversity of the microbial community native to Robins soil is substantially lower than that in Loring soil, as the Shannon (2.00 ± 0.06 vs. 5.64 ± 0.12), Simpson (0.81 ± 0.01 vs. 0.99 ± 0.00), and Chao1 (27.6 ± 2.5 vs. 726.6 ± 80.2) indices are much less in the day 7 samples from Robins soil microcosms than that in the day 0 samples from Loring soil microcosms (Table D-13). The lower diversity in Robins soil might be partially due to the heavier PFAS contamination detected in this site (Table D-9), as it has been reported that high concentrations of PFAS (e.g., $1 \mu\text{g}$ PFOS/g soil, $0.5 \mu\text{g}$ PFOA/g sediment) reduced the microbial community diversity and caused a shift in microbial community composition.^{139–141} The other reason may be the lack of sufficient carbon sources for the microbial growth at the site; the total organic carbon content in Robins AFB soil is as low as 0.5% while it is about 3.5% in Loring AFB soil. After the biostimulation with amendment of DGBE over 224 days, the microbial diversity in Robins AFB soil increased dramatically; the Chao1 and Shannon indices increased from 27.6 and 2.0 at day 7 samples to 123.9 and to 3.6 at day 224 samples, respectively (Table D-13). Conversely, the diversity and richness of Loring AFB soil microbial community decreased after a 224-day incubation with DGBE, as indicated by lower Chao1, Shannon, and Simpson indices at day 224 samples compared to day 0 samples (Table D-13). The decrease possibly resulted from the biased stimulated growth of certain species over others in original Loring soil by the DGBE amendment.

In both Loring or Robins soil microcosms, the significant difference ($p < 0.05$) in Chao1, Shannon, or Simpson indices was not found between day 224 samples from the live treatment ($\sim 1700 \mu\text{g/L}$ 6:2 FTS spiked) and the positive control ($0 \mu\text{g/L}$ 6:2 FTS spiked) (Table D-13), suggesting that the presences of spiked 6:2 FTS and its biotransformation products did not significantly change the microbial diversity in this study. Although the results are not in agreement with the previous studies that microbial diversity in river sediment and soil was reduced by the exposure to PFCA or 6:2 FTS biotransformation products, the concentrations of PFAS detected or applied in those studies were much higher (e.g., 15 mg/L) than that in the present study.^{139–141} Principle coordinate analysis (PCoA) was also analyzed on the Weighted Unifrac distance matrices as a measurement of beta diversity to visualize microbial community alteration among the different treatments in Loring and Robins microcosms. The minimal impact of spiked 6:2 FTS on overall diversity is further supported by the clear grouping of day 224 samples from the live treatment and positive controls (Figure D-3). In addition, the apparent separation of Loring and Robins soil samples revealed the distinct differences between the microbial community compositions at the two sites (Figure D-3).

D-S4. The impacts of 6:2 FTS and its biotransformation products on the microbial community compositions

At the phylum level, the increase in Myxococcota and Firmicutes were found in both Loring AFB and Robins AFB soil after being exposed to 6:2 FTS (Figure D-4). Specifically, the relative abundance of Myxococcota was $2.2 \pm 0.7\%$ and $1.1 \pm 0.4\%$ in non-spiked Loring AFB and Robins AFB soils, respectively; while it increased to $3.5 \pm 1.9\%$ and $3.5 \pm 0.3\%$ in the 6:2 FTS spiked soils, respectively. Likewise, Firmicutes increased from $1.3 \pm 0.1\%$ and $4.3 \pm 0.2\%$ in non-spiked soils, to $2.7 \pm 0.5\%$ and $7.5 \pm 1.1\%$ in the 6:2 FTS spiked Loring AFB and Robins AFB soil soils, respectively. The results suggest that Myxococcota and Firmicutes were relatively more tolerant to 6:2 FTS and/or its transformation products. Both of phyla were found capable of biotransformation of chlorinated solvents,^{176,177} and Firmicutes is a dominant phylum in the PFAS-contaminated soils.^{140,143}

Table D-1. Chemical names, acronyms, molecular structures, and suppliers of target poly- and perfluoroalkyl substances (PFAS) for LC-MS/MS targeted analysis.

Chemical name	Acronym	Molecular structure	Supplier
6:2 fluorotelomer sulfonate	6:2 FTS	$F(CF_2)_6CH_2CH_2SO_3^-$	Sigma-Aldrich (St. Louis, USA); Wellington Laboratories (Ontario, Canada)
6:2 fluorotelomer alcohol	6:2 FTOH	$F(CF_2)_6CH_2CH_2OH$	Wellington Laboratories
6:2 fluorotelomer saturated carboxylic acid	6:2 FTCA	$F(CF_2)_6CH_2COOH$	Wellington Laboratories
6:2 fluorotelomer unsaturated carboxylic acid	6:2 FTUA	$F(CF_2)_5CF=CHCOOH$	Wellington Laboratories
5:2 secondary fluorotelomer alcohol	5:2 sFTOH	$F(CF_2)_5CH(OH)CH_3$	Wellington Laboratories
5:3 fluorotelomer carboxylic acid	5:3 acid	$F(CF_2)_5CH_2CH_2COOH$	Wellington Laboratories
3:3 fluorotelomer carboxylic acid	3:3 acid	$F(CF_2)_3CH_2CH_2COOH$	Wellington Laboratories
Perfluorobutanoic acid	PFBA	$F(CF_2)_3COOH$	PFAC-MXC stock, Wellington Laboratories
Perfluoropentanoic acid	PFPeA	$F(CF_2)_4COOH$	
Perfluorohexanoic acid	PFHxA	$F(CF_2)_5COOH$	
Perfluoroheptanoic acid	PFHpA	$F(CF_2)_6COOH$	
Perfluorooctanoic acid	PFOA	$F(CF_2)_7COOH$	

Table D-2. Physical and chemical properties of Loring and Robins soils.

	Loring soil	Robins soil
Sand, Silt, Clay (%)	53.1 ± 3.1, 32.7 ± 2.3, 14.2 ± 0.8	77.5 ± 1.3, 5.6 ± 1.0, 16.9 ± 0.3
USDA Textual Class	Loam/Sandy Loam	Sandy Loam
CEC (meq/100 grams)	18.7 ± 0.0	2.8 ± 0.5
Organic Carbon (%)	3.5 ± 0.1	0.6 ± 0.1
Moisture Content (%)	24.1 ± 1.1	7.0 ± 0.1
pH (1-part soil: 1-part deionized water)	7.2 ± 0.2	5.1 ± 0.1

Table D-3. Microcosm set-up of 6:2 FTS aerobic biotransformation in Loring and Robins soils.

Treatment	Soil	Spiked 6:2 FTS ^a	Carbon source & electron donor	Electron acceptor	Other ^c
<i>Loring AFB soil microcosms</i>					
Live treatment	Loring AFB soil	Yes	DGBE ^b	Oxygen	/
Abiotic control	Loring AFB soil	Yes	DGBE	Oxygen	NaN ₃
Positive control	Loring AFB soil	No	DGBE	Oxygen	/
<i>Robins AFB soil microcosms</i>					
Live treatment	Robins AFB soil	Yes	DGBE	Oxygen	/
Abiotic control	Robins AFB soil	Yes	DGBE	Oxygen	NaN ₃
Positive control	Robins AFB soil	No	DGBE	Oxygen	/

^aThe initial concentration of 6:2 FTS spiked into the microcosms was ~1700 µg/L.

^bDGBE was added into the microcosms with an initial concentration of ~5 mM.

^cOne gram per liter sodium azide was added to inhibit the microbial activity.

Table D-4. Instrument conditions and LC gradient used for the detection and quantification of 6:2 FTS and its polyfluorinated transformation products by UPLC-MS/MS.

LC conditions			
LC system:	Waters ACQUITY UPLC I-Class fitted with PFC kit		
Column:	Waters BEH C-18 column (1.7 μ m dia., 2.1 \times 50 mm)		
Column temp:	30 $^{\circ}$ C		
Sample temp:	4 $^{\circ}$ C		
Injection volume:	50 μ L		
Mobile phase A:	Water		
Mobile phase B:	Methanol		
LC gradient			
Time (min)	Flow rate (mL/min)	%A	%B
0	0.25	50	50
2	0.25	10	90
4	0.25	0	100
6	0.25	0	100
7	0.25	50	50
10	0.25	50	50
MS conditions			
MS system:	Waters Xevo TQ-S Micro		
Ionization mode:	ESI-		
Capillary voltage:	5 kV		
Desolvation temp:	350 $^{\circ}$ C		
Desolvation gas flow:	750 L/hr		
Source temp:	120 $^{\circ}$ C		
Cone gas flow:	50 L/hr		

Table D-5. Multiple reaction monitoring (MRM) parameters used for the detection and quantification of 6:2 FTS and its polyfluorinated transformation products by UPLC-MS/MS.

Compound	Molecular Ion (m/z)	Cone Voltage (V)	Collision Energy (V)	Quant. Ion (m/z)	Cone Voltage (V)	Collision Energy (V)	Confirmation Ion (m/z)
6:2 FTS	427.10	25	18	407.09	25	34	80.84
6:2 FTOH	363.00	18	8	303.00			
6:2 FTCA	377.03	20	20	293.05	20	8	63.03
6:2 FTUA	357.00	30	14	293.00			
5:2 sFTOH	293.10	50	18	119.04			
5:3 Acid	340.97	32	14	237.1	32	20	217.06
3:3 Acid	241.00	10	10	177.00	10	20	219

Table D-6. Instrument conditions and LC gradient used for the detection and quantification of PFAAs by UPLC-MS/MS.

LC conditions			
LC system:	Waters ACQUITY UPLC I-Class fitted with PFC kit		
Column:	Waters BEH C-18 column (1.7 μ m dia., 2.1 \times 50 mm)		
Column temp:	50 $^{\circ}$ C		
Sample temp:	4 $^{\circ}$ C		
Injection volume:	10 μ L		
Mobile phase A:	95:5 Water:methanol + 2 mM ammonium acetate		
Mobile phase B:	Methanol + 2 mM ammonium acetate		
LC gradient			
Time (min)	Flow rate (mL/min)	%A	%B
0	0.4	85	15
1.2	0.4	85	15
17	0.4	15	85
17.5	0.4	0	100
18	0.4	85	15
20	0.4	85	15
MS conditions			
MS system:	Waters Xevo TQ-S Micro		
Ionization mode:	ESI-		
Capillary voltage:	0.50 kV		
Desolvation temp:	350 $^{\circ}$ C		
Desolvation gas flow:	650 L/hr		
Source temp:	150 $^{\circ}$ C		
Cone gas flow:	20 L/hr		

Table D-7. Multiple reaction monitoring (MRM) parameters used for the detection and quantification of PFAAs by UPLC-MS/MS.

Compound	Molecular Ion (m/z)	Cone Voltage (V)	Collision Energy (V)	Quant. Ion (m/z)	Cone Voltage (V)	Collision Energy (V)	Confirmation Ion (m/z)
PFBA	212.93	10	10	169.09			
PFPeA	262.95	10	5	219.09			
PFHxA	312.94	5	10	269.12	5	20	119.02
PFHpA	362.90	15	10	319.14	15	15	169.08
PFOA	412.93	10	10	369.12	10	15	169.03

Table D-8. Limits of detection (LODs) and limits of quantification (LOQs) of target PFAS.

Analytes	LOD ^a (ng/mL)	LOQ ^b (ng/mL)
6:2 FTS	0.02	0.06
6:2 FTOH ^c	0.63	11.10
6:2 FTCA	0.02	0.10
6:2 FTUA	0.02	0.03
5:2 sFTOH ^c	0.26	4.20
5:3 acid	0.01	0.02
3:3 acid	0.03	0.13
PFBA	0.01	0.05
PFPeA	0.01	0.05
PFHxA	0.01	0.05
PFHpA	0.01	0.05
PFOA	0.01	0.05

^aLODs are determined based on EPA Method 537.1

^bLOQs are determined with the Lowest Concentration Minimum Reporting Level (LCMRL) Calculator distributed by EPA.

^cThe LODs and LOQs for 6:2 FTOH and 5:2 sFTOH were run-dependent, and the values reported here were the highest levels during the analysis of all microcosm samples.

Table D-9. Background levels (nmole/g dw) of 6:2 FTS and its potential per- and polyfluorinated transformation products in Loring and Robins soils.

Category	PFAS	Loring AFB soil	Robins AFB soil
Polyfluorinated compounds	6:2 FTS	0.278 ± 0.067	2.821 ± 0.150
	6:2 FTOH	N.D.	N.D.
	6:2 FTCA	N.D.	N.D.
	6:2 FTUA	N.D.	N.D.
	5:2 sFTOH	N.D.	N.D.
	5:3 acid	0.071 ± 0.010	0.026 ± 0.006
	3:3 acid	0.036 ± 0.009	0.027 ± 0.007
Perfluorinated compounds	PFBA	0.033 ± 0.004	0.072 ± 0.013
	PFPeA	0.052 ± 0.010	0.073 ± 0.011
	PFH _x A	0.036 ± 0.005	0.291 ± 0.039
	PFHpA	0.016 ± 0.004	0.035 ± 0.008

N.D.: not detected in the sample.

Table D-10. Changes in the mass (nmole) of 6:2 FTS and its potential transformation products in Loring soil microcosms.

Time (day)	6:2 FTS	6:2 FTOH	6:2 FTUA	6:2 FTCA	5:2 sFTOH	5:3 acid	3:3 acid	PFBA	PFPeA	PFHxA	PFHpA
Live treatment											
0	154.7 ± 15.8	N.D.	N.D.	N.D.	N.D.	0.203 ± 0.004	0.136 ± 0.005	0.093 ± 0.009	0.146 ± 0.038	0.097 ± 0.024	0.047 ± 0.011
7	143.0 ± 8.3	N.D.	N.D.	N.D.	N.D.	0.226 ± 0.026	0.116 ± 0.016	0.120 ± 0.031	0.179 ± 0.020	0.106 ± 0.005	0.061 ± 0.023
28	99.6 ± 13.7	N.D.	5.729 ± 0.834	N.D.	8.237 ± 0.660	1.632 ± 0.337	0.105 ± 0.026	0.120 ± 0.019	0.186 ± 0.008	1.221 ± 0.242	0.079 ± 0.009
56	60.7 ± 3.2	N.D.	3.752 ± 1.470	0.309 ± 0.001	15.746 ± 1.777	2.306 ± 0.917	0.137 ± 0.011	0.109 ± 0.011	0.578 ± 0.077	2.722 ± 0.006	0.095 ± 0.019
98	46.3 ± 11.7	N.D.	1.205 ± 0.762	0.048 ± 0.019	15.148 ± 1.947	7.083 ± 0.924	0.107 ± 0.025	0.136 ± 0.007	0.720 ± 0.126	2.423 ± 0.390	0.321 ± 0.034
154	0.3 ± 0.1	N.D.	3.217 ± 0.109	N.D.	17.840 ± 1.887	13.698 ± 1.925	0.098 ± 0.025	0.615 ± 0.078	1.988 ± 0.464	2.454 ± 0.402	0.138 ± 0.010
224	0.5 ± 0.1	N.D.	0.469 ± 0.205	N.D.	19.832 ± 9.649	0.261 ± 0.118	0.124 ± 0.018	2.300 ± 0.780	10.964 ± 4.215	8.196 ± 1.067	0.508 ± 0.165
Positive control											
0	0.835 ± 0.200	N.D.	N.D.	N.D.	N.D.	0.172 ± 0.014	0.094 ± 0.004	0.093 ± 0.013	0.141 ± 0.036	0.117 ± 0.004	0.034 ± 0.001
7	0.632 ± 0.446	N.D.	N.D.	N.D.	N.D.	0.219 ± 0.028	0.100 ± 0.031	0.103 ± 0.008	0.176 ± 0.011	0.096 ± 0.008	0.054 ± 0.000
28	0.002 ± 0.000	N.D.	N.D.	N.D.	0.161 ± 0.013	0.195 ± 0.040	0.112 ± 0.021	0.122 ± 0.003	0.150 ± 0.048	0.130 ± 0.022	0.070 ± 0.018
56	0.002 ± 0.002	N.D.	N.D.	N.D.	0.453 ± 0.045	0.493 ± 0.085	0.099 ± 0.027	0.113 ± 0.003	0.127 ± 0.020	0.141 ± 0.010	0.100 ± 0.020
98	0.028 ± 0.004	N.D.	0.005 ± 0.002	N.D.	0.410 ± 0.120	0.623 ± 0.050	0.090 ± 0.012	0.149 ± 0.010	0.154 ± 0.027	0.149 ± 0.016	0.255 ± 0.015
154	0.038 ± 0.018	N.D.	0.002 ± 0.001	N.D.	0.340 ± 0.060	0.534 ± 0.008	0.087 ± 0.003	0.174 ± 0.053	0.111 ± 0.006	0.239 ± 0.085	0.104 ± 0.009
224	0.029 ± 0.001	N.D.	N.D.	N.D.	0.303 ± 0.219	0.282 ± 0.061	0.087 ± 0.045	0.235 ± 0.010	0.464 ± 0.012	0.355 ± 0.045	0.309 ± 0.052
Abiotic control											
0	145.7 ± 3.6	N.D.	N.D.	N.D.	N.D.	0.183 ± 0.018	0.096 ± 0.013	0.101 ± 0.012	0.137 ± 0.024	0.105 ± 0.021	0.054 ± 0.012
7	145.4 ± 1.4	N.D.	N.D.	N.D.	N.D.	0.221 ± 0.001	0.142 ± 0.004	0.098 ± 0.008	0.175 ± 0.007	0.120 ± 0.006	0.053 ± 0.008
28	156.2 ± 3.3	N.D.	N.D.	N.D.	N.D.	0.226 ± 0.014	0.136 ± 0.001	0.124 ± 0.003	0.150 ± 0.022	0.132 ± 0.020	0.065 ± 0.003
56	159.1 ± 1.8	N.D.	N.D.	N.D.	N.D.	0.218 ± 0.025	0.107 ± 0.039	0.158 ± 0.014	0.121 ± 0.018	0.131 ± 0.003	0.084 ± 0.010
98	137.0 ± 5.5	N.D.	N.D.	N.D.	N.D.	0.286 ± 0.006	0.125 ± 0.009	0.118 ± 0.010	0.140 ± 0.014	0.158 ± 0.006	0.266 ± 0.019
154	153.8 ± 0.2	N.D.	N.D.	N.D.	N.D.	0.455 ± 0.025	0.091 ± 0.006	0.154 ± 0.040	0.178 ± 0.059	0.121 ± 0.020	0.117 ± 0.001
224	152.3 ± 7.8	N.D.	N.D.	N.D.	N.D.	0.214 ± 0.092	0.150 ± 0.112	0.245 ± 0.039	0.373 ± 0.050	0.267 ± 0.115	0.200 ± 0.010

Table D-11. Changes in the mass (nmole) of 6:2 FTS and its potential transformation products in Robins soil microcosms.

Time (day)	6:2 FTS	6:2 FTOH	6:2 FTUA	6:2 FTCA	5:2 sFTOH	5:3 acid	3:3 acid	PFBA	PFPeA	PFHxA	PFHpA
Live treatment											
0	186.1 ± 15.3	N.D.	N.D.	N.D.	N.D.	0.082 ± 0.006	0.091 ± 0.013	0.240 ± 0.054	0.212 ± 0.015	0.984 ± 0.139	0.108 ± 0.017
7	182.8 ± 2.1	N.D.	N.D.	N.D.	N.D.	0.098 ± 0.008	0.082 ± 0.014	0.249 ± 0.032	0.176 ± 0.014	1.126 ± 0.091	0.126 ± 0.022
28	182.5 ± 3.7	N.D.	N.D.	N.D.	N.D.	0.076 ± 0.017	0.081 ± 0.023	0.200 ± 0.015	0.219 ± 0.026	1.008 ± 0.217	0.100 ± 0.009
56	208.6 ± 19.8	N.D.	N.D.	N.D.	N.D.	0.081 ± 0.007	0.071 ± 0.011	0.188 ± 0.027	0.227 ± 0.015	0.833 ± 0.090	0.112 ± 0.026
98	149.8 ± 7.7	0.006 ± 0.000	N.D.	N.D.	N.D.	0.077 ± 0.025	0.082 ± 0.029	0.232 ± 0.025	0.233 ± 0.011	0.868 ± 0.146	0.135 ± 0.018
154	121.3 ± 12.2	0.188 ± 0.000	0.857 ± 0.685	0.064 ± 0.000	6.804 ± 1.387	0.929 ± 0.428	0.099 ± 0.002	0.555 ± 0.114	0.768 ± 0.000	4.709 ± 0.323	0.325 ± 0.105
224	118.5 ± 11.2	N.D.	3.872 ± 1.907	0.522 ± 0.378	3.743 ± 0.095	4.365 ± 3.474	0.228 ± 0.015	0.605 ± 0.194	0.821 ± 0.016	3.891 ± 0.467	0.651 ± 0.304
Positive control											
0	8.252 ± 0.347	N.D.	N.D.	N.D.	N.D.	0.089 ± 0.014	0.094 ± 0.003	0.174 ± 0.018	0.220 ± 0.037	0.798 ± 0.024	0.087 ± 0.005
7	8.871 ± 0.274	N.D.	N.D.	N.D.	N.D.	0.090 ± 0.004	0.093 ± 0.010	0.217 ± 0.048	0.216 ± 0.004	1.032 ± 0.032	0.107 ± 0.004
28	8.058 ± 0.020	N.D.	N.D.	N.D.	N.D.	0.058 ± 0.006	0.067 ± 0.012	0.232 ± 0.008	0.211 ± 0.044	0.935 ± 0.041	0.138 ± 0.018
56	9.920 ± 1.111	N.D.	N.D.	N.D.	N.D.	0.074 ± 0.001	0.065 ± 0.012	0.194 ± 0.025	0.270 ± 0.001	0.776 ± 0.208	0.092 ± 0.029
98	7.026 ± 2.009	N.D.	N.D.	N.D.	N.D.	0.057 ± 0.009	0.062 ± 0.013	0.207 ± 0.039	0.244 ± 0.048	0.898 ± 0.015	0.167 ± 0.018
154	3.637 ± 3.581	N.D.	0.625 ± 0.574	N.D.	1.079 ± 0.504	0.081 ± 0.017	0.111 ± 0.089	0.437 ± 0.211	0.664 ± 0.000	3.338 ± 1.084	0.536 ± 0.070
224	1.815 ± 0.914	N.D.	0.331 ± 0.130	0.053 ± 0.006	2.225 ± 1.085	0.480 ± 0.131	0.261 ± 0.188	0.350 ± 0.004	0.797 ± 0.005	2.436 ± 0.227	0.578 ± 0.108
Abiotic control											
0	189.2 ± 8.3	N.D.	N.D.	N.D.	N.D.	0.056 ± 0.001	0.066 ± 0.023	0.243 ± 0.033	0.211 ± 0.033	0.805 ± 0.058	0.109 ± 0.023
7	156.5 ± 2.0	N.D.	N.D.	N.D.	N.D.	0.080 ± 0.024	0.073 ± 0.017	0.228 ± 0.003	0.235 ± 0.038	0.860 ± 0.117	0.121 ± 0.037
28	188.6 ± 2.3	N.D.	N.D.	N.D.	N.D.	0.081 ± 0.016	0.044 ± 0.001	0.199 ± 0.033	0.202 ± 0.007	0.731 ± 0.086	0.142 ± 0.025
56	173.3 ± 4.5	N.D.	N.D.	N.D.	N.D.	0.058 ± 0.015	0.091 ± 0.002	0.236 ± 0.028	0.213 ± 0.045	0.780 ± 0.025	0.127 ± 0.025
98	186.5 ± 13.6	N.D.	N.D.	N.D.	N.D.	0.077 ± 0.019	0.074 ± 0.010	0.224 ± 0.072	0.208 ± 0.029	0.570 ± 0.035	0.160 ± 0.001
154	183.5 ± 7.3	N.D.	N.D.	N.D.	N.D.	0.101 ± 0.072	0.059 ± 0.046	0.240 ± 0.013	0.653 ± 0.139	1.574 ± 0.686	0.392 ± 0.020
224	174.7 ± 3.6	N.D.	N.D.	N.D.	N.D.	0.063 ± 0.000	0.050 ± 0.020	0.277 ± 0.053	0.512 ± 0.058	1.609 ± 0.005	0.307 ± 0.031

Table D-12. Comparison of 6:2 FTS biotransformation in environmental matrices and pure cultures under aerobic conditions.

Environmental matrix/pure culture	Duration (days)	Biotransformation rate (half-life, if applicable)	Biotransformation products at the end of experiment (yield in mol%, if determined)	Reference
Activated sludge	90	63.7 mol% remaining at day 90	5:2 ketone & 5:2 sFTOH (3.4), 5:3 acid (0.1), PFBA (0.1), PFPeA (1.5), PFHxA (1.1)	24
River sediment	90	1.9 mol% remaining at day 90 (<5 days)	6:2 FTOH (<2.5), 6:2 FTCA (12), 5:2 sFTOH (<8), 5:2 ketone (<8), 5:3 acid (16), PFPeA(21), PFHxA(20), PFHpA (0.6)	25
Wetland slurry	142	91.1 mol% remaining at day 142	5:3 acid (2.7), PFPeA (6.1), PFHxA (2.1)	28
Landfill leachate and sediment	90	~50 mol% remaining at day 90 (86 days)	5:2 sFTOH (0.6), 5:3 acid (0.2), PFBA (0.6), PFPeA (5.6), PFHxA (3.1)	29
Landfill leachate and sediment	10	80-93 mol% remaining at day 10	Sum of PFBA, PFPeA and PFHxA (2)	30
<i>Pseudomonas</i> sp. strain D2	1	Not available	Not available	113
<i>Gordonia</i> sp. strain NB4-1Y	5	56 mol% remaining at day 5	6:2 FTCA, 6:2 FTUA, 5:3 acid, and 5:3 U acid	111
<i>Gordonia</i> sp. strain NB4-1Y	7	0.1 mol% remaining at day 7	6:2 FTOH (4.1), 6:2 FTCA (4.3), 6:2 FTUA (13.7), 5:2 sFTOH (9.0), 5:2 ketone (43.9), 5:3 acid (0.4), PFBA (<0.1), PFPeA(<0.1), PFHxA(0.6)	110
<i>Rhodococcus jostii</i> RHA1	6	<1 mol% remaining at day 6	6:2 FTCA, 6:2 FTUA, α -OH-5:3 acid, and PFHpA	112
<i>Dietzia aurantiaca</i> J3	7	0 mol% remaining at day 6	6:2 FTCA, 6:2 FTUA, 5:3 acid, PFPeA, PFHxA	114
Loring AFB soil	224	0.2 mol% remaining at day 224 (43.3 days)	6:2 FTUA (0.3), 5:2 sFTOH (12.8), 5:3 acid (0.2), PFBA (1.3), PFPeA (7.0), PFHxA (5.3), and PFHpA (0.2)	This study
Robins AFB soil	224	63.7 mol% remaining at day 224	6:2 FTUA (2.1), 6:2 FTCA (0.3), 5:2 sFTOH (2.0), 5:3 acid (2.3), PFBA (0.3), PFPeA (0.1), and PFHxA (0.8)	This study

Table D-13. Microbial richness and diversity in Loring and Robins soils.

Soil type	6:2 FTS (µg/L)	Sampling time	Mapped reads	OTUs	Chao1	Shannon	Simpson
Loring AFB soil	0	Day 0	10428	554	726.6 ± 80.2	5.64 ± 0.12	0.99 ± 0.00
	0	Day 0	6148	483			
	0	Day 224	14522	285	460.5 ± 44.6	4.38 ± 0.09	0.96 ± 0.00
	0	Day 224	16627	326			
	~1700	Day 224	18059	322	502.8 ± 36.8	4.58 ± 0.07	0.97 ± 0.00
	~1700	Day 224	14988	326			
Robins AFB soil	0	Day 7	3609	30	27.6 ± 2.5	2.00 ± 0.06	0.81 ± 0.01
	0	Day 7	1878	25			
	0	Day 224	3034	86	123.9 ± 12.1	3.64 ± 0.37	0.95 ± 0.02
	0	Day 224	6343	120			
	~1700	Day 224	15083	109	149.9 ± 17.2	3.61 ± 0.08	0.95 ± 0.00
	~1700	Day 224	14554	131			

Table D-14. Potential biotransformation products of 6:2 FTS identified by HRMS analysis

Chemical name	Formula	Mass (<i>m/z</i>)	Mass error [ppm]	Level of confidence ^a
1H-perfluoropentane	C ₅ HF ₁₁	268.98271	-1.00	1
1H-perfluorobutane	C ₄ HF ₉	218.98587	-1.39	1
1,2,2,3,3,4,4,4-octafluorobutan-1-ol	C ₄ H ₂ F ₈ O	216.98912	-6.39	2
Perfluoropentanal	C ₅ HF ₉ O	246.98080	-1.16	4
N/A ^b	C ₇ H ₂ F ₈	236.99543	-0.71	3
N/A	C ₇ H ₃ F ₉	257.00159	-0.93	4
N/A	N/A	292.98316	0.6	5

^a The level of confidence of each identified biotransformation product was assigned using a scheme reported by Schymanski et al.²⁰¹

^b Not applicable.

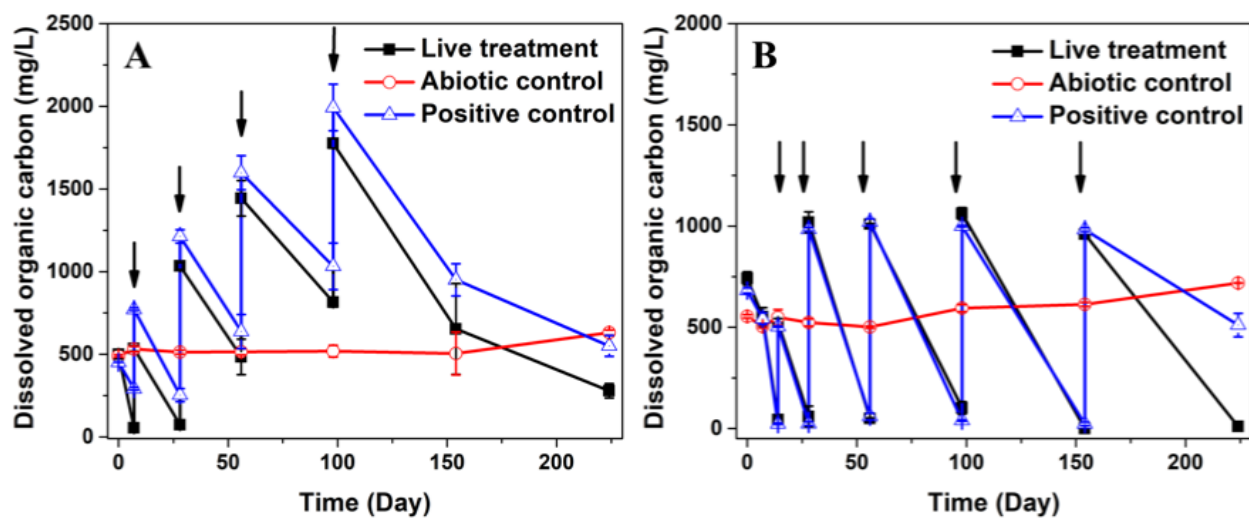


Figure D-1. Concentrations of dissolved organic carbon (DOC) in Loring (Panel A) and Robins (Panel B) soil microcosms. Solid arrows represent the amendment of 10 mM DGBE to live treatments and positive controls. Error bars represent the standard deviation of triplicate live treatment microcosms, and of duplicate control microcosms.

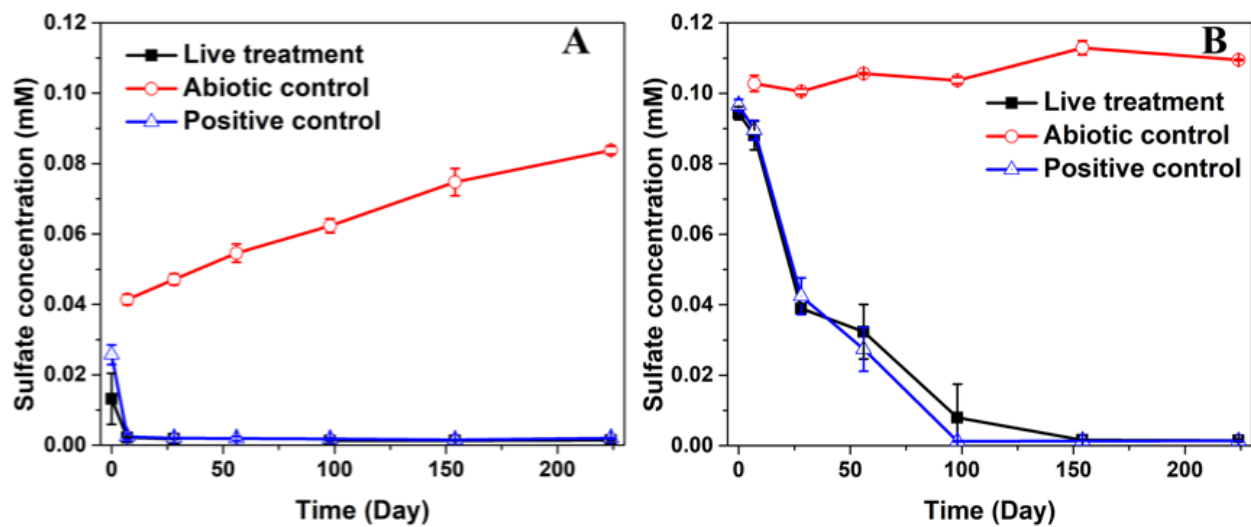


Figure D-2. Changes in sulfate concentrations during 6:2 FTS aerobic biotransformation in Loring (Panel A) and Robins (Panel B) soil microcosms. Error bars represent the standard deviation of triplicate live treatment microcosms, and of duplicate control microcosms.

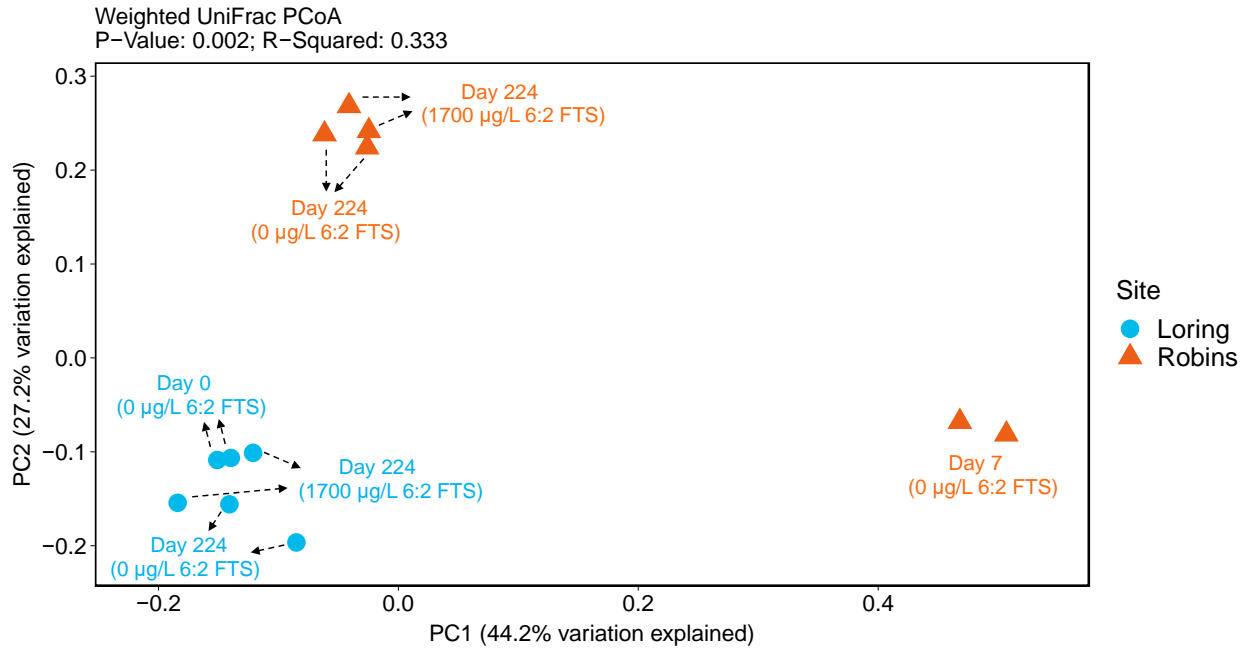


Figure D-3. Principal coordinate analysis (PCoA) plot of phylogenetic microbial community changes among the treatments from Loring or Robins soil microcosms, as described by weighted UniFrac distance matrices. The PC1 and PC2 axes explain 44.2% and 27.2% of the variation, respectively.

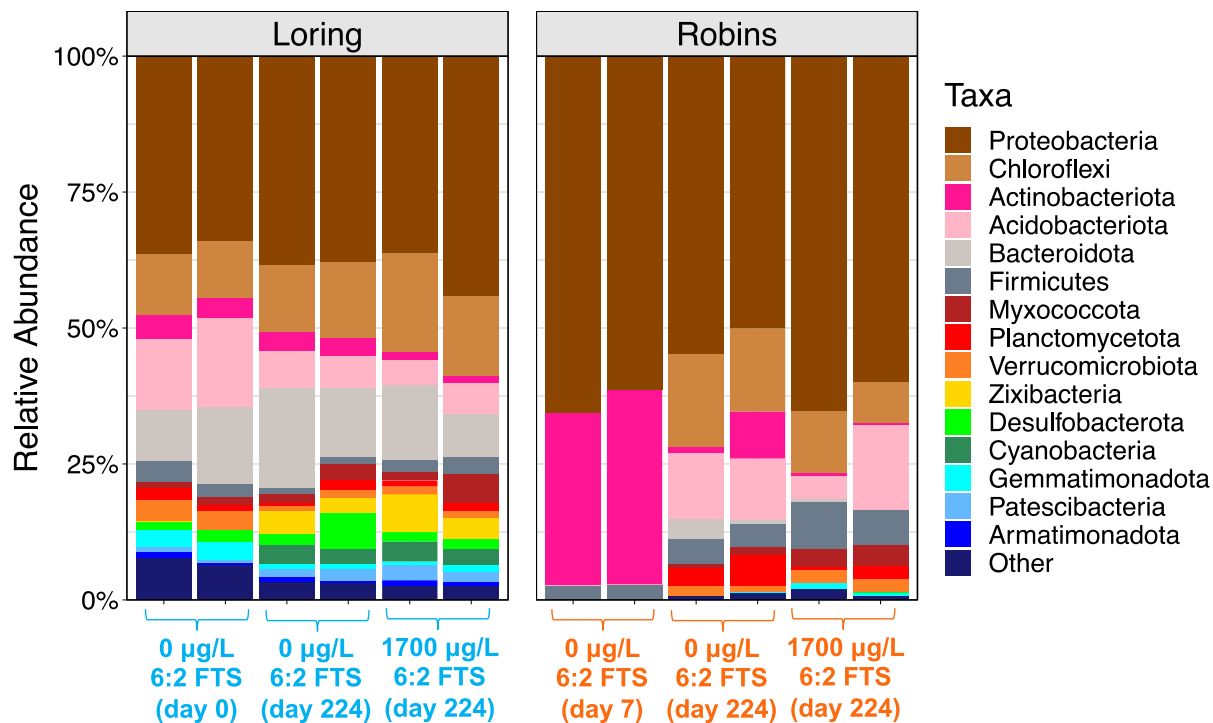


Figure D-4. The relative abundance of microbial community composition at the phylum level in Loring (left) and Robins (right) soil microcosms.

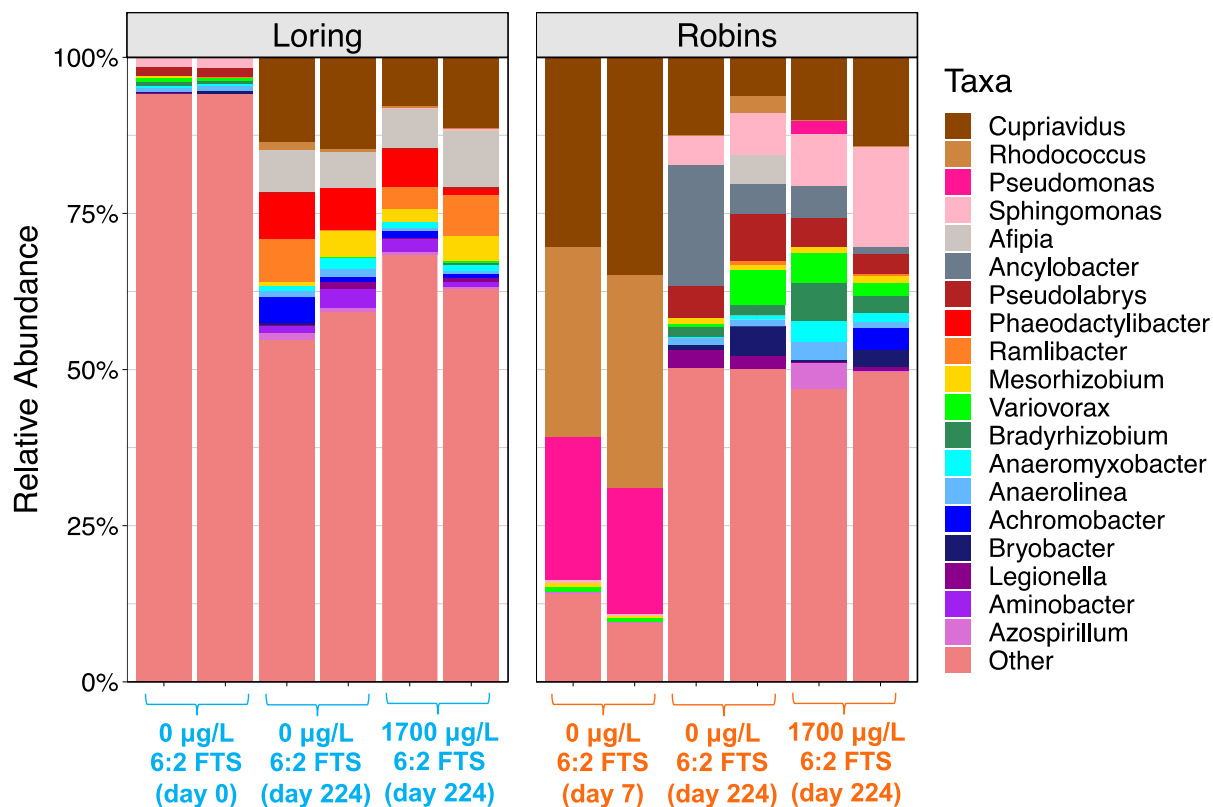


Figure D-5. The relative abundance of microbial community composition at the genus level in Loring (left) and Robins (right) soil microcosms.

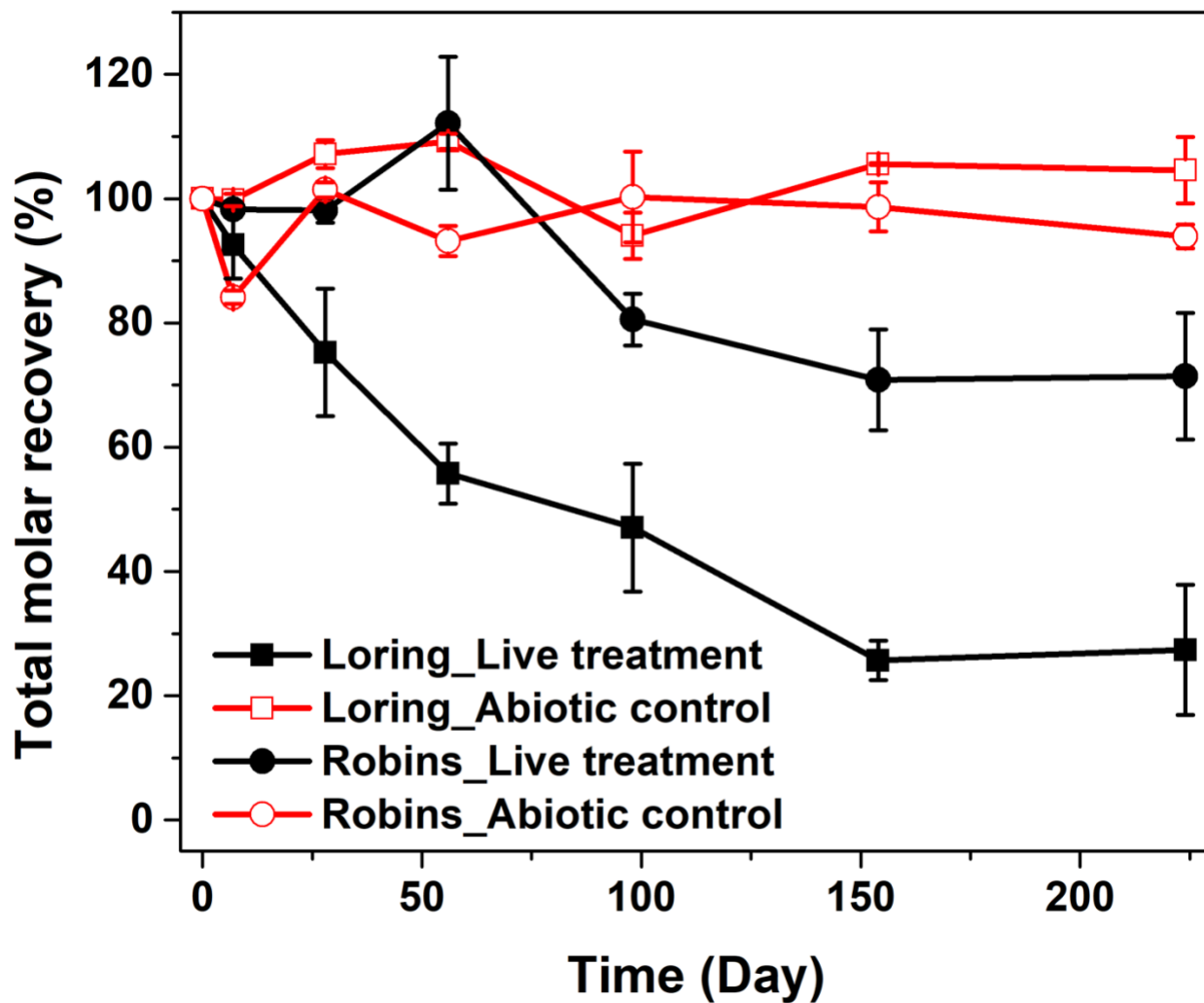


Figure D-6. The total molar recoveries (6:2 FTS and quantifiable biotransformation products) in live treatments and abiotic controls from Loring and Robins soil microcosms.

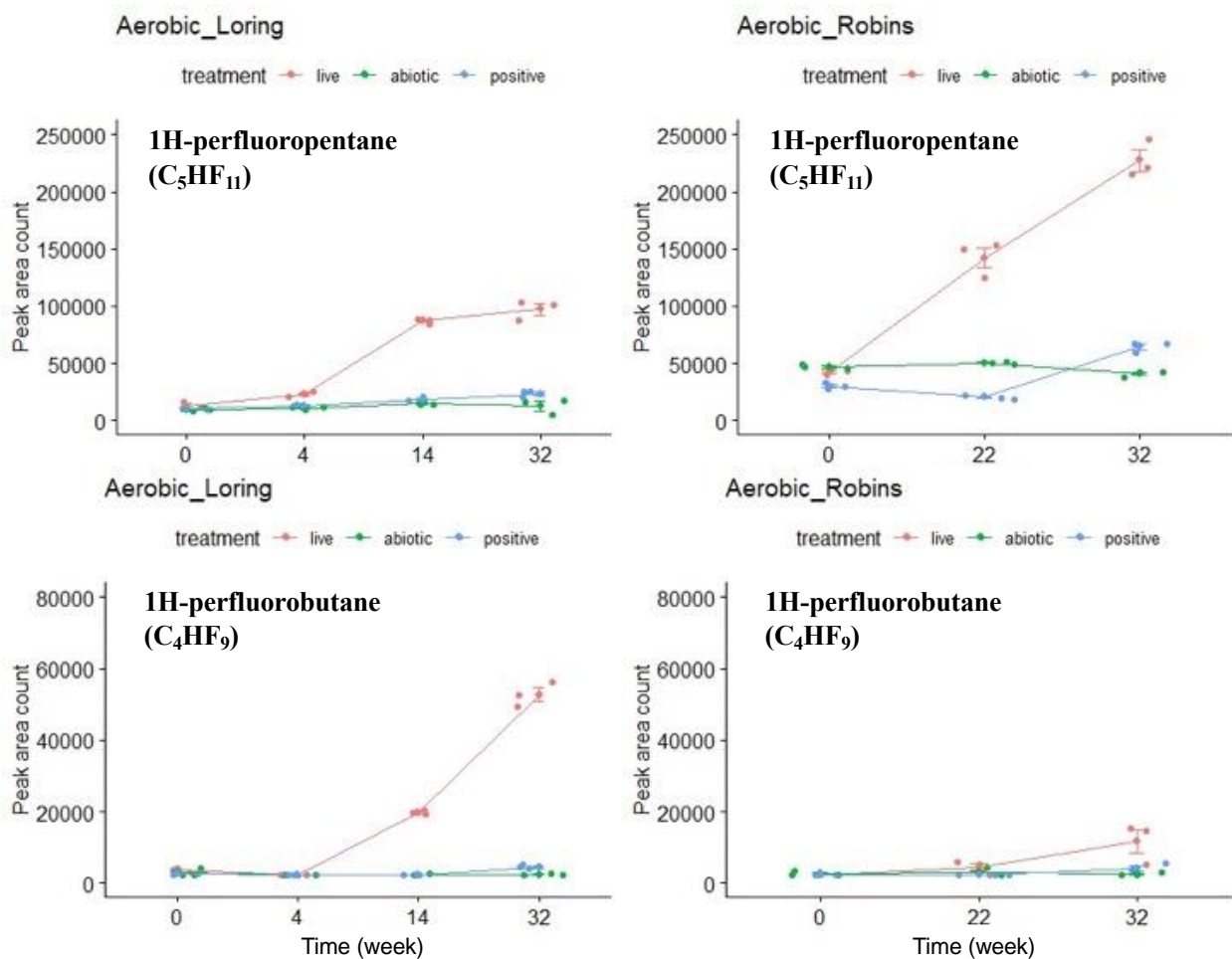


Figure D-7. The time trends of 1H-perfluoropentane (C_5HF_{11} , m/z 268.98271) and 1H-perfluorobutane (C_4HF_9 , m/z 218.98587) during 6:2 FTS biotransformation in each treatment of Loring and Robins soil microcosms based on peak areas of extracted ion chromatograms.

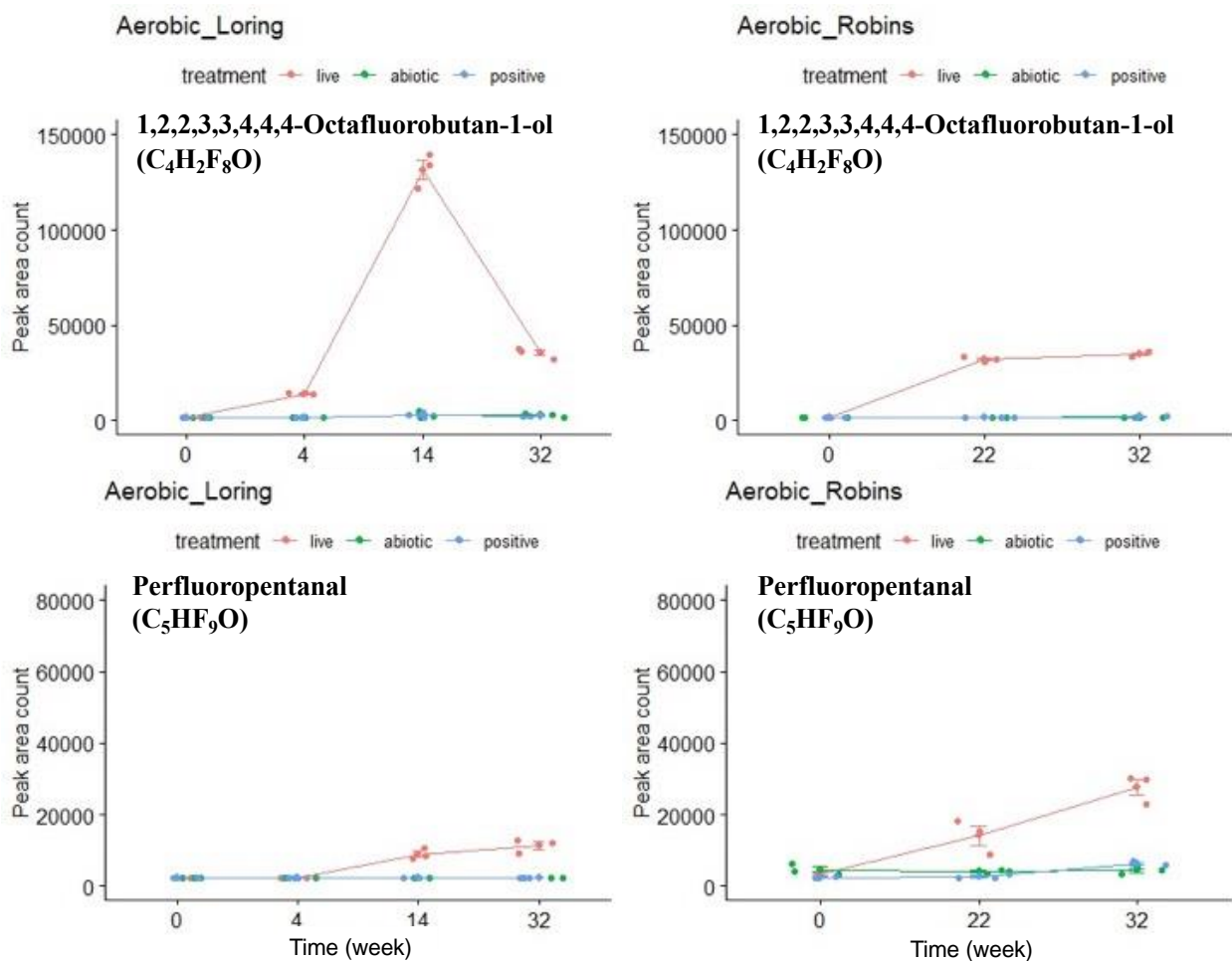


Figure D-8. The time trends of 1,2,2,3,3,4,4,4-Octafluorobutan-1-ol ($C_4H_2F_8O$, m/z 216.98912) and Perfluoropentanal (C_5HF_9O , m/z 246.9808) during 6:2 FTS biotransformation in each treatment of Loring and Robins soil microcosms based on peak areas of extracted ion chromatograms.

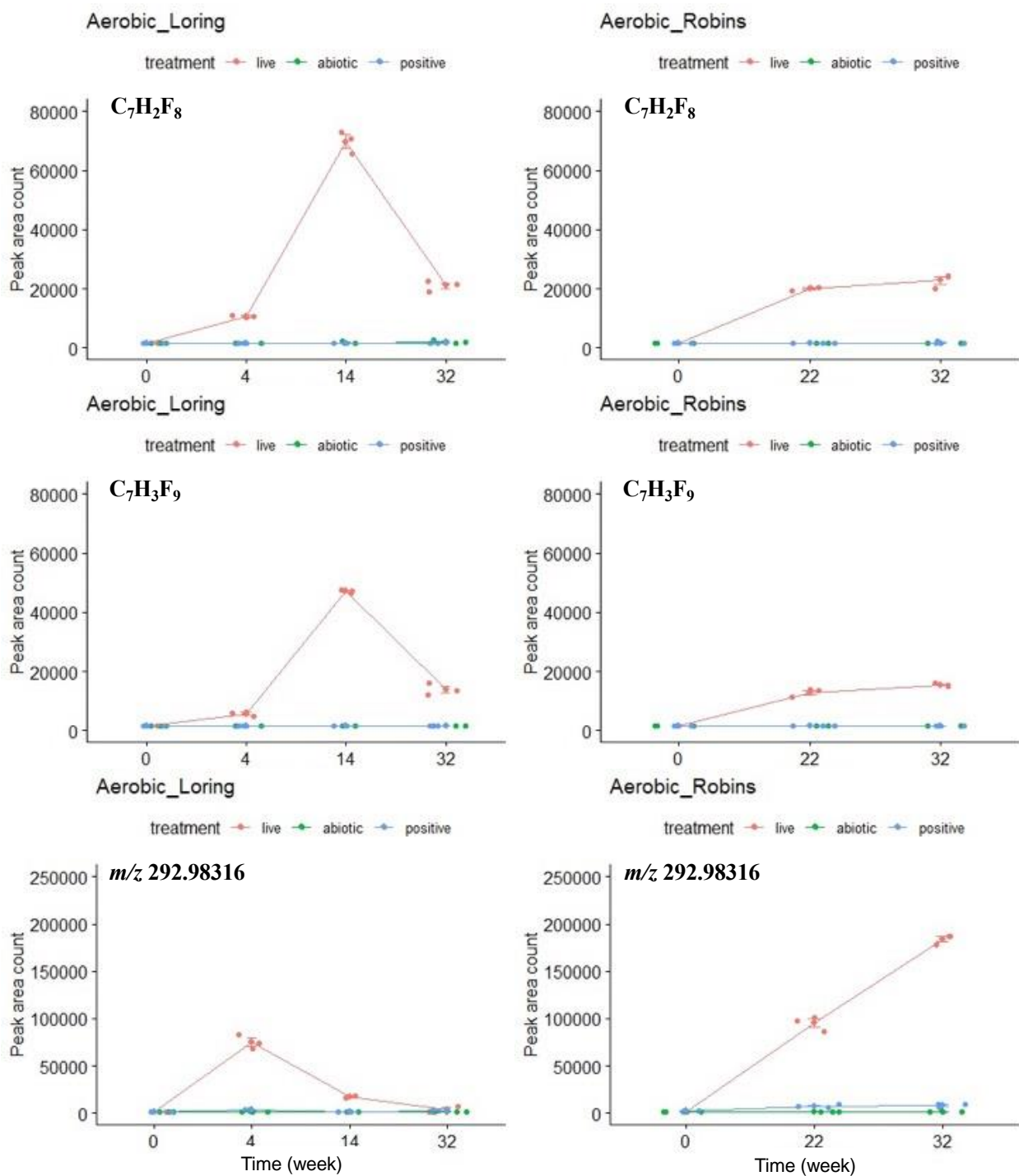
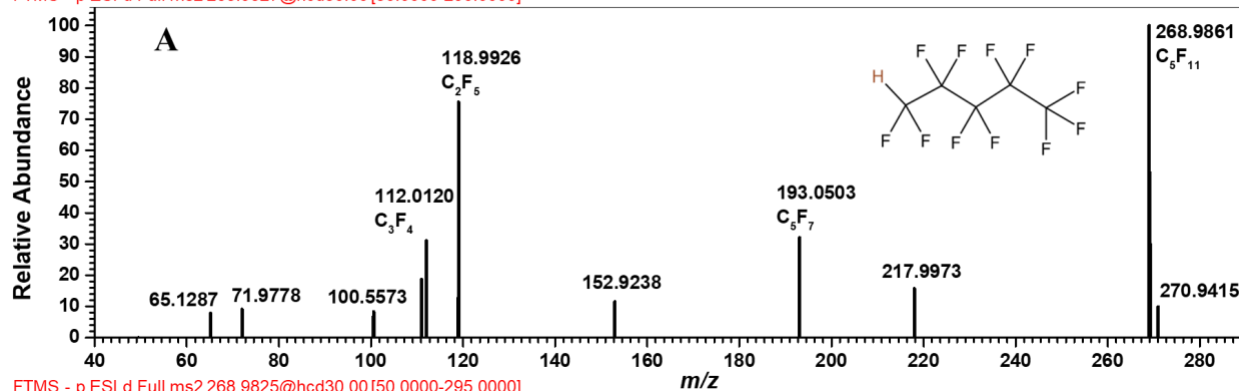


Figure D-9. The time trends of C₇H₂F₈ (m/z 236.99543), C₇H₃F₉ (m/z 257.00159), and m/z 292.98316 during 6:2 FTS biotransformation in each treatment of Loring and Robins soil microcosms based on peak areas of extracted ion chromatograms.

FTMS - p ESI d Full ms2 268.9827@hcd30.00 [50.0000-290.0000]



FTMS - p ESI d Full ms2 268.9825@hcd30.00 [50.0000-295.0000]

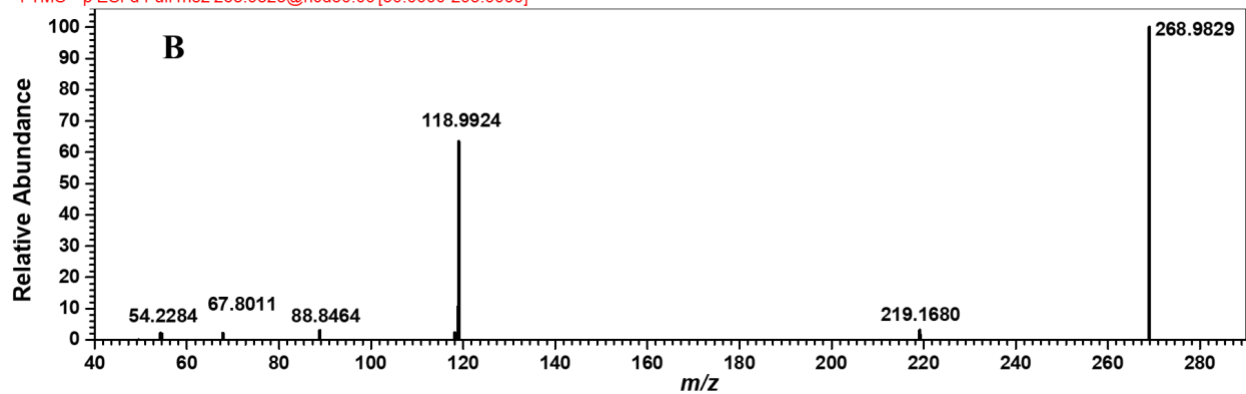
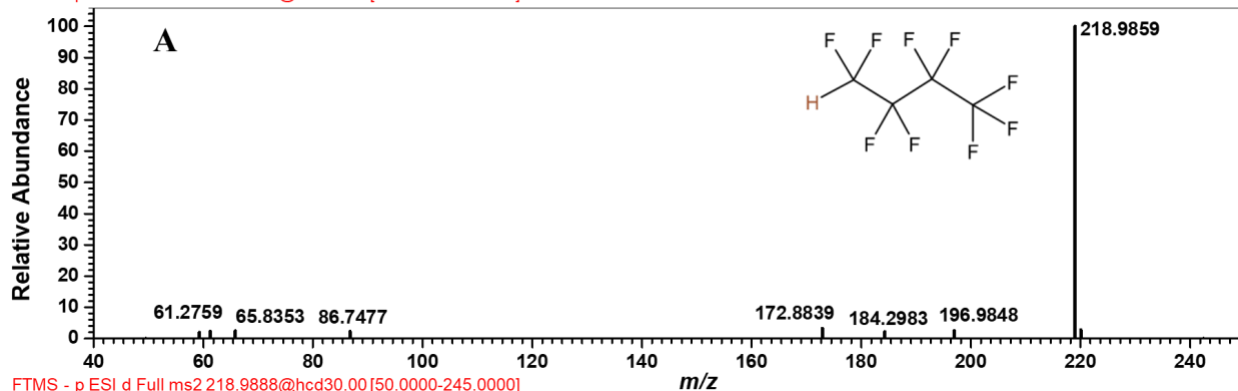


Figure D-10. MS² spectra of 1H-perfluoropentane (C₅HF₁₁, *m/z* 268.98271) obtained from the analysis of microcosm sample (Panel A), and the analysis of 1 ppb reference standard (Panel B).

FTMS - p ESI d Full ms2 218.9859@hcd30.00 [50.0000-240.0000]



FTMS - p ESI d Full ms2 218.9888@hcd30.00 [50.0000-245.0000]

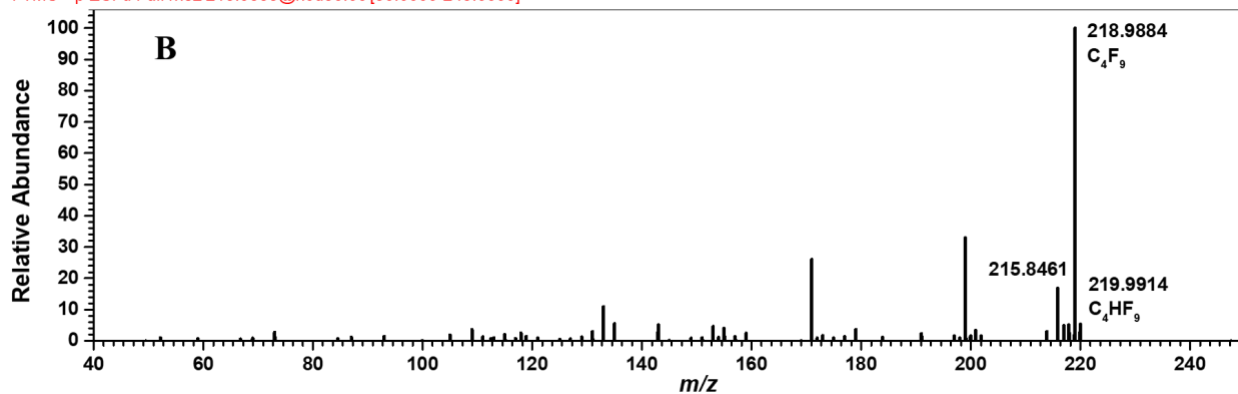
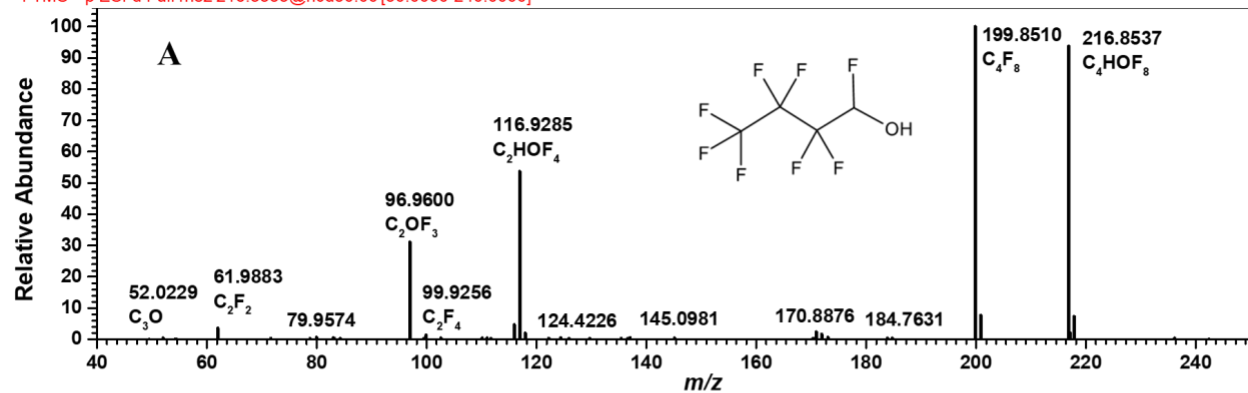


Figure D-11. MS² spectra of 1H-perfluorobutane (C₄HF₉, *m/z* 218.98587) obtained from the analysis of microcosm sample (Panel A), and the analysis of 1 ppb reference standard (Panel B).

FTMS - p ESI d Full ms2 216.8535@hcd30.00 [50.0000-240.0000]



FTMS - p ESI d Full ms2 236.9953@hcd55.00 [50.0000-260.0000]

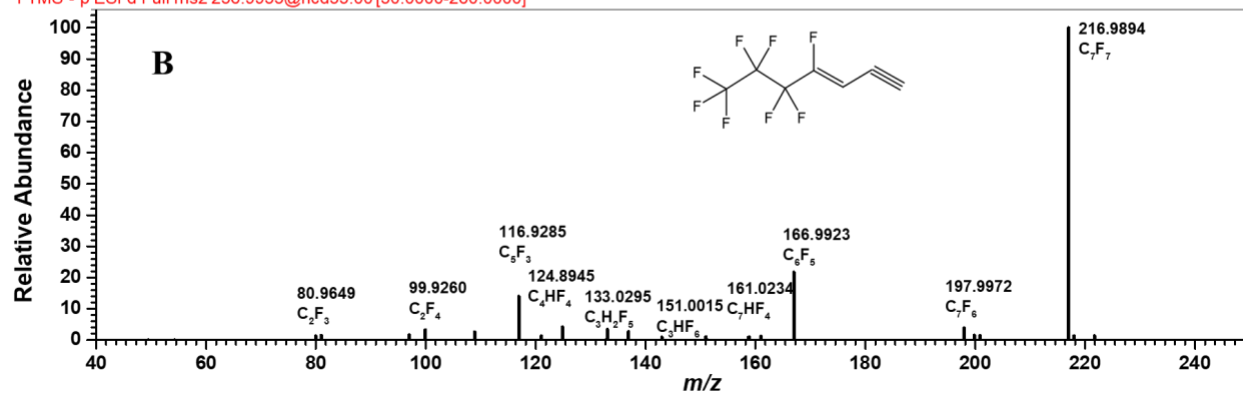


Figure D-12. MS² spectra of potential 6:2 FTS biotransformation products. Panel A, 1,2,2,3,3,4,4,4-octafluorobutan-1-ol ($C_4H_2F_8O$, m/z 216.98912); Panel B, $C_7H_2F_8$ (m/z 236.99543).

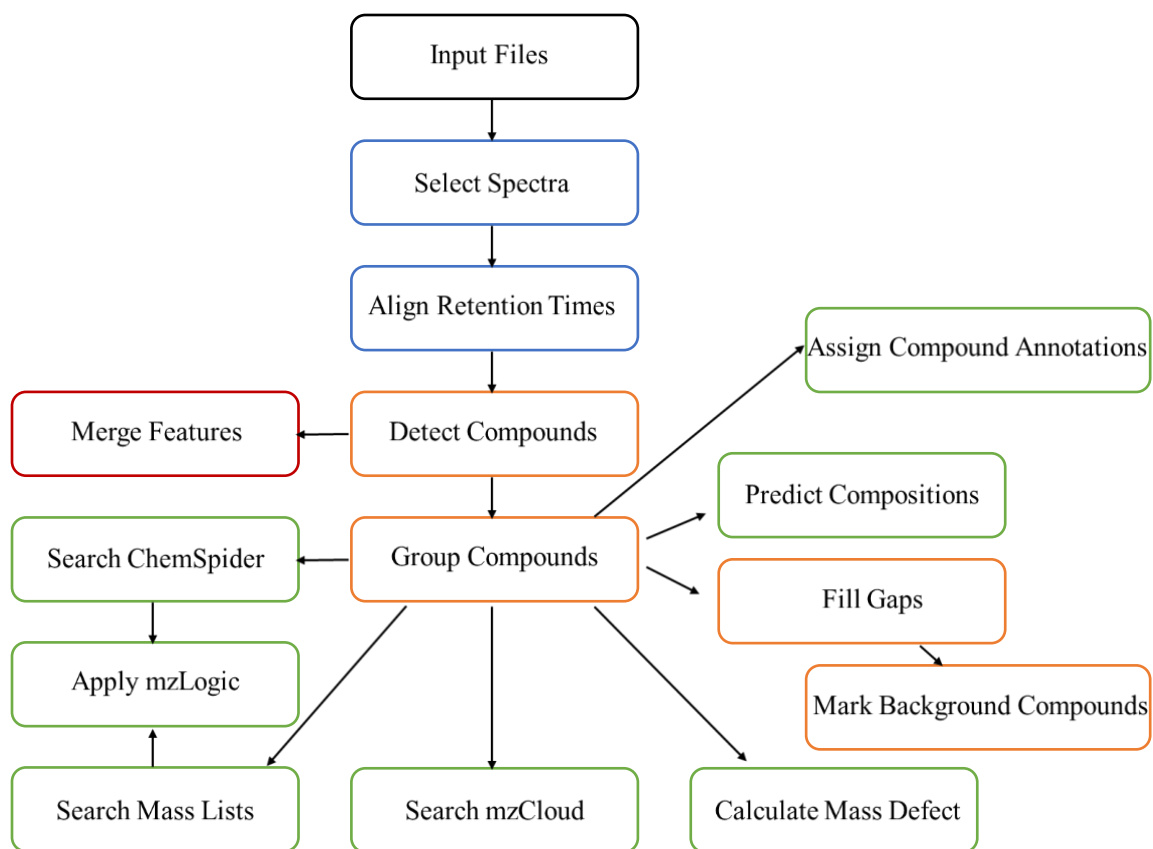


Figure D-13. Compound Discoverer Workflow.

Appendix E. Supporting Information for Chapter 6: Biotransformation of 6:2 Fluorotelomer Sulfonate in Aqueous Film-Forming Foam (AFFF)-impacted Soil under Continuous Flow Conditions

Table E-1. Chemical names, acronyms, molecular structures, and suppliers of target poly- and perfluoroalkyl substances (PFAS) for LC-MS/MS targeted analysis.

Chemical name	Acronym	Molecular structure	Supplier
6:2 fluorotelomer sulfonate	6:2 FTS	$F(CF_2)_6CH_2CH_2SO_3^-$	Sigma-Aldrich (St. Louis, USA); Wellington Laboratories (Ontario, Canada)
6:2 fluorotelomer alcohol	6:2 FTOH	$F(CF_2)_6CH_2CH_2OH$	Wellington Laboratories
6:2 fluorotelomer saturated carboxylic acid	6:2 FTCA	$F(CF_2)_6CH_2COOH$	Wellington Laboratories
6:2 fluorotelomer unsaturated carboxylic acid	6:2 FTUA	$F(CF_2)_5CF=CHCOOH$	Wellington Laboratories
5:2 secondary fluorotelomer alcohol	5:2 sFTOH	$F(CF_2)_5CH(OH)CH_3$	Wellington Laboratories
5:3 fluorotelomer carboxylic acid	5:3 acid	$F(CF_2)_5CH_2CH_2COOH$	Wellington Laboratories
3:3 fluorotelomer carboxylic acid	3:3 acid	$F(CF_2)_3CH_2CH_2COOH$	Wellington Laboratories
Perfluorobutanoic acid	PFBA	$F(CF_2)_3COOH$	PFAC-MXC stock, Wellington Laboratories
Perfluoropentanoic acid	PFPeA	$F(CF_2)_4COOH$	
Perfluorohexanoic acid	PFHxA	$F(CF_2)_5COOH$	
Perfluoroheptanoic acid	PFHpA	$F(CF_2)_6COOH$	
Perfluorooctanoic acid	PFOA	$F(CF_2)_7COOH$	

Table E-2. Packed dry porous media mass, total porosity, and pore volume (PV) for experimental columns.

Column	Porous media	Mass of packed porous media (dry weight, gram)	Total porosity (n)	PV (mL)
A1	Loring soil	140.6	0.35	28.8
A2	and Federal	139.6	0.35	28.7
B1	Fine sand	138.7	0.35	28.6
B2	(1:1 w/w)	139.5	0.36	29.3

Table E-3. Oxidation-reduction potential (ORP) of biotic column samples collected at different time points.

Column samples	ORP (mV)*
<i>Collected during Phase I (25.5-27.5 PVs)</i>	
Influent	476.7 ± 3.7
Port 1	450.6 ± 53.4
Port 2	562.1 ± 39.7
Port 3	469.9 ± 7.5
Effluent	498.6 ± 9.0
<i>Collected during Phase II (40.6-43.0 PVs)</i>	
Influent	539.5 ± 0.6
Port 1	586.8 ± 21.3
Port 2	532.8 ± 14.2
Port 3	542.2 ± 19.8
<i>Collected after Phase II-B (47.4-48.9 PVs)</i>	
Port 3	569.5 ± 22.7

*Values are reported as E_h (mV), relative to standard hydrogen electrode (SHE).

Table E-4. The average molar percent of 6:2 FTS and its biotransformation products (unit: mol%) at different time points in prior microcosm study (see Chapter 5).

	Day 7	Day 28	Day 56	Day 98	Day 154	Day 224
6:2 FTS	92.4 ± 5.2	64.4 ± 8.9	39.2 ± 2.1	29.9 ± 7.6	0.2 ± 0.0	0.3 ± 0.0
6:2 FTCA	N.D.	N.D.	0.4 ± 0.0	0.0 ± 0.0	N.D.	N.D.
6:2 FTUA	N.D.	3.7 ± 0.5	2.4 ± 0.9	0.8 ± 0.5	2.1 ± 0.1	0.3 ± 0.1
5:2 sFTOH	0.0 ± 0.0	5.3 ± 0.4	10.2 ± 1.1	9.8 ± 1.3	11.5 ± 1.2	13.3 ± 5.1
5:3 acid	0.0 ± 0.0	1.1 ± 0.2	1.5 ± 0.6	4.6 ± 0.6	8.9 ± 1.2	0.2 ± 0.1
PFBA	N.D.	N.D.	N.D.	N.D.	0.2 ± 0.0	1.3 ± 0.5
PFPeA	0.0 ± 0.0	0.0 ± 0.0	0.3 ± 0.0	0.4 ± 0.1	1.2 ± 0.3	7.0 ± 2.7
PFHxA	N.D.	0.8 ± 0.2	1.8 ± 0.0	1.6 ± 0.3	1.6 ± 0.3	5.3 ± 0.7
PFHpA	N.D.	N.D.	N.D.	0.0 ± 0.0	0.0 ± 0.0	0.2 ± 0.1
Transformation products	0.1 ± 0.0	10.9 ± 1.3	16.5 ± 2.7	17.2 ± 2.7	25.5 ± 3.1	27.6 ± 9.3
Total mass recovery	92.5 ± 5.4	75.3 ± 10.2	55.8 ± 4.8	47.1 ± 10.3	25.7 ± 3.2	27.9 ± 9.4

Table E-5. The average molar percent of 6:2 FTS and its biotransformation products (unit: mol%) at different phases.

Phases	I-B (11.5-17.5 PVs)	I-C (17.5-33.1 PVs)	II-A (33.1-47.4 PVs)	II-B (47.4-54.1 PVs)	II-C (54.1-58.8 PVs)
6:2 FTS	41.5 ± 12.6*	70.8 ± 11.9	55.4 ± 15.0	45.1 ± 17.3	52.3 ± 5.8
6:2 FTCA	5.4 ± 3.4	5.2 ± 3.8	3.7 ± 2.6	6.6 ± 4.0	4.7 ± 3.4
6:2 FTUA	3.4 ± 1.9	5.1 ± 2.5	4.2 ± 2.6	6.0 ± 4.1	2.9 ± 2.6
5:2 sFTOH	2.4 ± 2.1	3.8 ± 3.2	1.4 ± 1.4	1.7 ± 1.6	2.9 ± 2.2
5:3 acid	1.8 ± 1.4	2.0 ± 1.9	4.7 ± 2.7	10.4 ± 3.4	7.3 ± 2.4
PFBA	0.1 ± 0.1	0.0 ± 0.1	0.1 ± 0.2	0.7 ± 0.3	0.7 ± 0.2
PFPeA	0.0 ± 0.0	0.1 ± 0.1	0.1 ± 0.1	0.3 ± 0.1	0.1 ± 0.0
PFHxA	0.3 ± 0.2	0.2 ± 0.2	0.7 ± 0.4	1.4 ± 0.4	0.6 ± 0.1
PFHpA	0.1 ± 0.1	0.0 ± 0.1	0.1 ± 0.1	0.1 ± 0.0	0.0 ± 0.0
Transformation products	13.5 ± 9.3	16.4 ± 11.7	15.1 ± 10.0	27.2 ± 13.8	19.1 ± 10.9
Total mass recovery	55.0 ± 21.9	87.1 ± 23.7	70.6 ± 24.9	72.3 ± 31.1	71.4 ± 16.7

* The average molar percent of one compound represents the average value of its molar yields measured in all sampling points during the corresponding phase.

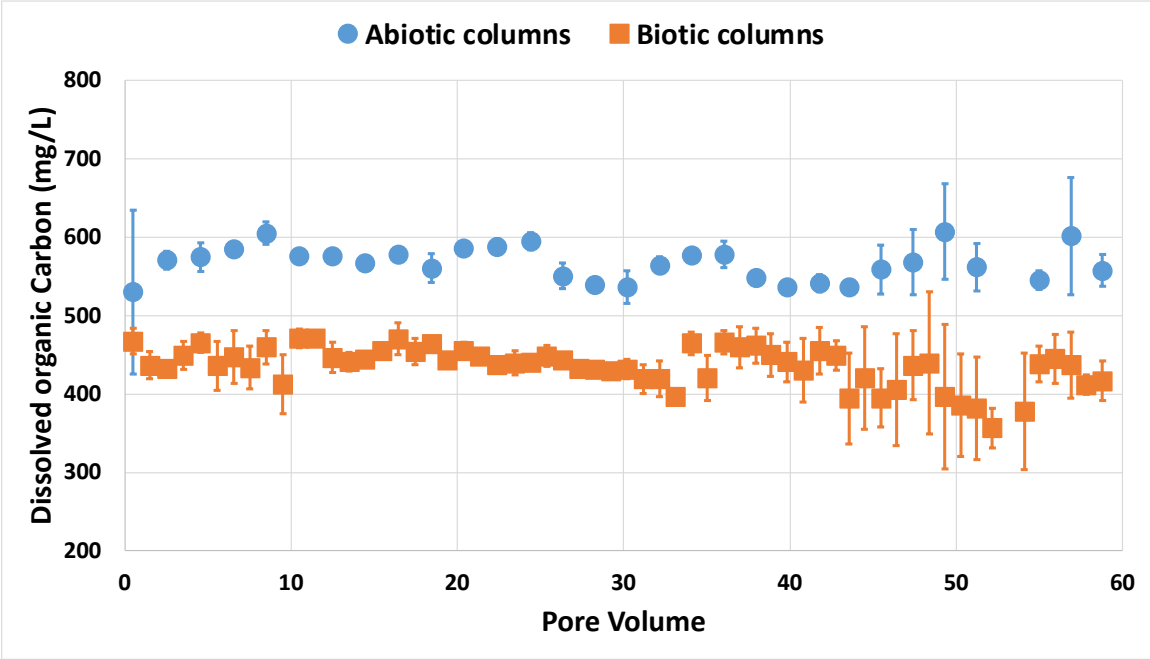


Figure E-1. Concentrations of dissolved organic carbon (DOC) in the effluent samples collected from abiotic and biotic columns.